Defining the role of individual gut commensal microbes and host-microbe interactions

by

Tingting Ju

A thesis submitted in partial fulfillment of the requirements for the degree of

Doctor of Philosophy

In

Animal Science

Department of Agricultural, Food and Nutritional Science
University of Alberta

ABSTRACT

Changes in the gut microbiota have been correlated with positive and negative health outcomes; however, the mechanisms of causality in microbial modifications and resulting host responses are largely unknown. In this thesis, a mouse model was successfully established by colonizing mice with gut microbial communities that differ only in the presence of a single commensal bacterium. Mouse commensal *Escherichia coli* and *Parasutterella* strains were selected as model microorganisms to investigate the mechanisms of host-microbe interactions with different perturbations.

To determine the impact of *E. coli* colonization on host response after antibiotic treatment, mice were colonized with *E. coli* and subsequently treated with metronidazole. *E. coli* colonized the mouse gut readily without causing notable changes in microbiota or host response. However, the presence of *E. coli* strongly affected metronidazole-induced microbial community structural shifts. Remarkably, *E. coli* in the context of a complex microbiota led to variations in the host response to metronidazole treatment including increased expression of antimicrobial peptide genes and intestinal inflammation. This proof of concept study provides an explanation for variability in animal models using antibiotics, and also encourages the development of personalized medication in antibiotic therapies.

The enrichment of family *Enterobacteriaceae* induced by high-fat diet (HFD) feeding has been correlated with impaired glucose homeostasis. To investigate the relationship between the enriched *Enterobacteriaceae* and the development of HFD-induced metabolic disease, the commensal *E. coli* strain was added to the mouse model with HFD intervention. When mice were maintained on a standard chow diet for 16 weeks, no difference in metabolic outcomes was observed between the control and *E. coli*-colonized mice. In contrast, under the

HFD regime, the presence of *E. coli* significantly increased body weight and adiposity as well as induced an impaired glucose tolerance, which was accompanied by elevated levels of plasma leptin. In addition, with HFD treatment, the colonization of *E. coli* led to increased inflammation in adipose tissue. The results demonstrated the role of commensal *E. coli* in glucose homeostasis and energy metabolism responding to HFD treatment, indicating contributions of commensal bacteria to the pathogenesis of obesity and insulin resistance.

To characterize the role of the genus *Parasutterella*, a core component of the human and mouse gut microbiota, *Parasutterella* mc1 was isolated from the mouse gut and characterized *in vitro* and *in vivo*. Mouse, rat, and human *Parasutterella* isolates were all asaccharolytic and producers of succinate. The murine isolate stably colonized the mouse intestine without shifting bacterial composition. Notable changes in microbial-derived metabolites were aromatic amino acid, bilirubin, purine, and bile acid derivatives. The impacted bile acid profile was consistent with altered expression of ileal bile acid transporter genes and hepatic bile acid synthesis genes, supporting the potential role of *Parasutterella* in bile acid maintenance and cholesterol metabolism. This experiment provides the first indication of the role of *Parasutterella* in the gut, beyond correlation, and provides insight into how it may contribute to host health.

A preliminary study was conducted to investigate host adaptions of *Parasutterella* strains in colonizing mouse gut. The chicken *Parasutterella* strain and pig *Sutterellaceae* strain failed to colonize the mouse intestine, whereas the mouse and human strain were able to colonize and persist. However, the mouse strain outcompeted and overcame the human strain in the competitive colonization experiment, indicating a better ecological fitness of the

mouse isolate than the human strain. The study suggests host selectivity of *Parasutterella* species and the co-evolution between *Parasutterella* and the host.

Collectively, the thesis provides information about the role of commensal bacteria, *E. coli* and *Parasutterella*, in microbial interactions and host physiology using a well-controlled tractable mouse model.

PREFACE

This thesis is an original work by Tingting Ju.

Part of Chapter 1 has been included in the book chapter Tingting Ju, Jiaying Li, Benjamin P. Willing. 2016. Microbiota-related modulation of metabolic processes in the body. In: Jason A. Tetro, and Emma Allen-Vercoe, editors. Microbiome Handbook, DEStech Publications, Inc. ISBN: 978–1–60595–159–1. p. 171–200. T. Ju and J. Li compiled the relevant information and wrote the manuscript together with B. P. Willing.

Chapter 2 has been published as Tingting Ju, Yasmeen Shoblak, Yanhua Gao, Kaiyuan Yang, Janelle Fouhse, B. Brett Finlay, Yee Wee So, Paul Stothard, Benjamin P. Willing. 2017. Initial gut microbial composition as a key factor driving host response to antibiotic treatment, as exemplified by the presence or absence of commensal *Escherichia coli*. Applied Environmental Microbiology. 83:e01107–17. T. Ju designed, conducted the experiment, collected and analyzed the data, and wrote the manuscript. Y. Shoblak, Y. Gao, K. Yang, Y. W. So helped with data collection. J. Fouhse and P. Stothard contributed to data analysis. B. B. Finlay provided conceptual advice. B. P. Willing designed the experiment, supervised data analyses, wrote and edited the manuscript.

The study in Chapter 3 was designed by T. Ju and B. P. Willing. T. Ju conducted the experiment, collected and analyzed the data, and wrote the manuscript. B. C. T. Bourrie helped with data collection. The manuscript is in preparation as Tingting Ju, Benjamin C. T. Bourrie, and Benjamin P. Willing. 2019. The presence of gut commensal *Escherichia coli* aggravated high-fat diet-induced obesity and insulin resistance in mice.

Chapter 4 has been published as Tingting Ju, Ji Yoon Kong, Paul Stothard, and Benjamin P. Willing. 2019. Defining the role of *Parasutterella*, a previously uncharacterized

member of the core gut microbiota. ISME J. 13:1520–1534. T. Ju designed, conducted the experiment, collected and analyzed the data, and wrote the manuscript. J. Kong helped with data collection. P. Stothard contributed to data analysis. B. P. Willing designed the experiment, supervised data analyses, wrote and edited the manuscript.

The study in Chapter 5 was designed by B. P. Willing. T. Ju was responsible for designing, conducting the experiments with A. Gilliland and writing the manuscript.

ACKNOWLEDGMENTS

I would like to express my deepest gratitude to my supervisor, Dr. Benjamin P. Willing, for his great insights, guidance, and support at every step of this journey. Thank you for providing me with numerous opportunities to develop my skills, knowledge, and experience in teaching and research.

I would also like to thank Dr. Michael Ganzle and Dr. Karen Madsen for serving on my supervisory committee, giving me invaluable advice and support throughout my research program. I would like to extend my gratitude to Dr. Paul Stothard and Dr. Jun Han for their help with the whole genome sequencing and metabolomic analyses. I am grateful for my examining committee members Dr. Thomas Clavel and Dr. Norman Neumann for reading my thesis and providing me with insightful feedbacks.

I want to thank the present and past members of the Willing lab for their continued support. Special thanks to Benjamin Bourrie, Andrew Forgie, Ashley Gilliland, and Deanna Pepin for their kind help with my sample collection. Sincere gratitude is also extended to Nicole Coursen and Stephanie Tollenaar for all the help with animal trials.

I am very grateful to the Department of Agricultural, Food, and Nutritional Science, the Faculty of Graduate Studies and Research at the University of Alberta and the Alberta Innovates for the financial support and academic guidance.

I would like to thank my friends for their support and care over the years. Finally, I want to thank my family for their enduring love and support. My parents, my sister, my brother and my fiancé, Jiyao have been constant sources of joy and support in my life. This thesis is dedicated to them.

TABLE OF CONTENTS

LIST OF TABLES

LIST OF FIGURES

1. CHAPTER 1: INTRODUCTION

1.1. Gut microbiota

The complex consortium of microbes that inhabits the mammalian gastrointestinal tract (GIT), termed the gut microbiota, are well known to have a tremendous impact on host health and disease. Driven by technological advances in the past decade, the scientific interest in the microbiome research field is moving beyond correlations to focus on addressing mechanisms and causations of host-microbe interactions (1). Although identifying the underlying mechanisms by which gut microbes impact host physiology remains challenging, several mediators of host-microbe interactions have been characterized, establishing a foundational understanding of the symbiont (2). The mediating factors include, but not limited to the immunomodulatory effects of the gut microbiome and the microbial-derived metabolites (2).

Host immune system plays an important role in shaping the gut microbiota which largely impacts the symbiotic relationships in the gut (1). The gut immune system prevents overgrowth of resident microbiota through multiple antimicrobial mechanisms to maintain immune homeostasis (3). Gut microbes can elicit distinct immune responses, however, the underlying mechanisms with respect to specified commensal microbes remain to be fully elucidated (4). In addition, it is still not clear to what extent individual bacterial species impacts the immune homeostasis in the context of a complex microbial community, suggesting the necessity of investigating the biology and function of individual bacterial species.

Microbial-derived metabolites in the gut actively foster intestinal homeostasis, however, our understanding of metabolites produced by the gut microbiota is still in its

infancy as a substantial proportion of the molecules and associated pathways have yet to be functionally characterized (5). Currently, several metabolites such as short-chain fatty acids, trimethylamine, and bile acids have been identified to exert a crucial influence on host health outcomes (5). In this section, the characteristics of bile acids and the involvement of the gut microbiota in bile acid metabolism will be briefly discussed.

1.1.1 The gut microbiota and bile acid metabolism

Bile acids are widely known for their role in promoting the absorption of dietary lipids and lipid-soluble nutrients in the intestine. However, more recently bile acids have been identified in metabolic regulation as signaling molecules that regulate a network of lipid, glucose, drug and energy metabolism (6). Bile acid signaling has also been identified as a mechanism through which microbes regulate host metabolism regarding the modifications of bile acid structure and abundance by the gut microbiota.

1.1.1.1 Biosynthesis and transport of bile acids

Bile acids are derived from cholesterol in the liver through a multi-enzyme process. The full complement of bile acid synthesis requires at least 16 enzymes that catalyze as many as 17 reactions to convert cholesterol into conjugated bile salts (7). The immediate products of these reactions are referred to as primary bile acids. In humans, there are two primary bile acids, which are chenodeoxycholic acid (CDCA) and cholic acid (CA). Mice synthesize CA and muricholic acid (MCA), the latter of which is significant in that βMCA is the primary bile acid responsible for activating some signaling pathways discussed below. Bile acids are conjugated with taurine or glycine at the last step of primary bile acids biosynthesis. The conjugation reduces the ability of bile acids to cross the cell membrane lipid bilayer, leading to a high intraluminal concentration of bile acids, which is essential for facilitating fat

digestion and absorption (8). More than 95% of excreted conjugated bile salts are reabsorbed in the distal ileum and returned to the liver through the enterohepatic circulation (9). The size of the bile acid pool can be maintained at a constant level, approximately 2 to 4 g in humans (10).

1.1.1.2 Microbial involvement in bile acid circulation

Gut bacteria modify primary bile acids via three mechanisms including deconjugation, 7α-dehydrogenation, and 7α-dehydroxylation (11). The process results in the formation of secondary bile acids, increasing the chemical diversity of the bile acid pool (12). In humans, the primary bile acids CA and CDCA are converted into the secondary bile acids deoxycholic acid (DCA) and lithocholic acids (LCA), respectively. The differences in bile acid profile between human and mice have been nicely summarized previously (13). The transformation of bile acids by the gut microbiota is mainly attributed to anaerobic bacterial genera including *Bacteroides*, *Eubacterium*, and *Clostridium* (12). The deconjugation process is performed by various genera such as *Bacteroides*, *Proteus*, *Lactobacillus*, *Clostridium*, and streptococci. The dehydrogenase activity is performed by a wide range of bacteria including *E. coli*, *Pseudomonas*, *Bacteroides*, *Eubacterium*, *Bacillus*, and *Clostridium* (14). In addition, *Bifidobacterium* and *Lactobacillus* species have been widely found to produce bile salt hydrolase (15, 16).

The gut microbiota alters the size of the bile acid pool and bile acid composition. Microbial colonization increases the fecal loss of bile acids, which coincides with an overall reduction in the bile acid pool (16). Germ-free rats have a circulating bile acid profile dominated by conjugated bile acids whereas bile acids are primarily unconjugated in

conventionalized mice (17). Collectively, the gut microbiota reduces the bile acid pool size, however, increases chemical diversity of bile acids (16).

1.1.1.3. Gut microbiota impacts host health by modulating bile acids metabolism

Obese patients treated with vancomycin showed reduced fecal secondary bile acids and simultaneous postprandial increase of plasma primary bile acids. Meanwhile, vancomycin treatment decreased peripheral insulin sensitivity, linking alterations in bile acids and glucose metabolism (17). It has been proposed that the gut microbiota affects signaling properties of bile acids via the Farnesoid X receptor (FXR) and the G protein-coupled membrane receptor 5 (TGR5) signaling pathway to influence the lipid and glucose metabolism (18).

1.1.1.3.1. FXR signaling pathway and bile acids metabolism

The FXR signaling pathway is important in maintaining bile acid pool as it controls both bile acid biosynthesis and enterohepatic cycling (19). The FXR pathway affects the biosynthesis of bile acids in the liver by repressing the expression of rate-limiting enzyme, cholesterol 7α-hydroxylase (CYP7A1), through direct regulation of the short heterodimer partner (SHP). Interruption of this feedback loop results in increased bile acid pool as evidenced by an altered bile acid pool size in $SHP^{-/-}$ mice (19). The activation of FXR signaling pathway in the intestine induces the expression of fibroblast growth factor (Fgf)-19 which is secreted into the circulation, inducing a repressed expression of CYP7A1 in the liver (20). The FXR-mediated repression of CYP7A1 contributes to the negative feedback regulation of bile acid synthesis, and this feedback mechanism is impacted by microbial modification of bile acids (21).

1.1.1.3.2. FXR signaling pathway in glucose and lipid metabolism

Substantial evidence indicates that the FXR signaling pathway plays an important role in the regulation of glucose metabolism. However, due to opposing findings, it is as yet unclear in which direction FXR signaling should be promoted/inhibited to result in a healthy outcome. FXR deficiency benefited body weight and glucose homeostasis in mice on a leptin-deficient (ob/ob) background (22). However, $FXR^{-/-}$ mice on a wild-type background developed severe fatty liver and impaired glucose tolerance (23). It has been proposed that FXR may have beneficial effects in mice under chow-diet fed conditions, whereas in mice maintained on HFD, FXR may exert deleterious outcomes by altering lipid and glucose metabolism (13). The mechanism by which the activation of FXR signaling pathway induces distinct responses in different contexts has yet to be established (24).

1.1.1.3.3. TGR5 signaling pathway and bile acid metabolism

Bile acids act as ligands for TGR5 in the liver and intestine, and TGR5 has been recognized to promote glucose homeostasis (25). LCA and DCA promoted glucagon-like peptide-1 (GLP-1) secretion in a murine enteroendocrine cell line via the TGR5 signaling pathway (26). TGR5 overexpression led to a dramatically improved glucose tolerance in mice fed HFD by inducing the secretion of GLP-1 (25). The association between TGR5 activation and GLP-1 secretion may provide a novel strategy to treat metabolic diseases such as diabetes and non-alcoholic fatty liver disease (NAFLD) (27). In addition, bile acid-activated TGR5 increased energy expenditure in brown adipose tissue, which prevented obesity and insulin resistance in mouse models (28). TGR5 signaling has also shown anti-inflammatory effect, making the pathway as essential machinery for fine-tuning energy and immune homeostasis (29).

Taken together, bile acids shape the gut microbiome, and in turn, the shift in the gut microbiota can influence the bile acid profile and thereby change host metabolism and health (13). Microbial-derived modifications of bile acids reveal an opportunity to improve obesity and metabolic diseases via bile acid signaling pathways.

1.2. Model systems for investigating microbe-microbe and host-microbe interactions

The establishment of effective model systems has been critical to the development of new knowledge in gut microbial ecology and host-microbial interactions. (30). To date, multiple model systems coupled with functional assays have been developed to evaluate the bioactivities of the gut microbiota and to explore mechanisms by which gut commensal microbes are linked to host health outcomes. These model systems use a range of approaches including *in vitro*, *ex vivo*, and *in vivo*. In this section, the applications and limitations of the major types of models in gut microbiome research will be discussed, particularly pertaining to the understanding of gut commensal bacteria (Figure 1.1).

1.2.1. *In vitro* models to study gut commensal bacteria

The *in vitro* models are considered as excellent tools for large scale screen of components of interest, ranging from commensal microbes to dietary nutrients or other bioactive compounds, to assess microbe-microbe or host-microbe interactions (30). Although there are limitations to mimic the complexity of the intestinal environment, these *in vitro* models provide invaluable information on host-microbe interplay.

1.2.1.1. *In vitro* fermentation models

To dynamically monitor the microbial activity, several *in vitro* fermentation models have been developed, including simple batch fermentations and dynamic fermentations that consist of complex multicompartmental continuous systems (31). Batch fermentation systems

represent static models using test tubes or controlled reactors inoculated with a variety of bacterial cultures or fecal microbial suspensions to test the impact of intestinal microorganisms on different substrates, and vice versa. Batch fermentations usually operate over a short-term period and under anaerobic conditions. Although the rate of substrate depletion and end product accumulation are normally altered compared to that in the gut environment, the considerable variations among inoculations and the high-throughput of batch fermentations make the models appropriate for initial assessment of microbial activity (31, 32). For longer fermentations, the semi-continuous culture systems were developed to mimic the large intestine in which part of the bacterial culture was removed and replenished once or twice daily (33). In addition, continuous culture models have been established to keep the bacterial population close to a steady state by continuously adding fresh growth medium and removing the spent culture (33). Currently, continuous culture models, particularly multi-compartmental models, have been widely used due to the capability of maintaining a relatively stable microbial ecosystem (31). The major *in vitro* continuous culture models have been listed in Table 1.1; Among them, the EnteroMix colon simulator, the TNO Gastro-Intestinal Model (TIM) 2, and the Simulator of the Human Intestinal Microbial Ecosystem (SHIME) have been widely used to simulate different compartments of GIT (31). These model systems allow the investigation of a dynamic fermentation process in different gut regions with high reproducibility, providing information about the bioactivities of microbial communities.

1.2.1.2. Cell culture system simulating intestine

The ability to simulate the host functionality in gut fermentation models remains limited. Therefore, intestinal cell culture system has been incorporated into the models, which

represents a common approach to explore interactions between gut commensal bacteria and the host. Several established cell lines including Caco-2, HT-29, T84, IEC-6, IEC-18, and IPEC-J2 have been extensively used to perform as intestinal epithelial cells (34). While the cell lines mimic characteristics of the intestinal epithelium, the single-cell type system is not sufficient to recapitulate the gut environment. An alternative approach is to use epithelial cell coculture models integrating multiple cell types, including epithelial cells, lymphocytes, macrophages, and dendritic cells, to simulate host immune response. The coculture model provides invaluable information about reactions generated from multiple cell types responding to commensal bacteria with respect to communications between different cell lineages (35).

Remarkably, recent advances in microfluidics-based systems provide a better simulation of the gut environment. The establishment of a gut-on-a-chip model includes a provision for peristalsis-like motions in the co-culture of intestinal epithelial cells and bacteria (36). Another device, the Host-Microbiota Interaction (HMI) module, has been developed to interface with the SHIME model culturing gut commensal microbes, incorporating a semi-permeable polyamide membrane between co-cultured bacteria and enterocytes (37). The module allows the co-culture of a monolayer of enterocytes with gut microbial communities under microaerophilic condition up to 48 h. Recently, another model, HuMiX, has been established showing a better capability of controlling oxygen levels in the co-culture system and the ability to incorporate other cell types within the model (38). However, the question remains whether the peripheral blood mononuclear cells (PBMCs) mostly used in cell co-culture models represent a similar behavior with gut-resident immune

cells. The phenotype observed from cell culture systems may need to be further validated *in vivo*.

1.2.2. *Ex vivo* models simulating intestine

In vitro and *ex vivo* models represent a powerful strategy to investigate specific effects of gut commensal microbes on host cells using a highly controlled approach. *Ex vivo* models provide more physiological relevance compared with cell culture systems, which have been widely used for measuring intestinal functionality such as intestinal permeability (39, 40). Several models have been developed such as the Ussing chamber, tissue explant, organoid, and intestinal organ culture system to investigate host-microbe interactions (39, 41, 42). These models open the door to exploring the immediate or early response of the intestinal tissue to bacterial exposure which can be difficult to assess *in vivo*. The systems, however, have limitations in supporting long-term investigations due to the viability, behavior changes, and the occurrence of apoptosis of intestinal tissue over time. In addition, models such as organoids lack other intestinal components, especially immunocytes, making it less suited to study the interactions between gut microbes and host immunity. Careful attention should also be paid to the substantial variations among intestinal segments in the tissue explant model. Taken together, these limitations regarding the time limit and multi-cell communications should be acknowledged when choosing *ex vivo* models to study the impact of the gut microbiota on intestinal physiology.

1.2.3. *In vivo* models to study host-microbe interactions

Currently, our understanding of mechanisms underpinning the interaction between the gut microbiota and the host is largely derived from animal studies due to the effectively controlled environment and diet (43). Animal models represent a robust tool to study the

impact of the gut microbiota on host health outcomes ranging from nutrient metabolism to disease resistance. Germ-free animals, including *Drosophila melanogaster*, zebrafish, mice, rats, and pigs have been developed as effective models combined with genomic and physiological characterizations. Advantages and disadvantages of each animal model in studying host-microbe interactions have been summarized previously (44). This section will mainly focus on rodent model systems which have been extensively used in gut microbiome research.

1.2.3.1. The anatomical and physiological features of mouse GIT

Regarding the anatomy, physiology, and biochemistry of the GIT, there are several differences between humans and mice (45). For instance, the stomach of rodents contain a non-glandular forestomach portion that is absent in humans. The non-glandular stomach is used for food storage without secretory activity, which is lined by keratinizing squamous mucosa and generally thin-walled and transparent (45). The feature of the forestomach in rodents allows the formation of a biofilm comprised of a variety of *Lactobacillus* spp (46). The jejunum is the longest segment of the small intestine in mice with Peyer's patches as the most prominent feature, whereas these characteristics are found in human ileum (47). The mucosal surface of the human small intestine contains the *plicae circularis* structure to increase the surface area, providing a niche for mucus-associated bacteria, which is absent in the mouse small intestine (46). The relative size of the cecum in rodents is significantly larger compared with humans, and rodents recapture vitamins produced by microbial fermentation in the cecum through coprophagy. The human colon is segmented with transverse fold structure in mucosa whereas mucosal folds in mice vary by colonic region (46). In addition, the glycan composition of mucus in the gut displays differences between humans and mice,

which may be involved in shaping gut microbial communities (46). These distinct features throughout the GIT should be considered when interpreting and translating results using mouse models.

1.2.3.2. Microbial composition of mouse GIT

The reported gut microbial composition in mice is largely influenced by multiple factors such as genetics, diet, antibiotics, and other environmental factors (48). Although it has been reported that 85% of sequences represent genera found in mice have not been detected in humans, in general, mouse and human microbiota are similar at the phylum level and certain genera are shared by both species (49, 50). A deep investigation of the microbial function in addition to taxonomic profiling will help to link the trait observed in mouse models to the human gut microbiome. Notably, laboratory mice, especially mice housed under the specific-pathogen-free (SPF) condition, may not be exposed to certain microbes that they would encounter naturally (51). For example, SPF mice purchased in this thesis did not harbor commensal *Enterobacteriaceae* and *Parasutterella*, which provide us a suitable model for conducting colonization studies in the context of a complex microbial community.

1.2.3.3. Antibiotic-treated mouse model

Antibiotic treatment has emerged as one of the primary tools for gut microbial manipulation, generally leading to a reduction in bacterial populations. Broad-spectrum antibiotics are commonly used in mouse models to study the altered bacterial composition and its impact on host physiological changes. Antibiotic treatment has been considered as an extreme perturbation to the gut microbiome and antibiotic regimens used in mouse models have been summarized previously (52) Although selecting certain classes of bacteria is possible, it remains difficult to manipulate gut microbial community at low taxonomic levels

by antibiotic treatment even with a narrow spectrum of activity. Therefore, the host response associated with altered gut microbiota is likely to be a consequence of changes in overall structure or in a group of bacteria, making the model less suitable for studying interactions between the host and specific bacterial species. In addition, antibiotics could directly affect host tissues by altering mitochondrial gene expression and inducing apoptosis of intestinal epithelial cells (53). The involvement of host-associated factors and relatively broad alterations in the gut microbial composition should be acknowledged using the antibiotic-treated models.

1.2.3.4. Germ-free mouse model

Germ-free animals highlight the impact of the gut microbiota on host physiology by comparing to conventionalized animals. Germ-free mice have an underdeveloped immune system featured by poorly formed Peyer's patches and altered lymphocyte distributions in the gut. Germ-free mouse model in combination with the recolonization of gut microbes is commonly used to better reflect the physiological conditions (54).

1.2.3.4.1. Monoclonization gnotobiotic mouse model

Germ-free mice can be monocolonized with microbes from many sources, including, but not limited to members isolated from the human and mouse gut microbiota (1). The monocolonization model is limited by the ability of microbes to get adapted to specific environmental conditions in germ-free mice. Microbe-microbe interactions play a fundamental role in microbial colonization as evidenced by the role of aerobic and facultative anaerobic bacteria in supporting the colonization of Clostridia in neonates gut (55). *Parasutterella* species, as strict anaerobic bacteria, monocolonized the germ-free mouse gut at a relatively low level compared to that in SPF mice, indicating the enhanced colonization

by microbial interactions (56). In addition, the lack of microbial complexity limited the display of normal physiological responses of the host, and choosing a proper control group is usually difficult in monocolonization models (1). However, monocolonization studies could still provide important information about the function of a single microorganism especially for the ones with low abundance in the context of a complex microbial community (1). A recent study using the monocolonization gnotobiotic mouse model coupled with immunophenotyping and transcriptomic analysis defined the impact of 53 human gut commensal bacteria on host immune response, providing evidence about immunomodulatory functions of these commensal bacteria (57). Further research in the presence of a complex microbial community is needed to validate findings from the monocolonization models.

1.2.3.4.2. Defined communities mouse model

Germ-free mice colonized with defined communities have provided an opportunity to understand the mechanisms that underlie host-commensal mutualism under different conditions. The defined microbial communities simplify the natural gut microbiota; however, they are complex enough to allow examination of microbe-microbe and host-microbe interactions. The altered Schaedler flora (ASF), which triggers the development of a relatively normal immune system and gastrointestinal function, have been widely used to reconstitute a defined community in germ-free mice (58). It has been shown that the metabolic function of ASF is more representative of wild microbiome than random consortia of similar or large size, and *Parabacteroides* ASF519 may be a vital contributor to the ASF genomic potential and metabolic activities (59). However, ASF was insufficient to provide colonization resistance against *Salmonella* infection, whereas a bacterial consortium comprising 12 mouse bacterial isolates, the Oligo-Mouse-Microbiota (Oligo-MM12), coupled

with three facultative anaerobic bacteria were able to protect mice from *Salmonella* infection (60). Therefore, the Oligo-MM12 represents a suitable fundamental model for gut microbiome research in the settings of enteric infection, highlighting the importance of selecting an appropriate defined community in investigating host-microbe interactions under different contexts.

Humanized gnotobiotic mouse models, resulted from colonizing germ-free mice with the human gut microbial community or a defined community of human-derived microbes, have been used to recapitulate biological features of human microbial communities (61). The metabolomic analysis of urine and fecal samples in mice colonized with human microbiota revealed that the majority of metabolomic features are transmissible to mice (62). However, more investigations are needed to demonstrate the extent of humanized mouse models represent the real relationship between the host and gut microbiota observed in humans regarding the absence of the host-microbe coevolution (50). In contrast, colonizing mice with mouse-derived microbes represents a relatively natural tool to study host-microbe interactions. Identifying gut microbial functions shared between different hosts such as immunomodulatory effects and microbial-derived metabolites may be a better approach to recapitulate the situation in host species of interest.

Collectively, the development of model systems has greatly advanced the field of gut microbiome research, which allows us to understand the impact of the gut microbiota on host physiology. The awareness of advantages and limitations of each model will provide an efficient way to decipher the mechanism of host-microbe interactions and promote practical application of gut microbiome research.

In this thesis, a SPF mouse model was established by adding a single mouse-derived bacterium to a complex gut microbial community, which did not harbor the bacterium, with the bacterial fermentation model and omics techniques integrated (Figure 1.2). The commensal *E. coli* and *Parasutterella* strains were selected as model microorganisms for the model system to explore their interactions with the host metabolism and immunity.

1.3. The commensal *E. coli* in the gastrointestinal tract (GIT)

The family *Enterobacteriaceae* has been recognized as one of the most taxonomically diverse bacterial families, which used to be the single constituent family within the order Enterobacteriales. At the time of writing, the newly delimited family *Enterobacteriaceae* consists of 53 genera, encompassing 211 species, with a validly published name (www.namesforlife.com) (63, 64). In a family as diverse as the *Enterobacteriaceae*, it is difficult to cover phenotypic characteristics and phylogenetic relationships of each genus within the family; however, with respect to gut residency, *Escherichia coli* is the most widely-found *Enterobacteriaceae* in mammals (65).

First identified by Theodor Escherich in 1885 from feces of neonates, *E. coli* has been widely associated with both animal and human health outcomes. Traditionally, the serotyping of *E. coli* was based on the somatic (O), flagellar (H) and capsular polysaccharide antigens (K) (66, 67). Multilocus sequence typing and genome sequence data expand the understanding of phylogenetic structures of *E. coli*, classifying *E. coli* strains into one of the seven phylogenetic groups (A, B1, B2, C, D, E, and F) (68). With substantial phylogenetic diversity, *E. coli* has engaged in a variety of host interactions ranging from mutualistic to pathogenic lifestyles. For example, *E. coli* of the A, B2, and F phylogroups are more likely to have a long-term persistence in the healthy human gut compared to other lineages (69).

A recent human study investigating the *Enterobacteriaceae* population in healthy human gut confirmed that *E. coli* is the most dominant *Enterobacteriaceae* in the gut, and clonal populations of *E. coli* are dynamic which are not consistent at the strain level (69). From the study, the authors suggested that the gut microbiota is not as stable as previously reported which is evidenced by the low stability of *Enterobacteriaceae* population; however, the question remains to what extent the strain-level differences impact functional dynamics at the community level. Nevertheless, the low stability of *E. coli* population may partially explain the expansion of *Enterobacteriaceae* commonly observed in various biological contexts such as inflammation. In this section, the potential role of *Enterobacteriaceae*, in particular *E. coli*, as gut commensals in host health outcomes regarding microbiome development, obesity, and type 2 diabetes (T2D) will be discussed.

1.3.1. *Enterobacteriaceae* in early life microbiome development

Being the dominant facultative anaerobe in the GIT, *Enterobacteriaceae* has been widely found in the infant intestinal microbiota during the first days of life (70, 71). The analysis of fecal microbiota in children sampled longitudinally up until 2 years of age demonstrated that three OTUs classified as *Bifidobacterium*, *Bifidobacterium longum*, and *Enterobacteriaceae* dominated the gut throughout the entire first year of life, indicating the involvement of *Enterobacteriaceae* in gut microbiome development in early life (72).

Indeed, the colonization of *Enterobacteriaceae* plays a crucial role in the establishment of colonization resistance and in the protection against infectious diseases. The susceptibility to intestinal infections in neonates has been attributed to a developing immune system and immature gut microbiome featured by a low microbial diversity (70). In neonatal chicks which are highly susceptible to *Salmonella* infection, the presence of both spore-

forming bacteria and commensal *Enterobacteriaceae* are required to confer colonization resistance against *Salmonella* (73). It has been shown that the low abundant keystone taxon, commensal *Enterobacteriaceae* competes with *Salmonella* for oxygen through the aerobic respiration. Therefore, the consumption of oxygen by *Enterobacteriaceae* and the maintenance of epithelial hypoxia by Clostridia limit the access to oxygen for *Salmonella* in the intestinal lumen, contributing to the niche protection (73–75). In a mouse study, the transplantation of facultative anaerobic commensals including *E. coli*, *Streptococcus danieliae*, and *Staphylococcus xylosus* to a defined microbial community increased colonization resistance against *Salmonella enterica serovar* Typhimurium infection (60). In addition, colonizing germ-free mice with cecal contents of neonatal and adult mice demonstrated that the neonatal microbiota is unable to mediate colonization resistance against *S.* Typhimurium and *Citrobacter rodentium* due to the lack of Clostridiales in neonatal microbiota (55). In the same study, reducing the oxygen concentration in the intestine by succinate administration enhanced the colonization by Clostridia belonging to the cluster IV and XIVa, and concomitantly reduced *S.* Typhimurium load in the intestine (55). The result indicated that the consumption of oxygen by aerobic and facultative anaerobic bacteria, such as *Enterobacteriaceae*, in the intestine not only limits the availability of oxygen to enteric pathogens but also enhances the colonization of Clostridia to confer colonization resistance. Remarkably, it has been suggested that the order and timing of colonization determine the ecological niche of microbes colonizing the gut, therefore, the acquisition of both spore-forming bacteria such as Clostridia and commensal *Enterobacteriaceae* early in life is important to establish the colonization resistance against enteric pathogens (60, 76).

1.3.2. Lipopolysaccharides (LPS) structure and characteristics in *Enterobacteriaceae*

1.3.2.1. LPS structure

LPS is a major constituent of the outer leaflet of the outer membrane in Gram-negative bacteria that is made up of three elements: lipid A, core oligosaccharide and O-antigen (77). The structure of lipid A is highly conserved and consists of a bisphosphorylated disaccharide of glucosamine typically with four to seven acyl chains (77). The core oligosaccharide can be built up to 15 sugar residues and can be further divided into the inner core region and outer core region. The O-antigen structure consists of repeating units of usually no more than five sugar units, which can only be found in smooth type LPS as the presence of the O-antigenic polysaccharide leads to a smooth appearance to the colony on agar plates. On the other hand, the absence of the O-antigenic polysaccharide resulted in a rough aspect of the colony, defining the LPS type as "rough" (78). Lipid A is anchored in the bacterial outer membrane and the core oligosaccharide links the O-antigen, which extends from the bacterial cell to the external environment, to the lipid A structure (77). LPS protects Gram-negative bacteria from environmental stress factors and also plays an important role in interacting with the host immune system as one of the pathogen-associated molecular patterns (77).

LPS structure varies among bacterial species which is linked to the functional diversity of the molecule. LPS structure of *E. coli* and *S.* Typhimurium as model microorganisms have been thoroughly studied. The inner region of the core oligosaccharide in *E. coli* is more conserved among *Enterobacteriaceae* species which is composed of 3-deoxy-α-D-manno-oct-ulosonic acid (Kdo) and one or more L-glycero-α-D-manno-

heptopyranose (Hep), and phosphate residues (79, 80). The outer region of the core oligosaccharide structure contains wide variations in sugar residues, indicating a critical role of the conserved inner region in maintaining the stability of bacterial outer membrane (80, 81). The presence of O-antigen varies among *E. coli* strains whereas the lipid A and Kdo are considered to be the minimal LPS structure that is essential for growth (80, 82).

1.3.2.2. LPS activity impacts host innate immune response

The role of LPS in host-microbe interactions has been investigated in pathogenic bacteria such as *Helicobacter pylori*, *Salmonella*, and enterohemorrhagic *E. coli* (83–85). LPS is one of the key factors for these pathogens to establish colonization and persistence in the ecological niche; however, our knowledge about LPS from commensal microorganisms and its interaction with the host immune system remains limited. Toll-like 4 receptor (TLR4), as a member of pattern recognition receptors family, recognizes LPS as reflected by the hyporesponsive phenotype to LPS in $TLR4^{-/-}$ mice (86). The recognition of LPS triggers the activation of TLR4/myeloid differentiation factor (MD)-2 mediated pro-inflammatory signaling cascade (87). Independently of TLR4 activation, the intracellular sensing of LPS triggers cytosolic caspase activation by the non-canonical inflammasome as evidenced by responses in macrophages (88, 89). These pathways play an essential role in maintaining intestinal homeostasis as sensing LPS molecules from symbiotic and pathobiontic bacteria is important for a balanced immune system (77). Although the structure and function of LPS from different commensal bacteria are yet to be described, LPS derived from certain commensal bacteria has been associated with host immunity.

A study investigating the microbiome development from birth until three years in infants from Estonia, Finland, and Russian showed that the *Bacteroides* species enriched in

Finnish and Estonian infants produced a distinct form of LPS in structure and function compared with LPS from *E. coli* dominating the Russian infant microbiome (90). *E. coli* derived LPS, which contains the hexa-acylated lipid A structure, exerted a pro-inflammatory response in human PBMCs whereas LPS produced from *B. dorei* that harbored tetra- and penta-acylated lipid A structures inhibited the immune-stimulatory effects. It was hypothesized that the presence of *B. dorei* may prevent the establishment of protective immune tolerance by *E. coli* LPS in early life (90). Monocolonzing germ-free interleukin (IL)-$2^{-/-}$ mice with non-pathogenic *E. coli* strains resulted in colitis with higher levels of Kupffer cell induction than that in *B. vulgatus*-colonized mice, indicating the differences in LPS activity between these two species (91). Additional differences have been shown in LPS structure produced by *E. coli* and *Bacteroides* such as the absence of heptose in the core oligosaccharide structure of *Bacteroides fragilis* LPS and the lack of O-antigen in *B. thetaiotaomicron* LPS (92, 93). These findings suggested a potential mechanism linking gut microbiota-derived LPS and the susceptibility to immune-related diseases with respect to the immune education by microbial ligands.

Indeed, the immune education by commensal bacterial derived LPS is a critical process for the adaptation of the fetal and newborn (94). The expression of TLR4/MD-2 and LPS-mediated signaling pathways in the intestinal epithelial cells (IECs) of fetal, newborn, and adult mice demonstrated that the susceptibility of IECs to LPS, the major microbial stimulus for postnatal epithelial activation, was lost after birth. The hypo-responsive feature provides the epithelial tolerance to microbial ligands to support the subsequent colonization by the gut microbiota (94). As the predominant Gram-negative bacteria colonizing the GIT of

neonates, *Enterobacteriaceae* is important in educating gut epithelial cells to become hypo-responsive to microbial ligands during microbiome development.

Differences in immunogenic properties between LPS from *Bacteroides* species and *E. coli* have also been reported in the context of the mature gut microbiome. In patients with coronary artery disease, the abundance of *Bacteroides vulgatus* and *Bacteroides dorei* was significantly reduced compared to healthy controls, and supplementations of these two live bacteria in a mouse model led to an anti-inflammatory effect with a decreased level of fecal LPS and a strengthened gut barrier (95). The authors suggested that *Bacteroides* strains might have a direct impact on intestinal LPS synthesis and the associated TLR-dependent signaling (95). In contrast, an increase in the abundance of *Enterobacteriaceae* was accompanied by elevated LPS production by the gut microbiota (96).

1.3.2.3. *Enterobacteriaceae* and LPS in obesity and T2D

In a healthy intestine, luminal LPS does not alter intestinal epithelial barrier function, however, LPS in the interstitial fluid, even at a relatively low level, resulted in an increase in intestinal permeability through TLR4 signaling transduction pathway (97–99). Therefore, the paracellular permeation of LPS induced by multiple factors such as physiological stresses leads to increased intestinal permeability (98). The altered intestinal permeability has been correlated with microbial translocation and systemic endotoxemia which are involved in the onset and progression of diseases such as inflammatory bowel disease (IBD), obesity and metabolic syndromes, and non-alcoholic steatohepatitis (NASH) (100, 101).

In the development of obesity and metabolic syndromes, *Enterobacteriaceae*, in particular *E. coli*, has been identified as one of the microbial biomarkers enriched in obese and T2D patients (102, 103). LPS levels were also significantly higher in T2D patients than

that in healthy controls (104). In obese individuals, plasma levels of LPS were found to be significantly elevated compared with healthy controls, which were reduced after bariatric surgery (105). In animal models, the HFD diet has been shown to promote the endotoxemia (106). The chronic infusion of LPS in the context of control-diet feeding induced obese and diabetic phenotypes similar, to some extent, to HFD feeding in mice through a cluster of differentiation 14 (CD14)-dependent mechanism (106). LPS levels in plasma and cecal contents were reduced by antibiotic treatment in both HFD-fed and ob/ob mice, which was correlated with reduced glucose intolerance and systemic inflammation (107). These results indicated the correlation between *Enterobacteriaceae* enrichment, LPS, and the pathogenesis of obesity and T2D, however, mechanisms have not been fully elucidated due to the complex and multifactorial nature of the diseases.

It has been suggested that a high energy diet tends to elevate plasma LPS and dietary fat was more efficient in transporting bacterial LPS from the intestinal lumen into the bloodstream (108). A study comparing the fecal microbiota from children consuming a modern western diet and a rural diet indicated that dietary fiber depletion may favor the establishment of *Enterobacteriaceae*, such as *Escherichia* and *Shigella* (109), which might increase the chance of LPS translocation in children served the western diet. Recently, a study using a mouse model of obesity and T2D demonstrated that hyperglycemia, rather than obesity or leptin signaling, is a direct and specific cause for the intestinal barrier dysfunction and the susceptibility to enteric infection (110). During hyperglycemia, the metabolic function of epithelial cells undergoes a glucose-mediated reprogramming through glucose transporter GLUT2, leading to barrier dysfunction and subsequent microbial translocation to the systemic circulation (110). In addition, in dextran sodium sulfate (DSS)-treated mice with

impaired gut barrier function, exogenous LPS purified from *E. coli* significantly induced glucagon-like peptide-1 (GLP-1) secretion in the plasma, highlighting the role of the enteroendocrine L cell in protecting gut barrier function and nutrient metabolism (53). Therefore, the development of obesity and metabolic syndrome is a process involving the physiological change of intestinal barrier function, gut commensal microbiota as the reservoir of microbial molecules, and the microbial translocation to the systemic circulation.

Enterobacteriaceae species are able to thrive in an inflamed gut environment through a variety of mechanisms (111–113). With LPS that is well-known to be involved in the initiation and propagation of intestinal inflammation, commensal *E.coli* may contribute to the inflammation and dysbiosis through an enhanced LPS translocation upon intestinal barrier damage. However, mechanistic studies are still needed to demonstrate the causality of the impaired intestinal barrier function under different physiologic, metabolic, and immunological conditions. Variations in host-microbe interactions between bacterial species need to be further validated due to the specific structure in individual microbe as exemplified by the diverse activity of LPS.

1.4. The genus *Parasutterella*

Parasutterella, a genus of Betaproteobacteria, has been recognized as a common bacterial constituent of the human gut microbiota (114, 115). Having been discovered for approximately ten years, the relative abundance of *Parasutterella* has been observed to have a correlative relationship with different health outcomes. However, beyond simple associations between the abundance change and host phenotype, our understanding of the biology and functionalities of *Parasutterella* remains limited. This section focuses particularly on the

biological features of *Parasutterella* and its relationship with host health outcomes that can help advance future research.

1.4.1. Ecology of the genus *Parasutterella*

The genus *Parasutterella* was first described in 2009 when the type strain *Parasutterella excrementihominis* YIT 11859 was successfully isolated from the human gut. The isolated strain was most closely phylogenetically related to the genus *Sutterella,* which was placed within the family *Alcaligenaceae*. However, *P. excrementihominis* YIT 11859 formed a separate cluster and represented a novel species of a new genus (116). In 2011, the type strain *Parasutterella secunda* YIT 12071 was isolated from human feces, and the distinct phylogenetic positions, as well as biological characteristics, of the genera *Parasutterella* and *Sutterella* were confirmed when comparing to other members in the family *Alcaligenaceae* (117). Therefore, the novel family *Sutterellaceae* was created to accommodate these two genera, with the genus *Parasutterella* containing two species, *P. excrementihominis* and *P. secunda* (118).

Parasutterella has been identified as a common inhabitant of the human and animal gut (115, 118, 119). Based on reported 16S ribosomal RNA (rRNA) gene sequences available in the Ribosomal Database Project (RDP), members of the genus *Parasutterella* have been found in humans, mice, rats, dogs, pigs, chickens, turkeys, and calves (Figure 1.3). In humans, as a member of the healthy fecal core microbiome, *Parasutterella* has a unique phylogenetic classification (115) as it stands out as one of the most frequently reported taxa within the class Betaproteobacteria in the gut, and is largely represented by a single species, *P. excrementihominis*. The 16S rRNA gene sequence similarity indicates that the mouse isolate *Parasutterella* mc1 is most closely related to *P. excrementihominis* (56), which is

consistent with the phylogenetic position of the uncultured bacteria sequenced from mouse intestine and deposited in the RDP. Interestingly, among all host-specific lineages, the uncultured bacterium sequenced from the ileum and cecum of broiler chickens displayed the highest similarity to the *P. excrementihominis* type strain isolated from human feces (120). The host adaptation of gut bacterial species has indicated the joint evolution of gut commensal microbes and vertebrate hosts, as exemplified by host-specific lineages of *Lactobacillus reuteri*. Specifically, poultry isolates and human strains of *L. reuteri* share an evolutionary history with chickens as both strains performed well in colonizing the chicken gut (121). Similar to *L. reuteri*, *Parasutterella* has diversified into host-specific lineages which can be used as a model organism to study evolutionary mechanisms of a vertebrate gut symbiont.

1.4.2. Genomic and biological characteristics of *Parasutterella*

1.4.2.1. Isolation and culture condition

The type strain *P. excrementihominis* YIT 11859 and *P. secunda* YIT 12071 were isolated from human feces on anaerobe basal agar (pH = 6.0) and on Gifu anaerobic agar (GAM) supplemented with oxacillin (4 μg/mL), respectively (116, 117). We were able to isolate *Parasutterella* from human and mouse feces using the selective media including GAM (pH = 6.0) and GAM supplemented with 4 μg/mL oxacillin (56). Both human and mouse isolates can be grown on the fastidious anaerobic agar (FAA); however, with a significantly reduced bacterial colony size, indicating that GAM is more suitable for cultivation of *Parasutterella* strains. Cells of *Parasutterella* are Gram-negative, obligately anaerobic cocci to coccobacilli. The biochemical characteristics of *Parasutterella* are largely unreactive and asaccharolytic, which is consistent with the absence of genes for transporting and

metabolizing exogenous sugars (56, 118). Although the growth in broth culture is weak and the end product of metabolism is limited, *Parasutterella* is a succinate-producing bacterium as reflected by a significant succinate production in broth culture of human, mouse, and rat isolates (56). In addition, mouse models have shown positive correlations between *Parasutterella* abundance and fecal succinate levels (56, 122).

1.4.2.2. *Parasutterella* uses amino acids as energy sources

Currently, there are four complete genomes of *Parasutterella* strains deposited at the Genbank database. The basic genomic features for strains of the genus *Parasutterella* including our mouse isolate *Parasutterella* mc1 are listed in Table 1.2. Incorporating the genome analysis into biochemical experiments provides us a strong tool to understand the metabolic characteristics of gut microbes. Based on the capacity of catabolizing amino acids as well as corresponding genes in the genome, the major substrates for *Parasutterella* to survive in the gut are likely to be amino acids. We have shown that asparagine is the most rapid and preferable amino acid metabolized by *Parasutterella* mc1 in the context of complex medium (56). In congruence, the genome of *Parasutterella* mc1 contains genes encoding L-asparaginase, aspartate ammonia-lyase, and a putative aspartate dehydrogenase, indicating that asparagine and its initial product aspartate are the key amino acids for fumarate formation in *Parasutterella*. Previous studies have identified the type I and type II L-asparaginase in *Escherichia coli,* and *Parasutterella* genome contains both types of L-asparaginase genes, validating the ability of the species to metabolize asparagine (123, 124). When rats were fed with diets containing milk casein, soy protein or fish meal, *P. excrementihominis* was only detected in the cecum of the fish meal group (125). The significantly higher percentages of total free asparagine in the fish meal (2.09 ± 0.08%) than

that in milk product casein (0.21 ± 0.01%) as well as in plant products such as soybean meal (0.21 ± 0.01%) may contribute to the successful detection of *P. excrementihominis* (126). In contrast to dietary aspartate which is mostly catabolized in the small intestine, nearly all of the dietary asparagine is absorbed into the portal circulation for protein synthesis in the whole body with less than 1% of asparagine metabolized in the small intestine (127–129). However, the mucin produced by goblet cells may contain asparagine in the peptide which can potentially be a nutrient source for *Parasutterella* (130). In addition, *Parasutterella* has the genomic capacity to utilize serine, an amino acid enriched in mucin peptide, with pyruvate, ammonia and other amino acids as products. Therefore, the preferential catabolism of these non-essential amino acids for the host may indicate the adaptation of *Parasutterella* to the gut environment.

1.4.2.3. Electron acceptors in *Parasutterella*

Fumarate, one of the products from asparagine metabolism, is likely to perform as an electron acceptor in *Parasutterella* for proton translocation, which is evidenced by the presence of fumarate reductase in genome sequences. In facultative anaerobic bacteria such as *E. coli* and *Campylobacter jejuni*, succinate dehydrogenase (expressed under aerobic condition) and fumarate reductase (expressed under anaerobic condition) catalyze the interconversion of fumarate and succinate (131, 132). The gene encoding succinate dehydrogenase is absent in the genome of *Parasutterella*, indicating the anaerobic respiration of this strict anaerobe in the gut. It has been reported in *C. jejuni* that the aspartase plays a very important role in providing fumarate for anaerobic respiration when oxygen is severely limited, which is a potential survival mechanism for *C. jejuni* in the mammalian and avian gut

(132). *Parasutterella* may adopt a similar survival approach with *C. jejuni* due to the preferable utilization of asparagine and its metabolized product, aspartate.

In addition to fumarate as the electron acceptor, nitrate is an anaerobic electron acceptor that could support the colonization of *Parasutterella* in the GIT based on the presence of nitrate reductases genes and the positive nitrate reduction activity (133). However, the intestinal environment contains limited nitrate, therefore, fumarate may be the more important anaerobic electron acceptor for the established populations of *Parasutterella* in the intestine (134). The colonic luminal fumarate has been positively correlated with the relative abundance of *Parasutterella* spp in a mouse model (135). In *E. coli,* fumarate respiration provides a more significant colonization advantage than nitrate respiration for long-term persistence in the GIT (134). Therefore, the ability to respire both fumarate and nitrate may contribute to the initial colonization of *Parasutterella* and the maintenance of the competitive advantage in the gut. In bacterial fumarate and nitrate respiration, the quinone pool is the link between respiratory dehydrogenases and terminal reductases for electron transport (134, 136). Predominantly, the electron flow to fumarate and nitrate is via menaquinone (MQ)-6 and methylmenaquinone (MMK)-6 in *P. excrementihominis* and via MQ-5 and MMK-5 in *P. secunda* (116, 117). These anaerobic quinones together support the colonization of *Parasutterella* using the most energy-efficient respiratory electron acceptors in the intestine, suggesting that *Parasutterella* has specialized to allow for the occupation of the intestinal niche.

1.4.2.4. Heme biosynthesis

Recently, a novel member of the family *Sutterellaceae*, *Mesosutterella multiformis* JCM 32464^{T}, was isolated from human feces (133). The strain is phylogenetically located

between the genera *Parasutterella* and *Sutterella*, which shares the same major respiratory quinones with *P. excrementihominis* (137). This new species was predicted to process a heme biosynthesis pathway to generate energy as evidenced by the presence of the protoporphyrinogen IX dehydrogenase (*hemG*) gene. The authors proposed that *M. multiformis* JCM 32464^T is able to utilize fumarate reductase, nitrate reductase, and F-type ATPase along with HemG and MQ to generate ATP under anaerobic conditions (137). In contrast, the genome of *Parasutterella* shows all heme biosynthetic genes (*hemA*, *hemL*, *hemB*, *hemC*, *hemE*, *hemN*, and *hemH*) except for *hemD* and *hemG* genes, indicating a different metabolic pathway for synthesizing heme or intermediates in the genus *Parasutterella*.

1.4.2.5. CRISPR-Cas system

CRISPR refers to a family of DNA repeats found in genomes of various archaea and bacteria. CRISPR, in combination with Cas proteins, forms the CRISPR-Cas system which provides acquired immunity against foreign genetic elements (138). CRISPR-Cas immunity proceeds in three steps: first (the adaptation phase), a part of an invading genetic element is incorporated as a new spacer within the CRISPR array and the infection is thereby memorized; second (the expression phase), the array is transcribed as a precursor CRISPR RNA (pre-crRNA) molecule which is processed to generate short mature crRNAs; and third (the interference phase), crRNAs direct other Cas proteins to cleave newly invading nucleic acids (139). The systems have been classified into type I, II, III, which are further divided into several subtypes based on the nature of *cas* genes and the organization of the operon (139). The types I and III share similar mechanisms whereas the type II CRISPR-Cas system has evolved distinct features regarding the processing of pre-crRNA and the interference step.

The type II group is the rarest bacterial CRISPR-Cas system, which is absent in archaea, with an over-representation among commensals and pathogens. The subtype II-B system is notably narrow in its distribution which is presented only in several genera including *Francisella*, *Parasutterella*, *Sutterella*, *Legionella*, *Wolinella*, and *Leptospira* (139). Most of these genera are host-associated bacteria and the unique system in *Sutterella* and *Parasutterella* may attract interest for understanding the evolutionary processes of these phylogenetic groups.

1.4.2.6. Central metabolic pathways

Two alternative pathways have been reported in *E. coli* for gluconeogenesis to generate phosphoenolpyruvate (PEP), including the decarboxylation of oxaloacetate by PEP carboxykinase (PckA) and the alternative decarboxylation of malate to pyruvate by the malic enzyme (MaeB). The pyruvate generated from malate decarboxylation is further converted into PEP by PEP synthase (PPsA) (140, 141). *Parasutterella* genome contains all the enzymes involved in the gluconeogenic pathways including PcKA, MaeB, and PPsA, indicating the capability of synthesizing carbohydrate intermediates. On the other hand, *Parasutterella* possesses an incomplete glycolytic pathway as the genome lacks the key enzymes phosphofructokinase, phosphoglycerate mutase, and pyruvate kinase, consistent with the asaccharolytic characteristics of the genus *Parasutterella*.

The TCA cycle in *Parasutterella* species is incomplete, owing to the absence of citrate synthase, aconitase, and isocitrate dehydrogenase. The likely arrangement of TCA cycle reactions in *Parasutterella* is shown in Figure 1.4. Due to limited experimental evidence for biochemistry validation of enzymes expressed by *Parasutterella*, the summary of individual enzymes participating in the TCA cycle listed below are mainly based on the presence of enzyme-encoding genes.

1.4.2.6.1. Pyruvate:flavodoxin oxidoreductase

The generation of acetyl-Coenzyme A (acetyl-CoA) from the oxidative decarboxylation of pyruvate is necessary for reactions in the TCA cycle, fatty acids synthesis and the other metabolic process. Aerobic bacteria and mammalian system decarboxylate pyruvate to generate acetyl-CoA by pyruvate dehydrogenase multienzyme complex (142). In *E. coli*, the decarboxylation reaction is catalyzed by pyruvate dehydrogenase during aerobic growth and by pyruvate formate-lyase during anaerobic growth; however, the participation of the third enzyme, pyruvate:ferredoxin oxidoreductase (POR) in this reaction is limited (143). In contrast, the decarboxylation of pyruvate in anaerobic microorganisms is commonly carried out by POR, a single enzyme-containing Fe-S clusters and thiamine pyrophosphate as necessary cofactors (144). With the presence of pyruvate and CoA, POR catalyzes the reduction of flavodoxin (ferredoxin) to generate CO_2 and acetyl-CoA. POR also has catalytic proficiency for the reverse reaction to synthesize pyruvate from acetyl-CoA with ferredoxin as an electron carrier (145). *Parasutterella* converts pyruvate to acetyl-CoA by POR as reflected by the POR gene in the genome while neither pyruvate dehydrogenase nor formate-lyase gene is found.

1.4.2.6.2. Citrate synthase, aconitase, and isocitrate dehydrogenase

In the complete TCA cycle, the first step generating citrate and CoA from acetyl-CoA and oxaloacetate is carried out by citrate synthase. The next step in this oxidative branch of the TCA cycle is catalyzed by aconitase to generate isocitrate from citrate. The following step is to decarboxylate isocitrate to generate 2-oxoglutarate and CO_2 by isocitrate dehydrogenase. *Parasutterella* exhibited a non-cyclic TCA cycle lacking citrate synthase, aconitase, and isocitrate dehydrogenase. Citrate synthase is absent in *Clostridium sporosphaeroides* and

some human pathogens such as *Streptococcus pyogenes*; however, citrate lyase is expressed instead to process the conversion of citrate to oxaloacetate in these microorganisms (146, 147). Both citrate synthase and citrate lyase genes are not present in the genome of *Parasutterella*. It is likely that *Parasutterella* is incapable of utilizing citrate converted from acetyl-CoA to generate 2-oxoglutarate.

Integrating detailed functional characterization and genomic analysis is necessary to validate enzymes in the TCA cycle (148). For example, when aligning the protein sequence of an *E. coli* aconitase against the *Haemophilus influenzae* genome, which has no annotated aconitase gene, the alignment detects an unrelated gene, 3-isopropylmalate dehydratase (3-IPMD). It is likely due to the close relationship between the aconitase and 3-IPMD enzyme families that leads to the difficulties in accurate annotation, indicating limitations in predicting functions using genomic analysis approach (148). Interestingly, enzymes involved in the oxidative branch of the TCA cycle have been found in members of *Sutterella*. The genome of *Sutterella wadsworthensis* contains citrate lyase and the genome of *Sutterella sp.* CAG:397 has citrate synthase, aconitase as well as isocitrate dehydrogenase annotated. There is no significant similarity found when aligning the citrate synthase or citrate lyase sequences of *Sutterella* species against *Parasutterella* genome. The aconitase and isocitrate dehydrogenase protein sequences of *Sutterella* sp. CAG:397 share 28% (query coverage, 44%) and 32% identity (query coverage, 71%) with 3-IPMD enzyme of *P. excrementihominis*, respectively. Therefore, functional assay with experimental evidence is required to further confirm the metabolic pathway of the TCA cycle in *Parasutterella*.

It is not surprising to find the incomplete TCA cycle in microorganisms, especially in anaerobes; however, the capability of generating 2-oxoglutarate, oxaloacetate, and succinyl-

CoA from pyruvate is normally retained in bacteria with an incomplete TCA cycle. For instance, lactobacilli exhibit a non-cyclic and branched TCA cycle with the absence of isocitrate, 2-oxoglutarate, and succinate dehydrogenases, but demonstrate the activities of citrate lyase, malate dehydrogenase, and fumarase, suggesting the retained ability to reductively synthesize succinate (149). During anaerobic growth, with the repressed activity of 2-oxoglutarate dehydrogenase complex, the TCA cycle in *E. coli* serves in a branched, non-cyclic pathway including an oxidative branch to produce 2-oxoglutarate and a reductive branch to generate succinate (150). A human pathogen, *Chlamydia trachomatis* utilizes an inner-membrane transmembrane transporter, dicarboxylate transporter orthologue, to transport 2-oxoglutarate into the cytoplasm after diffusion through the outer membrane to initiate the incomplete TCA cycle, which lacks citrate synthase, aconitase, and isocitrate dehydrogenase (151). Understanding the metabolic fate of 2-oxoglutarate, one of the key intermediates in the TCA cycle, will increase our knowledge of the mechanism by which *Parasutterella* survive as a core anaerobe in the gut microbiota.

1.4.2.6.3. Metabolism of 2-oxoglutarate

Although it appears that the oxidative branch of the conventional TCA cycle in *Parasutterella* is incomplete, the pathway of oxidative decarboxylating 2-oxoglutarate to produce succinyl-CoA and CO_2 is present and is carried out by a 2-oxoglutarate dehydrogenase multi-enzyme complex. The enzyme complex contains multiple copies of three different types of subunits: a 2-oxoglutarate dehydrogenase with thiamin pyrophosphate as an essential co-factor (E1), dihydrolipoamide acyltransferase (E2) and FAD-containing dihydrolipoamide dehydrogenase (E3) (152). The E2 component forms a core structure of the enzyme complexes which binds multiple copies of the peripheral E1 and E3 subunits and

provides attachment sites for lipoic acid as a cofactor(153, 154). The E2 component also catalyzes the reaction to form the acyl-CoA product (155). The genome of *Parasutterella* contains genes encoding all three components of 2-oxoglutarate dehydrogenase multi-enzyme complex, indicating the capability of interconverting 2-oxoglutarate to succinyl-CoA. Interestingly, it has been well recognized that the pyruvate dehydrogenase multienzyme complex and 2-oxoglutarate dehydrogenase multienzyme complex share a high similarity in structural and functional properties, and they are responsible for producing acyl-CoA products from glycolysis and TCA cycle, respectively. The genome of *Parasutterella* shows an absence of pyruvate dehydrogenase multienzyme complex and a presence of 2-oxoglutarate dehydrogenase multienzyme complex, suggesting a unique feature of the TCA cycle in the genus *Parasutterella*.

1.4.2.6.4. Interconversion of succinyl-CoA and succinate

The conversion of succinyl-CoA to succinate and CoA, under the concomitant generation of a nucleotide triphosphate (NTP), is carried out by succinate-CoA synthetase (succinate-CoA ligase), which is the only enzyme in the TCA cycle to carry out a substrate-level phosphorylation reaction. The enzyme can also catalyze the reverse reaction that forms succinyl-CoA from succinate (156). Succinate-CoA synthetases consist of two subunits: the α subunit containing a histidine residue, which is transiently phosphorylated during catalysis, and the β subunit providing the nucleotide-binding site (157, 158). Eukaryotes generate GTP and ATP by succinate-CoA synthetases during the phosphorylation of succinyl-CoA (159). *E. coli* succinate-CoA synthetase hydrolyzes succinyl-CoA to form ATP, CoA, and succinate; however, during anaerobic growth, the enzyme plays an important role in providing succinyl-CoA from the reverse reaction (160). *Parasutterella* has succinate-CoA synthetases to

catalyze the interconversion of succinyl-CoA and succinate with the preference of ADP/ATP. Although it appears that the TCA cycle in *Parasutterella* consists of a reductive branch with succinate as the end metabolite owing to the accumulation of succinate in broth culture, the direction of the reaction catalyzed by succinate-CoA synthetases in this strict anaerobic bacterium remains to be validated by biochemical experiments.

1.4.2.6.5. Fumarate reductase

Succinate dehydrogenase and fumarate reductase catalyze the interconversion of fumarate and succinate in *E. coli* under aerobic and anaerobic conditions, respectively (131). *Parasutterella* lacks succinate dehydrogenase, whereas shows the presence of a fumarate reductase. The fumarate reductase contains multiple subunits, including an iron-sulfur subunit, a flavoprotein catalytic subunit, and one or two hydrophobic transmembrane subunits (161). The genome of *Parasutterella* contains genes encoding fumarate reductase with *frdA* gene encodes the flavoprotein subunit, the *frdB* gene encodes the iron-sulfur protein subunit, and a predicted gene for transmembrane subunits. In mouse models, fumarate reductase plays a crucial role in supporting the colonization of the stomach by *Helicobacter pylori*, which is likely due to the high availability of fumarate to the microbe in the colonization niche (162, 163). Hence, fumarate reductase may play an active role in the physiology and colonization of *Parasutterella* in the gut.

1.4.2.6.6. Fumarase and malate dehydrogenase

The reversible hydration of fumarate to L-malate is catalyzed by fumarase, and the gene encoding fumarate hydratase is present in *Parasutterella* genomes. Three fumarase genes have been isolated from *E. coli*, including *fumA*, *fumB*, and *fumC*, and these genes show different catalyzing activity under aerobic and anaerobic conditions (164). In *H. polyri*,

the fumC enzyme has been identified which functions preferentially in the direction of forming fumarate from L-malate (165). The form of fumarase in *Parasutterella* and its function during the colonization requires future validations.

Malate dehydrogenase catalyzes the reversible oxidation of malate to oxaloacetate with the concomitant reduction of NAD. In *E. coli*, malate dehydrogenase is required under both aerobic and anaerobic growth conditions, and the electron acceptors, as well as carbon substrates, are important determinants in regulating malate dehydrogenase expression (166). *Campylobacter* strains display different malate dehydrogenase patterns grown under aerobic and anaerobic conditions, indicating the diverse activity of the enzyme (167). The genome of *Parasutterella* contains a malate dehydrogenase gene and the direction of the reaction catalyzed by the enzyme remains to be determined.

In summary, the genus *Parasutterella* has an incomplete TCA cycle which operates in a reductive branched pathway. It lacks genes encoding citrate synthase, aconitase, and isocitrate dehydrogenase. Instead, the genus *Parasutterella* contains the 2-oxoglutarate dehydrogenase multi-enzyme complex, succinate-CoA synthetase, fumarase, and malate dehydrogenase. The incomplete TCA cycle reflects the fumarate respiration approach used by *Parasutterella* to maintain redox and energy balance.

1.4.3. The genus *Parasutterella* and health outcomes

As a common inhabitant of human and various animal GIT, *Parasutterella* has been correlated with beneficial and deleterious health outcomes. Changes in the relative abundance of *Parasutterella* have been observed in multiple studies in the context of dietary treatment, antibiotic administration, and different pathological conditions. The summary below focuses

on the potential role of *Parasutterella* in host physiology and discusses possible manipulation strategies of this commensal bacterium.

1.4.3.1. Colonization of the GIT by *Parasutterella*

In mouse models and human studies, *Parasutterella* has been detected in the luminal content as well as in the mucosa of cecum and colon (168–170). Human and mouse *Parasutterella* isolates have limited capabilities of mono-colonizing germ-free mouse intestine, reaching counts from 4 to 5 log CFUs/g feces (unpublished data). However, in SPF mice, *Parasutterella* rapidly and stably colonized the mouse GIT with a single environmental exposure, representing an average of 9.31 ± 0.16 log10 16S rRNA gene copies per gram of feces (56). The differences in intestinal environments between germ-free mice and SPF mice may contribute to *Parasutterella* colonization capabilities, whereas the success to colonize the mature mouse gut after a single exposure indicate that *Parasutterella* fills an ecological niche in the GIT.

1.4.3.2. *Parasutterella* as one of the early colonizers in the gut

Parasutterella has been observed to be transmitted between mother and vaginally born infants, and the relative abundance gradually increases during the first 12 months of age, indicating *Parasutterella* as one of the early colonizers in the newborn gut (171). Interestingly, the sequence of *Parasutterella* spp was presented in the colostrum of Italian mothers, which was collected within 3 days postpartum. In contrast, the species was not detected in the colostrum of Burundian mothers; however, it became one of the main bacterial species in Burundian mature milk collected at 1 month of life (172). As a succinate producing bacterium, *Parasutterella* may promote the colonization of strict anaerobes in the gut through an indirect mechanism which boosts oxygen consumption by aerobic or facultative anaerobic

bacteria (55). Limiting oxygen in the intestine significantly reduced *S.* Typhimurium load, indicating that *Parasutterella* may therefore play a role in microbiome development and infection resistance against enteric pathogens in early life (61).

1.4.3.3. *Parasutterella* and secretory IgA

Secretory IgA produced at mucosal surfaces is critical in mediating intestinal immunity by binding to specific resident microbes, dietary components, and luminal antigens (173, 174). Pathogen-specific IgA is high-affinity and T-cell dependent, whereas the commensal-induced IgA is characterized largely by low affinity and specificity that are shared by multiple bacterial species (173). As there are only certain bacterial species in the gut are highly coated with IgA, the previous study has revealed that the high-IgA coating selectively marks inflammatory and potentially disease-driving commensals in mice and humans (173). However, bacteria that are coated by IgA are not always colitogenic, instead, they can help improve the barrier function such as *Akkermansia muciniphila* and *Clostridium scindens* (175). The phylum Proteobacteria in the human intestine is likely to be coated by IgA, and members from *Sutterellaceae*, including *Parasutterella* and *Sutterella*, are commonly retrieved from the IgA-coated bacterial fractions (176, 177). Interestingly, specific microbes could induce an IgA-low phenotype in mice which led to an enhanced DSS sensitivity and increased intestinal damage compared to IgA-high mice. *Sutterella* species was identified as one of the IgA-low-inducing microbes and these microbes were able to degrade a peptide that protects dimeric IgA from degradation by bacterial proteases, known as secretory component (178). There is no evidence showing the ability of *Parasutterella* to degrade the secretory component. Overall, the exact role of the secretory IgA-coated commensals in gut immunity is still unclear; however, as a crucial physical barrier, IgA plays

an important role in maintaining the symbiotic relationship between the host and gut microorganisms.

1.4.3.4. The genus *Parasutterella* impacts bile acid metabolism

Bile acids promote the absorption of dietary lipids and lipid-soluble nutrients in the intestine, and also play a role as important endocrine signaling molecules impacting host physiology (13). *Parasutterella* species grow in broth with the presence of bile acids and they have been correlated with bile acid metabolism in multiple studies (116, 117). In an *in vitro* culture study, a reduced rate of deconjugating taurocholic acid, a major primary bile acid, was observed in donors with a greater abundance of *Parasutterella* and *Akkermansia* (179). However, the *in vitro* model system has potential limitations which exclude the significant differences in absorption rate between conjugated and deconjugated bile acids by enterocytes, and eliminates the effect of host signaling cascades, including the enterohepatic FXR/Fgf15 axis, on bile acid metabolism (180). Therefore, the positive correlations between the deconjugation rate and the abundance of *Parasutterella* need further investigation by incorporating host factors which significantly impact bile acid synthesis and turnover. In a NASH-hepatocellular carcinoma (HCC) mouse model, the relative abundance of *Parasutterella* was negatively correlated with TCDCA and TLCA levels in the liver, and in feces it was inversely correlated with DCA and LCA (181). *Parasutterella* has also been positively associated with fecal β-MCA and 7-ketoDCA in a study using a humanized microbiota mouse model (182). In addition, human studies focusing on fecal microbiota transplantation (FMT) in *Clostridium difficile* infection patients or alcoholic hepatitis patients consistently demonstrated the correlation of *Parasutterella* with bile acid metabolism (183, 184). In line with these results, our trackable mouse model, which added *Parasutterella* mc1

to a complex gut microbial community, showed that the colonization of *Parasutterella* strain altered the bile acid metabolism in the intestine (56). Consistent with changes in bile acid profiling, the gene expression of ileal bile aid transporters and genes involved in the FXR signaling pathway were significantly altered by *Parasutterella* colonization (56). However, there remains a paucity of information regarding the ability of *Parasutterella* to utilize bile acids, which requires future work focusing on the mechanism driving altered bile acid metabolism by *Parasutterella* colonization.

1.4.3.5. *Parasutterella* in obesity and metabolic syndromes

Multiple studies have reported changes in the relative abundance of *Parasutterella* in the development of obesity and metabolic syndrome. A human study, which recruited 57 obese human subjects and 54 non-obese control subjects, showed that obese patients exhibited the hypothalamic inflammation and gliosis, and the inflammation was significantly inversely correlated with the relative abundance of *P. excrementihominis* and unclassified *Marinilabiliaceae* (185). In animal models, however, inconsistent alterations of *Parasutterella* abundance in the pathogenesis of obesity and metabolic syndromes have been demonstrated. Male Sprague-Dawley rats with hypertriglyceridemia induced by HFD showed an elevated abundance of fecal *Parasutterella* compared to that in the control rats (186). A safflower oil based high fat/high sucrose diet treatment significantly decreased the relative abundance of *Parasutterella* in the cecum and colon in C57BL/6 male mice, which coincided with the initiation of the inflammation in liver and insulin resistance (187). In another study, C57BL/6 male mice received HFD exhibited impaired glucose tolerance with an increase in fecal *Desulfovibrionaceae* and a reduction of *Parasutterella* within the phylum Proteobacteria compared with the chow-diet fed group (188). In addition, comparisons between C57BL/6

male mice fed a HFD that became diabetic or were diabetes-resistant, the genus *Parasutterella* remained unchanged between groups, suggesting that *Parasutterella* responds to diet rather than the diabetic phenotype (189). Interestingly, male Wistar rats received berberine and metformin, which are two clinically effective drugs for treating obesity and T2D, both showed enrichment of fecal *Parasutterella* (190). However, the underlying mechanism of these two drugs in stimulating certain microbial populations including *Parasutterella* remains unclear, which could involve the calorie restriction effect as a result of reduced food intake or involve the microbial cross-feeding by increasing short-chain fatty acid-producing bacteria (190). Furthermore, prediabetic subjects showed altered gut microbial genera including a reduction in *Parasutterella* compared with healthy subjects (191). These studies demonstrate a relationship between *Parasutterella* and obesity as well as metabolic syndromes; however, the causal role of changes in *Parasutterella* needs further investigation. Our previous study has shown that *Parasutterella* colonization alters bile acid metabolism, which could impact lipid and glucose homeostasis in obesity and diabetes. Therefore, the genus *Parasutterella* may contribute to health improvement strategies for obesity and metabolic syndromes (56).

1.4.3.6. *Parasutterella* and liver health

The genus *Parasutterella* has been linked to liver injury in multiple studies. An imbalanced gut microbiota induced by alcohol consumption could contribute to liver injury, and it has been reported that chronic alcohol administration in male C57BL/6 mice for 6 weeks resulted in a significant reduction of fecal *Parasutterella* (192, 193). In a human study, *Parasutterella* represented 5.76% of total microbiota in an alcoholic patient without alcoholic hepatitis, and represented 0.001% in the alcoholic patient with severe alcoholic hepatitis. The

liver injury phenotype in the patients was transmissible to germ-free mice and the authors speculated that *Parasutterella* may play a role in protecting the liver in the progression of hepatitis (184). In addition, fecal *Parasutterella* was significantly reduced in a NASH-HCC mouse model, suggesting a potential role of *Parasutterella* in the progression of liver injury and carcinogenesis (181). The reduction of *Parasutterella* with the pathogenesis of hepatocellular carcinoma has also been reported in the human study as the *Parasutterella* population was significantly decreased in patients who developed hepatocellular carcinoma regardless of hepatitis virus infection compared to the healthy controls (194). From the study, *Parasutterella* was negatively correlated with clinical hepatic function indexes including the alanine aminotransferase and aspartate aminotransferase (AST) levels in the blood which are indicators of hepatocyte injury (194). In healthy infants, the negative correlation between hepatic AST levels and the genera *Parasutterella* and *Enterococcus* has been reported; however, the variations in ages and delivery patterns of the infants recruited in the study may strongly impact the establishment of the gut microbiota, thereby potentially contributing to the observed results (195). Therefore, it will be worthwhile to investigate the mechanisms by which *Parasutterella* could potentially exert protective effects on liver health, specifically on the aspect of liver injury.

1.4.3.7. *Parasutterella* in IBD and gastrointestinal disorders

In Crohn's disease patients, certain genera including *Parasutterella* were enriched within submucosa tissues of the terminal ileum, indicating these bacteria are capable of penetrating mucosal barriers (196). Alterations in *Parasutterella* populations have been reported in DSS-induced colitis mouse models; however, confounding factors in the treatments such as a strong dietary effect led to difficulties to address the role of

Parasutterella in the pathogenesis of colitis (197). It remains unclear whether the changed population of *Parasutterella* caused the inflammation or the bacterial genus has a better ability to thrive in an inflamed environment. The same situation applies to the altered relative abundance of *Parasutterella* in irritable bowel syndrome (IBS) patients and a functional gastrointestinal disorders (FGID) study (198, 199). The pathogenesis mechanism of FGID hasn't been clearly characterized due to multiple factors contributing to the central nerve system (CNS) alteration. *Parasutterella*, among 15 genera that were differentially expressed, was significantly increased in IBS patients compared to that in healthy controls. The inflammatory phenotype was transmitted to germ-free mice through FMT and six genera including *Parasutterella* were associated with the IBS phenotype (198). As a common inhabitant in human and mouse gut, it is not surprising that *Parasutterella* was able to colonize the germ-free mouse intestine by FMT; however, the increased abundance of *Parasutterella* in IBS patients and IBS mice were not sufficient to demonstrate the causal relationship between the bacterial genus and IBS development. Further studies are needed to better characterize the role of *Parasutterella* in inflammation and gut physiology.

1.4.3.8. *Parasutterella* and *C. difficile* infection (CDI)

Although the abundance of Proteobacteria was dramatically increased by *C. difficile* infection, the genus *Parasutterella* was significantly lower in CDI patients and asymptomatic carriers than that in healthy controls (200). In addition, in a randomized clinical trial of FMT in CDI patients, subjects who were cured after receiving FMT using autologous fecal microbiota had increased relative abundance of *Parasutterella*. The author hypothesized that *Parasutterella* may be active in bile acid metabolism (183). Contradictorily, the presence of *Parasutterella* has been associated with the moribund phenotype in a humanized microbiota

mouse model challenged with *C. difficile*. However, the antibiotic cocktail administration followed by clindamycin injection as the pretreatment in the study may exert a strong impact on the microbial composition, which weakens the correlation between specific taxonomies and the progression of CDI (201). Another study which compared the microbiota in CDI patients prior to and after FMT showed a decreased abundance of *Parasutterella* post-transplant. However, differing from the autologous fecal microbiota, there was a potential variability in microbiota among different donors based on the transplant approach, which resulted in limited ability to interpret the causality of altered *Parasutterella* population post-transplant and its relationship with the disease status in CDI patients (202). CDI has been strongly associated with restorage of secondary bile acids, therefore, *Parasutterella* could contribute to the CDI treatment by actively impacting bile acid profiling.

1.4.3.9. The genus *Parasutterella* in aging

A strong decrease in the relative abundance of *Parasutterella* has been reported in the fecal microbiota of aged rats compared to that in young rats (203). Consistently, in an aging C57BL/6J mouse model, the relative abundance of *Parasutterella* was significantly decreased during aging, which was positively correlated with fumarate and negatively correlated with methanol in the colonic luminal content (135). Calorie restriction attenuated age-related declines in the relative abundance of bacterial genera including *Parasutterella* (204). In the same study, *Parasutterella* was negatively correlated with immune-related genes in the colon, including *Cybb* and *Cxcl13*, and also inversely correlated with the levels of identified bile acids such as a CDCA derivate in the colonic luminal content (204). The authors proposed that caloric restriction in aging mice prevented an imbalanced colonic microbial ecosystem, which consequently diminished the exposure to certain microbial-derived components such as

secondary bile acids and LPS, and hence prevented the chronic colonic inflammation (204). In another aging mouse model focusing on influenza responses, serum chemokine, CXCL10, was negatively correlated with the relative abundance of *Parasutterella*, indicating the involvement of *Parasutterella* and other gut microbes in antiviral immune responses (205). Taken together, the genus *Parasutterella* has been reported as one of the aging indicators and has been correlated with various metabolites. However, on the basis of limited evidence with few human studies, our understanding of the role of gut microbes and the metabolites in aging is still rather limited. Further insight into the mechanisms underlying the complex aging process regarding microbial factors is required.

1.4.3.10. The genus *Parasutterella* in neurological and neuropsychiatric diseases

Recent discoveries have suggested that alterations in host-microbe interactions may contribute to the physiological function of the CNS, demonstrating that the gut microbiota not only impacts host metabolism, but also regulate immunity and even mediate brain functions (206). However, the studies investigating gut microbes in neurological and neuropsychiatric diseases are still in their infancy. The proposed mechanism through which the gut microbiota impact the brain function and behavior include the modulation of the immune system, the stimulation of neuroendocrine signaling pathways, and the direct activation of neurons (207, 208). Exploring which components of the microbiome are mediating the effects on the gut-brain axis will contribute to the maintenance of brain health.

Changes in the relative abundance of *Parasutterella* have been reported in a variety of CNS disorders including autism spectrum disorder, depression, and Parkinson's disease. The evidence from experimental and clinical studies are summarized in Table 1.3. However, these findings did not demonstrate the causal relationship between changes in gut microbes,

including *Parasutterella*, and the disease phenotype. Future research, with an emphasis on the role of gut microbes as a causal factor in CNS disorders, will help to develop strategies to maintain the homeostasis of CNS, extending current research focused on simple associations.

1.4.4. Manipulation of the *Parasutterella* population

1.4.4.1. Host factors impact *Parasutterella* population

Host-related factors, such as genetics and immune homeostasis, have a large impact on microbiome composition (209). Multiple models, in particular mouse models, with different genetic determinants have shown alterations in *Parasutterella* abundance. For example, the knockout of the *Fut2* gene in mice, which encodes an α-1,2-fucosyltransferase responsible for the expression of ABO bold group antigens in mucus and other secretions, significantly increased the relative abundance of genera including *Parasutterella* in feces, indicating the availability of fucosylated glycans in the gut could shape the microbial community (210, 211). In humans, approximately 20% of individuals who are homozygous for this "non-secretor" allele are unable to express antigens on mucosal surfaces, which could alter the gut microbial composition and its functionalities (210). Another host factor impacting *Parasutterella* relative abundance are hepatic circadian-related genes. Conditionally knocking out the circadian transcription factor, neuronal PAS domain protein 2 (*Npas2*), in the liver of mice led to a significantly lower percentage of body weight loss compared to wild-type mice in the setting of restricted feeding. *Parasutterella* were positively correlated with the weight loss in the knock-out mice but showed opposing correlations in the wild-type mice, indicating the effects of hepatic circadian gene expression on the gut microbiota (212).

In addition to host genetic variations, bile acids are an important host factor shaping gut microbial communities due to their antimicrobial activity. Conversely, alterations of gut microbial composition can influence host bile acid metabolism. In mice, knockout of the gene *Klb*, which encodes a type I membrane protein mediating both FGF15 and FGF21 signaling pathways, resulted in a phenotype with hepatic inflammation and initiation of fibrosis, which is associated with a high level of secondary bile acids in the serum and liver (213). The shift in bile acid composition induced remodeling of the gut microbiota in the knock-out mice featured by a significant increase in the genera *Parasutterella* and *Desulfovibrio*, highlighting the high tolerance to bile acid of these bacteria (213).

A recent study showed that proteolytic digestion of Paneth-cell human defensin 5 (HD-5) led to the generation of novel antimicrobial fragments which altered the proportion of certain bacteria in mouse fecal microbiota without affecting the overall community structure (214). More specifically, the relative abundance of the genera *Bacteroides* and *Lactobacillus* were decreased whereas *Parasutterella* and *Akkermansia* sp. were increased compared with nontreated mice, indicating that *Parasutterella* may be less susceptible to HD-5 (214). Furthermore, the functional mucosal barrier is a key component in modulating intestinal mucosal immune responses, which may lead to changes in the gut microbiome (215). Knocking out the intestinal brush border electroneutral Na^+/H^+ exchange (NHE) in mice led to spontaneous distal chronic colitis and altered gut microbial composition including an increase in *Parasutterella* abundance (216). In agreement with the changed abundance of *Parasutterella* in the inflammation as discussed previously, the ability of the genus to survive in the inflamed gut may partially be attributed to the changes in colonocyte metabolism featured by the increased availability of nitrate in the gut lumen as a by-product of colitis

(217). It is to be noted that *Parasutterella* responded inconsistently to different anti-inflammatory drugs such as 5-aminosalicylic acid and nonsteroidal anti-inflammatory drugs, indicating the response to interventions is context-dependent due to the complexity of the diseases (218, 219). Taken together, to manipulate *Parasutterella* population with respect to incorporating host-associated factors, it is necessary to demonstrate the direct causal relationship between changes in *Parasutterella* populations and specific physiologic, metabolic, and immunologic phenotypes of the host.

1.4.4.2. Antibiotic impacts on the *Parasutterella* population

The summary of the impact of antibiotic treatment on *Parasutterella* in human studies and animal models is shown in Table 1.4. The genus *Parasutterella* is susceptible to certain antibiotics belonging to fluoroquinolones, macrolides, and phenicol, whereas it has shown resistance to rifamycins and the common antibiotic cocktails used in mouse models. The susceptibility of *Parasutterella* to fluoroquinolones has been verified by the protective effects on the genus exerted by DAV132, a powerful nonspecific adsorbent reducing fecal antibiotic concentration, in moxifloxacin treated volunteers (220). Interestingly, *Parasutterella* has displayed resistance to the antibiotic cocktail including ampicillin, however, the genus was susceptible to another β-lactam, amoxicillin (221). The differences in the efficacy of these two β-lactam antibiotics may be attributed to the dosage (oral gavage vs. drinking water) or to variations in the resistance mechanisms of *Parasutterella* that remain to be elucidated.

In addition, *Parasutterella* seemed to survive and persist in the gut after streptomycin treatment which disrupted the gut microbiota by largely decreasing the proportion of Firmicutes. However, the presence of the quorum-sensing signal molecule (the autoinducer 2, AI-2)-producing bacteria promoted gut colonization by microbial taxa including members in

the Firmicutes and *Parasutterella*, suggesting that the microbial group behavior could also shape the gut microbiome after antibiotic treatment (222).

1.4.4.3. Effect of dietary components on *Parasutterella* population

It has been reported in human studies that dietary composition may drive changes in *Parasutterella* abundance. The genera *Parasutterella* and *Marinilabiliaceae* have been negatively correlated with hypothalamus inflammation in humans. A follow-up food frequency questionnaire was applied to investigate whether the dietary macronutrient intake had an influence on the abundance of these two bacterial genera. *P. excrementihominis* was inversely associated with dietary fat intake, not the total energy, carbohydrate, or protein intake, in obese patients (77). Specifically, *P. excrementihominis* showed negative correlations with dietary glycerin and lipoids as well as long-chain fatty acids, although the associations need further confirmation in experimental studies (77). Another human trial investigating the influence of exercise types and athlete diet patterns on the gut microbiota showed that the relative abundance of fecal *Bifidobacterium* and *Parasutterella* were the lowest in bodybuilders compared with that in healthy controls and distance runners. The dietary pattern in bodybuilders which is featured by high protein, high fat, low carbohydrate, and low dietary fiber may contribute to the change in the level of *Parasutterella* (223).

In animal models, the fecal microbiota of C57BL/6J mice that received lowly-digestible starch diet was enriched with certain genera including *Parasutterella* compared with that in the highly-digestible starch diet mice. *Parasutterella* and *Bacteroides* were significantly correlated with *in vivo* H_2 production as a reflection of carbohydrate digestibility (224). The cross-feeding interactions may contribute to the enriched *Parasutterella* due to its asaccharolytic characteristics. A study conducted in C57BL/6J mice, which were fed a

methionine–choline-deficient diet with or without sodium butyrate supplementation, indicated that butyrate markedly promoted the abundance of *Parasutterella* and *Akkermensia* in feces (225). Consistent with the idea that butyrate promotes *Parasutterella*, HFD feeding in male C57BL/6J mice reduced the relative abundance of *Parasutterella* in feces compared with the control mice, however, supplementation of sodium butyrate reversed the reduction in *Parasutterella* (226). In-feed supplementation of a butyrate-producing strain, *Butyricicoccus pullicaecorum*, to broilers significantly increased the abundance of specified genera such as *Parabacteroides* and *Parasutterella* in the ileum and cecum compared to that in the control group (227). In addition, *Parasutterella* was more abundant in feces of mice supplemented with prebiotics including galacto-oligosaccharide and oligofructose in the diet compared with the control mice (228–230). Male Wistar rats received a diet containing laminaran for 2 weeks harbored *Parabacteroides, Lachnospiraceae*, and *Parasutterella* which were not present in rats given alginate or basal diet, indicating a potential role of the highly fermentable polysaccharide in modulating *Parasutterella* abundance in the gut (231). Collectively, the cross-feeding interactions, particularly regarding the availability of butyrate, may support the survival of *Parasutterella* in the GIT but requires further validation.

In vitro fermentation studies have demonstrated modulatory effects of certain dietary components on *Parasutterella*. A study investigating how the microbial composition of fecal donor impacts fermentation properties of dietary fiber showed that *Parasutterella* decreased during the fermentation process independently of supplemented fiber type (232). Certain genera including *Parasutterella* exhibited positive correlations with ammonia production (232). In another *in vitro* model of the proximal colon, lactulose significantly stimulated the

growth of *Parasutterella* (233). These findings from the *in vitro* models provide potential strategies to manipulate the *Parasutterella* population in the GIT.

Other dietary components have also been reported to have a modulating effect on *Parasutterella* abundance. For example, administration of fructose and glucose in juvenile male Sprague-Dawley rats through the entire juvenile and adolescent period significantly elevated *Bacteroides*, *Alistipes*, *Lactobacillus*, *Clostridium sensu stricto*, *Bifidobacteriaceae*, and *Parasutterella* abundance in feces, suggesting that early-life sugar consumption impacts the gut microbiota independently of obese parameters and caloric intake in the rodent model (234). In another study, mice treated with HFD for 12 weeks showed an increased relative abundance of *Parasutterella* in colonic content compared to mice that received standard chow diet, and the increase was further promoted by krill oil supplementation (235). In addition, vitamin A-deficient diet significantly decreased the abundance of *Anaerotruncus*, *Oscillibacter*, *Lachnospiraceae_NK4A136_*group*, and Mucispirillum*, whereas increased the abundance of *Parasutterella* in colon samples, suggesting the role of vitamin A in modulating the intestinal mucosa-associated microbes (169). The dietary copper level has also displayed an inhibitory effect on fecal *Parasutterella* abundance (236). Collectively, the mechanism of modulating the gut microbiota by these dietary components is commonly multifactorial and remains unclear. Future studies are necessary in order to reveal the underlying mechanism of microbial changes by specified dietary ingredients, and therefore to provide strategies to maintain the beneficial host-microbe interactions.

To conclude, the genus *Parasutterella*, as a core member of the gut microbiota, has evolved unique genomic and biological features to adapt to the intestinal niche. The association between the *Parasutterella* population and host health outcomes, including

beneficial and deleterious, suggests a potential approach to provide health benefits on the host by manipulating the gut microbiota.

1.5. Hypotheses and Objectives

This thesis aimed to establish an effective model system to investigate the causal relationship between changes in microbial population and host physiology with following hypotheses and objectives.

1.5.1 Hypotheses

1.5.1.1 The presence of gut commensal *E. coli* impacts immune activation resulting from antibiotic perturbation.

1.5.1.2. *E. coli* contributes to the pathogenesis of obesity and metabolic syndrome.

1.5.1.3. *Parasutterella* plays a unique role in shaping the intestinal metabolite profile resulting in altered host physiology.

1.5.1.4. *Parasutterella* species are host-adapted.

1.5.2 Objectives

1.5.2.1. To establish a mouse model system to investigate the biological and physiological features of model microorganisms, *E. coli* and *Parasutterella*

1.5.2.2. To investigate the impact of commensal *E. coli* colonization on host immune responses in the context of metronidazole treatment (Chapter 2)

1.5.2.3. To explore the role of *E. coli* in the development of obesity and insulin resistance (Chapter 3)

1.5.2.4. To characterize the biology and lifestyle of *Parasutterella* and its interactions with the host (Chapter 4 and 5)

1.6. References

1. Round JL, Palm NW. 2018. Causal effects of the microbiota on immune-mediated diseases. Sci Immunol 3:eaao1603.
2. Fischbach MA. 2018. Microbiome: focus on causation and mechanism. Cell 174:785–790.
3. Abraham C, Medzhitov R. 2011. Interactions between the host innate immune system and microbes in inflammatory bowel disease. Gastroenterology 140:1729–1737.
4. Surana NK, Kasper DL. 2017. Moving beyond microbiome-wide associations to causal microbe identification. Nature 552:244–247.
5. Postler TS, Ghosh S. 2017. Understanding the holobiont: how microbial metabolites affect human health and shape the immune system. Cell Metab 26:110–130.
6. Chiang JYL. 2009. Bile acids: regulation of synthesis. J Lipid Res 50:1955–1966.
7. Russell DW. 2003. The enzymes, regulation, and genetics of bile acid synthesis. Annu Rev Biochem 72:137–174.
8. Hofmann AF, Mysels KJ. 1992. Bile acid solubility and precipitation *in vitro* and *in vivo*: the role of conjugation, pH, and Ca_2^+ ions. J Lipid Res 33:617–626.
9. Macdonald IA, Bokkenheuser VD, Winter J, McLernon AM, Mosbach EH. 1983. Degradation of steroids in the human gut. J Lipid Res 24:675–700.
10. Dawson PA. 2011. Role of the intestinal bile acid transporters in bile acid and drug disposition. Handb Exp Pharmacol 201:169–203.
11. Midtvedt T. 1974. Microbial bile acid transformation. Am J Clin Nutr 27:1341–1347.
12. Ridlon JM, Kang D-J, Hylemon PB. 2006. Bile salt biotransformations by human intestinal bacteria. J Lipid Res 47:241–259.
13. Wahlström A, Sayin SI, Marschall HU, Bäckhed F. 2016. Intestinal crosstalk between bile acids and microbiota and its impact on host metabolism. Cell Metab 24:41–50.
14. Floch MH. 2002. Bile salts, intestinal microflora and enterohepatic circulation. Dig Liver Dis 34:S54–57.
15. Jones B V, Begley M, Hill C, Gahan CGM, Marchesi JR. 2008. Functional and comparative metagenomic analysis of bile salt hydrolase activity in the human gut microbiome. Proc Natl Acad Sci 105:13580–13585.

16. O'Flaherty S, Briner Crawley A, Theriot CM, Barrangou R. 2018. The *Lactobacillus* bile salt hydrolase repertoire reveals niche-specific adaptation. mSphere 3:e00140–18.
17. Vrieze A, Out C, Fuentes S, Jonker L, Reuling I, Kootte RS, Van Nood E, Holleman F, Knaapen M, Romijn JA, Soeters MR, Blaak EE, Dallinga-Thie GM, Reijnders D, Ackermans MT, Serlie MJ, Knop FK, Holst JJ, Van Der Ley C, Kema IP, Zoetendal EG, De Vos WM, Hoekstra JBL, Stroes ES, Groen AK, Nieuwdorp M. 2014. Impact of oral vancomycin on gut microbiota, bile acid metabolism, and insulin sensitivity. J Hepatol 60:824–831.
18. Nieuwdorp M, Gilijamse PW, Pai N, Kaplan LM. 2014. Role of the microbiome in energy regulation and metabolism. Gastroenterology 146:1525–1533.
19. Kerr TA, Saeki S, Schneider M, Schaefer K, Berdy S, Redder T, Shan B, Russell DW, Schwarz M. 2002. Loss of nuclear receptor SHP impairs but does not eliminate negative feedback regulation of bile acid synthesis. Dev Cell 2:713–720.
20. Wang L, Lee YK, Bundman D, Han Y, Thevananther S, Kim CS, Chua SS, Wei P, Heyman RA, Karin M, Moore DD. 2002. Redundant pathways for negative feedback regulation of bile acid production. Dev Cell 2:721–731.
21. Lefebvre P, Cariou B, Lien F, Kuipers F, Staels B. 2009. Role of bile acids and bile acid receptors in metabolic regulation. Physiol Rev 89:147–191.
22. Prawitt J, Abdelkarim M, Stroeve JHM, Popescu I, Duez H, Velagapudi VR, Dumont J, Bouchaert E, Van Dijk TH, Lucas A, Dorchies E, Daoudi M, Lestavel S, Gonzalez FJ, Oresic M, Cariou B, Kuipers F, Caron S, Staels B. 2011. Farnesoid X receptor deficiency improves glucose homeostasis in mouse models of obesity. Diabetes 60:1861–1871.
23. Ma K, Saha PK, Chan L, Moore DD. 2006. Farnesoid X receptor is essential for normal glucose homeostasis. J Clin Invest 116:1102–1109.
24. Staels B, Handelsman Y, Fonseca V. 2010. Bile acid sequestrants for lipid and glucose control. Curr Diab Rep 10:70–77.
25. Thomas C, Gioiello A, Noriega L, Strehle A, Oury J, Rizzo G, Macchiarulo A, Yamamoto H, Mataki C, Pruzanski M, Pellicciari R, Auwerx J, Schoonjans K. 2009. TGR5-mediated bile acid sensing controls glucose homeostasis. Cell Metab 10:167–177.

26. Katsuma S, Hirasawa A, Tsujimoto G. 2005. Bile acids promote glucagon-like peptide-1 secretion through TGR5 in a murine enteroendocrine cell line STC-1. Biochem Biophys Res Commun 329:386–390.
27. Pols TWH, Auwerx J, Schoonjans K. 2010. Targeting the TGR5-GLP-1 pathway to combat type 2 diabetes and non-alcoholic fatty liver disease. Gastroentérologie Clin Biol 34:270–273.
28. Watanabe M, Houten SM, Mataki C, Christoffolete MA, Kim BW, Sato H, Messaddeq N, Harney JW, Ezaki O, Kodama T, Schoonjans K, Bianco AC, Auwerx J. 2006. Bile acids induce energy expenditure by promoting intracellular thyroid hormone activation. Nature 439:484–489.
29. Yoneno K, Hisamatsu T, Shimamura K, Kamada N, Ichikawa R, Kitazume MT, Mori M, Uo M, Namikawa Y, Matsuoka K, Sato T, Koganei K, Sugita A, Kanai T, Hibi T. 2013. TGR5 signalling inhibits the production of pro-inflammatory cytokines by in vitro differentiated inflammatory and intestinal macrophages in Crohn's disease. Immunology 139:19–29.
30. Joice R, Yasuda K, Shafquat A, Morgan XC, Huttenhower C. 2014. Determining microbial products and identifying molecular targets in the human microbiome. Cell Metab 20:731–741.
31. Venema K, Van Den Abbeele P. 2013. Experimental models of the gut microbiome. Best Pract Res Clin Gastroenterol 27:115–126.
32. Part VI. 2015. In vitro fermentation models: General introduction. p 175. In: Verhoeckx K, Cotter P, López-Expósito I, Kleiveland C, Lea T, Mackie A, Requena, T., Swiatecka, D., Wichers, H. (ed), The impact of food bioactives on health: *in vitro* and *ex vivo* models. Springer.
33. Rumney CJ, Rowland IR. 1992. *In vivo* and *in vitro* models of the human colonic flora. Crit Rev Food Sci Nutr 31:299–331.
34. Bermudez-Brito M, Plaza-Díaz J, Fontana L, Muñoz-Quezada S, Gil A. 2013. *In vitro* cell and tissue models for studying host–microbe interactions: a review. Br J Nutr 109:S27–S34.

35. Haller D, Bode C, Hammes WP, Pfeifer AM, Schiffrin EJ, Blum S. 2000. Non-pathogenic bacteria elicit a differential cytokine response by intestinal epithelial cell/leucocyte co-cultures. Gut 47:79–87.
36. Kim HJ, Huh D, Hamilton G, Ingber DE. 2012. Human gut-on-a-chip inhabited by microbial flora that experiences intestinal peristalsis-like motions and flow. Lab Chip 12:2165–2174.
37. Marzorati M, Vanhoecke B, De Ryck T, Sadaghian Sadabad M, Pinheiro I, Possemiers S, Van Den Abbeele P, Derycke L, Bracke M, Pieters J, Hennebel T, Harmsen HJ, Verstraete W, Van De Wiele T. 2014. The HMITM module: a new tool to study the host-microbiota interaction in the human gastrointestinal tract *in vitro*. BMC Microbiol 14:133.
38. Shah P, Fritz J V., Glaab E, Desai MS, Greenhalgh K, Frachet A, Niegowska M, Estes M, Jäger C, Seguin-Devaux C, Zenhausern F, Wilmes P. 2016. A microfluidics-based *in vitro* model of the gastrointestinal human-microbe interface. Nat Commun 7:11535.
39. Pearce SC, Coia HG, Karl JP, Pantoja-Feliciano IG, Zachos NC, Racicot K. 2018. Intestinal *in vitro* and *ex vivo* models to study host-microbiome interactions and acute stressors. Front Physiol 9:1584.
40. Sun EW, De Fontgalland D, Rabbitt P, Hollington P, Sposato L, Due SL, Wattchow DA, Rayner CK, Deane AM, Young RL, Keating DJ. 2017. Mechanisms controlling glucose-induced GLP-1 secretion in human small intestine. Diabetes 66:2144–2149.
41. Leushacke M, Barker N. 2014. *Ex vivo* culture of the intestinal epithelium: Strategies and applications. Gut 63:1345–1354.
42. Yissachar N, Zhou Y, Ung L, Lai NY, Mohan JF, Ehrlicher A, Weitz DA, Kasper DL, Chiu IM, Mathis D, Benoist C. 2017. An intestinal organ culture system uncovers a role for the nervous system in microbe-immune crosstalk. Cell 168:1135–1148.
43. Lacroix C, de Wouters T, Chassard C. 2015. Integrated multi-scale strategies to investigate nutritional compounds and their effect on the gut microbiota. Curr Opin Biotechnol 32:149–155.
44. Fritz J V., Desai MS, Shah P, Schneider JG, Wilmes P. 2013. From meta-omics to causality: experimental models for human microbiome research. Microbiome 1:14.

45. Kararli TT. 1995. Comparison of the gastrointestinal anatomy, physiology, and biochemistry of humans and commonly used laboratory animals. Biopharm Drug Dispos 16:351–380.
46. Hugenholtz F, de Vos WM. 2018. Mouse models for human intestinal microbiota research: a critical evaluation. Cell Mol Life Sci 75:149–160.
47. Treuting PM, Dintzis SM. 2012. 12-Lower gastrointestinal tract. p 212–228. In: Treuting PM, Dintzis SM, Liggitt D, Frevert CW, (ed), Comparative anatomy and histology, 1st ed. Academic Press.
48. Ericsson AC, Davis JW, Spollen W, Bivens N, Givan S, Hagan CE, McIntosh M, Franklin CL. 2015. Effects of vendor and genetic background on the composition of the fecal microbiota of inbred mice. PLoS One 10:e0116704.
49. Ley RE, Backhed F, Turnbaugh P, Lozupone CA, Knight RD, Gordon JI. 2005. Obesity alters gut microbial ecology. Proc Natl Acad Sci 102:11070–11075.
50. Nguyen TLA, Vieira-Silva S, Liston A, Raes J. 2015. How informative is the mouse for human gut microbiota research? Dis Model Mech 8:1–16.
51. Rosshart SP, Vassallo BG, Angeletti D, Hutchinson DS, Morgan AP, Takeda K, Hickman HD, McCulloch JA, Badger JH, Ajami NJ, Trinchieri G, Pardo-Manuel de Villena F, Yewdell JW, Rehermann B. 2017. Wild mouse gut microbiota promotes host fitness and improves disease resistance. Cell 171:1015–1028.
52. Kennedy EA, King KY, Baldridge MT. 2018. Mouse microbiota models: comparing germ-free mice and antibiotics treatment as tools for modifying gut bacteria. Front Physiol 9:1534.
53. Morgun A, Dzutsev A, Dong X, Greer RL, Sexton DJ, Ravel J, Schuster M, Hsiao W, Matzinger P, Shulzhenko N. 2015. Uncovering effects of antibiotics on the host and microbiota using transkingdom gene networks. Gut 64:1732–1743.
54. Smith K, McCoy KD, Macpherson AJ. 2007. Use of axenic animals in studying the adaptation of mammals to their commensal intestinal microbiota. Semin Immunol 19:59–69.
55. Kim YG, Sakamoto K, Seo SU, Pickard JM, Gillilland MG, Pudlo NA, Hoostal M, Li X, Wang TD, Feehley T, Stefka AT, Schmidt TM, Martens EC, Fukuda S, Inohara N,

Nagler CR, Núñez G. 2017. Neonatal acquisition of Clostridia species protects against colonization by bacterial pathogens. Science 356:315–319.

56. Ju T, Kong JY, Stothard P, Willing BP. 2019. Defining the role of *Parasutterella*, a previously uncharacterized member of the core gut microbiota. ISME J 13:1520–1534.
57. Geva-Zatorsky N, Sefik E, Kua L, Pasman L, Tan TG, Ortiz-Lopez A, Yanortsang TB, Yang L, Jupp R, Mathis D, Benoist C, Kasper DL. 2017. Mining the human gut microbiota for immunomodulatory organisms. Cell 168:928–943.
58. Dewhirst FE, Chien CC, Paster BJ, Ericson RL, Orcutt RP, Schauer DB, Fox JG. 1999. Phylogeny of the defined murine microbiota: altered Schaedler flora. Appl Env Microbiol 65:3287–3292.
59. Biggs MB, Medlock GL, Moutinho TJ, Lees HJ, Swann JR, Kolling GL, Papin JA. 2017. Systems-level metabolism of the altered Schaedler flora, a complete gut microbiota. ISME J 11:426–438.
60. Brugiroux S, Beutler M, Pfann C, Garzetti D, Ruscheweyh HJ, Ring D, Diehl M, Herp S, Lötscher Y, Hussain S, Bunk B, Pukall R, Huson DH, Münch PC, McHardy AC, McCoy KD, MacPherson AJ, Loy A, Clavel T, Berry D, Stecher B. 2016. Genome-guided design of a defined mouse microbiota that confers colonization resistance against *Salmonella enterica* serovar Typhimurium. Nat Microbiol 2:16215.
61. Turnbaugh PJ, Ridaura VK, Faith JJ, Rey FE, Knight R, Gordon JI. 2009. The effect of diet on the human gut microbiome: a metagenomic analysis in humanized gnotobiotic mice. Sci Transl Med 1:6ra14.
62. Marcobal A, Kashyap PC, Nelson TA, Aronov PA, Donia MS, Spormann A, Fischbach MA, Sonnenburg JL. 2013. A metabolomic view of how the human gut microbiota impacts the host metabolome using humanized and gnotobiotic mice. ISME J 7:1933–1943.
63. Parte AC. 2014. LPSN-List of prokaryotic names with standing in nomenclature. Nucleic Acids Res 42:D613–D616.
64. Adeolu M, Alnajar S, Naushad S, Gupta RS. 2016. Genome-based phylogeny and taxonomy of the 'Enterobacteriales': Proposal for enterobacterales ord. nov. divided into the families *Enterobacteriaceae*, *Erwiniaceae* fam. nov., *Pectobacteriaceae* fam.

nov., *Yersiniaceae* fam. nov., *Hafniaceae* fam. nov., Morgane. Int J Syst Evol Microbiol 66:5575.

65. Kittana H, Gomes-Neto JC, Heck K, Geis AL, Segura Muñoz RR, Cody LA, Schmaltz RJ, Bindels LB, Sinha R, Hostetter JM, Benson AK, Ramer-Tait AE. 2018. Commensal *Escherichia coli* strains can promote intestinal inflammation via differential interleukin-6 production. Front Immunol 9:2318.
66. Nataro JP, Kaper BJ. 1998. Diarrheagenic *Escherichia coli*. Clin Microbiol Rev 11:142–201.
67. Fratamico PM, DebRoy C, Liu Y, Needleman DS, Baranzoni GM, Feng P. 2016. Advances in molecular serotyping and subtyping of *Escherichia coli*. Front Microbiol 7:644.
68. Clermont O, Christenson JK, Denamur E, Gordon DM. 2013. The Clermont *Escherichia coli* phylo-typing method revisited: improvement of specificity and detection of new phylo-groups. Environ Microbiol Rep 5:58–65.
69. Martinson JNV, Pinkham N V., Peters GW, Cho H, Heng J, Rauch M, Broadaway SC, Walk ST. 2019. Rethinking gut microbiome residency and the *Enterobacteriaceae* in healthy human adults. ISME J.
70. Milani C, Duranti S, Bottacini F, Casey E, Turroni F, Mahony J, Belzer C, Delgado Palacio S, Arboleya Montes S, Mancabelli L, Lugli GA, Rodriguez JM, Bode L, de Vos W, Gueimonde M, Margolles A, van Sinderen D, Ventura M. 2017. The first microbial colonizers of the human gut: composition, activities, and health implications of the infant gut microbiota. Microbiol Mol Biol Rev 81:e00036–17.
71. Palmer C, Bik EM, DiGiulio DB, Relman DA, Brown PO. 2007. Development of the human infant intestinal microbiota. PLoS Biol 5:e177.
72. Avershina E, Lundgård K, Sekelja M, Dotterud C, Storrø O, Øien T, Johnsen R, Rudi K. 2016. Transition from infant- to adult-like gut microbiota. Environ Microbiol 18:2226–2236.
73. Litvak Y, Mon KKZ, Nguyen H, Chanthavixay G, Liou M, Velazquez EM, Kutter L, Alcantara MA, Byndloss MX, Tiffany CR, Walker GT, Faber F, Zhu Y, Bronner DN, Byndloss AJ, Tsolis RM, Zhou H, Bäumler AJ. 2019. Commensal *Enterobacteriaceae*

protect against *Salmonella* colonization through oxygen competition. Cell Host Microbe 25:128–139.

74. Rivera-Chávez F, Zhang LF, Faber F, Lopez CA, Byndloss MX, Olsan EE, Xu G, Velazquez EM, Lebrilla CB, Winter SE, Bäumler AJ. 2016. Depletion of butyrate-producing Clostridia from the gut microbiota drives an aerobic luminal expansion of *Salmonella*. Cell Host Microbe 19:443–454.
75. Velazquez EM, Nguyen H, Heasley KT, Saechao CH, Gil LM, Rogers AWL, Miller BM, Rolston MR, Lopez CA, Litvak Y, Liou MJ, Faber F, Bronner DN, Tiffany CR, Byndloss MX, Byndloss AJ, Bäumler AJ. 2019. Endogenous *Enterobacteriaceae* underlie variation in susceptibility to *Salmonella* infection. Nat Microbiol 4:1057–1064.
76. Litvak Y, Bäumler AJ. 2019. The founder hypothesis: a basis for microbiota resistance, diversity in taxa carriage, and colonization resistance against pathogens. PLOS Pathog 15:e1007563.
77. Steimle A, Autenrieth IB, Frick JS. 2016. Structure and function: lipid A modifications in commensals and pathogens. Int J Med Microbiol 306:290–301.
78. Silipo A, Molinaro A. 2010. The diversity of the core oligosaccharide in lipopolysaccharides. Subcell Biochem 53:69–99.
79. Klein G, Müller-Loennies S, Lindner B, Kobylak N, Brade H, Raina S. 2013. Molecular and structural basis of inner core lipopolysaccharide alterations in *Escherichia coli*: incorporation of glucuronic acid and phosphoethanolamine in the heptose region. J Biol Chem 288:8111–8127.
80. Caroff M, Karibian D. 2003. Structure of bacterial lipopolysaccharides. Carbohydr Res 338:2431–2447.
81. Ebbensgaard A, Mordhorst H, Aarestrup FM, Hansen EB. 2018. The role of outer membrane proteins and lipopolysaccharides for the sensitivity of *Escherichia coli* to antimicrobial peptides. Front Microbiol 9:2153.
82. Frirdich E, Whitfield C. 2005. Lipopolysaccharide inner core oligosaccharide structure and outer membrane stability in human pathogens belonging to the *Enterobacteriaceae*. J Endotoxin Res 11:133–144.

83. Monteiro MA. 2001. Helicobacter pylori: A wolf in sheep's clothing: The glycotype families of *Helicobacter pylori* lipopolysaccharides expressing histo-blood groups: structure, biosynthesis, and role in pathogenesis. Adv Carbohydr Chem Biochem 57:99–158.
84. Hoare A, Bittner M, Carter J, Alvarez S, Zaldívar M, Bravo D, Valvano MA, Contreras I. 2006. The outer core lipopolysaccharide of *Salmonella enterica* serovar Typhi is required for bacterial entry into epithelial cells. Infect Immun 74:1555–1564.
85. Ståhl AL, Svensson M, Mörgelin M, Svanborg C, Tarr PI, Mooney JC, Watkins SL, Johnson R, Karpman D. 2006. Lipopolysaccharide from enterohemorrhagic *Escherichia coli* binds to platelets through TLR4 and CD62 and is detected on circulating platelets in patients with hemolytic uremic syndrome. Blood 108:167–176.
86. Hoshino K, Takeuchi O, Kawai T, Sanjo H, Ogawa T, Takeda Y, Takeda K, Akira S. 1999. Cutting edge: Toll-like receptor 4 (TLR4)-deficient mice are hyporesponsive to lipopolysaccharide: evidence for TLR4 as the Lps gene product. J Immunol 162:3749–3752.
87. Rosadini C V., Kagan JC. 2017. Early innate immune responses to bacterial LPS. Curr Opin Immunol 44:14–19.
88. Kayagaki N, Wong MT, Stowe IB, Ramani SR, Gonzalez LC, Akashi-Takamura S, Miyake K, Zhang J, Lee WP, Muszyński A, Forsberg LS, Carlson RW, Dixit VM. 2013. Noncanonical inflammasome activation by intracellular LPS independent of TLR4. Science 341:1246–1249.
89. Shi J, Zhao Y, Wang Y, Gao W, Ding J, Li P, Hu L, Shao F. 2014. Inflammatory caspases are innate immune receptors for intracellular LPS. Nature 514:187–192.
90. Vatanen T, Kostic AD, D'Hennezel E, Siljander H, Franzosa EA, Yassour M, Kolde R, Vlamakis H, Arthur TD, Hämäläinen AM, Peet A, Tillmann V, Uibo R, Mokurov S, Dorshakova N, Ilonen J, Virtanen SM, Szabo SJ, Porter JA, Lähdesmäki H, Huttenhower C, Gevers D, Cullen TW, Knip M, Xavier RJ. 2016. Variation in microbiome LPS immunogenicity contributes to autoimmunity in humans. Cell 165:1551.
91. Waidmann M, Bechtold O, Frick J-S, Lehr H-A, Schubert S, Dobrindt U, Loeffler J, Bohn E, Autenrieth IB. 2003. *Bacteroides vulgatus* protects against *Escherichia coli*-

induced colitis in gnotobiotic interleukin-2-deficient mice. Gastroenterology 125:162–177.

92. Kasper DL. 1976. Chemical and biological characterization of the lipopolysaccharide of *Bacteroides fragilis* subspecies fragilis. J INFECT DIS 134:59–66.

93. Jacobson AN, Choudhury BP, Fischbach MA. 2018. The biosynthesis of lipooligosaccharide from *Bacteroides thetaiotaomicron*. MBio 9:e02289–17.

94. Lotz M, Gütle D, Walther S, Ménard S, Bogdan C, Hornef MW. 2006. Postnatal acquisition of endotoxin tolerance in intestinal epithelial cells. J Exp Med 203:973–984.

95. Yoshida N, Emoto T, Yamashita T, Watanabe H, Hayashi T, Tabata T, Hoshi N, Hatano N, Ozawa G, Sasaki N, Mizoguchi T, Amin HZ, Hirota Y, Ogawa W, Yamada T, Hirata KI. 2018. *Bacteroides vulgatus* and *Bacteroides dorei* reduce gut microbial lipopolysaccharide production and inhibit atherosclerosis. Circulation 138:2486–2498.

96. Jang SE, Lim SM, Jeong JJ, Jang HM, Lee HJ, Han MJ, Kim DH. 2018. Gastrointestinal inflammation by gut microbiota disturbance induces memory impairment in mice. Mucosal Immunol 11:369–379.

97. Ge Y, Ezzell RM, Warren HS. 2002. Localization of endotoxin in the rat intestinal epithelium. J Infect Dis 182:873–881.

98. Guo S, Al-Sadi R, Said HM, Ma TY. 2013. Lipopolysaccharide causes an increase in intestinal tight junction permeability *in vitro* and *in vivo* by inducing enterocyte membrane expression and localization of TLR-4 and CD14. Am J Pathol 182:375–387.

99. Guo S, Nighot M, Al-Sadi R, Alhmoud T, Nighot P, Ma TY. 2015. Lipopolysaccharide regulation of intestinal tight junction permeability is mediated by TLR4 signal transduction pathway activation of FAK and MyD88. J Immunol 195:4999–5010.

100. Utzschneider KM, Kratz M, Damman CJ, Hullarg M. 2016. Mechanisms linking the gut microbiome and glucose metabolism. J Clin Endocrinol Metab 101:1445–1454.

101. Rojo ÓP, San Román AL, Arbizu EA, Martínez ADLH, Sevillano ER, Martínez AA. 2007. Serum lipopolysaccharide-binding protein in endotoxemic patients with inflammatory bowel disease. Inflamm Bowel Dis 13:269–277.

102. Santacruz A, Collado MC, García-Valdés L, Segura MT, Marítn-Lagos JA, Anjos T, Martí-Romero M, Lopez RM, Florido J, Campoy C, Sanz Y. 2010. Gut microbiota

composition is associated with body weight, weight gain and biochemical parameters in pregnant women. Br J Nutr 104:83–92.

103. Qin J, Li Y, Cai Z, Li S, Zhu J, Zhang F, Liang S, Zhang W, Guan Y, Shen D, Peng Y, Zhang D, Jie Z, Wu W, Qin Y, Xue W, Li J, Han L, Lu D, Wu P, Dai Y, Sun X, Li Z, Tang A, Zhong S, Li X, Chen W, Xu R, Wang M, Feng Q, Gong M, Yu J, Zhang Y, Zhang M, Hansen T, Sanchez G, Raes J, Falony G, Okuda S, Almeida M, LeChatelier E, Renault P, Pons N, Batto J-M, Zhang Z, Chen H, Yang R, Zheng W, Li S, Yang H, Wang J, Ehrlich SD, Nielsen R, Pedersen O, Kristiansen K, Wang J. 2012. A metagenome-wide association study of gut microbiota in type 2 diabetes. Nature 490:55–60.

104. Creely SJ, McTernan PG, Kusminski CM, Fisher FM, Da Silva NF, Khanolkar M, Evans M, Harte AL, Kumar S. 2006. Lipopolysaccharide activates an innate immune system response in human adipose tissue in obesity and type 2 diabetes. Am J Physiol Metab 292:E740–E747.

105. Trøseid M, Nestvold TK, Rudi K, Thoresen H, Nielsen EW, Lappegård KT. 2013. Plasma lipopolysaccharide is closely associated with glycemic control and abdominal obesity: evidence from bariatric surgery. Diabetes Care 36:3627–3632.

106. Cani PD, Amar J, Iglesias MA, Poggi M, Knauf C, Bastelica D, Neyrinck AM, Fava F, Tuohy KM, Chabo C, Waget A, Delmée E, Cousin B, Sulpice T, Chamontin B, Ferrières J, Tanti J-F, Gibson GR, Casteilla L, Delzenne NM, Alessi MC, Burcelin R. 2007. Metabolic endotoxemia initiates obesity and insulin resistance. Diabetes 56:1761–1772.

107. Cani PD, Bibiloni R, Knauf C, Waget A, Neyrinck AM, Delzenne NM, Burcelin R. 2008. Changes in gut microbiota control metabolic endotoxemia-induced inflammation in high-fat diet-induced obesity and diabetes in mice. Diabetes 57:1470–1481.

108. Amar J, Burcelin R, Ruidavets JB, Cani PD, Fauvel J, Alessi MC, Chamontin B, Ferriéres J. 2008. Energy intake is associated with endotoxemia in apparently healthy men. Am J Clin Nutr 87:1219–1223.

109. De Filippo C, Cavalieri D, Di Paola M, Ramazzotti M, Poullet JB, Massart S, Collini S, Pieraccini G, Lionetti P. 2010. Impact of diet in shaping gut microbiota revealed by

a comparative study in children from Europe and rural Africa. Proc Natl Acad Sci 107:14691–14696.

110. Thaiss CA, Levy M, Grosheva I, Zheng D, Soffer E, Blacher E, Braverman S, Tengeler AC, Barak O, Elazar M, Ben-Zeev R, Lehavi-Regev D, Katz MN, Pevsner-Fischer M, Gertler A, Halpern Z, Harmelin A, Aamar S, Serradas P, Grosfeld A, Shapiro H, Geiger B, Elinav E. 2018. Hyperglycemia drives intestinal barrier dysfunction and risk for enteric infection. Science 359:1376–1383.
111. Singh V, Yeoh BS, Xiao X, Kumar M, Bachman M, Borregaard N, Joe B, Vijay-Kumar M. 2015. Interplay between enterobactin, myeloperoxidase and lipocalin 2 regulates *E. coli* survival in the inflamed gut. Nat Commun 6:7113.
112. Lupp C, Robertson ML, Wickham ME, Sekirov I, Champion OL, Gaynor EC, Finlay BB. 2007. Host-mediated inflammation disrupts the intestinal microbiota and promotes the overgrowth of *Enterobacteriaceae*. Cell Host Microbe 2:119–129.
113. Winter SE, Winter MG, Xavier MN, Thiennimitr P, Poon V, Keestra AM, Laughlin RC, Gomez G, Wu J, Lawhon SD, Popova IE, Parikh SJ, Adams LG, Tsolis RM, Stewart VJ, Bäumler AJ. 2013. Host-derived nitrate boosts growth of *E. coli* in the inflamed gut. Science 339:708–711.
114. Lawley TD, Walker AW. 2013. Intestinal colonization resistance. Immunology 138:1–11.
115. Willing B, Dicksved J, Halfvarson J, Andersson A, Lucio M, Zeng Z, Jarnerot G, Tysk C, Jansson JK, Engstrand L. 2010. A pyrosequencing study in twins shows that GI microbial profiles vary with inflammatory bowel disease phenotypes. Gastroenterology 139:1844–1854.
116. Nagai F, Morotomi M, Sakon H, Tanaka R. 2009. *Parasutterella excrementihominis* gen. nov., sp. nov., a member of the family *Alcaligenaceae* isolated from human faeces. Int J Syst Evol Microbiol 59:1793–1797.
117. Morotomi M, Nagai F, Watanabe Y. 2011. *Parasutterella* secunda sp. nov., isolated from human faeces and proposal of *Sutterellaceae* fam. nov. in the order Burkholderiales. Int J Syst Evol Microbiol 61:637–643.

118. Morotomi M. 2014. The family *Sutterellaceae*. p. 1005–1012. In: Rosenberg E, DeLong EF, Lory S, Stackebrandt E, Thompson F (ed), The prokaryotes: Alphaproteobacteria and Betaproteobacteria, 4th ed. Springer, Berlin, Heidelberg.
119. Wang J, Lang T, Shen J, Dai J, Tian L, Wang X. 2019. Core gut bacteria analysis of healthy mice. Front Microbiol 10:887.
120. Bjerrum L, Engberg RM, Leser TD, Jensen BB, Finster K, Pedersen K. 2006. Microbial community composition of the ileum and cecum of broiler chickens as revealed by molecular and culture-based techniques. Poult Sci 85:1151–1164.
121. Duar RM, Frese SA, Lin XB, Fernando SC, Burkey TE, Tasseva G, Peterson DA, Blom J, Wenzel CQ, Szymanski CM, Walter J. 2017. Experimental evaluation of host adaptation of *Lactobacillus reuteri* to different vertebrate species. Appl Environ Microbiol 83:e00132–17.
122. Osaka T, Moriyama E, Arai S, Date Y, Yagi J, Kikuchi J, Tsuneda S. 2017. Meta-analysis of fecal microbiota and metabolites in experimental colitic mice during the inflammatory and healing phases. Nutrients 9:E1329.
123. Campbell HA, Mashburn LT, Boyse EA, Old LJ. 1967. Two L-asparaginases from *Escherichia coli* B. Their separation, purification, and antitumor activity. Biochemistry 6:721–730.
124. Cedar H, Schwartz JH. 1968. Production of L-asparaginase II by *Escherichia coli.* J Bacteriol 96:2043–2048.
125. An C, Kuda T, Yazaki T, Takahashi H, Kimura B. 2014. Caecal fermentation, putrefaction and microbiotas in rats fed milk casein, soy protein or fish meal. Appl Microbiol Biotechnol 98:2779–2787.
126. Li X, Rezaei R, Li P, Wu G. 2011. Composition of amino acids in feed ingredients for animal diets. Amino Acids 40:1159–1168.
127. Windmueller HG, Spaeth AE. 1976. Metabolism of absorbed aspartate, asparagine, and arginine by rat small intestine *in vivo*. Arch Biochem Biophys 175:670–676.
128. Windmueller HG, Spaeth AE. 1980. Respiratory fuels and nitrogen metabolism *in vivo* in small intestine of fed rats. Quantitative importance of glutamine, glutamate, and aspartate. J Biol Chem 255:107–112.

129. Wu G. 2010. Functional amino acids in growth, reproduction, and health. Adv Nutr 1:31–37.
130. Corfield AP. 2018. The interaction of the gut microbiota with the mucus barrier in health and disease in human. Microorganisms 6:78–135.
131. Cecchini G, Schröder I, Gunsalus RP, Maklashina E. 2002. Succinate dehydrogenase and fumarate reductase from *Escherichia coli*. Biochim Biophys Acta 1553:140–157.
132. Guccione E, Del Rocio Leon-Kempis M, Pearson BM, Hitchin E, Mulholland F, Van Diemen PM, Stevens MP, Kelly DJ. 2008. Amino acid-dependent growth of *Campylobacter jejuni*: key roles for aspartase (AspA) under microaerobic and oxygen-limited conditions and identification of AspB (Cj0762), essential for growth on glutamate. Mol Microbiol 69:77–93.
133. Sakamoto M, Ikeyama N, Kunihiro T, Iino T, Yuki M, Ohkuma M. 2018. *Mesosutterella multiformis* gen. nov., sp. nov., a member of the family *Sutterellaceae* and *Sutterella megalosphaeroides* sp. nov., isolated from human faeces. Int J Syst Evol Microbiol 68:3942–3950.
134. Jones SA, Chowdhury FZ, Fabich AJ, Anderson A, Schreiner DM, House AL, Autieri SM, Leatham MP, Lins JJ, Jorgensen M, Cohen PS, Conway T. 2007. Respiration of *Escherichia coli* in the mouse intestine. Infect Immun 75:4891–4899.
135. van der Lugt B, Rusli F, Lute C, Lamprakis A, Salazar E, Boekschoten M V., Hooiveld GJ, Müller M, Vervoort J, Kersten S, Belzer C, Kok DEG, Steegenga WT. 2018. Integrative analysis of gut microbiota composition, host colonic gene expression and intraluminal metabolites in aging C57BL/6J mice. Aging (Albany NY) 10:930–950.
136. Kern M, Simon J. 2008. Characterization of the NapGH quinol dehydrogenase complex involved in *Wolinella succinogenes* nitrate respiration. Mol Microbiol 69:1137–1152.
137. Ikeyama N, Ohkuma M, Sakamoto M. 2019. Draft genome sequence of *Mesosutterella multiformis* jcm 32464T, a member of the family *Sutterellaceae*, isolated from human feces. Microbiol Resour Announc 8:e00478–19.
138. Horvath P, Barrangou R. 2010. CRISPR/Cas, the immune system of bacteria and archaea. Science 327:167–170.

139. Chylinski K, Makarova KS, Charpentier E, Koonin E V. 2014. Classification and evolution of type II CRISPR-Cas systems. Nucleic Acids Res 42:6091–6105.
140. Netzer R, Krause M, Rittmann D, Peters-Wendisch PG, Eggeling L, Wendisch VF, Sahm H. 2004. Roles of pyruvate kinase and malic enzyme in *Corynebacterium glutamicum* for growth on carbon sources requiring gluconeogenesis. Arch Microbiol 182:354–363.
141. Bologna FP, Andreo CS, Drincovich MF. 2007. *Escherichia coli* malic enzymes: two isoforms with substantial differences in kinetic properties, metabolic regulation, and structure. J Bacteriol 189:5937–5946.
142. Patel MS, Roche TE. 1990. Molecular biology and biochemistry of pyruvate dehydrogenase complexes. FASEB J 4:3224–3233.
143. Knappe J, Sawers G. 1990. A radical-chemical route to acetyl-CoA: the anaerobically induced pyruvate formate-lyase system of *Escherichia coli*. FEMS Microbiol Lett 6:383–398.
144. Charon MH, Volbeda a, Chabriere E, Pieulle L, Fontecilla-Camps JC. 1999. Structure and electron transfer mechanism of pyruvate:ferredoxin oxidoreductase. Curr Opin Struct Biol 9:663–669.
145. Furdui C, Ragsdale SW. 2000. The role of pyruvate ferredoxin oxidoreductase in pyruvate synthesis during autotrophic growth by the Wood-Ljungdahl pathway. J Biol Chem 275:28494–28499.
146. Antranikian G, Giffhorn F. 1987. Citrate metabolism in anaerobic bacteria. FEMS Microbiol Lett 46:175–198.
147. Fuchs TM, Eisenreich W, Heesemann J, Goebel W. 2012. Metabolic adaptation of human pathogenic and related nonpathogenic bacteria to extra- and intracellular habitats. FEMS Microbiol Rev 36:435–462
148. Cordwell SJ. 1999. Microbial genomes and “missing” enzymes: redefining biochemical pathways. Arch Microbiol 172:269–279.
149. Morishita T, Yajima M. 1995. Incomplete operation of biosynthetic and bioenergetic functions of the citric acid cycle in multiple auxotrophic Lactobacilli. Biosci Biotechnol Biochem 59:251–255.

150. Amarasingham CR, Davis BD. 1965. Regulation of alpha-ketoglutarate dehydrogenase formation in *Escherichia coli*. J Biol Chem 240:3664–3668.
151. Kubo A, Stephens RS. 2001. Substrate-specific diffusion of select dicarboxylates through *Chlamydia trachomatis* PorB. Microbiology 147:3135–3140.
152. Aevarsson A, Seger K, Turley S, Sokatch JR, Hol WG. 1999. Crystal structure of 2-oxoisovalerate and dehydrogenase and the architecture of 2-oxo acid dehydrogenase multienzyme complexes. Nat Struct Biol 6:785–792.
153. Frank RAW, Price AJ, Northrop FD, Perham RN, Luisi BF. 2007. Crystal structure of the e1 component of the *Escherichia coli* 2-oxoglutarate dehydrogenase multienzyme complex. J Mol Biol 368:639–651.
154. Mark AR, Clore GM, James GO, Angela MG, Richard NP, Ettore A, Kazuyasu S. 1992. Three-dimensional solution structure of the e3-binding domain of the dihydrolipoamide succinyltransferase core from the 2-oxoglutarate dehydrogenase multienzyme complex of *Escherichia coli*. Biochemistry 31:3463–3471.
155. Green JDF, Laue ED, Perham RN, Ali ST, Guest JR. 1995. Three-dimensional structure of a lipoyl domain fromthe dihydrolipoyl acetyltransferase component of the pyruvate dehydrogenase multienzyme complex of *Escherichia coli*. J Mol Biol 248:328–343.
156. Nolte JC, Schürmann M, Schepers CL, Vogel E, Wübbeler JH, Steinbüchel A. 2014. Novel characteristics of succinate coenzyme a (succinate-coa) ligases: Conversion of malate to malyl-coa and coa-thioester formation of succinate analogues *in vitro*. Appl Environ Microbiol 80:166–176.
157. Wolodko WT, Fraser ME, James MN, Bridger WA. 1994. The crystal structure of succinyl-CoA synthetase from *Escherichia coli* at 2.5-A resolution. J Biol Chem 269:10883–10890.
158. Joyce MA, Fraser ME, James MNG, Bridger WA, Wolodko WT. 2000. ADP-binding site of *Escherichia coli* succinyl-CoA synthetase revealed by X-ray crystallography. Biochemistry 39:17–25.
159. Lambeth DO. 2006. Reconsideration of the significance of substrate-level phosphorylation in the citric acid cycle. Biochem Mol Biol Educ 34:21–29.

160. Buck D, Spencer ME, Guest JR. 1985. Primary structure of the succinyl-CoA synthetase of *Escherichia coli*. Biochemistry 24:6245–6252.
161. Roy CDL. 2001. Succinate:quinone oxidoreductases-what can we learn from *Wolinella succinogenes* quinol:fumarate reductase? FEBS Letters 504:133–141.
162. Ge Z, Feng Y, Dangler CA, Xu S, Taylor NS, Fox JG. 2000. Fumarate reductase is essential for *Helicobacter pylori* colonization of the mouse stomach. Microb Pathog 29:279–287.
163. Ge Z. 2005. Potential of fumarate reductase as a novel therapeutic target in *Helicobacter pylori* infection. Expert Opin Ther Targets 6:135–146.
164. Woods SA, Schwartzbach SD, Guest JR. 1988. Two biochemically distinct classes of fumarase in *Escherichia coli*. Biochim Biophys Acta (BBA)-Protein Struct Mol 954:14–26.
165. Pitson SM, Mendz GL, Srinivasan S, Hazell SL. 1999. The tricarboxylic acid cycle of *Helicobacter pylori*. Eur J Biochem 260:258–267.
166. Park SJ, Cotter PA, Gunsalus RP. 1995. Regulation of malate dehydrogenase (mdh) gene expression in *Escherichia coli* in response to oxygen, carbon, and heme availability. J Bacteriol 177:6652–6656.
167. Wexler HM, Reeves D, Summanen PH, Molitoris E, McTeague M, Duncan J, Wilson KH, Finegold SM. 1996. *Sutterella wadsworthensis* gen. nov., sp. nov., bile-resistant microaerophilic *Campylobacter gracilis*-like clinical isolates. Int J Syst Bacteriol 46:252–258.
168. Li H, Limenitakis JP, Fuhrer T, Geuking MB, Lawson MA, Wyss M, Brugiroux S, Keller I, Macpherson JA, Rupp S, Stolp B, Stein J V., Stecher B, Sauer U, McCoy KD, Macpherson AJ. 2015. The outer mucus layer hosts a distinct intestinal microbial niche. Nat Commun 6:8292.
169. Xiao L, Chen B, Feng D, Yang T, Li T, Chen J. 2019. TLR4 may be involved in the regulation of colonic mucosal microbiota by Vitamin A. Front Microbiol 10:268.
170. Dong LN, Wang JP, Liu P, Yang YF, Feng J, Han Y. 2017. Faecal and mucosal microbiota in patients with functional gastrointestinal disorders: correlation with toll-like receptor 2/toll-like receptor 4 expression. World J Gastroenterol 23:6665–6673.

171. Bäckhed F, Roswall J, Peng Y, Feng Q, Jia H, Kovatcheva-Datchary P, Li Y, Xia Y, Xie H, Zhong H, Khan MT, Zhang J, Li J, Xiao L, Al-Aama J, Zhang D, Lee YS, Kotowska D, Colding C, Tremaroli V, Yin Y, Bergman S, Xu X, Madsen L, Kristiansen K, Dahlgren J, Wang J. 2015. Dynamics and stabilization of the human gut microbiome during the first year of life. Cell Host Microbe 17:690–703.
172. Drago L, Toscano M, De Grandi R, Grossi E, Padovani EM, Peroni DG. 2016. Microbiota network and mathematic microbe mutualism in colostrum and mature milk collected in two different geographic areas: Italy versus Burundi. ISME J 11:875–884.
173. Palm NW, De Zoete MR, Cullen TW, Barry NA, Stefanowski J, Hao L, Degnan PH, Hu J, Peter I, Zhang W, Ruggiero E, Cho JH, Goodman AL, Flavell RA. 2014. Immunoglobulin A coating identifies colitogenic bacteria in inflammatory bowel disease. Cell 158:1000–1010.
174. Honda K, Littman DR. 2016. The microbiota in adaptive immune homeostasis and disease. Nature 535:75–84
175. Kau AL, Planer JD, Liu J, Rao S, Yatsunenko T, Trehan I, Manary MJ, Liu TC, Stappenbeck TS, Maleta KM, Ashorn P, Dewey KG, Houpt ER, Hsieh CS, Gordon JI. 2015. Functional characterization of IgA-targeted bacterial taxa from undernourished Malawian children that produce diet-dependent enteropathy. Sci Transl Med 7:276ra24.
176. D'Auria G, Peris-Bondia F, Džunková M, Mira A, Collado MC, Latorre A, Moya A. 2013. Active and secreted IgA-coated bacterial fractions from the human gut reveal an under-represented microbiota core. Sci Rep 3:3515.
177. Goedert JJ, Hua X, Bielecka A, Okayasu I, Milne GL, Jones GS, Fujiwara M, Sinha R, Wan Y, Xu X, Ravel J, Shi J, Palm NW, Feigelson HS. 2018. Postmenopausal breast cancer and oestrogen associations with the IgA-coated and IgA-noncoated faecal microbiota. Br J Cancer 118:471–479.
178. Moon C, Baldridge MT, Wallace MA, Burnham CAD, Virgin HW, Stappenbeck TS. 2015. Vertically transmitted faecal IgA levels determine extra-chromosomal phenotypic variation. Nature 521:90–93.

179. Martin G, Kolida S, Marchesi JR, Want E, Sidaway JE, Swann JR. 2018. *In vitro* modeling of bile acid processing by the human fecal microbiota. Front Microbiol 9:1153.
180. Degirolamo C, Rainaldi S, Bovenga F, Murzilli S, Moschetta A. 2014. Microbiota modification with probiotics induces hepatic bile acid synthesis via downregulation of the Fxr-Fgf15 axis in mice. Cell Rep 7:12–18.
181. Xie G, Wang X, Huang F, Zhao A, Chen W, Yan J, Zhang Y, Lei S, Ge K, Zheng X, Liu J, Su M, Liu P, Jia W. 2016. Dysregulated hepatic bile acids collaboratively promote liver carcinogenesis. Int J Cancer 139:1764–1775.
182. Dey N, Wagner VE, Blanton LV, Cheng J, Fontana L, Haque R, Ahmed T, Gordon JI. 2015. Regulators of gut motility revealed by a gnotobiotic model of diet-microbiome interactions related to travel. Cell 163:95–107.
183. Staley C, Kelly CR, Brandt LJ, Khoruts A, Sadowsky MJ. 2016. Complete microbiota engraftment is not essential for recovery from recurrent *Clostridium difficile* infection following fecal microbiota transplantation. MBio 7:e01965–16.
184. Llopis M, Cassard AM, Wrzosek L, Boschat L, Bruneau A, Ferrere G, Puchois V, Martin JC, Lepage P, Le Roy T, Lefèvre L, Langelier B, Cailleux F, González-Castro AM, Rabot S, Gaudin F, Agostini H, Prévot S, Berrebi D, Ciocan D, Jousse C, Naveau S, Gérard P, Perlemuter G. 2016. Intestinal microbiota contributes to individual susceptibility to alcoholic liver disease. Gut 65:830–839.
185. Kreutzer C, Peters S, Schulte DM, Fangmann D, Türk K, Wolff S, van Eimeren T, Ahrens M, Beckmann J, Schafmayer C, Becker T, Kerby T, Rohr A, Riedel C, Heinsen FA, Degenhardt F, Franke A, Rosenstiel P, Zubek N, Henning C, Freitag-Wolf S, Dempfle A, Psilopanagioti A, Petrou-Papadaki H, Lenk L, Jansen O, Schreiber S, Laudes M. 2017. Hypothalamic inflammation in human obesity is mediated by environmental and genetic factors. Diabetes 66:2407–2415.
186. Huang C, Chen J, Wang J, Zhou H, Lu Y, Lou L, Zheng J, Tian L, Wang X, Cao Z, Zeng Y. 2017. Dysbiosis of intestinal microbiota and decreased antimicrobial peptide level in paneth cells during hypertriglyceridemia-related acute necrotizing pancreatitis in rats. Front Microbiol 8:776.

187. Danneskiold-Samsøe NB, Andersen D, Radulescu ID, Normann-Hansen A, Brejnrod A, Kragh M, Madsen T, Nielsen C, Josefsen K, Fretté X, Fjære E, Madsen L, Hellgren LI, Brix S, Kristiansen K. 2017. A safflower oil based high-fat/high-sucrose diet modulates the gut microbiota and liver phospholipid profiles associated with early glucose intolerance in the absence of tissue inflammation. Mol Nutr Food Res 61:1600528.
188. Zhang C, Zhang M, Pang X, Zhao Y, Wang L, Zhao L. 2012. Structural resilience of the gut microbiota in adult mice under high-fat dietary perturbations. ISME J 6:1848–1857.
189. Serino M, Luche E, Gres S, Baylac A, Bergé M, Cenac C, Waget A, Klopp P, Iacovoni J, Klopp C, Mariette J, Bouchez O, Lluch J, Ouarné F, Monsan P, Valet P, Roques C, Amar J, Bouloumié A, Théodorou V, Burcelin R. 2012. Metabolic adaptation to a high-fat diet is associated with a change in the gut microbiota. Gut 61:543–553.
190. Zhang X, Zhao Y, Xu J, Xue Z, Zhang M, Pang X, Zhang X, Zhao L. 2015. Modulation of gut microbiota by berberine and metformin during the treatment of high-fat diet-induced obesity in rats. Sci Rep 5:14405.
191. Yang J, Summanen PH, Henning SM, Hsu M, Lam H, Huang J, Tseng CH, Dowd SE, Finegold SM, Heber D, Li Z. 2015. Xylooligosaccharide supplementation alters gut bacteria in both healthy and prediabetic adults: a pilot study. Front Physiol 6:216.
192. Canesso MCC, Lacerda, NL, Ferreira CM, Gonçalves, JL, Almeida D, Gamba C, Pedroso SH, Moreira C, Martins FS, Nicoli JR, Teixeira MM, Godard ALB, Vieira AT. 2014. Comparing the effects of acute alcohol consumption in germ-free and conventional mice: the role of the gut microbiota. BMC Microbiol 14:240.
193. Zhang X, Wang H, Yin P, Fan H, Sun L, Liu Y. 2017. Flaxseed oil ameliorates alcoholic liver disease via anti-inflammation and modulating gut microbiota in mice. Lipids Health Dis 16:44.
194. Liu Q, Li F, Zhuang Y, Xu J, Wang J, Mao X, Zhang Y, Liu X. 2019. Alteration in gut microbiota associated with hepatitis B and non-hepatitis virus related hepatocellular carcinoma. Gut Pathog 11:1.

195. Guo C, Li Y, Wang P, Li Y, Qiu C, Li M, Wang D, Zhao R, Li D, Wang Y, Li S, Dai W, Zhang L. 2018. Alterations of gut microbiota in cholestatic infants and their correlation with hepatic function. Front Microbiol 9:2682.
196. Chiodini RJ, Dowd SE, Chamberlin WM, Galandiuk S, Davis B, Glassing A. 2015. Microbial population differentials between mucosal and submucosal intestinal tissues in advanced Crohn's disease of the ileum. PLoS One 10:e0134382.
197. Ritchie LE, Sturino JM, Carroll RJ, Rooney LW, Andrea Azcarate-Peril M, Turner ND. 2015. Polyphenol-rich sorghum brans alter colon microbiota and impact species diversity and species richness after multiple bouts of dextran sodium sulfate-induced colitis. FEMS Microbiol Ecol 91:fiv008.
198. Chen Y-J, Wu H, Wu S-D, Lu N, Wang Y-T, Liu H-N, Dong L, Liu T-T, Shen X-Z. 2018. *Parasutterella*, in association with irritable bowel syndrome and intestinal chronic inflammation. J Gastroenterol Hepatol 33:1844–1852.
199. Luna RA, Oezguen N, Balderas M, Venkatachalam A, Runge JK, Versalovic J, Veenstra-VanderWeele J, Anderson GM, Savidge T, Williams KC. 2017. Distinct microbiome-neuroimmune signatures correlate with functional abdominal pain in children with autism spectrum disorder. Cell Mol Gastroenterol Hepatol 3:218–230.
200. Zhang L, Dong D, Jiang C, Li Z, Wang X, Peng Y. 2015. Insight into alteration of gut microbiota in *Clostridium difficile* infection and asymptomatic *C. difficile* colonization. Anaerobe 34:1–7.
201. Collins J, Auchtung JM, Schaefer L, Eaton KA, Britton RA. 2015. Humanized microbiota mice as a model of recurrent *Clostridium difficile* disease. Microbiome 3:35.
202. Low DE, Shahinas D, Silverman M, Sittler T, Chiu C, Kim P, Allen-Vercoe E, Weese S, Wong A, Pillaij DR. 2012. Toward an understanding of changes in diversity associated with fecal microbiome transplantation based on 16s rRNA gene deep sequencing. MBio 3:e00338–12.
203. Wu J, Ren W, Li L, Luo M, Xu K, Shen J, Wang J, Chang G, Lu Y, Qi Y, Xu B, He Y, Hu Y. 2018. Effect of aging and glucagon-like peptide 2 on intestinal microbiota in SD rats. Aging Dis 9:566–577.

204. Kok DEG, Rusli F, van der Lugt B, Lute C, Laghi L, Salvioli S, Picone G, Franceschi C, Smidt H, Vervoort J, Kampman E, Müller M, Steegenga WT. 2018. Lifelong calorie restriction affects indicators of colonic health in aging C57Bl/6J mice. J Nutr Biochem 56:152–164.
205. Bartley JM, Zhou X, Kuchel GA, Weinstock GM, Haynes L. 2017. Impact of age, caloric restriction, and influenza infection on mouse gut microbiome: an exploratory study of the role of age-related microbiome changes on influenza responses. Front Immunol 8:1164.
206. Rieder R, Wisniewski PJ, Alderman BL, Campbell SC. 2017. Microbes and mental health: a review. Brain Behav Immun 66:9–17.
207. Erny D, De Angelis ALH, Jaitin D, Wieghofer P, Staszewski O, David E, Keren-Shaul H, Mahlakoiv T, Jakobshagen K, Buch T, Schwierzeck V, Utermöhlen O, Chun E, Garrett WS, Mccoy KD, Diefenbach A, Staeheli P, Stecher B, Amit I, Prinz M. 2015. Host microbiota constantly control maturation and function of microglia in the CNS. Nat Neurosci 18:965–977.
208. Martin CR, Osadchiy V, Kalani A, Mayer EA. 2018. The brain-gut-microbiome axis. Cell Mol Gastroenterol Hepatol 6:133–148.
209. Kurilshikov A, Wijmenga C, Fu J, Zhernakova A. 2017. Host genetics and gut microbiome: challenges and perspectives. Trends Immunol 38:633–647.
210. Kashyap PC, Marcobal A, Ursell LK, Smits SA, Sonnenburg ED, Costello EK, Higginbottom SK, Domino SE, Holmes SP, Relman DA, Knight R, Gordon JI, Sonnenburg JL. 2013. Genetically dictated change in host mucus carbohydrate landscape exerts a diet-dependent effect on the gut microbiota. Proc Natl Acad Sci 110:17059–17064.
211. Rausch P, Künzel S, Suwandi A, Grassl GA, Rosenstiel P, Baines JF. 2017. Multigenerational influences of the Fut2 gene on the dynamics of the gut microbiota in mice. Front Microbiol 8:991.
212. O'Neil DS, Stewart CJ, Chu DM, Goodspeed DM, Gonzalez-Rodriguez PJ, Shope CD, Aagaard KM. 2017. Conditional postnatal deletion of the neonatal murine hepatic circadian gene, Npas2, alters the gut microbiome following restricted feeding. Am J Obstet Gynecol 217:218.e1–218.e15.

213. Somm E, Henry H, Bruce SJ, Bonnet N, Montandon S A, Niederländer NJ, Messina A, Aeby S, Rosikiewicz M, Fajas L, Sempoux C, Ferrari S, Greub G, Pitteloud N. 2018. β-Klotho deficiency shifts the gut-liver bile acid axis and induces hepatic alterations in mice. Am J Physiol Endocrinol Metab 315:E833–E847.
214. Ehmann D, Wendler J, Koeninger L, Larsen IS, Klag T, Berger J, Marette A, Schaller M, Stange EF, Malek NP, Jensen BAH, Wehkamp J. 2019. Paneth cell α-defensins HD-5 and HD-6 display differential degradation into active antimicrobial fragments. Proc Natl Acad Sci 116:3746–3751.
215. Turner JR. 2009. Intestinal mucosal barrier function in health and disease. Nat Rev Immunol 9:799–809
216. Larmonier CB, Laubitz D, Hill FM, Shehab KW, Lipinski L, Midura-Kiela MT, McFadden R-MT, Ramalingam R, Hassan KA, Golebiewski M, Besselsen DG, Ghishan FK, Kiela PR. 2013. Reduced colonic microbial diversity is associated with colitis in NHE3-deficient mice. Am J Physiol Liver Physiol 305:G667–G677.
217. Litvak Y, Byndloss MX, Bäumler AJ. 2018. Colonocyte metabolism shapes the gut microbiota. Science 362:eaat9076.
218. Xu J, Chen N, Wu Z, Song Y, Zhang Y, Wu N, Zhang F, Ren X, Liu Y. 2018. 5-aminosalicylic acid alters the gut bacterial microbiota in patients with ulcerative colitis. Front Microbiol 9:1274.
219. Maseda D, Zackular JP, Trindade B, Kirk L, Roxas JL, Rogers LM, Washington MK, Du L, Koyama T, Viswanathan VK, Vedantam G, Schloss PD, Crofford LJ, Skaar EP, Aronoff DM. 2019. Nonsteroidal anti-inflammatory drugs alter the microbiota and exacerbate *Clostridium difficile* colitis while dysregulating the inflammatory response. MBio 10:e02282–18.
220. De Gunzburg J, Ghozlane A, Ducher A, Le Chatelier E, Duval X, Ruppé E, Armand-Lefevre L, Sablier-Gallis F, Burdet C, Alavoine L, Chachaty E, Augustin V, Varastet M, Levenez F, Kennedy S, Pons N, Mentré F, Andremont A. 2018. Protection of the human gut microbiome from antibiotics. J Infect Dis 217:628–636.
221. Tulstrup MV-L, Roager HM, Thaarup IC, Frandsen HL, Frøkiær H, Licht TR, Bahl MI. 2018. Antibiotic treatment of rat dams affects bacterial colonization and causes decreased weight gain in pups. Commun Biol 1:145.

222. Thompson JA, Oliveira RA, Djukovic A, Ubeda C, Xavier KB. 2015. Manipulation of the quorum sensing signal AI-2 affects the antibiotic-treated gut microbiota. Cell Rep 10:1861–1871.
223. Jang L-G, Choi G, Kim S-W, Kim B-Y, Lee S, Park H. 2019. The combination of sport and sport-specific diet is associated with characteristics of gut microbiota: an observational study. J Int Soc Sports Nutr 16:21.
224. Fernández-Calleja JMS, Konstanti P, Swarts HJM, Bouwman LMS, Garcia-Campayo V, Billecke N, Oosting A, Smidt H, Keijer J, van Schothorst EM. 2018. Non-invasive continuous real-time *in vivo* analysis of microbial hydrogen production shows adaptation to fermentable carbohydrates in mice. Sci Rep 8:15351.
225. Ye J, Lv L, Wu W, Li Y, Shi D, Fang D, Guo F, Jiang H, Yan R, Ye W, Li L. 2018. Butyrate protects mice against methionine–choline-deficient diet-induced non-alcoholic steatohepatitis by improving gut barrier function, attenuating inflammation and reducing endotoxin levels. Front Microbiol 9:1967.
226. Zhou D, Pan Q, Xin FZ, Zhang RN, He CX, Chen GY, Liu C, Chen YW, Fan JG. 2017. Sodium butyrate attenuates high-fat diet-induced steatohepatitis in mice by improving gut microbiota and gastrointestinal barrier. World J Gastroenterol 23:60–75.
227. Eeckhaut V, Wang J, Van Parys A, Haesebrouck F, Joossens M, Falony G, Raes J, Ducatelle R, Van Immerseel F. 2016. The probiotic butyricicoccus pullicaecorum reduces feed conversion and protects from potentially harmful intestinal microorganisms and necrotic enteritis in broilers. Front Microbiol 7:1416.
228. Cheng W, Lu J, Lin W, Wei X, Li H, Zhao X, Jiang A, Yuan J. 2018. Effects of a galacto-oligosaccharide-rich diet on fecal microbiota and metabolite profiles in mice. Food Funct 9:1612–1620.
229. Everard A, Lazarevic V, Derrien M, Girard M, Muccioli GM, Neyrinck AM, Possemiers S, Van Holle A, François P, de Vos WM, Delzenne NM, Schrenzel J, Cani PD. 2011. Responses of gut microbiota and glucose and lipid metabolism to prebiotics in genetic obese and diet-induced leptin-resistant mice. Diabetes 60:2775–2786.
230. Bindels LB, Neyrinck AM, Claus SP, Le Roy CI, Grangette C, Pot B, Martinez I, Walter J, Cani PD, Delzenne NM. 2015. Synbiotic approach restores intestinal

homeostasis and prolongs survival in leukaemic mice with cachexia. ISME J 10:1456–1470.

231. An C, Kuda T, Yazaki T, Takahashi H, Kimura B. 2013. Flx pyrosequencing analysis of the effects of the brown-algal fermentable polysaccharides alginate and laminaran on rat cecal microbiotas. Appl Environ Microbiol 79:860–866.
232. Brahma S, Martínez I, Walter J, Clarke J, Gonzalez T, Menon R, Rose DJ. 2017. Impact of dietary pattern of the fecal donor on *in vitro* fermentation properties of whole grains and brans. J Funct Foods 29:281–289.
233. Aguirre M, Jonkers DMAE, Troost FJ, Roeselers G, Venema K. 2014. *In vitro* characterization of the impact of different substrates on metabolite production, energy extraction and composition of gut microbiota from lean and obese subjects. PLoS One 9:e113864.
234. Noble EE, Hsu TM, Jones RB, Fodor AA, Goran MI, Kanoski SE. 2017. Early-life sugar consumption affects the rat microbiome independently of obesity. J Nutr 147:20–28.
235. Lu C, Sun T, Li Y, Zhang D, Zhou J, Su X. 2018. Microbial diversity and composition in different gut locations of hyperlipidemic mice receiving krill oil. Appl Microbiol Biotechnol 102:355–366.
236. Zhang F, Zheng W, Guo R, Yao W. 2017. Effect of dietary copper level on the gut microbiota and its correlation with serum inflammatory cytokines in Sprague-Dawley rats. J Microbiol 55:694–702.
237. Kong F, Singh RP. 2010. A human gastric simulator (HGS) to study food digestion in human stomach. J Food Sci 75:E627–E635.
238. Thuenemann EC, Giuseppina GM, Rich GT, Faulks RM. 2015. Dynamic gastric model (DGM), p 47–59. In: Verhoeckx K, Cotter P, López-Expósito I, Kleiveland C, Lea T, Mackie A, Requena, T., Swiatecka, D., Wichers, H. (ed), The impact of food bioactives on health: *in vitro* and *ex vivo* models. Springer.
239. Minekus M, Marteau P, Havenaar R, Huis in ’t Veld JHJ. 1995. A multicompartmental dynamic computer-controlled model simulating the stomach and small intestine. Altern to Lab Anim 23:197.

240. Minekus M, Smeets-Peeters M, Havenaar R, Bernalier A, Fonty G, Marol-Bonnin S, Alric M, Marteau P, Huis In't Veld JHJ. 1999. A computer-controlled system to simulate conditions of the large intestine with peristaltic mixing, water absorption and absorption of fermentation products. Appl Microbiol Biotechnol 1:108–114.
241. Cinquin C, Le Blay G, Fliss I, Lacroix C. 2006. New three-stage *in vitro* model for infant colonic fermentation with immobilized fecal microbiota. FEMS Microbiol Ecol 57:324–336.
242. Molly K, Vande Woestyne M, Verstraete W. 1993. Development of a 5-step multi-chamber reactor as a simulation of the human intestinal microbial ecosystem. Appl Microbiol Biotechnol 39:254–258.
243. Van den Abbeele P, Roos S, Eeckhaut V, Mackenzie DA, Derde M, Verstraete W, Marzorati M, Possemiers S, Vanhoecke B, Van Immerseel F, Van de Wiele T. 2012. Incorporating a mucosal environment in a dynamic gut model results in a more representative colonization by Lactobacilli. Microb Biotechnol 5:106–115.
244. Macfarlane GT, Gibson GR, Cummings JH. 1992. Comparison of fermentation reactions in different regions of the human colon. J Appl Bacteriol 72:57–64.
245. De Angelis, Maria and Piccolo, Maria and Vannini, Lucia and Siragusa, Sonya and De Giacomo, Andrea and Serrazzanetti, Diana Isabella and Cristofori, Fernanda and Guerzoni, Maria Elisabetta and Gobbetti, Marco and Francavilla R. 2013. Fecal microbiota and metabolome of children with autism and pervasive developmental disorder not otherwise specified. PLoS One 8:e76993.
246. Hu S, Li A, Huang T, Lai J, Li J, Sublette ME, Lu H, Lu Q, Du Y, Hu Z, Ng CH, Zhang H, Lu J, Mou T, Lu S, Wang D, Duan J, Hu J, Huang M, Wei N, Zhou W, Ruan L, Li MD, Xu Y. 2019. Gut microbiota changes in patients with bipolar depression. Adv Sci 0:1900752.
247. Evans SJ, Bassis CM, Hein R, Assari S, Flowers SA, Kelly MB, Young VB, Ellingrod VE, McInnis MG. 2017. The gut microbiome composition associates with bipolar disorder and illness severity. J Psychiatr Res 87:23–29.
248. Jiang H, Ling Z, Zhang Y, Mao H, Ma Z, Yin Y, Wang W, Tang W, Tan Z, Shi J, Li L, Ruan B. 2015. Altered fecal microbiota composition in patients with major depressive disorder. Brain Behav Immun 48:186–194.

249. Li N, Wang Q, Wang Y, Sun A, Lin Y, Jin Y, Li X. 2019. Fecal microbiota transplantation from chronic unpredictable mild stress mice donors affects anxiety-like and depression-like behavior in recipient mice via the gut microbiota-inflammation-brain axis. Stress 24:1–11.
250. Qian Y, Yang X, Xu S, Wu C, Qin N, Chen S Di, Xiao Q. 2018. Detection of microbial 16S rRNA gene in the blood of patients with Parkinson's disease. Front Aging Neurosci 10:156.
251. Hu X, Wang T, Liang S, Li W, Wu X, Jin F. 2015. Antibiotic-induced imbalances in gut microbiota aggravates cholesterol accumulation and liver injuries in rats fed a high-cholesterol diet. Appl Microbiol Biotechnol 99:9111–9122.
252. Isaac S, Scher JU, Djukovic A, Jiménez N, Littman DR, Abramson SB, Pamer EG, Ubeda C. 2017. Short- and long-term effects of oral vancomycin on the human intestinal microbiota. J Antimicrob Chemother 72:128–136.
253. Li J, Hao H, Cheng G, Liu C, Ahmed S, Shabbir MAB, Hussain HI, Dai M, Yuan Z. 2017. Microbial shifts in the intestinal microbiota of *Salmonella* infected chickens in response to enrofloxacin. Front Microbiol 8:1711.
254. Li R, Wang H, Shi Q, Wang N, Zhang Z, Xiong C, Liu J, Chen Y, Jiang L, Jiang Q. 2017. Effects of oral florfenicol and azithromycin on gut microbiota and adipogenesis in mice. PLoS One 12:e0181690.
255. Feng Y, Huang Y, Wang Y, Wang P, Song H, Wang F. 2019. Antibiotics induced intestinal tight junction barrier dysfunction is associated with microbiota dysbiosis, activated NLRP3 inflammasome and autophagy. PLoS One 14:e0218384.
256. Shen B, Hu J, Song H, Wang Z, Fan J, Sun Y, Wang Q. 2019. Antibiotics exacerbated colitis by affecting the microbiota, Treg cells and SCFAs in IL10-deficient mice. Biomed Pharmacother 114:108849.

Table 1.1. Summary of *in vitro* continuous culture models to study host-microbe interactions

Model	Simulated gut compartment	pH	Ref
HGS	Stomach	pH = 1.35 at the end of 3 hours digestion	(237)
DGM	Stomach and duodenum	pH = 2 and 6.8, respectively	(238)
TIM1	Stomach, duodenum, jejunum, and ileum	pH = 1.7, 6.2, 6.5, and 7.4, respectively	(239)
TIM2	Proximal colon	pH = 5.8	(240)
EnteroMix	Ascending colon, transverse colon, descending colon, and distal colon	pH = 5.5, 6.0, 6.5, and 7.0, respectively	(31)
Lacroix model	Proximal colon, transverse, and distal colon of infants	pH = 5.9, 6.2, and 6.6-6.7, respectively	(241)
SHIME	Stomach, small intestine, ascending colon, transverse colon, and descending colon	pH = 5.6-5.9, 6.15-6.4, 6.6-6.9 in the three colon compartments, respectively	(242)
M-SHIME	Stomach, small intestine, ascending colon, transverse colon, and descending colon	pH = 2, 6.6, 5.6-5.9, 6.15-6.4, 6.6-6.9, respectively	(243)
MacFarlane/Gibson	Ascending colon, transverse colon, and descending colon	pH = 6.0, 6.5, and 7.0, respectively	(244)

HGS, the Human Gastric Simulator; DGM, the Dynamic Gastric Model; TIM1, the TNO Gastro-Intestinal Model (TIM) 1; EnteroMix, The EnteroMix of Danisco; SHIME, Simulator of the Human Intestinal Microbial Ecosystem; M-SHIME, mucosal-SHIME.

Table 1.2. Basic genomic features for strains of the genus *Parasutterella*

Strain	Host	Genome size (bp)	G+C content (%)	CDS
Parasutterella excrementihominis YIT 11859^T	Human, gut	2,831,860	48.1	2,751
Parasutterella excrementihominis CAG:233	Environment	2,501,740	48.3	2,228
Parasutterella excrementihominis UBA11789	Human, gut	2,478,509	48.7	2,402
Parasutterella excrementihominis UBA9121	Human, gut	2,370,147	48.9	2,180
Parasutterella mc1	Mouse, gut	2,845,554	44.1	2,648

Data of *P. excrementihominis* strains are obtained from the GenBank database. *P. excrementihominis* YIT 11859 (ID: 267788), *P. excrementihominis* CAG:233 (ID: 738428), *P. excrementihominis* UBA11789 (ID: 7276318), *P. excrementihominis* UBA9121 (ID: 7371238).

Table 1.3. Summary of experimental and clinical studies on *Parasutterella* in CNS disorders

CNS disorder	Model	Methods	*Parasutterella*	Ref
ASD	Human	ASD children with FGID (ASD-FGID, n = 14), NT children with FGID (NT-FGID, n = 15), NT children without abdominal pain (NT, n = 6)	*P. excrementihominis* and *Tyzzerella* species were significantly associated with the ASD-FGID group with pain (n = 9) compared with the ASD-FGID group with no pain (n = 5).	(199)
	Human	ASD children (AD, n = 10), POD-NOS children (POD-NOS, n = 10), healthy children (HC, n = 10)	*P. excrementihominis* was higher in the AD group compared to HC and POD-NOS children.	(245)
BD	Human	BD patients (BD, n = 52), healthy controls (HCs, n = 45)	Genera *Parasutterella*, *Roseburia, Faecalibacterium*, *Ruminococcus*, *Gemmiger*, and *Coprococcus* were more abundant in HCs compared to the BD group.	(246)
	Human	BD patients (BD, n = 115), healthy controls (HCs, n = 64)	No difference was found in the relative abundance of *Parasutterella* in the feces between BD (0.6 ± 1.2) and HCs (0.7 ± 1.3) groups.	(247)
Depression	Human	Active-MDD group (A-MDD, n = 29), responding-MDD group (R-MDD, n = 17), healthy controls group (HCs, n = 30)	*Parasutterella*, together with other predominant genera, such as *Blautia* and *Clostridium XIX*,	(248)

			were relatively more abundant in the A-MDD patients compared with the HC group.	
	Mouse	CUMS group (CUMS, n = 8), control group (CON, n = 8)	Genera *Helicobacter*, *Turicibacter*, *Parasutterella*, *Alistipes*, *Odoribacter*, *and Akkermansia* were increased in CUMS group compared with the CON group.	(133)
PD	Human	PD patients (PD; 23 females, 22 males; age, 68.1 ± 8.0), healthy spouses (HC; 22 females, 23 males, age, 67.9 ± 8.0)	Genera *Parasutterella*, *Kocuria*, and *Phascolarctobacterium* were negatively associated with NMS scores.	(134)

CNS, central nervous system; ASD, Autism spectrum disorder; FGID, functional gastrointestinal disorders; NT, neurotypical; POD-NOS, Pervasive Developmental Disorder Not Otherwise Specified; BD, Bipolar disorder; MDD, major depressive disorder; CUMS, chronic unpredictable mild stress; PD, Parkinson's disease; NMS, non-motor symptoms

Table 1.4. Effects of antibiotic treatment on *Parasutterella* abundance

Antibiotics	Model	Methods	*Parasutterella*	Ref
Broad-spectrum antibiotic cocktail	Rat Sprague-Dawley (male)	Ampicillin, neomycin, and metronidazole (1 g/L for each type) in drinking water for 4 weeks Chow diet (CT); high cholesterol diet (HCD); CT + antibiotic (CT + Ab); HCD + antibiotic (HCD + Ab)	The abundance of *Parasutterella* was higher in HCD + Ab mice compared to that in CT, HCD, and CT + Ab mice.	(251)
Vancomycin	Human Rheumatoid arthritis patients (female, male)	Vancomycin (250 mg four times a day) received orally for 2 weeks	The abundance of *Parasutterella* was not changed by vancomycin administration.	(252)
Enrofloxacin	Chicken (male)	Enrofloxacin (0.1 mg/kg, 4 mg/kg, and 100 mg/kg body weight) administered orally for three rounds of 7-day treatment following with 7-day withdrawal Chicks were infected with *Salmonella* Typhimurium at 4 days old and received enrofloxacin at 8 days old	Five genera including *Parasutterella* were significantly decreased in the antibiotic treated groups than in the control group for both the treatment period and the withdrawal period. These genera have been identified as highly susceptible to enrofloxacin.	(253)

Azithromycin and florfenicol	Mouse C57BL/6 (female, male)	Azithromycin (35 mg/L) or florfenicol (33 mg/L) in drinking water for four weeks	The abundance of *Parasutterella* was reduced in both antibiotic treatment groups.	(254)
Isoniazid, rifampin, and pyrazinamide	Mouse C57BL/6J-CD45a (Ly5a) (female)	A combination of isoniazid (25 mg/mL), rifampin (1 mg/mL), and pyrazinamide (150 mg/mL) by oral gavage Mice were infected with *Mycobacterium tuberculosis* received the combination of drugs 5 days a week for the first 2 months, and isoniazid and rifampin only for an additional 2 months	Relative levels of genera *Barnesiella*, *Porphyromonas*, and *Paraprevotella* of the phylum Bacteroidetes and genera *Parasutterella* and *Desulfovibrio* of the phylum Proteobacteria were increased by the treatment and further increased following cessation of therapy.	(250)
Amoxicillin and vancomycin	Rat Wistar Hannover (female)	A daily dosage of 0.5 mL of Amoxicillin (60 mg/mL) or vancomycin (8 mg/mL), or water by oral gavage Antibiotic treatment of dams started on 8 days before the expected birth of pups and continued until pups were weaned at 4 weeks of age	The relative abundance of *Parasutterella* was significantly reduced in dams received amoxicillin compared to that in the water group, whereas vancomycin treatment did not alter the level of fecal *Parasutterella*.	(221)
Broad-spectrum	Mouse C57BL/6 (female)	Ampicillin (1 g/L), neomycin sulfate (1 g/L), metronidazole (1 g/L), and vancomycin (0.5 g/L) in drinking water for 1, 3, 4, 7, or 14 days	Several genera, majorly belonging to the phylum Proteobacteria, such	(255)

antibiotic cocktail			as *Parasutterella* was significantly increased in antibiotic-treated mice.	
Broad-spectrum antibiotic cocktail	Mouse C3H IL10$^{-/-}$ (male)	Ampicillin (1 g/L), novobiocin sodium salt (1 g/L), metronidazole (1 g/L) and vancomycin hydrochloride (0.5 g/L) in drinking water for 19 days	Ten genera including *Parasutterella* were significantly increased in mice treated with antibiotics compared to that in water-treated mice.	(256)
Moxifloxacin	Human (female, male)	Moxifloxacin (400 mg/day) was administered orally for 5 days	Genera including *Parasutterella* and *Sutterella* were decreased in moxifloxacin treated volunteers.	(220)

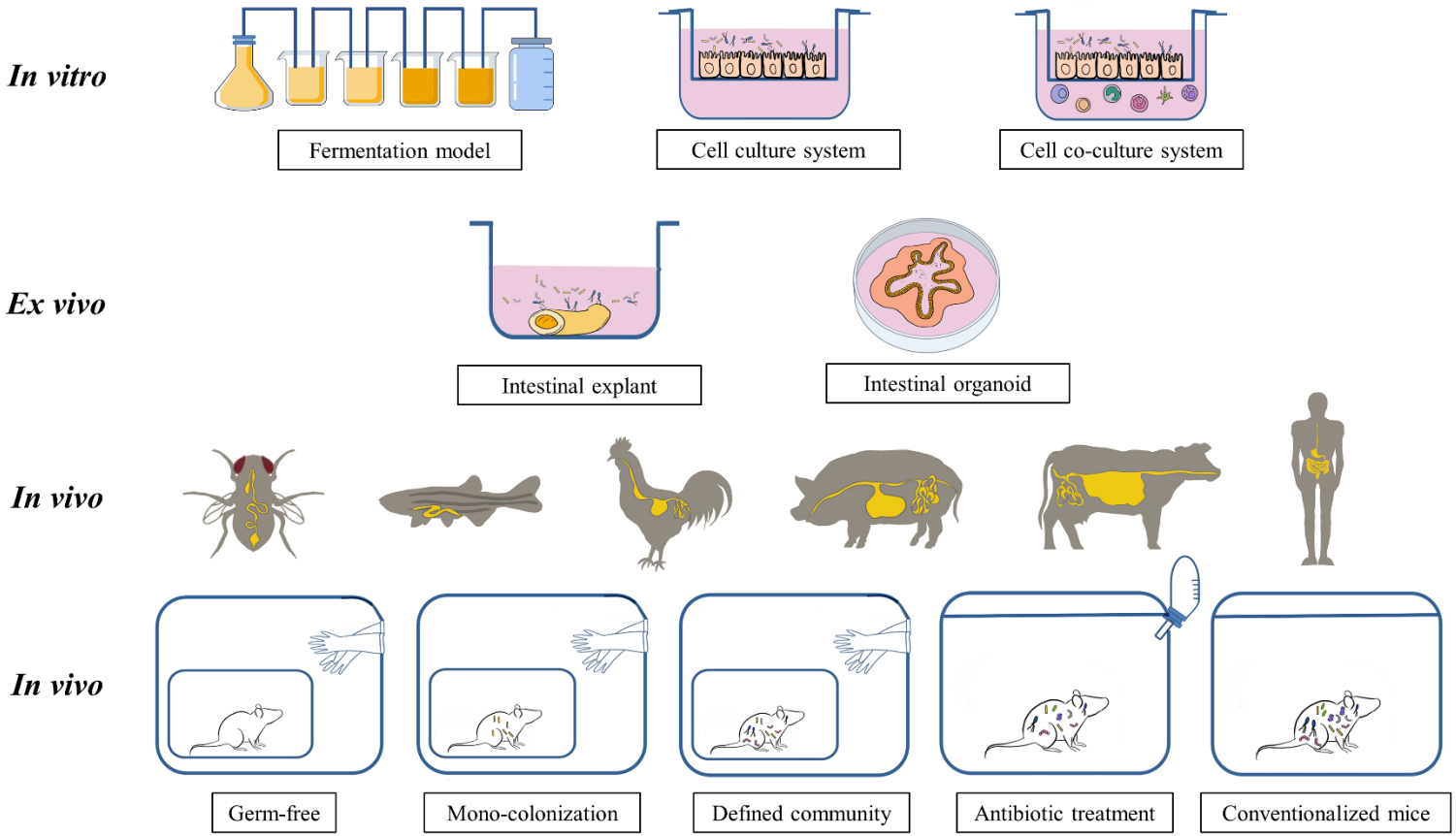

Figure 1.1. Overview of representative model systems to investigate host-microbe interactions in gut microbiome research.

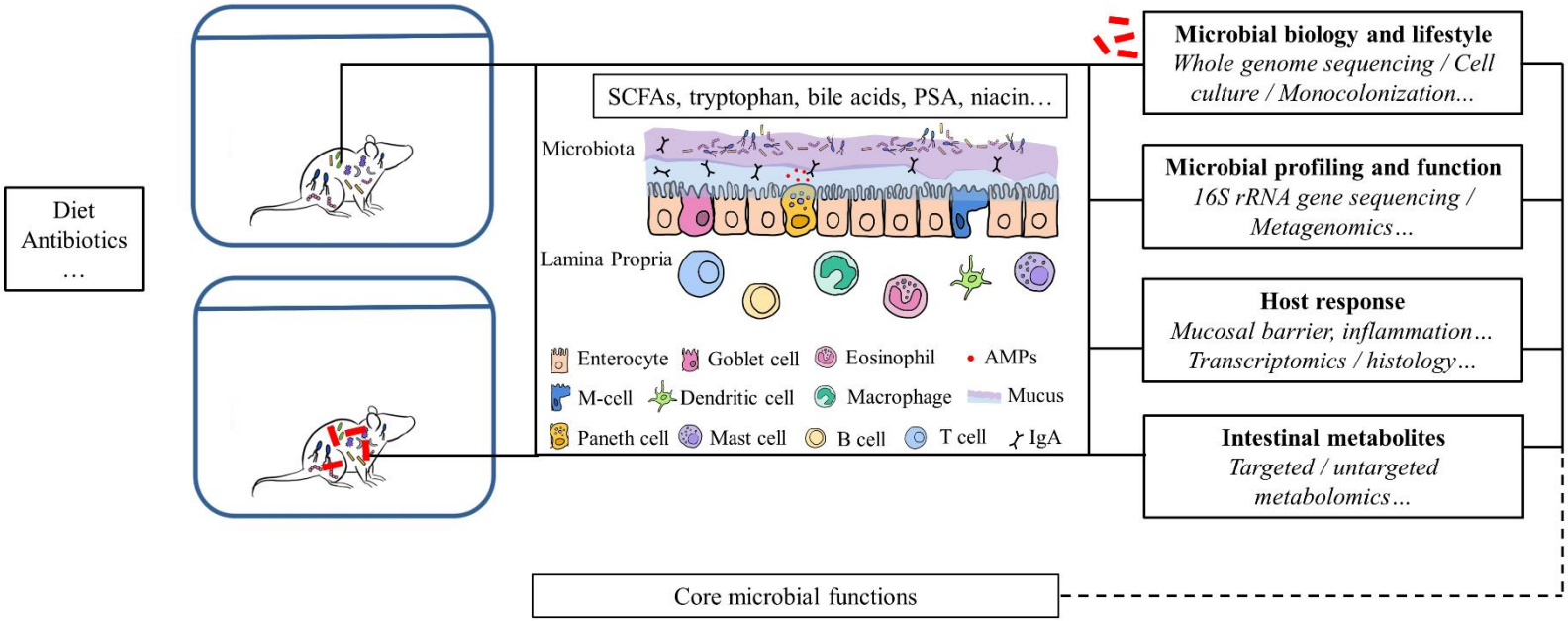

Figure 1.2. The mouse model established in this thesis. SPF mice colonized with/without a single commensal bacterium were used to compare the impact of the single bacterium on microbial community and host physiology.

PSA, polysaccharide A; AMPs, antimicrobial peptides

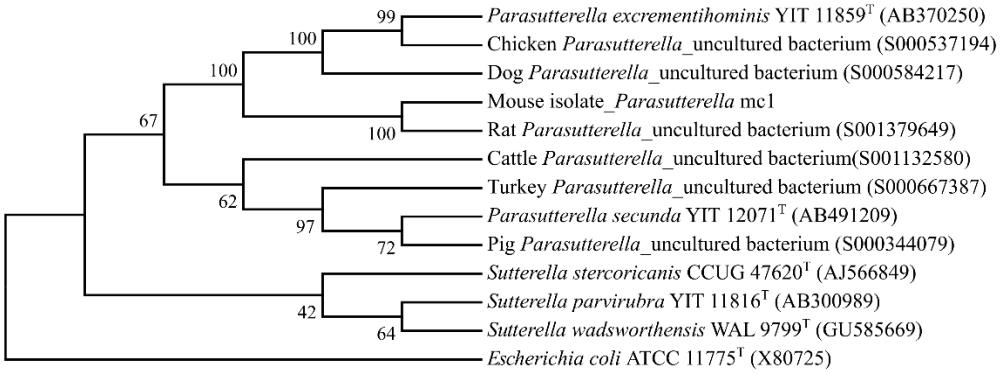

Figure 1.3. Maximum likelihood phylogenetic tree based on 16S rRNA gene sequences of *Parasutterella* isolate and uncultured bacterium, including type strains within the family *Sutterellaceae*. Sequences were obtained from RDP and the sequence belonging to *E. coli* type strain was used as the outgroup. For each node bootstrap values (1,000 replicates) greater than 50% are shown.

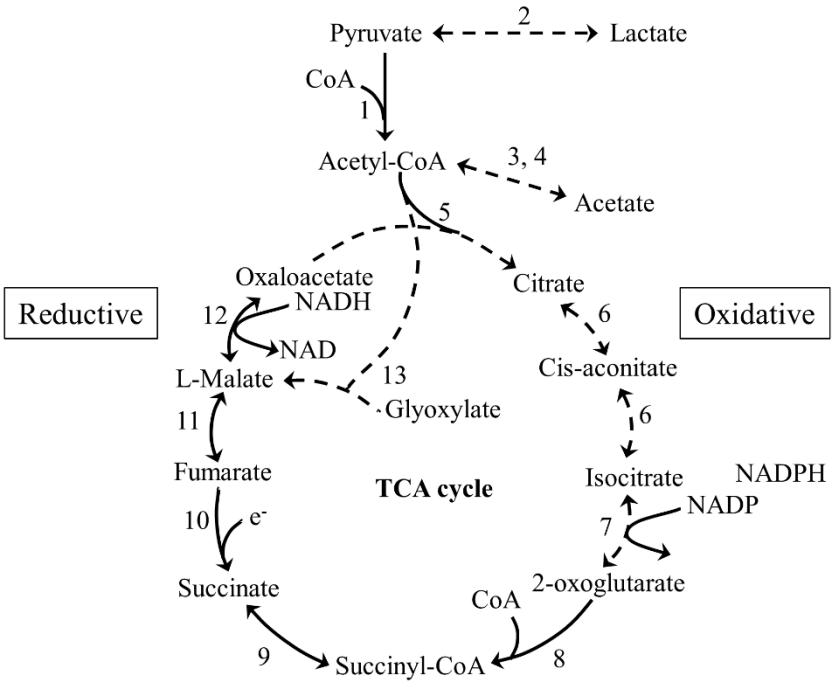

Figure 1.4. Predicted TCA cycle and related reactions in *Parasutterella*. Enzymes are labeled by numbers. 1, pyruvate:flavodoxin oxidoreductase; 2, L-lactate dehydrogenase; 3, phosphotransacetylase; 4, acetate kinase; 5, citrate synthase; 6, aconitase; 7, isocitrate dehydrogenase; 8, 2-oxoglutarate dehydrogenase multi-enzyme complex; 9, succinate-CoA synthetase; 10, fumarate reductase; 11, fumarase; 12, NAD-linked malate dehydrogenase malate:quinone oxidoreductase; 13, malate synthase. Solid lines indicate reactions involved in the TCA cycle of *Parasutterella* and the dashed lines represent the absent pathways based on predicted genes in the genome.

2. CHAPTER 2: INITIAL GUT MICROBIAL COMPOSITION AS A KEY FACTOR DRIVING HOST RESPONSE TO ANTIBIOTIC TREATMENT, AS EXEMPLIFIED BY THE PRESENCE OR ABSENCE OF COMMENSAL *ESCHERICHIA COLI*

2.1. Introduction

Antibiotics have been extensively used in the therapy of human and animal infections. The rational mechanisms of antibiotic therapies include decreasing bacterial density, eliminating targeted detrimental bacteria, inhibiting secondary bacterial proliferation, and reducing bacterial translocation, however, at the expense of strong alteration in the commensal microbiota (1). It is well-known that antibiotics have strong effects on the gut microbiota, resulting in imbalances of the microbial ecosystem and concomitantly affecting host physiology, particularly involving innate defense mechanisms (2–4). Antibiotic treatment that might help one individual can cause adverse outcomes in another (5). For instance, in inflammatory bowel disease (IBD) trials, antibiotic therapies using metronidazole and ciprofloxacin resulted in contradictory outcomes (6–8). Moreover, compositional changes of gut commensal microbiota in response to antibiotic therapies are variable between individuals. A large cohort study showed variation in the diversity and richness of antibiotic resistance genes in the human gut microbiota, which indicated the differences in altered microbiota by antibiotic usage (9). Administration of 500 mg ciprofloxacin twice a day for 5 days affected about 30% of bacterial taxa in the gut, however, with interindividual variation in the magnitude of the effect (10, 11). The mechanism by which antibiotic administration leads to inconsistent host outcome are not entirely clear.

Several studies have illustrated the importance of monitoring the initial composition of the gut microbiota prior to antibiotic administration. A recent human study, which

recruited 18 healthy volunteers to take a therapeutic dosage of the antibiotic cefprozil for a week, showed that a subset of participants had a dramatic increase of a specific group of bacteria in response to antibiotic treatment. The subset was participants who initially categorized as a *Bacteroides* enterotype with lower microbial diversity (12). While the study pointed out the necessity of monitoring initial microbial composition, it did not provide direct evidence of variations in host response resulting from the initial difference in the microbiota. The understanding of the host response underlying functional changes in the microbiota responding to antibiotic treatments remains limited, primarily because most studies to date have focused on compositional changes in microbiota and fail to provide information on corresponding changes in host response.

Our previous independent studies showed contradictory results for host gene expression of *MUC2*, regenerating islet-derived protein 3β (*Reg3β*) and regenerating islet-derived protein 3*γ* (*Reg3γ*) in the mouse colon in response to metronidazole administration ((13) and unpublished data). Metronidazole is a broad-spectrum antibiotic, which is highly active against gram-negative anaerobic microbes (14). It was first used by Shinn in 1962 to treat acute ulcerative gingivitis and more recently it has been extensively used in treating diseases such as IBD and *Clostridium difficile* infection (15). The colonic mucosal barrier plays an important role in protecting epithelium integrity and functionality. The secretion of mucus, which is predominated by secretory mucin MUC2, as well as other components such as antimicrobial peptides and immunoglobulins forms a complex biochemical matrix to maintain a dynamic and healthy barrier (16, 17). The C-type lectin Reg3β and Reg3γ are members of the REG gene family, which are antimicrobial peptides synthesized by Paneth cells in the small intestine and by crypt epithelium in the colon (18), and are a key element of

host defense supporting the mucosal barrier (19). Reg3β and Reg3γ have been reported to influence host-commensal and host-pathogen interactions in the GI tract, and regulate innate immune response (20, 21). It has been shown that metronidazole treatment significantly increased the expression of *Reg3γ* in the distal colon of mice, indicating increased microbial stimulation of the epithelium and weakened mucosal barrier (13). However, in subsequent unpublished studies we have observed reduced *Reg3γ* expression in response to metronidazole treatment. It was noted that in studies where *Reg3γ* dropped in response to metronidazole, there was a lack of *Escherichia coli,* whereas in experiments where *Reg3γ* increased, *E. coli* flourished in response to metronidazole treatment. Therefore, we hypothesized that the initial commensal microbiota, particularly the presence or absence of *E. coli*, contributed to the difference in the host response to metronidazole treatment. In this study, it is shown that the addition of a single commensal *E. coli* results in a distinct pattern of microbial shift and host response after metronidazole treatment. While this study focuses on a single commensal organism and a single antibiotic, it was designed as a proof of concept study to demonstrate that variations in membership of the pre-existing microbiota impact the subsequent change in microbial composition as well as the host response to antibiotic treatment.

2.2. Materials and methods

2.2.1. Mice. 6-8-week-old C57BL/6J female mice (Jackson Laboratory, Bar Harbor, ME) were housed in the animal facility at the University of Alberta. Mice were kept in filter-topped cages, fed autoclaved food and water, and handled in biosafety cabinet under specific pathogen-free (SPF) conditions. Mice were randomly grouped into eight cages with 4 mice per cage by a blinded lab animal technician and balanced for average body weight. Cages

were allocated to 4 treatments: control (CON), *E. coli* colonization (EC), metronidazole treatment (MET), and metronidazole treatment after *E. coli* colonization (EC-MET). The protocol of the study is shown in Figure 2.1A1. Briefly, mice from the group EC and EC-MET were exposed to a commensal *E. coli* by oral gavage, while group CON and MET received PBS. 10 days post-colonization, MET and EC-MET mice were given metronidazole (Sigma-Aldrich, Oakville, ON) at 750 mg/L in drinking water for 4 days, while the CON and EC groups continued on sterilized water. Mice were euthanized after 4 days of metronidazole/water administration and tissues were harvested. The experiment was repeated 3 times with the sample size of 4, 8, and 8, respectively (n = 20 in total).

To further investigate whether the effect of metronidazole on *E. coli* abundance and host response were transient or long-term, twenty mice were randomly grouped into eight cages with 2 or 3 mice per cage. The cages were allocated to 4 treatments as described above (n = 5). The procedure is shown in Figure 2.1A2 for the 14-day metronidazole treatment. Additionally, in order to study if the host response to metronidazole administration with the presence of *E. coli* is unique to the specific strain studied, two additional commensal *E. coli* were added to repeat the protocol as shown in Figure 2.1A1. Forty mice were randomly grouped into 16 cages with 2 or 3 mice per cage. The cages were allocated to 6 treatments (n = 5): control (CON), wild mouse *E. coli* isolate colonization (WMEC), rat *E. coli* isolate colonization (REC), metronidazole treatment (MET), metronidazole treatment after wild mouse *E. coli* isolate colonization (WMEC-MET) and after rat *E. coli* isolate colonization (REC-MET). The protocols employed were approved by the University of Alberta's Animal Care Committee and in direct accordance with the guideline of the Canadian Council on the Use of Laboratory Animals.

2.2.2. Bacterial strains. Commensal *E. coli* strains were isolated from a healthy NIH Swiss mouse (Harlan Laboratories, Inc., Indianapolis, IN), a wild mouse feces (glycerol stock), and rat feces on MacConkey agar. Bacterial strains were cultivated in 5 mL of Luria-Bertani (LB) medium (Fisher Scientific, Nepean, ON) at 37℃ for 16 h. The culture medium containing approximately 2.0×10^8 colony forming units (CFUs)/mL of *E. coli* was centrifuged at 5,000 x g for 10 min to harvest bacterial cells. Pellets of *E. coli* cells were suspended in 1 x PBS and mice were exposed to *E. coli* by oral gavage with 0.1 mL of suspension. Enumeration of *E. coli* was conducted by serial dilutions of fecal samples plated on MacConkey agar (BD, Sparks, MD) and total CFUs per gram fecal contents were then calculated.

2.2.3. Whole genome sequencing and annotation. To determine whether the *E. coli* isolated from a healthy mouse had any known virulence factors the genome was sequenced. The whole-genome sequence of the isolated commensal *E. coli* strain was generated on the Illumina Miseq Platform. Illumina fragment libraries were generated using Nextera XT DNA Library Preparation Kit (Illumina, San Diego, CA) and quantified by Qubit 2.0 Fluorometer (Invitrogen, Carlsbad, CA). Libraries were normalized to 2 nM and denatured using 0.1 N NaOH and mixed with 5% PhiX genomic DNA as the positive control. The sequencing flow cell cluster amplification was performed with 2 x 300 base paired-end reads on an Illumina MiSeq instrument, using the V3 MiSeq sequencing-by-synthesis kits (Illumina, San Diego, CA). The draft genome was assembled with the SPAdes assembler (22) and the Rapid Annotations using Subsystems Technology (RAST) (23) was used for genome annotation. IslandViewer was used for predicting toxin-related virulence in the whole genome of the *E. coli* isolate (24).

2.2.4. Tissue collection. Four days or 14 days after metronidazole treatment, mice were euthanized by CO_2 asphyxiation followed by cervical dislocation. The terminal 5 mm piece of distal colon was collected for histological analysis and the remaining colon tissue was harvested for subsequent gene expression and cytokine analysis. Colonic contents were collected for microbial composition analysis. All tissue samples were immediately placed in 10% neutral buffered formalin for histological studies or snap frozen in liquid nitrogen.

2.2.5. Microbial composition analysis. Total DNA was extracted from colonic contents using the QIA stool extraction kit (Qiagen Inc., Valencia, CA) with the addition of a bead-beating step as described in a previous study (25). Amplicon libraries were constructed from colonic content samples that amplified the V3-V4 region of the 16S rRNA gene according to the protocol from Illumina (16S Metagenomic Sequencing Library Preparation). Primers targeting the region were:
(Forward: 5'-TCGTCGGCAGCGTCAGATGTGTATAAGAGACAGCCTACGGGNGGCWGCAG-3';
Reverse: 5'-GTCTCGTGGGCTCGGAGATGTGTATAAGAGACAGGACTACHVGGGTATCTAATCC-3'). A paired-end sequencing run was performed on the Illumina MiSeq Platform (Illumina Inc. San Diego, CA) using 2 x 300 cycles. The raw sequence data obtained was filtered through a quality control pipeline, and bases with quality scores lower than 33 were filtered using FASTX-Toolkit. Paired-end sequencing reads were merged using the PANDAseq algorithm. The QIIME 1.9.1 (Quantitative Insight into Microbial Ecology) toolkit and Usearch version 7.1 was applied for obtaining an operational taxonomic units (OUTs) table (26, 27) using the following procedures. First, merged sequences were dereplicated and filtered for chimaeras against the ChimeraSlayer reference database. Secondly, the high-quality reads were mapped against the database of usearch_global and the OTU table was

obtained using the script of 'uc2otutab.py'. The classification of representative sequences for each OTU was carried out using the QIIME pipeline with the default algorithm of the Ribosome Database Project (RDP) classifier (confidence threshold, 80%). The Greengenes (GG) v.13_8 reference database clustered at 97% identity was used for assigning taxonomy. The alpha diversity parameters for the microbial community, including the Chao1 and Shannon index, were estimated by normalizing the number of sequences per sample to the lowest counts among all samples.

2.2.6. RNA isolation and cDNA synthesis. Colon tissue was excised, snap frozen in liquid nitrogen, and subsequently stored at -80℃ until RNA extraction. RNA was extracted using the GeneJET RNA Purification Kit (Thermo Scientific, Nepean, ON) following the manufacturer's instructions. The RNA quality was verified by gel electrophoresis using 2x RNA GEL Loading Dye (Thermo Scientific, Nepean, ON). The concentration of RNA was determined by a NanoDrop ND-2000 spectrophotometer (NanoDrop Technologies, Wilmington, DE) and 1 μg RNA was used for reverse transcription (RT) using the Maxima First Strand cDNA Synthesis kit (Thermo Scientific, Nepean, ON).

2.2.7. Quantitative polymerase chain reaction (qPCR). qPCR was performed using PerfeCTa SYBR Green Supermix (Quantabio, Gaithersburg, MD). Primers for host gene expression (*Reg3β*, *Reg3γ*, *MUC2*, and *IL-22*) are listed in Table 2.1. qPCR was conducted on an ABI StepOne™ real-time System (Applied Biosystems, Foster City, CA), and followed the cycles: 95℃ for 20 s and 40 cycles of 94℃ for 10 s, 60℃ for 30 s. Glyceraldehyde-3-phosphate dehydrogenase (*GAPDH*) was used as the housekeeping gene for normalization. The fold change of gene expression compared to the control group was calculated using the $2^{-\Delta\Delta Ct}$ method.

2.2.8 Cytokine determination. For protein extraction, 50-100 mg snap frozen colon tissues were stored at -80℃ and subsequently homogenized in 150 µL RIPA buffer which contains 50 mM Tris-HCl (pH = 8.0), 150 mM NaCl, 0.1% Triton X-100, 0.5% Sodium deoxycholate, 1 mM Sodium orthovanadate, 1 mM NaF, and Protease inhibitors cocktail (Sigma-Aldrich, Oakville, ON). The homogenates were centrifuged at 10,000 x g for 20 min, and the supernatant was collected. Protein concentrations in the supernatant were determined using the Pierce BCA protein assay kit (Thermo Scientific, Nepean, ON). The MSD Proinflammatory Panel 1 (mouse) kit (Meso Scale Discovery, Gaithersburg, MD) was used to quantify cytokines according to the manufacturer's recommendations with input protein concentration at 5 mg/mL. Cytokine concentrations were normalized to protein content.

2.2.9. Histology. The distal 5 mm of the colon were collected and immediately placed in 10% neutral buffered formalin at room temperature for 24 h, and then placed into 70% ethanol. Fixed tissue was embedded in paraffin, sectioned into 5 µm slices and subjected to hematoxylin and eosin (H&E) staining (13). Images were taken using an EVOS FL Auto Imaging System (Thermo Scientific, Nepean, ON). The well-oriented cross sections were assessed for pathology as previous described (13).

2.2.10. Statistical analysis and visualization. Data were analyzed in a completely randomized design and fixed effects of the treatment in the model were *E. coli* presence, metronidazole treatment, and their interaction. Mice were considered as the experimental unit. To compare the enumeration of *E. coli* at different time points, Kruskal-Wallis test was used to calculate *P* values and Dunn's test was used for multiple comparisons (SAS Inst. Inc., Cary, NC). Data of body weight, gene expression, cytokine and microbial abundance (regularized log (x + 1) transformed) were analyzed by PROC GLM with Bonferroni

correction in SAS. Microbial diversity indices (Chao1 and Shannon) for each sample was calculated using the vegan package in R (R 3.3.2). Results are expressed as mean value with standard error of the mean (SEM). Probability values less than 0.05 were considered as significant difference. Principle Component Analysis (PCA) derived from weighted UniFrac distance was performed to evaluate the overall difference between groups using the JMP software program (version 10.0.2, SAS Inst. Inc.). The permutational multivariate analysis of variance (adonis) was used to compare beta-diversity of four groups based on Bray-Curtis dissimilarities with permutations number of 999 using R. Correlation of colonic *E. coli* bacterial load with tumor necrosis factor-alpha (TNF-α) levels was analyzed by Spearman Rank Correlation using SAS. Graphpad Prism 6 software (Graphpad Software, Inc, La Jolla, CA) was used for data graphing.

2.2.11. Accession number(s). The whole genome sequence of the mice commensal *E. coli* isolate was deposited in the Sequence Read Archive (SRA) under accession number SUB2077929. Raw sequence reads of the 16S rRNA gene amplicon data are available through the SRA with accession number SUB2077113.

2.3. Results

2.3.1. Metronidazole stimulated an overgrowth of colonic commensal *E. coli*. A commensal *E. coli* was isolated from a fresh mouse fecal sample on MacConkey agar. The genome of the mouse *E. coli* isolate consisted of a single circular chromosome of 5,190,098 bp with an average GC content of 50.60%. The number of predicted unique genes encoded by the chromosome is 4,826. There were no identified hits of toxin virulence factors (VFs)-related genes in the genome of the *E. coli* isolate.

Wild-type C57BL/6 mice obtained from the Jackson laboratory were identified to be free of *E. coli* by the selective culture of fecal samples on MacConkey agar. The commensal *E. coli* successfully colonized the mouse intestine with a single dose in the EC and EC-MET group, ranging from 2.22 x 10^5 to 2.25 x 10^6 CFUs/g feces 2 days after exposure. The abundance varied from 1.07 x 10^5 to 6.21 x 10^6 CFUs/g feces 10 days after *E. coli* treatment, indicating the stability of *E. coli* colonization (Figure 2.1B). Enumeration of *E. coli* in mouse feces collected after 4 days metronidazole/water administration showed that *E. coli* were 6830-fold more abundant in the EC-MET group than the EC group (CFUs/g feces) (Figure 2.1B). Neither body weight loss nor death was observed with the colonization of *E. coli*. There were no differences in body weight between metronidazole treated groups and vehicle control groups (Figure 2.1C).

2.3.2. Metronidazole treatment reduced enteric microbial biodiversity. The intestinal microbiota after 4 days metronidazole/water treatment was characterized by sequencing of 16S rRNA gene tags (V3-V4 region) from colonic contents using Illumina MiSeq platform. The number of sequencing reads obtained was 3,134,825, with an average of 101,123 ± 36,174 (mean ± SD) quality-controlled and chimera-checked reads per sample. OTU clustering (97% cutoff) yielded a total of 535 OTUs for the entire data set, which included 373 OTUs associated with CON dataset, 167 OTUs with the MET group, 262 OTUs with the EC-MET group, and 320 OTUs with the EC group.

To evaluate phylogenetic richness and evenness of the intestinal microbiota, Chao1 diversity index and Shannon index were calculated in each sample. The numbers of sequences per library were normalized to 29,037 for the bacterial community according to the minimum reads number among all libraries. *E. coli* x metronidazole interactions were

observed in Chao1 ($P < 0.05$) and Shannon indexes ($P < 0.01$) (Figure 2.2A). The Chao1 index and Shannon values of the intestinal microbiota in CON and EC were significantly higher than that in both metronidazole treated groups, indicating a lower alpha diversity resulted from metronidazole treatment ($P < 0.05$) (Figure 2.2A). When treated with metronidazole, the group with *E. coli* colonization showed a greater reduction in alpha diversity than the MET group (Shannon index, $P < 0.05$; Figure 2.2A).

2.3.3. Overall structural changes of gut microbiota in response to metronidazole. To assess the abundance profile of different phyla and genera, all sequences were assigned to taxonomy using RDP Classifier. There were significant differences between groups at different taxonomic levels. Bacteroidetes was the most predominant phylum in the CON and EC groups, contributing an average of 77.8% and 72.6% of the microbial communities, respectively. Firmicutes was the next most dominant phylum, representing an average of 21.5% and 26.2%, respectively. In the MET group, the most abundant phylum was Firmicutes (71.7%), while Actinobacteria (23.2%) and Verrucomicrobia (4.6%) constituted the next most abundant phyla. However, in EC-MET group, Proteobacteria was the dominant phylum with 81.8% of the microbiota, and with much less Firmicutes (10.1%), Actinobacteria (6.2%), and Bacteroidetes (1.8%) (Figure 2.2B). Principal component analysis based on weighted UniFrac distance revealed distinct clustering of MET and EC-MET groups but no separation of CON and EC group based on the first two principal component (PC) scores, which accounted for 88.30% and 9.82% of the total variation, respectively (Figure 2.3A). The permutational multivariate analysis of variance (adonis) exhibited the separation of MET and EC-MET groups from the CON and EC group ($P < 0.01$).

Multivariate analysis performed on the OTUs suggested that colonization of *E. coli* isolate did not result in major shifts in microbial composition compared to the microbial profile in the CON group. The most profound changes were the enrichment of genera *Allobaculum* (0.65% vs. 0.04%, $P < 0.01$), *Akkermansia* (0.85% vs. 0.2%, $P < 0.01$), *Lactobacillus* (2.16% vs. 0.76%, $P < 0.01$), and *Ruminococcus* (0.66% vs. 0.29%, $P < 0.01$) in EC vs. CON (Figure 2.2B). In addition, the microbiota in the MET group underwent profound losses ($P < 0.05$) of genera *Clostridiales*_unclassified and *Rikenellaceae*_unclassified and became dominated by *Lactobacillus*, *Bifidobacterium*, *Enterococcaceae*_unclassified, *Turicibacter*, and *Akkermansia* species in comparison to CON and EC group (Figure 2.2B; Figure 2.3B). However, with the presence of *E. coli*, metronidazole treatment induced a distinct pattern of microbial composition. The EC-MET group showed marked expansion of *Enterobacteriaceae* proportions (represented by only the inoculated *E. coli*) compared to the EC group (81.74% vs. 0.02%) and contractions of previously dominant populations, which were substantial for *Bacteroidales_S24-7*_unclassified and *Clostridiales*_unclassified, and modest for *Turicibacter* (Figure 2.2B; Figure 2.3B). The presence of *E. coli* and metronidazole administration interacted in producing significant effects on the abundance of certain bacterial families including *Bifidobacteriaceae*, *Lactobacillaceae*, *Enterococcaceae*, and *Enterobacteriaceae* (Figure 2.3B). The distinct effect of metronidazole on colonic microbial composition confirms that the alterations in bacterial communities were highly dependent on the presence of *E. coli* before antibiotic administration.

Because analysis of microbial composition is based on relative abundance, and the increase in *E. coli* alone could reduce relative abundance of other taxa without reducing their

actual number, the microbiota of EC-MET to MET groups were compared with the OTU representing *E. coli* removed. Even with *E. coli* removed from the analysis, community composition based on beta-diversity was still significantly different between EC-MET and MET groups (adonis analysis, $P < 0.05$; permutations number of 999). In addition, there were differences in the abundance of some genera between metronidazole treated groups including a reduced abundance of *Turicibacteraceae* in the EC-MET group (17.9 ± 5.81%, mean ± SEM) compared to the MET (0.69 ± 0.23%, mean ± SEM) group.

2.3.4. Host response to metronidazole is driven by initial bacterial composition.

As mentioned above, our previous studies in mice showed inconsistent changes in mRNA expression of host antimicrobial protein Reg3γ in response to metronidazole treatment. Based on the hypothesis that the pre-existing gut microbiota may play a role in driving the difference in host response towards antibiotics administration, the mRNA expression of *Reg3β*, *Reg3γ*, *MUC2*, and *IL-22* were analyzed using qPCR assay. As shown in Figure 2.4A, EC-MET mice exhibited a significant increase in mRNA expression of both *Reg3β* and *Reg3γ* compared to that in the CON group ($P < 0.05$). Mice without *E. coli* colonization showed substantial variation (7.94 ± 4.43 fold change, mean ± SEM) in *Reg3β* mRNA expression level in response to metronidazole treatment whereas the group with *E. coli* showed a consistent increase in *Reg3β* expression (13.07 ± 2.07 fold change, mean ± SEM) with metronidazole treatment (Figure 2.4A). In contrast, the increased mRNA expression of *Reg3γ* in response to metronidazole treatment was tightly associated with the enrichment of *E. coli* (Figure 2.4B). It has been reported that metronidazole treatment induced a reduction in *MUC2* mRNA expression and a thinning of the mucus layer in the distal colon in mice (13). In the current study, colonization of *E. coli* tended to stimulate the mRNA expression of

MUC2 ($0.05 < P \leq 0.1$) (Figure 2.4C). Although the MET group had slightly lower expression levels of *MUC2* mRNA, there was no significant difference between the MET and the CON group in *MUC2* expression. There was no significant change in *IL-22* expression detected in the MET, EC, and EC-MET group compared to CON ($P > 0.05$, Figure 2.4D).

To determine whether increased *Reg3β* and *Reg3γ* expression were associated with intestinal inflammation, colonic cytokines were measured by ELISA. The most profound change in the colonic cytokine profile was the level of TNF-α, as shown in Figure 2.5A1. TNF-α was induced in EC-MET mice as compared to all other treatment groups ($P < 0.01$). There was an *E. coli* x metronidazole interaction for the expression level of TNF-α ($P < 0.05$), which indicated that the combination of *E. coli* and metronidazole was required to drive this response. Metronidazole treatment in the absence of *E. coli* did not increase TNF-α, however did increase the expression level of IL-1β ($P < 0.05$), IL-6 ($P < 0.01$), and IL-10 ($P < 0.01$) (Figure 2.5B).

The correlation between the enriched *E. coli* abundance in the EC-MET group and levels of TNF-α was analyzed using Spearman's rank correlation. As shown in Figure 2.5A2, there was a trend for TNF-α expression levels to be correlated with colonic *E. coli* counts ($r = 0.643$, $P = 0.096$). Collectively, there was a clear pattern of increased pro-inflammatory cytokines in *E. coli* colonized mice in response to metronidazole administration (TNF-α), though the histological analysis of distal colon sections from all groups did not show significant evidence of inflammation (Figure 2.6). In contrast, with the absence of *E. coli*, the MET group did not exhibit upregulation of TNF-α. The result suggested that the immune homeostatic imbalance of colonic epithelium triggered by metronidazole treatment was driven by the initial commensal microbial composition profile.

In the long-term metronidazole treatment experiment, the stimulating effects of metronidazole on colonic commensal *E. coli* growth was stable (Figure 2.7A1). The abundance of *E. coli* after metronidazole treatment for 14 days ranged from 1.50 x 10^8 to 2.08 x 10^{10} CFUs/g feces, whereas the abundance of *E. coli* in the group that received water for 14 days varied from 7.50 x 10^4 to 9.44 x 10^5 CFUs/g feces (Figure 2.7A1). With the overgrowth of *E. coli* during the long-term metronidazole administration, the expression level of *Reg3β* and *Reg3γ* mRNA persisted ($P < 0.05$) (Figure 2.7A2; Figure 2.7A3).

Commensal *E. coli* strains isolated from a wild mouse and healthy rat stably colonized the mouse intestine with an average abundance of 5.57 x 10^6 and 1.15 x 10^5 CFUs/g feces, respectively. Four-day metronidazole treatment significantly increased the abundance of *E. coli* to an average of 3.35 x 10^9 and 1.24 x 10^9 CFUs/g feces, in WMEC-MET and REC-MET respectively (Figure 2.7B1; Figure 2.7C1). In the wild mouse *E. coli* isolate colonized mice, metronidazole administration also increased ($P < 0.05$) the expression level of *Reg3β* and *Reg3γ* mRNA, which were 2.8- and 7.7-fold change respectively compared to the level in the CON group (Figure 2.7B2; Figure 2.7B3). However, in the rat *E. coli* isolate colonized mice, metronidazole did not significantly affect the expression of these two genes in conjunction with *E. coli* proliferation (Figure 2.7C2; Figure 2.7C3).

2.4. Discussion

The result of this study showed that the pre-existing composition of commensal microbes plays an important role in how the host responds to antibiotic treatment. In particular, the presence or absence of a commensal *E. coli* impacts mucosal immunity of the colon and alters the shift in microbial composition induced by metronidazole treatment. Our current study showed that metronidazole administration dramatically reduced the biodiversity

of the gut microbiota, as indicated by Chao1 and Shannon index. Changes in the gut microbiome largely reflected an increase in *E. coli,* which induced the expression of genes coding antimicrobial peptides and inflammation.

It is well recognized that broad-spectrum antibiotics significantly reduce the richness and evenness of the intestinal microbiota (28, 29). In the current study, we have observed lower biodiversity in the gut microbiota after four-day metronidazole treatment. Within the metronidazole treated mice, the presence of *E. coli* accelerated the reduction in the diversity of the gut microbiota, as indicated by Shannon index. The observation suggested that the gut microbial composition before metronidazole treatment could be predictive of the degree of reduction in diversity, at least for this specific antibiotic administration.

Previously published studies have shown that metronidazole treatment induced a significant disturbance in the microbial composition of the colon, targeting the depletion of obligate anaerobic *Bacteroidales* communities (13, 14, 31). Consistent with previous findings, the comparison of the MET group and CON group exhibited a dramatic decrease in the relative abundance of the family *Bacteroidales_S24-7.* Studies in human and animal models have demonstrated that broad-spectrum antibiotics targeting specific pathogenic organisms can influence the commensal microbial community to a much greater degree than previously assumed. A recent study, which used metronidazole and vancomycin to treat wild-type C57BL/6 mice from Jackson Laboratory, showed that genera *Enterococcus*, unclassified_*Proteobacteria*, novel members of *Lactobacillus* and *Clostridium* greatly expanded with metronidazole treatment, while *Lactobacillus aviaries*, *Enterococcus faecalis*, *Klebsiella oxytoca*, and *Akkermansia muciniphilia* expanded with vancomycin. Moreover, the author observed that the expanding population was highly dependent on initially colonized

communities (31). Another study reported that a single dose of clindamycin treatment for one day in mice resulted in generally similar expansions and contractions of the gut microbiota, but occasional differences between individuals were observed. The author concluded that these differences between individuals were likely due to subtle differences in the initial commensal microbiota (32). Concordant with previous studies, we observed a great expansion of *Enterococcus*, *Lactobacillus* and *Clostridium* compared to the initial point in the MET group. In addition, the presence of commensal *E. coli* resulted in a very different expansion, showing remarkable effects of a subtle difference in the initial microbiota. It has been widely recognized that the composition of human gut microbiota varies among individuals as a result of different selection pressure from the host, microbial ecosystem, and environment. Therefore, it is essential to be aware of the initial difference when evaluating the outcome from antibiotic treatments.

In the current study, there was a distinct host response to metronidazole treatment with respect to innate immunity as well as mucosal homeostasis due to the addition of a single commensal microorganism to the initial microbiota. The evidence has correlated changes in host innate mucosal immunity with commensal microorganisms in previous studies. Acute colonization with commensal Schaedler's *E. coli* in immune competent germ-free BALB/c mice resulted in 1.6 to 3.5-fold induction of *Reg3β* and *Reg3γ* and no induction of *IFN-γ* (33). In the current study, the addition of *E. coli* alone did not result in an increased expression of *Reg3β* and *Reg3γ*. This likely reflects the much greater degree to which *E. coli* will colonize in a germ-free as compared to the conventional animal (34). Interestingly, in another study where germ-free C57BL/6 mice were monocolonized with a non-host adapted commensal *E. coli* JM83 strain for three weeks, *Reg3γ* expression was not increased (35), indicating *E. coli*

must be somewhat host-adapted and have the ability to penetrate to the mucosal surface to elicit this response. It has been reported that *Lactobacillus reuteri* exhibited different host-adapted lineages in mice, indicating the evolutionary host-driven diversification (36). In addition, a study using a germ-free mouse model colonized with single commensal bacterium clearly showed that *Reg3γ* is not driven by an enriched total number of bacteria but triggered by increased microbial-epithelial contact at the mucosal surface (18, 20). The increased expression of *Reg3β* and *Reg3γ* genes have been associated with an inflammatory response and bacterial reconstitution, which was accompanied by strengthened communication between gut commensal bacteria and mucosal surface (37). In the current study, the elicited expression of *Reg3β* and *Reg3γ* genes in the EC-MET (both 4 days and 14 days) and WMEC-MET group is likely due to increased contact between commensal bacteria and the mucosal surface, which is stimulated by the imbalanced microbiota to fortify epithelial barrier function. The lack of increase observed in *Reg3β* and *Reg3γ* genes in REC-MET group may reveal that host-adaptation is a prerequisite for the stimulation of gut epithelium by gut commensal bacteria.

The evidence has suggested that IL-22 is a key element for directly inducing the expression of Reg3γ in the colon (38, 39), however, increased *IL-22* mRNA expression was not observed in the current study. It has been shown that *Bifidobacterium breve* NCC2950 induced Reg3γ in the absence of IL-22, implying that the induction of the Reg3 family involves multiple pathways (35). Therefore, the induced expression of *Reg3β* and *Reg3γ* in the current study is likely through a non-IL-22 mediated mechanism.

Metronidazole treatment of C57BL/6 mice has previously been shown to reduce the mRNA expression of *MUC2*, which resulted in a thinner mucus layer (13). However, it has

been reported that metronidazole administration in rats increased bacteria penetrating the crypts and a thickening of the mucus layer in the proximal colon (40). In the current study, *E. coli* colonization significantly increased the expression of *MUC2* while metronidazole treatment didn't impact the expression of the gene. This difference may be explained by the nature of the shifts in the microbiome seen in the previous rat study as compared to the current study; supporting the concept that response to antibiotic treatment will vary depending on the pre-existing microbiota.

An array of cytokines was analyzed in the colon of mice in response to antibiotic treatment as an indicator of intestinal inflammation. The result showed a trend for a correlation between *E. coli* enrichment and the expression of TNF-α. Studies in different models, especially *in vitro* cell culture, have reported the stimulation of inflammatory cytokines by commensal bacteria. It has been reported that a commensal *E. coli* strain stimulated Caco-2 cells to produce TNF-α and IL-1β, but did not induce secretion of IFN-γ, IL-4, or IL-12 in Caco-2 cells (41). The increase of TNF-α expression by commensal *E. coli* has been shown in the HT-29 cell line model as well (42). TNF-α is a proinflammatory cytokine for which expression is enhanced by a variety of stimuli such as bacterial endotoxin (LPS) (43). The changes in this proinflammatory related cytokine in the current study suggest that with the acute and strong expansion of commensal *E. coli* in response to metronidazole treatment, the microbial changes triggered an imbalance in immune homeostasis. The immune homeostatic imbalance is likely due to the increase in contact between commensal bacteria and intestinal epithelium resulting from *E. coli* expansion, and in turn, the imbalance in immune homeostasis may further exaggerate the alteration of the gut microbiota.

While the relationship between *E. coli* and metronidazole is of direct interest, this study provides proof of concept in how care must be taken using antibiotics as a study tool since the difference in results from one experiment to the next can be attributed to the pre-existing microbiota. Furthermore, the study demonstrated that initial gut microbial composition is a key factor driving host response to antibiotic administration, creating a compelling argument to consider personalized medication based on individual variations in the gut microbiota.

2.5. References

1. Sartor RB. 2004. Therapeutic manipulation of the enteric microflora in inflammatory bowel diseases: antibiotics, probiotics, and prebiotics. Gastroenterology 126:1620–1633.
2. Jernberg C, Löfmark S, Edlund C, Jansson JK. 2007. Long-term ecological impacts of antibiotic administration on the human intestinal microbiota. ISME J 1:56–66.
3. Jernberg C, Löfmark S, Edlund C, Jansson JK. 2010. Long-term impacts of antibiotic exposure on the human intestinal microbiota. Microbiology 156:3216–3223.
4. Willing BP, Russell SL, Finlay BB. 2011. Shifting the balance: antibiotic effects on host-microbiota mutualism. Nat Rev Microbiol 9:233–243.
5. Langdon A, Crook N, Dantas G. 2016. The effects of antibiotics on the microbiome throughout development and alternative approaches for therapeutic modulation. Genome Med 8:39.
6. Colombel JF, Lemann M, Cassagnou M, Bouhnik Y, Duclos B, Dupas JL, Notteghem B, Mary JY. 1999. A controlled trial comparing ciprofloxacin with mesalazine for the treatment of active Crohn's disease. Groupe d'Etudes Therapeutiques des Affections Inflammatoires Digestives (GETAID). Am J Gastroenterol 94:674–678.
7. Arnold GL, Beaves MR, Pryjdun VO, Mook WJ. 2002. Preliminary study of ciprofloxacin in active Crohn's disease. Inflamm Bowel Dis 8:10–15.
8. Guslandi M. 2005. Antibiotics for inflammatory bowel disease: do they work? Eur J Gastroenterol Hepatol 17:145–147.

9. Hu Y, Yang X, Qin J, Lu N, Cheng G, Wu N, Pan Y, Li J, Zhu L, Wang X, Meng Z, Zhao F, Liu D, Ma J, Qin N, Xiang C, Xiao Y, Li L, Yang H, Wang J, Yang R, Gao GF, Wang J, Zhu B. 2013. Metagenome-wide analysis of antibiotic resistance genes in a large cohort of human gut microbiota. Nat Commun 4:2151.
10. Dethlefsen L, Huse S, Sogin ML, Relman DA. 2008. The pervasive effects of an antibiotic on the human gut microbiota, as revealed by deep 16s rRNA sequencing. PLoS Biol 6:e280.
11. Dethlefsen L, Relman DA. 2011. Incomplete recovery and individualized responses of the human distal gut microbiota to repeated antibiotic perturbation. Proc Natl Acad Sci U S A 1:4554–4561.
12. Raymond F, Ouameur A a, Déraspe M, Iqbal N, Gingras H, Dridi B, Leprohon P, Plante P-L, Giroux R, Bérubé È, Frenette J, Boudreau DK, Simard J-L, Chabot I, Domingo M-C, Trottier S, Boissinot M, Huletsky A, Roy PH, Ouellette M, Bergeron MG, Corbeil J. 2015. The initial state of the human gut microbiome determines its reshaping by antibiotics. ISME J 10:707–720.
13. Wlodarska M, Willing B, Keeney KM, Menendez A, Bergstrom KS, Gill N, Russell SL, Vallance BA, Finlay BB. 2011. Antibiotic treatment alters the colonic mucus layer and predisposes the host to exacerbated *Citrobacter rodentium*-induced colitis. Infect Immun 79:1536–1545.
14. Löfmark S, Edlund C, Nord CE. 2010. Metronidazole is still the drug of choice for treatment of anaerobic infections. Clin Infect Dis 50:16–23.
15. Eykyn SJ, Phillips I. 1976. Metronidazole and anaerobic sepsis. BrMedJ 2:1418–1421.
16. Van der Sluis M, De Koning BAE, De Bruijn ACJM, Velcich A, Meijerink JPP, Van Goudoever JB, Büller HA, Dekker J, Van Seuningen I, Renes IB, Einerhand AWC. 2006. Muc2-deficient mice spontaneously develop colitis, indicating that MUC2 is critical for colonic protection. Gastroenterology 131:117–129.
17. Zarepour M, Bhullar K, Montero M, Ma C, Huang T, Velcich A, Xia L, Vallance BA. 2013. The mucin Muc2 limits pathogen burdens and epithelial barrier dysfunction during *Salmonella enterica* serovar typhimurium colitis. Infect Immun 81:3672–3683.

18. Vaishnava S, Yamamoto M, Severson KM, Ruhn KA, Yu X, Koren O, Ley R, Wakeland EK, Hooper L V. 2011. The antibacterial lectin RegIIIgamma promotes the spatial segregation of microbiota and host in the intestine. Science 334:255–258.
19. Hiemstra PS. 2001. Epithelial antimicrobial peptides and proteins: their role in host defence and inflammation. Paediatr Respir Rev 2:306–310.
20. Cash HL, Whitham C V, Behrendt CL, Hooper L V. 2006. Symbiotic bacteria direct expression of an intestinal bactericidal lectin. Science 313:1126–1130.
21. Brandl K, Plitas G, Schnabl B, DeMatteo RP, Pamer EG. 2007. MyD88-mediated signals induce the bactericidal lectin RegIIIγ and protect mice against intestinal *Listeria monocytogenes* infection. J Exp Med 204:1891–1900.
22. Bankevich A, Nurk S, Antipov D, Gurevich AA., Dvorkin M, Kulikov AS, Lesin VM, Nikolenko SI, Pham S, Prjibelski AD, Pyshkin AV, Sirotkin AV, Vyahhi N, Tesler G, Alekseyev MA, Pevzner PA. 2012. SPAdes: a new genome assembly algorithm and its applications to single-cell sequencing. J Comput Biol 19:455–477.
23. Aziz RK, Bartels D, Best AA, DeJongh M, Disz T, Edwards RA, Formsma K, Gerdes S, Glass EM, Kubal M, Meyer F, Olsen GJ, Olson R, Osterman AL, Overbeek RA, McNeil LK, Paarmann D, Paczian T, Parrello B, Pusch GD, Reich C, Stevens R, Vassieva O, Vonstein V, Wilke A, Zagnitko O. 2008. The RAST Server: rapid annotations using subsystems technology. BMC Genomics 9:75.
24. Dhillon BK, Laird MR, Shay JA, Winsor GL, Lo R, Nizam F, Pereira SK, Waglechner N, McArthur AG, Langille MGI, Brinkman FSL. 2015. IslandViewer 3: more flexible, interactive genomic island discovery, visualization and analysis. Nucleic Acids Res 43:W104–W108.
25. Willing BP, Vacharaksa A, Croxen M, Thanachayanont T, Finlay BB. 2011. Altering host resistance to infections through microbial transplantation. PLoS One 6:e26988.
26. Caporaso JG, Kuczynski J, Stombaugh J, Bittinger K, Bushman FD, Costello EK, Fierer N, Peña AG, Goodrich JK, Gordon JI, Huttley GA, Kelley ST, Knights D, Koenig JE, Ley RE, Lozupone CA, McDonald D, Muegge BD, Pirrung M, Reeder J, Sevinsky JR, Turnbaugh PJ, Walters WA, Widmann J, Yatsunenko T, Zaneveld J, Knight R. 2010. QIIME allows analysis of high-throughput community sequencing data. Nat Methods 7:335–336.

27. Edgar RC. 2010. Search and clustering orders of magnitude faster than BLAST. Bioinformatics 26:2460–2461.
28. Perez-Cobas AE, Gosalbes MJ, Friedrichs A, Knecht H, Artacho A, Eismann K, Otto W, Rojo D, Bargiela R, von Bergen M, Neulinger SC, Daumer C, Heinsen FA, Latorre A, Barbas C, Seifert J, Santos VM Dos, Ott SJ, Ferrer M, Moya A, Pérez-Cobas AE, Bergen M Von, Däumer C, Martins V, Dos Santos VM. 2012. Gut microbiota disturbance during antibiotic therapy: a multi-omic approach. Gut 62:1591–1601.
29. Francino MP. 2016. Antibiotics and the human gut microbiome: dysbioses and accumulation of resistances. Front Microbiol 6:1543.
30. Gerritsen J, Smidt H, Rijkers GT, De Vos WM. 2011. Intestinal microbiota in human health and disease: the impact of probiotics. Genes Nutr 6:209–240.
31. Lewis BB, Buffie CG, Carter RA, Leiner I, Toussaint NC, Miller LC, Gobourne A, Ling L, Pamer EG. 2015. Loss of microbiota-mediated colonization resistance to *Clostridium difficile* infection with oral vancomycin compared with metronidazole. J Infect Dis 212:1656–1665.
32. Buffie CG, Jarchum I, Equinda M, Lipuma L, Gobourne A, Viale A, Ubeda C, Xavier J, Pamer EG. 2012. Profound alterations of intestinal microbiota following a single dose of clindamycin results in sustained susceptibility to *Clostridium difficile*-induced colitis. Infect Immun 80:62–73.
33. Keilbaugh S a, Shin ME, Banchereau RF, McVay LD, Boyko N, Artis D, Cebra JJ, Wu GD. 2005. Activation of RegIIIbeta/gamma and interferon gamma expression in the intestinal tract of SCID mice: an innate response to bacterial colonisation of the gut. Gut 54:623–629.
34. Willing BP, Van Kessel AG. 2007. Enterocyte proliferation and apoptosis in the caudal small intestine is influenced by the composition of colonizing commensal bacteria in the neonatal gnotobiotic pig. J Anim Sci 85:3256–3266.
35. Natividad JM, Hayes CL, Motta JP, Jury J, Galipeau HJ, Philip V, Garcia-Rodenas CL, Kiyama H, Bercik P, Verdu EF. 2013. Differential induction of antimicrobial REGIII by the intestinal microbiota and *Bifidobacterium breve* NCC2950. Appl Environ Microbiol 79:7745–7754.

36. Oh PL, Benson AK, Peterson DA, Patil PB, Moriyama EN, Roos S, Walter J, Lantbruksuniversitet S. 2010. Diversification of the gut symbiont *Lactobacillus reuteri* as a result of host-driven evolution. ISME J 4:377–387.
37. Loonen LMP, Stolte EH, Jaklofsky MTJ, Meijerink M, Dekker J, van Baarlen P, Wells JM. 2014. REG3γ-deficient mice have altered mucus distribution and increased mucosal inflammatory responses to the microbiota and enteric pathogens in the ileum. Mucosal Immunol 7:939–947.
38. Zheng Y, Valdez PA, Danilenko DM, Hu Y, Sa SM, Gong Q, Abbas AR, Modrusan Z, Ghilardi N, de Sauvage FJ, Ouyang W. 2008. Interleukin-22 mediates early host defense against attaching and effacing bacterial pathogens. Nat Med 14:282–289.
39. Sanos SL, Vonarbourg C, Mortha A, Diefenbach A. 2011. Control of epithelial cell function by interleukin-22-producing RORγt$^+$ innate lymphoid cells. Immunology 132:453–465.
40. Pélissier MA, Vasquez N, Balamurugan R, Pereira E, Dossou-Yovo F, Suau A, Pochart P, Magne F. 2010. Metronidazole effects on microbiota and mucus layer thickness in the rat gut. FEMS Microbiol Ecol 73:601–610.
41. Haller D, Bode C, Hammes WP, Pfeifer AM, Schiffrin EJ, Blum S. 2000. Non-pathogenic bacteria elicit a differential cytokine response by intestinal epithelial cell/leucocyte co-cultures. Gut 47:79–87.
42. Bahrami B, Macfarlane S, Macfarlane GT. 2011. Induction of cytokine formation by human intestinal bacteria in gut epithelial cell lines. J Appl Microbiol 110:353–363.
43. De Plaen IG, Tan XD, Chang H, Wang L, Remick DG, Hsueh W. 2000. Lipopolysaccharide activates nuclear factor kappaB in rat intestine: role of endogenous platelet-activating factor and tumour necrosis factor. Br J Pharmacol 129:307–314.
44. Goodrich ME, McGee DW. 1999. Effect of intestinal epithelial cell cytokines on mucosal B-cell IgA secretion: enhancing effect of epithelial-derived IL-6 but not TGF-β on IgA$^+$ B cells. Immunol Lett 67:11–14.
45. Vinderola G, Matar C, Perdigon G. 2005. Role of intestinal epithelial cells in immune effects mediated by gram-positive probiotic bacteria: involvement of toll-like receptors. Clin Diagn Lab Immunol 12:1075–1084.

46. Kuhn KA, Manieri NA, Liu TC, Stappenbeck TS. 2014. IL-6 stimulates intestinal epithelial proliferation and repair after injury. PLoS One 9:e114195.
47. Curtis MM, Hu Z, Klimko C, Narayanan S, Deberardinis R, Sperandio V. 2014. The gut commensal *Bacteroides thetaiotaomicron* exacerbates enteric infection through modification of the metabolic landscape. Cell Host Microbe 16:759–769.
48. Hoebler C, Gaudier E, De Coppet P, Rival M, Cherbut C. 2006. MUC genes are differently expressed during onset and maintenance of inflammation in dextran sodium sulfate-treated mice. Dig Dis Sci 51:381–389.
49. Satoh-Takayama N, Serafini N, Verrier T, Rekiki A, Renauld JC, Frankel G, DiSanto J. 2014. The chemokine receptor CXCR6 controls the functional topography of interleukin-22 producing intestinal innate lymphoid cells. Immunity 41:776–788.

Table 2.1. Primers and thermal cycling profiles for qPCR analysis

Targeted genes	Oligonucleotides sequences (5'-3')	Annealing Tm (°C)	Ref
Reg3β	Forward: GGCTTCATTCTTGTCCTCCA	60	(47)
	Reverse: TCCACCTCCATTGGGTTCT		
Reg3γ	Forward: AAGCTTCCTTCCTGTCCTCC	60	(47)
	Reverse: TCCACCTCTGTTGGGTTCAT		
MUC2	Forward: GCTGACGAGTGGTTGGTGAATG	60	(48)
	Reverse: GATGAGGTGGCAGACAGGAGAC		
IL-22	Forward: TTGAGGTGTCCAACTTCCAGCA	60	(49)
	Reverse: AGCCGGACGTCTGTGTTGTTA		
GAPDH	Forward: ATTGTCAGCAATGCATCCTG	60	(15)
	Reverse: ATGGACTGTGGTCATGAGCC		

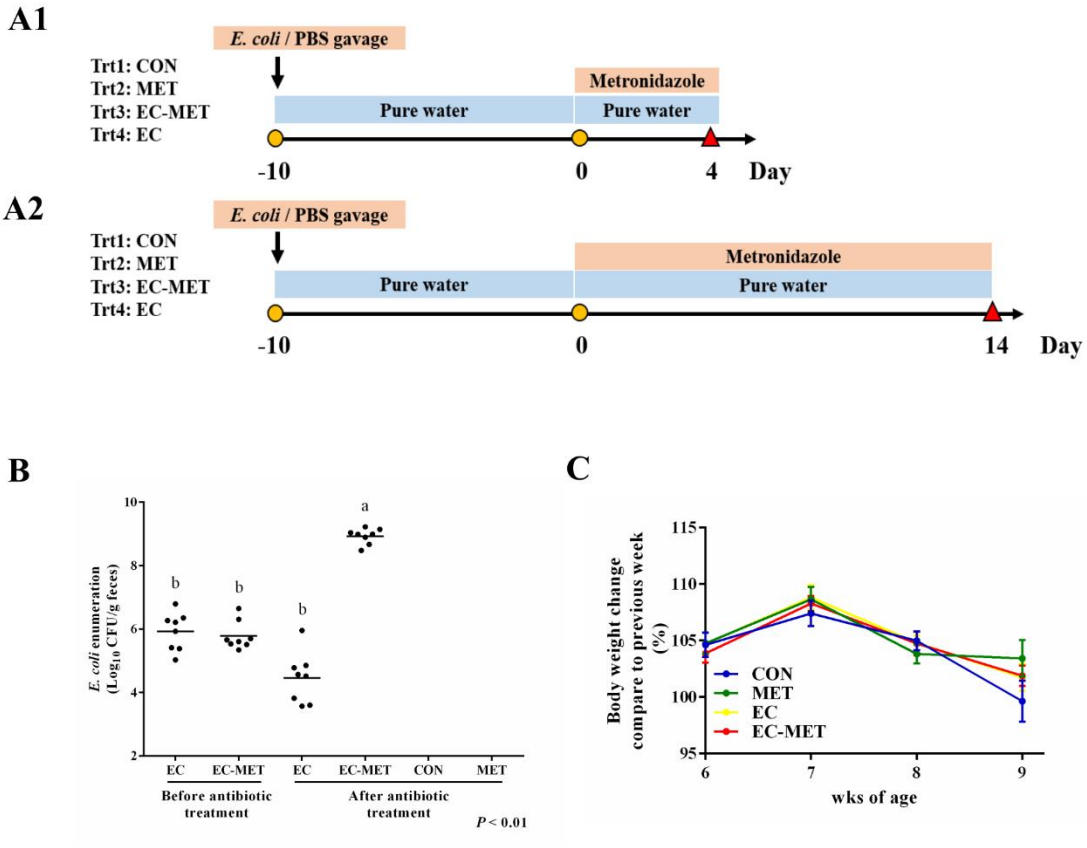

Figure 2.1. Experimental protocol. *E. coli*: Re-suspend bacteria in PBS with a concentration of 2.0 x 10^8 CFUs/mL was given to mice (0.1 mL/each mouse). Metronidazole: 750 mg/L in drinking water. Body weight was recorded weekly. Mice were sacrificed on **A1)** Day 4 or **A2**) Day 14. **B**) Enumeration of *E. coli* in mouse feces before metronidazole treatment and 4 days after metronidazole/water administration. Dots represent individual mice and lines depict the mean values. **C**) Body weight changes during the *E. coli* treatment and 4 days metronidazole/water treatment. For all treatment groups, n = 8. Data are shown as mean ± SEM. [a,b] Means that do not share a common letter are significantly different. $\alpha = 0.05$.

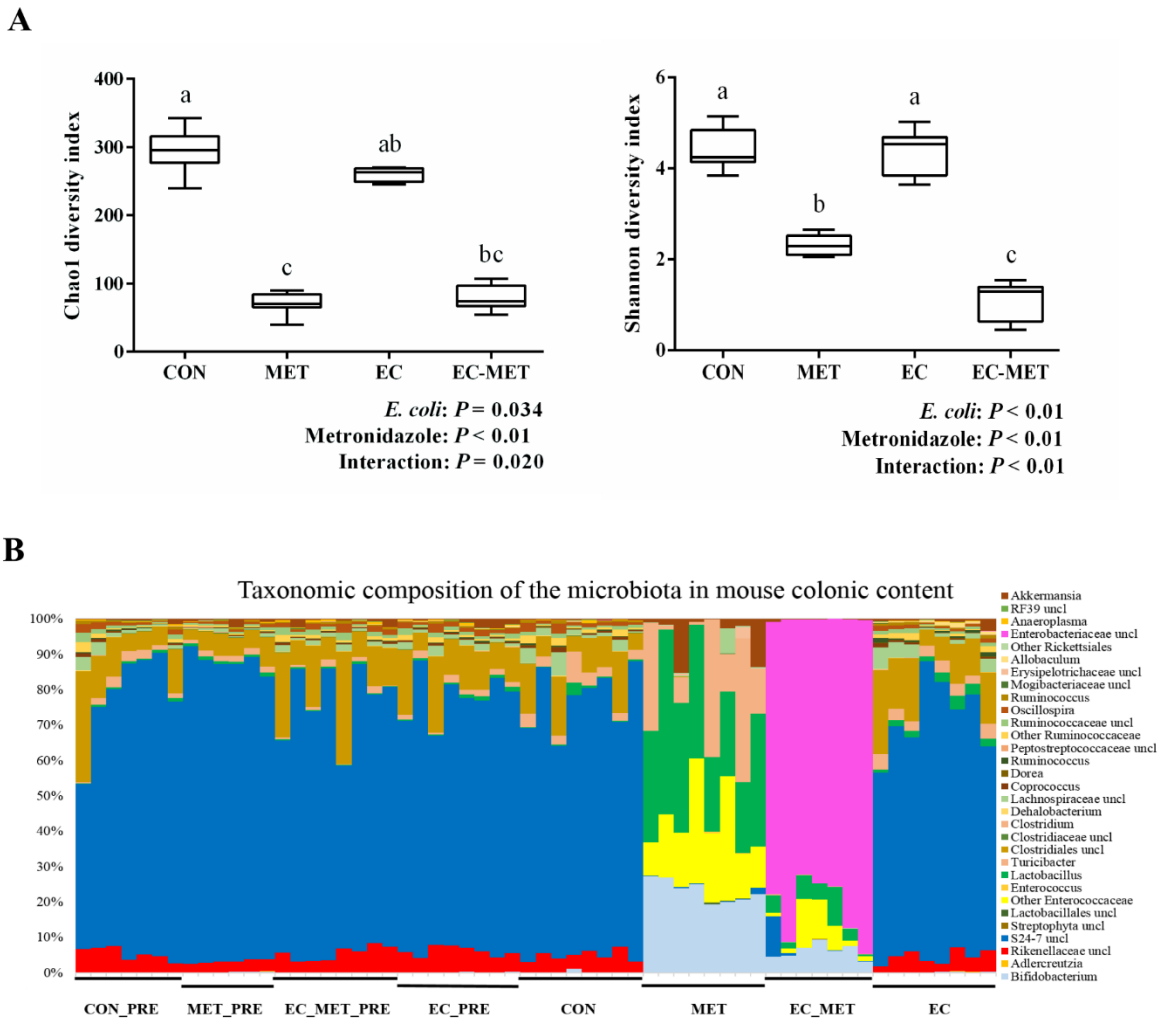

Figure 2.2. A) Alpha diversity analysis of bacterial communities in colon contents of mice. **B**) Bar chart indicating microbial community profiles between groups, summarized down to the genus level. All the colonic content were harvested after 4 days metronidazole/water administration. Data are shown as mean ± SEM. [a,b,c] Means that do not share a common letter are significantly different. $\alpha = 0.05$. Microbial composition of the four groups before experimental treatment are labeled as CON_PRE, MET_PRE, EC_MET_PRE, EC_PRE, respectively.

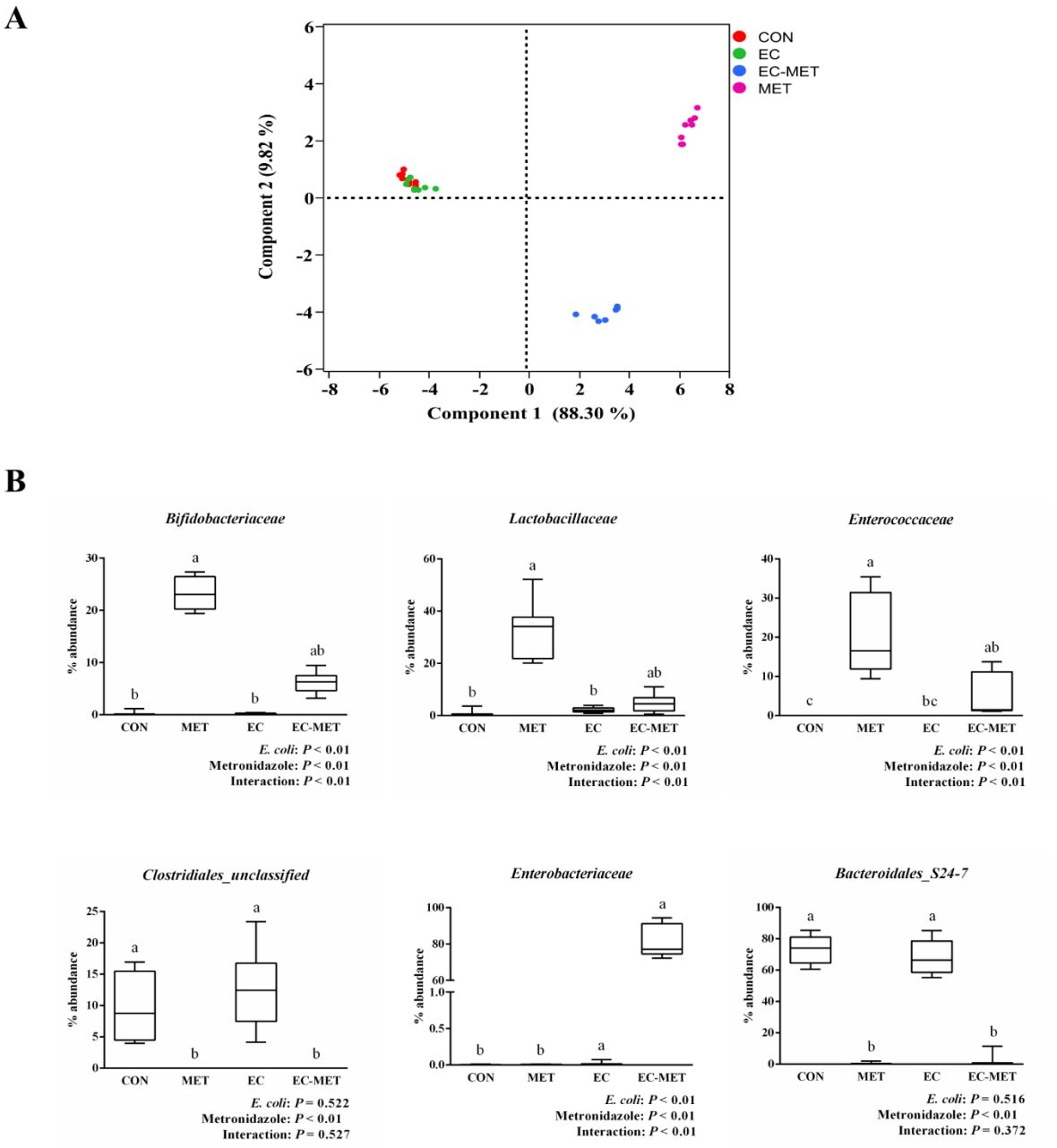

Figure 2.3. A) PCA plot of bacterial communities based on the weighted UniFrac distance matrix. Each point represents an individual mouse. **B**) Box-plots show selective bacterial abundance in different treated groups at the family level. Colonic contents were collected after 4 days of metronidazole/water treatment. For all treatment groups, n = 8. Data are shown as mean ± SEM. [a,b,c] Means that do not share a common letter are significantly different. α = 0.05.

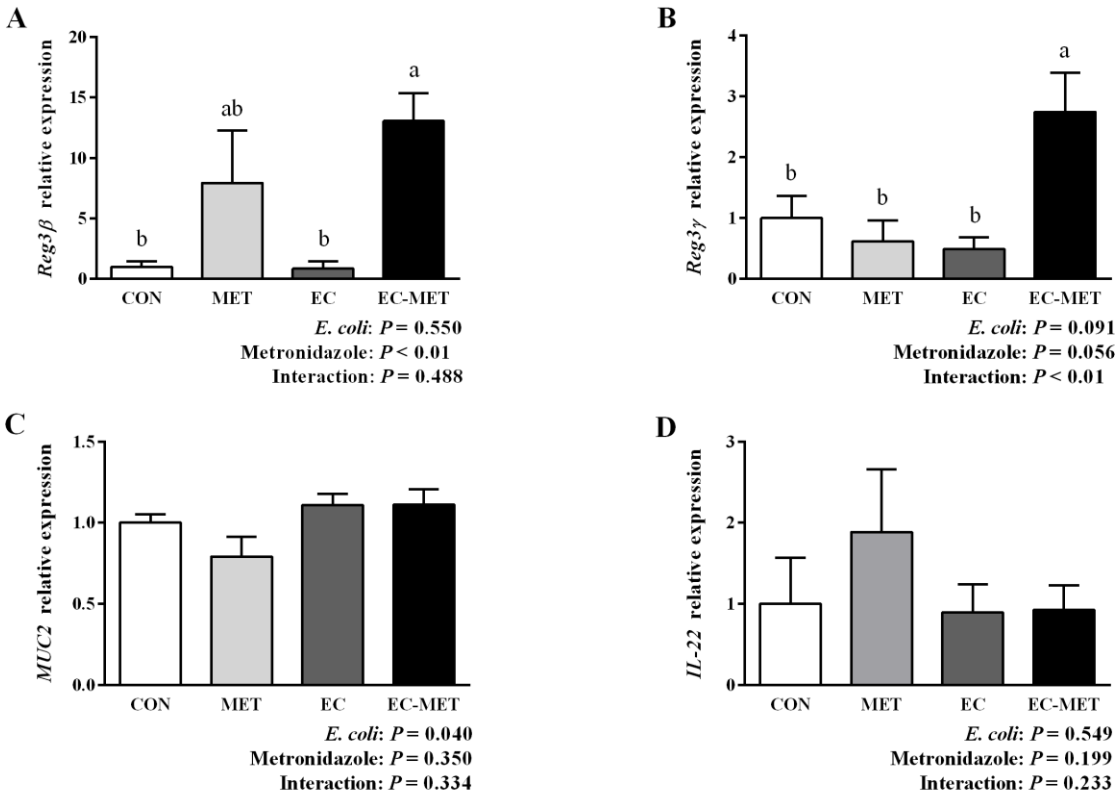

Figure 2.4. qPCR assay results of **A**) *Reg3β*, **B**) *Reg3γ*, **C**) *MUC2*, and **D**) *IL-22* expression in the colon of untreated, *E. coli* and metronidazole-treated mice. Colonic tissue samples were harvested after 4 days of metronidazole/water administration. For all treatment group, n = 8. Data are shown as mean ± SEM. [a,b,c] Means that do not share a common letter are significantly different. $\alpha = 0.05$.

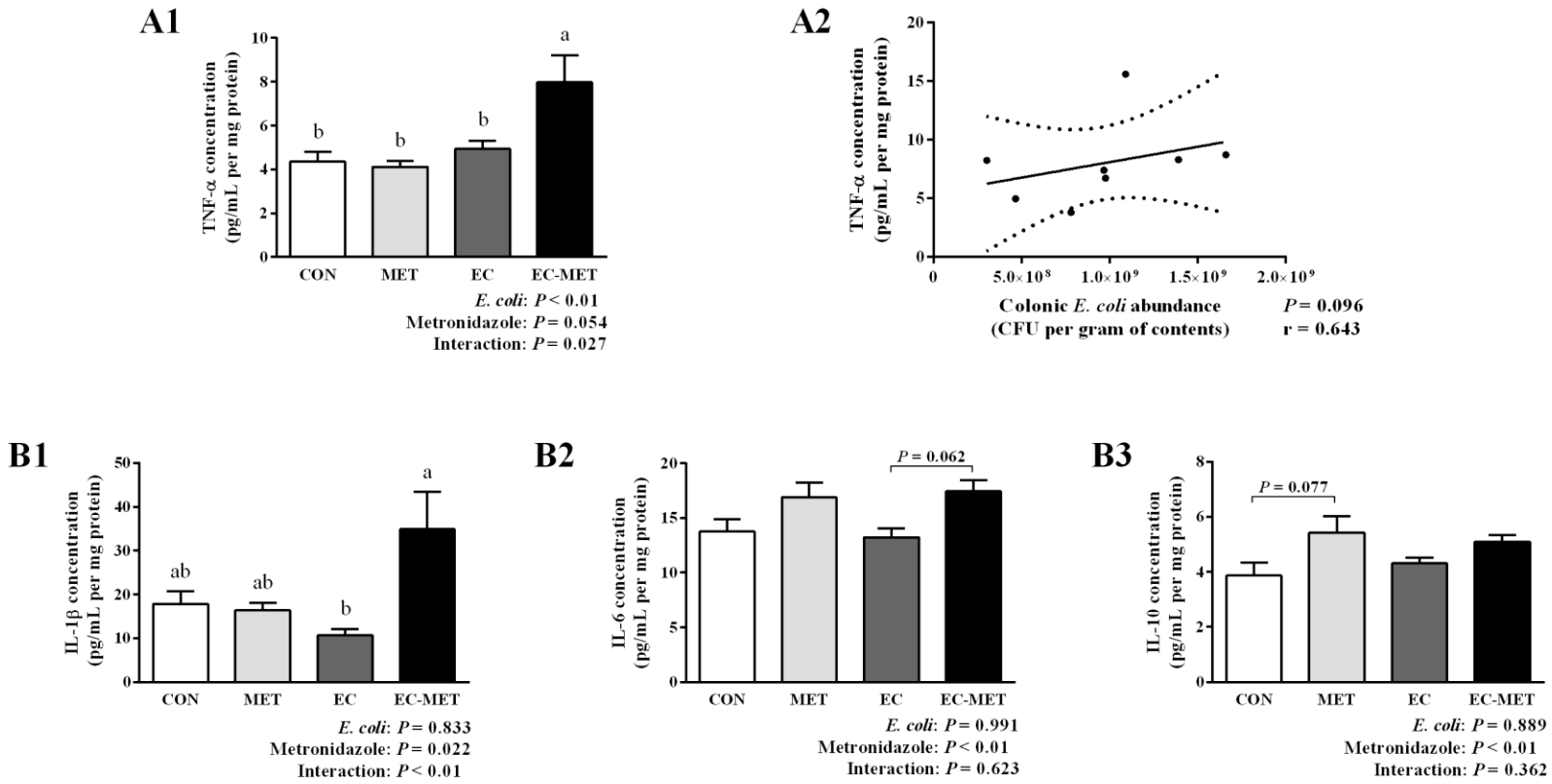

Figure 2.5. Cytokine analysis results of **A1**) TNF-α, **B1**) IL-1β, **B2**) IL-6, **B3**) IL-10 production in the colon. Colonic tissue samples were collected 4 days after metronidazole/water treatment. For all treatment groups, n = 8. Data are shown as mean ± SEM. [a,b,c] Means that do not share a common letter are significantly different. $\alpha = 0.05$. **A2**) Correlation of colonic *E. coli* bacterial load with TNF-α expression levels in EC-MET group. Spearman's correlation coefficient (r values) and significance *P* values are shown.

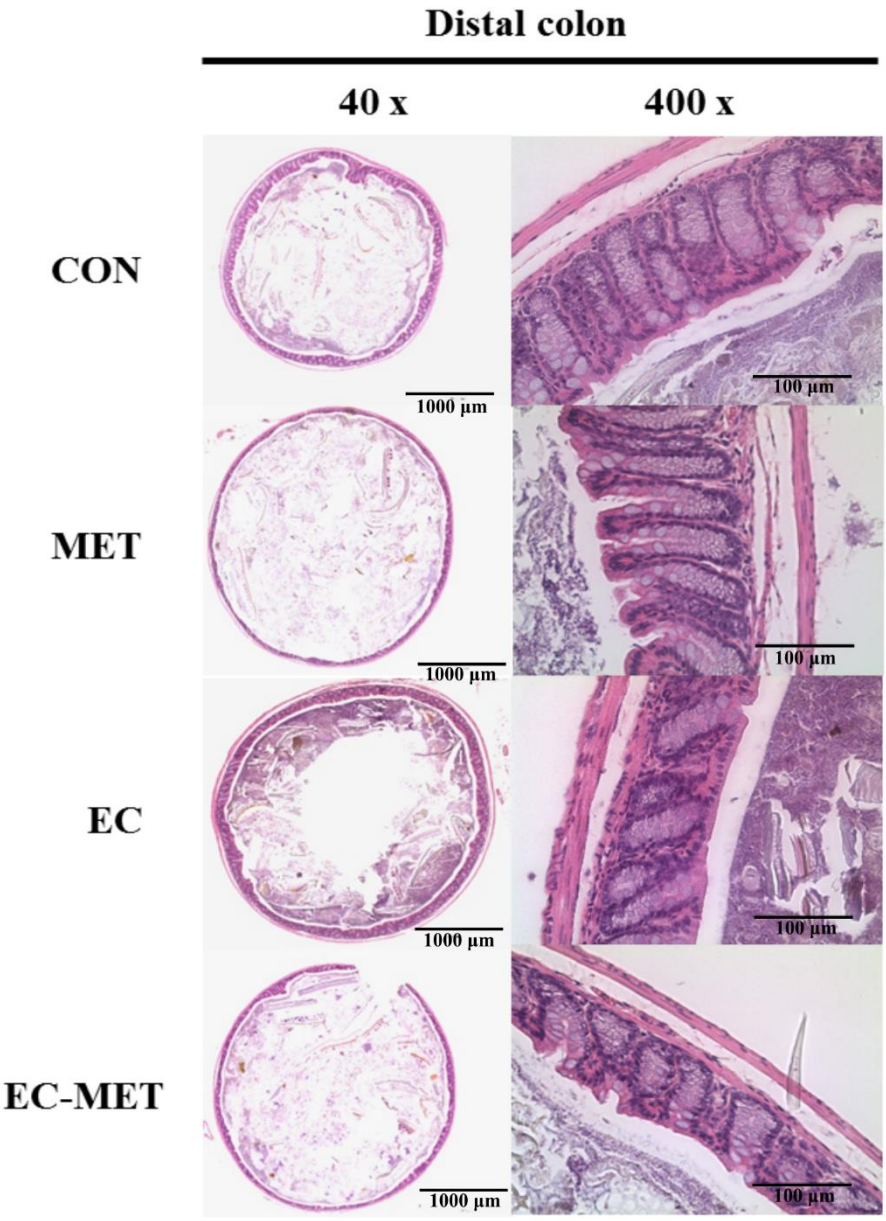

Figure 2.6. Distal colon sections from CON, MET, EC, and EC-MET mice 4 days after metronidazole/water treatment were stained with Haematoxylin and Eosin. There was no significant inflammation evidence in all treatments, including inflammation and damage of lumen, surface epithelium, mucosa, and submucosa, as well as the number of goblet cells. Original magnification and bars: Left: x 40, 1000 µm; right: x 400, 100 µm.

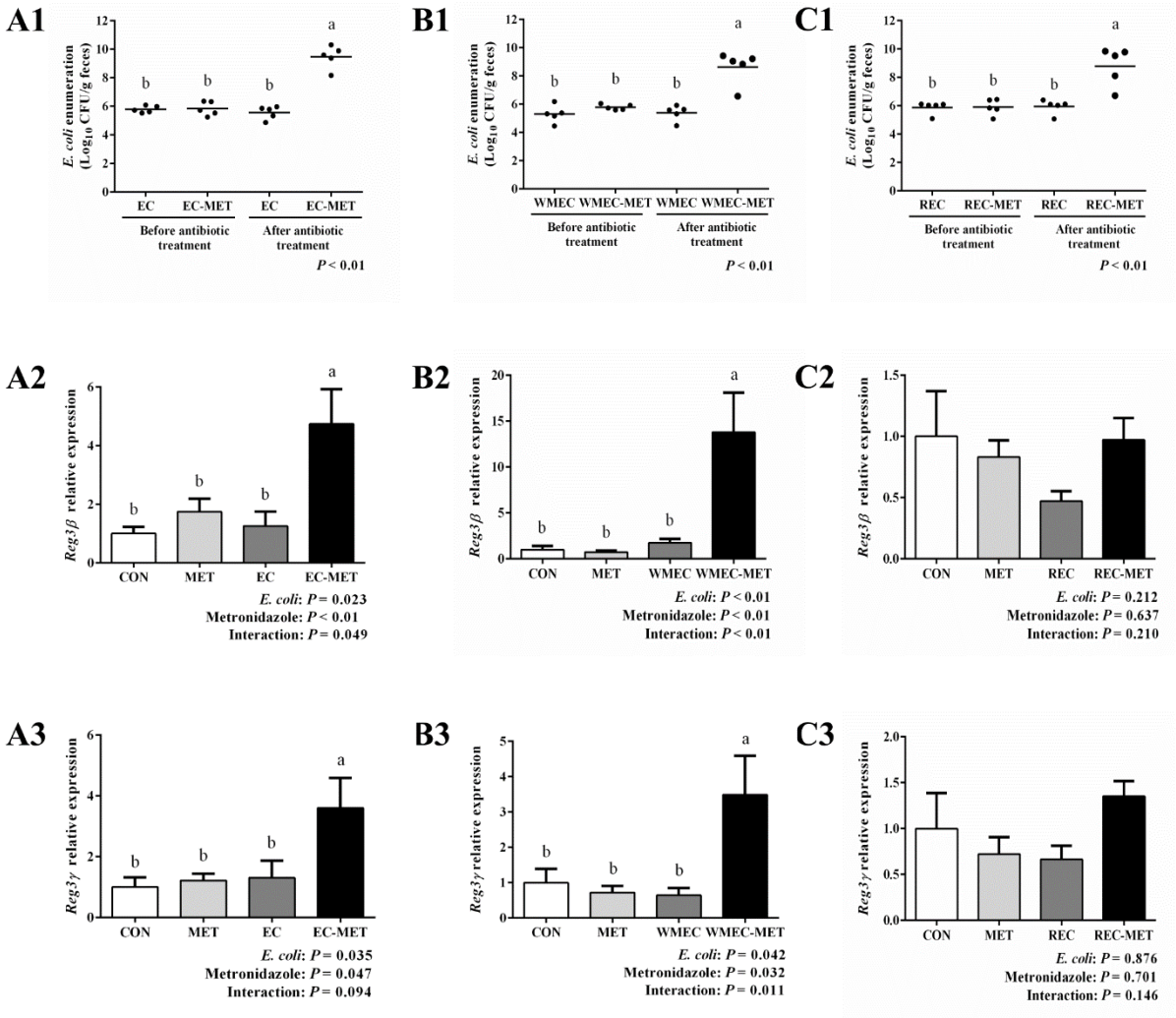

Figure 2.7. Enumeration of *E. coli* in mouse feces and colonic gene expression of mice colonized with **A**) commensal *E. coli* isolate, **B**) wild mouse *E. coli* isolate, and **C**) rat *E. coli* isolate. For enumeration of *E. coli* in mouse feces, samples were taken before metronidazole treatment and after **A1**) 14 days or **B1, C1**) 4 days of metronidazole/water treatment. Dots represent individual mice and lines depict mean values. *Reg3β* and *Reg3γ* expression in the colon of untreated, *E. coli* and metronidazole-treated mice was detected by qPCR. Colonic tissue samples were harvested after **A2**, **A3**) 14 days or **B2**, **B3**, **C2**, **C3)** 4 days metronidazole/water administration. For all treatment groups, n = 5. Data are shown as mean ± SEM. [a,b] Means that do not share a common letter are significantly different. $\alpha = 0.05$.

3. CHAPTER 3: THE PRESENCE OF GUT COMMENSAL *ESCHERICHIA COLI* AGGRAVATED HIGH-FAT DIET-INDUCED OBESITY AND INSULIN RESISTANCE IN MICE

3.1. Introduction

The gut microbiota has been suggested as a contributing factor to obesity and associated metabolic disorders, including type 2 diabetes (T2D) and its precursor, insulin resistance (IR) (1, 2). In mouse models, obesogenic high-fat diet (HFD) leads to significant changes in gut microbial composition and germ-free mice are protected from diet-induced obesity and IR (2–4). Alterations in the gut microbiota have been observed in obese human subjects and transferring to germ-free mice of fecal microbiota from obese donors resulted in increased adiposity (2, 5). These findings from both animal models and human studies demonstrated the contribution of the gut microbiota to obesity development and adiposity regulation. There are several proposed mechanisms through which changes in the gut microbiota influence host metabolic outcomes including the regulation of body weight and glucose homeostasis (3, 6, 7). It has been suggested that the gut microbiota could impact the capacity for energy harvest from the diet (6) and signal to the host through multiple pathways mediating glucose metabolism and insulin sensitivity (8, 9). Substantial experimental evidence indicates that the gut microbiota contributes to insulin resistance by inducing the chronic low-grade inflammation in multiple organs, which plays a crucial role in the pathogenesis of obesity and T2D (10, 11).

The chronic systemic inflammatory state related to the development of obesity and IR is typically reflected by the increased infiltration and activation of immune cells in white adipose tissue (WAT) (12). The gut microbiota contributes to fat accumulation and adipose

inflammation, which is supported by reduced macrophages in WAT and improved glucose metabolism in germ-free mice compared with conventionally raised mice (3, 11). In this process, bacterial endotoxin lipopolysaccharide (LPS), the major component of the outer membrane of Gram-negative bacteria, has been identified as a key factor in inducing an inflammatory response in WAT (11, 13). It has been hypothesized that the enhanced translocation of LPS into the systemic circulation on lipid-rich diet leads to adipose tissue inflammation (10, 14). Remarkably, LPS purified from *Escherichia coli* induced a strong stimulation of TLR4 signaling and inflammatory cytokines whereas *Bacteroides* species failed to generate inflammatory responses, indicating that LPS derived from different gut bacterial sources exhibited the significantly different capacity to elicit inflammatory response due to the distinct chemical structure of LPS molecules (15).

Indeed, the family *Enterobacteriaceae* and in particular the commensal *E. coli* in the gut have been linked to obese phenotype and IR, which is likely due to the immunostimulatory property of LPS and the capability to thrive in the inflamed gut (16, 17). Colonizing germ-free mice with an endotoxin-producing strain from the genus *Enterobacter* induced systemic inflammation and excessive fat accumulation in response to the HFD treatment (18). A chronic continuous infusion of low-dose *E. coli* LPS induced low-grade chronic inflammation and glucose intolerance in mouse models (10, 19). The monocolonization of germ-free mice with a wild type *E. coli* strain or isogenic mutant strain with reduced immunogenicity revealed that LPS was sufficient to induce macrophage infiltration into WAT and impaired glucose metabolism (11). Being one of the first bacterial species to colonize the intestine during infancy, commensal *E. coli* may play a key role in promoting the colonization of strict anaerobes by establishing the favorable

microenvironment in the intestine (20–22). However, commensal *E. coli* might exert adverse effects on the gut microbiota and host physiology under certain circumstances, such as gut microbiome dysbiosis and metabolic dysfunction (11, 23).

In monoclonization studies, the *Enterobacteriaceae* species colonized the mouse gut reaching a density of 10^{10}-10^{12} colony-forming units (CFUs)/g feces (11, 18), whereas the conventional mice typically harbor 10^{4}-10^{6} CFUs/g feces of these species (23). Therefore, with the robust colonization of *Enterobacteriaceae* species in the gut due to niche availability, monocolonization studies may not reflect the effects of the species on host metabolism as commensals, which also limited interactions between the microorganism and the complex microbial community. In previous studies, a commensal *E. coli* strain was successfully isolated from mouse feces and subsequently introduced to *Enterobacteriaceae*-free mice harboring a complex microbiota to investigate the effect of the commensal *E. coli* colonization on host physiology (23). This established mouse model was used in the present study to demonstrate the role of commensal *E. coli* in glucose homeostasis and energy metabolism responding to dietary treatment. The proof of concept study supports the importance of gut commensal bacteria in the pathogenesis of obesity and T2D, paving the way to the development of personalized nutrition and strategies to manipulate the gut microbiota.

3.2. Materials and methods

3.2.1. Mice. Six to eight weeks old C57BL/6J female mice (Jackson Laboratory, Bar Harbor, ME) were housed in the animal facility at the University of Alberta. Mice were kept in filter-topped cages with free access to food and water and handled in a biosafety cabinet under specific pathogen-free conditions. Mice were randomly grouped into 4 mice per cage

by a blinded lab animal technician and balanced for average body weight. Dietary treatments included a standard chow (5053 PicoLab® Rodent Diet 20, LabDiet, supplying energy as 13% fat, 25% protein, and 62% carbohydrate) and a HFD (D12451, Research Diets Inc., supplying energy as 45% fat, 20% protein, and 35% carbohydrate).

To investigate if the colonization of *E. coli* impacts glucose homeostasis in the setting of standard chow diet, mice were allocated to 2 treatments: standard chow (SC) and standard chow with *E. coli* colonization (SC_EC). In the HFD treatment arm, the mice were allocated to 3 treatments: standard chow (SC), high-fat diet (HF), and high-fat diet treatment with *E. coli* colonization (HF_EC) (n = 8 per treatment). The protocol of the study is shown in Figure 3.1A. Briefly, mice from the group SC_EC and HF_EC were exposed to a commensal *E. coli* strain by single oral gavage, while the group SC and HF received vehicle control (phosphate-buffered saline, PBS). Two weeks post-colonization, HF and HF_EC mice were switched to the HFD, while the SC group was continued on standard chow diet. Body weights and feed intake were recorded weekly. Mice were euthanized 16 weeks after dietary treatment to harvest tissue and gut content. The protocols employed were approved by the University of Alberta's Animal Care Committee and in direct accordance with the guideline of the Canadian Council on the Use of Laboratory Animals.

3.2.2. Bacterial strains. The commensal *E. coli* strain was previously isolated and cultured using MacConkey agar (BD, Sparks, MD) (23, 24). The bacterial strain was cultivated in 5 mL of Luria-Bertani medium (Fisher Scientific, Nepean, ON) at 37°C for 16 h, which contained approximately 2.0×10^8 CFUs/mL of *E. coli* cells. The culture was centrifuged at 5,000 x g for 10 min to collect cell pellets that were subsequently suspended in 1 x PBS. Mice were exposed to *E. coli* by oral gavage with 0.1 mL of the suspension. Fecal

E. coli was enumerated by conducting serial dilutions of feces and spread plating onto MacConkey agar. The total CFUs per gram fecal contents were then calculated.

3.2.3. Oral glucose tolerance test (OGTT). OGTT was performed following twelve weeks of dietary treatment. After fasting overnight for 16 hours, mice were weighed and the baseline glucose concentration in whole blood taken from the tail vein was measured using a glucometer (Accu-Check Compact Plus, Roche Diagnostics, Laval, Quebec, Canada). Mice were subsequently given a standard dose of glucose (1 g/kg body weight, 40% w/v in 1 x PBS) by oral gavage. The blood glucose concentration was measured at 15, 30, 45, 60, 90, and 120 min. The area under the curve (AUC) was calculated as described previously (25). Additional blood samples were collected and centrifuged to obtain plasma which was stored at -80°C for further analysis.

3.2.4. Tissue collection. Sixteen weeks after dietary treatment, mice were fasted for six hours and euthanized by CO_2 asphyxiation followed by cervical dislocation. Blood samples were collected by cardiac puncture in tubes containing EDTA, Complete® general protease inhibitor (Sigma) and dipeptidyl peptidase 4 inhibitor (EMD Millipore, MA). Plasma was obtained by centrifuging the blood sample at 3,000 x g for 10 min and frozen at -80°C. Liver and major white adipose tissue depots including inguinal, gonadal and retroperitoneal fat pad were weighed and collected. Ileal, cecal, and colonic contents were collected for microbial composition analyses. Samples were immediately placed in 10% neutral buffered formalin for histological studies or snap frozen in liquid nitrogen.

3.2.5. Microbial composition analysis. DNA was extracted from ileal, cecal, and colonic contents collected at the termination as well as from feces collected before dietary

treatment. The DNA extraction, amplicon library construction, paired-end sequencing and data analysis were performed using protocols published previously (23).

3.2.6. RNA isolation and cDNA synthesis. Liver and fat tissue were snap frozen in liquid nitrogen and subsequently stored at -80℃. Hepatic RNA was extracted using the GeneJET RNA Purification Kit (Thermo Scientific, Nepean, ON) following manufacturer's instructions. Gonadal fat RNA was extracted using the TRIzol™ reagent (Thermo Scientific, Nepean, ON). The concentration of RNA was determined by a NanoDrop ND-2000 spectrophotometer (NanoDrop Technologies, Wilmington, DE) and 1 μg RNA was used for reverse transcription using the qScript Flex cDNA synthesis kit (Quantabio, Gaithersburg, MD).

3.2.7. Quantitative polymerase chain reaction (qPCR). Primers for host gene expression are listed in Table 3.1. qPCR assay was performed on an ABI StepOne™ real-time System (Applied Biosystems, Foster City, CA) using the PerfeCTa SYBR Green Supermix (Quantabio, Gaithersburg, MD) which followed the cycles: 95℃ for 20 s and 40 cycles of 94℃ for 10 s, 60℃ for 30 s. β2-microglobulin (*B2M*) and glyceraldehyde-3-phosphate dehydrogenase (*GAPDH*) were used as reference genes for normalization. The fold change of gene expression compared to the SC group was calculated using the $2^{-\Delta\Delta Ct}$ method.

3.2.8. Plasma metabolic hormone measurements. Plasma leptin, active glucagon-like peptide-1 (GLP-1), insulin, total gastric inhibitory polypeptide (GIP), active ghrelin, peptide YY (PYY), glucagon, pancreatic polypeptide (PP), resistin, connecting peptide (C-peptide), and active amylin were determined using a multiplex bead panel assay (MRDMET, Eve Technology, Calgary, Canada).

3.2.9. Liver lipid extraction. The liver tissue was homogenized in a lysis buffer

containing 10 mM Tris-HCl, 150 mM NaCl, 1 mM EDTA, and Complete® general protease inhibitor (Sigma). The total protein concentration of liver homogenates were measured by a Micro-bicinchoninic acid protein assay kit (Pierce, Rockford, IL) and lipids were extracted from the homogenate (1 mg/mL, protein concentration) using the Folch procedure (26).

3.2.10. Plasma and liver lipid analysis. Plasma and hepatic triglyceride (TG) (Sekisui Diagnostics, Lexington, MA) and cholesterol (Wako Diagnostics, Richmond, VA) were determined using commercial colorimetric assay kits following the manufacturer's instruction.

3.2.11. Histology. The hepatic tissue was fixed in 10% neutral buffered formalin at room temperature for 24 h, and then placed into 70% ethanol. The fixed tissue was embedded in paraffin, sectioned at 3 μm, and stained with hematoxylin and eosin (H&E). Images were taken using an EVOS FL Auto Imaging System (Thermo Scientific, Nepean, ON).

3.2.12. Statistical analysis and visualization. The effect of diet and time on body weight was analyzed by the two-way repeated-measures ANOVA with Bonferroni post hoc adjustment in SAS (version 10.0.2, SAS Inst. Inc. Cary, NC). To compare the difference in the enumeration of fecal *E. coli* (log-transformed), gene expression, and metabolic hormone levels between treatments, the Shapiro-Wilk test was used to check the normality of data distribution and the one-way ANOVA was subsequently performed. For microbial composition analyses, the comparison of individual taxa/OTUs between groups were conducted using the Kruskal-Wallis test. Permutational multivariate analysis of variance (MANOVA) of the weighted UniFrac distance was used to determine the difference in overall microbial compositions across treatments (adonis function, vegan package, R v3.4.4) (27). The principal coordinate analysis (PCoA) based on a Bray-Curtis dissimilarity matrix

was plotted using the phyloseq package (R v3.4.4). *P* values indicate statistical significance as follows: **, $P < 0.01$; *, $P < 0.05$. R (v3.4.4) and GraphPad Prism was used for visualizing results.

3.3. Results

3.3.1. Commensal *E. coli* increased body weight and adiposity after HFD treatment.

C57BL/6J mice that did not harbor *E. coli* strains confirmed by plating were exposed to the commensal *E. coli* isolate by oral gavage. The *E. coli* isolate successfully colonized the mouse intestine in the SC_EC and HF_EC group, ranging from 1.30×10^5 to 2.14×10^6 CFUs/g feces as detected one week after exposure. The abundance of *E. coli* did not change throughout sixteen weeks of standard chow diet treatment (Figure 3.1B). In contrast, HFD induced an increase in the level of *E. coli* in feces one week after HFD treatment (with a 0.8-log CFUs/g increase), which was maintained through the HFD challenge (Figure 3.1C; Figure 3.2A).

The body weight of mice was recorded weekly during dietary treatment. When mice were fed the standard chow diet for 16 weeks, the body weight was comparable between SC and SC_EC group (23.0 ± 1.4 g vs. 23.7 ± 1.3 g, respectively, mean ± standard deviation, $P = 0.313$), indicating that *E. coli* colonization had no effect on body weight changes in the setting of chow-fed diet. Under the HFD regime, no difference in body weight was found between HF mice and SC mice after 12 weeks of dietary treatment (25.8 ± 1.6 g vs. 23.7 ± 2.2 g, mean ± standard deviation, $P = 0.311$, Figure 3.2B), whereas the HF_EC mice tended to be heavier than the SC mice ($P = 0.061$, Figure 3.1D). Sixteen weeks of HFD treatment significantly increased the body weight in HF_EC mice compared to SC mice (30.7 ± 2.7 g vs. 23.3 ± 2.7 g, mean ± standard deviation, $P = 0.028$, Figure 3.1D). No significant

difference was observed in food intake between SC, HF, and HF_EC groups, suggesting that the increased body weight gain in HF_EC mice was not attributed to alterations in energy input (Figure 3.1E).

When mice were maintained on HFD, notable differences were observed in the weight of major white adipose tissue (WAT) pads including inguinal, gonadal, and retroperitoneal fat depots among treatment groups. Specifically, when compared with SC mice, HF_EC mice developed a significantly higher visceral WAT pads including gonadal and retroperitoneal depots ($P < 0.05$, Figure 3.2C), however, there was no difference in visceral WAT pads between HF and SC mice. In addition, the presence of *E. coli* further increased the inguinal fat mass in response to HFD treatment (Figure 3.2C). When expressed as a percentage of total body weight, the proportion of fat was significantly higher in HF_EC mice relative to SC mice, as measured by the combined weight of fat depots (Figure 3.2D). No changes in the weight of liver and muscle were observed among groups, indicating that the increased body weight in HF_EC mice may mainly result from changes in adipose tissue mass. Consistent with the comparable body weight, there was no difference detected in weights of WAT pads, liver, and muscle between SC and SC_EC mice (Figure 3.1F).

3.3.2. *E. coli* aggravated impaired glucose tolerance induced by HFD. An OGTT was performed after 12 weeks of dietary intervention to investigate whether the presence of *E. coli* had any effect on glucose homeostasis. Under the HFD treatment, after an overnight fasting period of 16 hours, HF_EC mice tended to show higher levels of fasting glucose compared with SC mice ($P = 0.061$, Figure 3.3A), whereas no difference was observed in fasting blood glucose levels between HF and SC mice ($P = 0.450$). HF_EC mice displayed impaired glucose disposal during OGTT (Figure 3.3B) and exhibited 19.5% and 18.2%

higher glucose AUC compared to that in SC and HF mice, respectively (Figure 3.3C), implying that the presence of *E. coli* exacerbates HFD-induced glucose intolerance. No significant difference in the rate of clearing glucose from the circulation was detected between SC and HF mice. When fed a standard chow diet, there was no difference in fasting blood glucose levels or glucose disposal capacity between SC and SC_EC mice, suggesting the interaction between *E. coli* and HFD in altering glucose and insulin homeostasis (Figure 3.4A-C).

A panel of circulating metabolic hormones was assessed to gain insights into the effect of *E. coli* colonization on metabolic regulatory hormones under the HFD regime and standard chow diet. Plasma levels of leptin, an adipocyte-derived hormone, was significantly higher in HF_EC mice than that in SC and HF mice, which was consistent with the increased adiposity in HF_EC mice (Figure 3.3D). In addition, plasma C-peptide concentrations were significantly increased in HF_EC mice compared with SC mice (Figure 3.3E). The HFD administration significantly increased plasma insulin levels, however, the presence of *E. coli* did not affect the elevated plasma insulin concentration in response to HFD treatment (Table 3.2). Plasma levels of GLP-1, GIP, ghrelin, PYY, glucagon, PP, resistin, and amylin were not significantly different among SC, HF, and HF_EC groups (Table 3.2). No changes were detected in circulating metabolic hormones between SC and SC_EC mice (Table 3.3).

3.3.3. *E. coli*, in combination with HFD, enhanced lipid accumulation and inflammation in liver and adipose tissue. The impaired insulin sensitivity induced by HFD treatment is frequently associated with pathological changes in liver and adipose tissue which play a crucial role in maintaining blood glucose homeostasis. As expected, mice that received HFD treatment for 16 weeks developed hepatic steatosis as reflected by the notable

accumulation of lipid droplets in the liver. HF_EC mice showed the highest hepatic TG content among groups, which was consistent with histological changes in the liver (Figure 3.5A). HFD treatment significantly increased total cholesterol levels in the liver and plasma; however, there was no difference between HF and HF_EC groups (Figure 3.5B). In addition, plasma TG levels were not different between SC, HF, and HF_EC mice (Figure 3.5A). The increased hepatic lipid accumulation in HF_EC mice was associated with changes in lipogenic genes in the liver. Specifically, HF_EC mice showed a significant upregulation of sterol regulatory element-binding protein-1c (*SREBP-1c*), peroxisome proliferator-activated receptor γ2 (*PPARγ2*), and acyl-CoA: diacylglycerol acyltransferase-2 (*DGAT2*) compared to SC and HF mice (Figure 3.6A). Hepatic genes involved in lipogenesis (fatty acid synthase, *FASN*), fatty acid oxidation (carnitine palmitoyl transferase 1α, *CPT1α*), fatty acid update (liver fatty acid binding protein, *LFABP*), and VLDL secretion (apolipoprotein B, *ApoB*; microsomal triglyceride transfer protein, *MTTP*) were altered in the HF_EC group, indicating an impaired hepatic lipid metabolism resulting from *E. coli* colonization (Figure 3.6B). The expression of gluconeogenic genes (glucose-6-phosphatase, *G6Pase*; phosphoenolpyruvate carboxykinase, *PEPCK*) in the liver were repressed by HFD treatment regardless of *E. coli* presence (Figure 3.6C). There was no difference in cholesterol and TG levels in plasma and liver observed between SC and SC_EC mice (Figure 3.5C-D).

Consistent with increased adipose tissue mass observed in HF_EC mice, the gene expression of adiposity markers and lipid metabolizing mediators, including *SREBP-1c*, peroxisome proliferator-activated receptor α (*PPARα*), and *PPARγ2*, were upregulated in the gonadal fat of HF_EC mice compared to SC and HF mice (Figure 3.6D). The gene that involved in TG synthesis, *DGAT2*, exhibited a trend to be higher in HF_EC mice compared

with SC mice. Furthermore, the mRNA level of inflammation-related genes, *TNF-α*, was significantly higher in the gonadal fat of HF_EC mice than that in SC mice (Figure 3.6D). Overall, these results suggested that the presence of *E. coli* promoted the lipid load and low-grade chronic inflammation in the adipose tissue in response to HFD treatment.

3.3.4. Diet is a major driver of shifting gut microbial structure independently of *E. coli* colonization. To characterize the gut microbial composition of SC, HF, and HF_EC mice after 16 weeks of dietary treatment, intestinal contents obtained from the ileum, cecum, and colon were sequenced targeting the V3-V4 region of the 16S rRNA gene. Following the quality control and chimera removal, the sequencing obtained an average of 18,685 ± 6,019 (mean ± standard deviation) reads per sample. An OTU identified as the genus *Lactococcus* was absent or below detection in the gut microbiota before the initiation of HFD treatment, which was also absent in standard chow diet-fed mice. The PCoA plots revealed that the colonization of *E. coli* did not shift the microbial structure in the ileum ($R^2 = 0.057$, $P = 0.057$), cecum ($R^2 = 0.091$, $P = 0.642$) and colon ($R^2 = 0.079$, $P = 0.906$), which was determined by an adonis test (Figure 3.7A). The microbial communities separated by dietary type as reflected by a clear cluster of samples according to stand chow diet or HFD treatment (adonis, $P < 0.01$, Figure 3.7A).

The phylogenetic richness and evenness of microbial communities at different intestinal segments were evaluated by Chao1 diversity index and Shannon index. Ileal microbial communities from HFD-treated groups were more diverse and even than the SC group, as evidenced by a greater Shannon index value for HF and HF_EC mice (Figure 3.7B). However, no difference in Shannon index values calculated from cecal and colonic microbial communities was observed between SC, HF, and HF_EC groups. HFD treated mice had

significantly lower Chao1 index values than the SC mice in cecal and colonic microbial communities, indicating a decreased species richness induced by HFD administration (Figure 3.7B). Chao1 index values of ileal microbial communities were not affected by treatment.

The analysis of differential abundance in OTUs showed no notable changes in identified bacterial genera between HF and HF_EC mice except for the absence/presence of *E. coli* at all three intestinal segments, indicating the minimal effect of *E. coli* colonization on taxonomic structure of microbial communities (Table 3.4). In accordance with separations of the overall microbial structure by dietary type, multiple genera were altered by HFD treatment. In general, HFD consumption resulted in a significant decrease in the relative abundance of Bacteroidetes phylum and an increase in the Firmicutes phylum. Specifically, the relative abundance of the family Bacteroidales *S24-7* was significantly reduced at all intestinal sites after HFD treatment, whereas the family *Ruminococcaceae* and *Peptostreptococcaceae* were consistently increased in HF and HF_EC mice. In addition, the family *Rikenellaceae*, which belongs to the phylum Bacteroidetes, was drastically decreased in the cecal and colonic microbiota of HFD-treated mice. The genus *Akkermensia*, however, was significantly enriched in the cecum and colon of HF and HF_EC mice (Table 3.4). These results indicated that dietary type plays a major role in shaping gut microbial communities, whereas the colonization of commensal *E. coli* showed a minimal impact on the microbial structure.

3.4. Discussion

The correlation between the enrichment of the family *Enterobacteriaceae* and HFD-induced obese phenotype has been documented (16, 17, 28). The overgrowth of the family *Enterobacteriaceae* has been considered as a consequence of intestinal inflammation

provoked by HFD treatment which supports the growth of aerotolerant bacteria (29). However, mono-colonization of germ-free mice with *Enterobacter cloacae*, a member of *Enterobacteriaceae* isolated from human gut, induced obesity and insulin resistance under a HFD regime (18), indicating the contribution of endotoxin-producing bacteria to obesity pathogenesis. In the current study, a tractable mouse model was successfully established by adding a single bacterium, a mouse commensal *E. coli* strain, to a complex microbial ecosystem to investigate the effect of endotoxin-producing bacteria on metabolic outcomes and microbial interactions in the context of HFD administration. The result showed that the presence of commensal *E. coli* exacerbated the impairment of glucose intolerance under the HFD regime.

After 12 weeks of dietary treatment, HF_EC mice displayed a rapid weight gain and the increase was sustained up to 16 weeks of the treatment, which was accompanied by increased adiposity. In contrast, the difference in body weight and fat pad weights between SC and HF mice remained the same to 16 weeks of treatment. A previous study reported that a significant difference in body weight between the low-fat control and HFD group occurred from week 27 in female C57BL/6J mice (30). In the present study, the HFD treatment was not sufficient to induce significant changes in body weight of HF mice compared with the SC group. However, a combination of HFD treatment and commensal *E. coli* led to greater body weight and body fat than SC mice, indicating the contribution of *E. coli* to body weight gain and adipose tissue expansion in response to HFD administration. Consistent with observed body weight differences, HF_EC mice exhibited glucose intolerance during OGTT with significantly increased AUC, whereas no difference was shown in glucose disposal between SC and HF mice. The fat accretion and the concomitant increase in plasma leptin level, which

was significantly correlated with plasma insulin level, was observed in HF_EC mice, indicating a pronounced impairment of leptin action resulted from *E. coli* colonization and HFD treatment (31, 32).

In the present study, no statistical difference was observed between SC, HF, and HF_EC groups in food intake as well as energy intake calculated based on the dietary energy density although HFD treated groups showed increases in calorie intake. However, the insignificant calorie intake in HF_EC led to excess accumulation of WAT which is pivotal to lipid and glucose homeostasis. In the progression of obesity, the increased WAT mass is attributed to mechanisms including adipocyte hypertrophy and/or adipocyte hyperplasia (33). The WAT expansion in HF_EC mice indicated an increased capacity of fat storage in response to HFD administration. Concomitantly, the gene involved in adipogenesis and TG synthesis (*SREBP-1c*, *PPARγ2*, and *DGAT2*) were elevated in HF_EC mice, suggesting that the presence of *E. coli* in the gut promoted adipogenesis and lipid accumulation.

Liver weights were not significantly affected by dietary treatment, however, HF_EC mice displayed excess hepatic lipid accumulation. Consistent with the altered hepatic lipid metabolism, the colonization of *E. coli* significantly increased the expression level of genes related to lipid metabolism including *SREBP-1c*, *PPARγ2*, and *DGAT2*. The hepatic lipid metabolism is a complex and dynamic process with multiple biological functions, including lipogenesis, fatty acid update, fatty acid oxidation, and VLDL secretion. The transcriptional factor *SREBP-1c* regulates *de novo* lipogenesis, which plays an important role in hepatic lipid metabolism and development of steatosis (34). The expression of *PPARγ2* has been positively correlated with HFD-induced lipid accumulation in the liver (35) and *DGAT2* mediates hepatocyte TG synthesis and hepatic steatosis. In addition, the lipid disposal was also

enhanced in the liver of HF_EC mice as reflected by the elevated expression of genes involved in lipid oxidation and VLDL secretion such as *CPT1α* and *ApoB*. Therefore, HF_EC mice exhibited an altered lipid metabolism with an enhancement of *de novo* fatty acid synthesis and lipid removal in the liver; however, the disposal of TG may not be sufficient to compensate for the increases in fatty acid synthesis.

A state of low-grade inflammation in various tissues, including the hypothalamus, adipose tissue, and liver, is involved in the development of obesity and T2D (33, 36, 37). HFD feeding may lead to enhanced LPS translocation into the circulation which triggers adipose inflammation and impaired insulin and leptin actions (10). In the current study, the mRNA expression of *TNF-α*, the primary enhancers of the inflammatory response in adipose tissue, was significantly increased with the presence of *E. coli* in response to HFD treatment. The expression of *TNF-α*, *IL-1β*, and *MCP-1* gene expression in the liver were not different between SC, HF, HF_EC mice. No difference was detected in the inflammatory-related genes between SC and SC_EC groups, implying the interaction between HFD and *E. coli* to initiate an inflammatory response in the development of metabolic disorders such as obesity. A recent study reported that commensal *E. coli* isolates exhibited different capacities to elicit acute intestinal inflammation in mice harboring a minimal bacterial community treated by dextran sulfate sodium (38). Although we cannot entirely rule out the possibility that the pro-inflammatory response induced by *E. coli* depends on the characteristic of the strain due to the diversity of this species, the current study demonstrated the potential contribution of commensal *E. coli* to the low-grade systemic inflammation in the context of long-term HFD treatment. Future studies targeting a reduction in *E. coli* population, specifically, may result in improved metabolic outcomes in animal models harboring a greater diversity of *E. coli*

species. We also expect that other *Enterobacteriaceae*, and bacteria containing more immunogenic LPS that thrive in response to a western diet may result in similar adverse outcomes as observed for *E. coli* in this study.

The characterization of the gut microbiome after 16 weeks of dietary treatment revealed that the dietary type explained the largest variance in microbial composition as bacterial communities of SC mice were clearly distinct from the HF and HF_EC mice (Figure 3.7). Changes in the gut microbiota elicited by HFD consumption have been documented, which generally leads to an expansion of Firmicutes at the expense of Bacteroidetes (2, 39). In the current study, the altered ratio of abundance in Bacteroidetes and Firmicutes was observed in HFD treated groups, which was consistent with previous reports using similar dietary treatment (39–41). However, when comparing the difference between HF and HF_EC groups as well as between SC and SC_EC groups, *Enterobacteriaceae* which was represented by the *E. coli* isolate was the only significantly changed family. It is possible that the colonization of the commensal *E. coli* isolate led to strain-level differences in the gut microbiota that were not detected by 16S rRNA sequencing analysis, however, a lack of impact on the overall structure in the setting of standard chow diet or HFD implied that commensal *E. coli* primarily contributed to the exacerbated glucose intolerance and inflammatory responses with minimal interactions with the microbial community under HFD feeding conditions, and that the shift from Bacteroidetes to Firmicutes was less important. The findings of the current study are somewhat counter to what has been found in patients that received Roux-en-Y gastric bypass (RYGB). In RYGB patients, increased *Enterobacteriaceae* is associated with improved body composition, metabolic and inflammatory profiles after the surgery (42–44). However, the markedly increased

Enterobacteriaceae abundance is most likely explained by the fact that the shortened small bowel favors aerobic and facultative anaerobic microbes (42). Given the result of the current study, increased *Enterobacteriaceae* in RYGB patients likely reflects the severity to which the intestinal microbial ecosystem is disrupted, and does not support a causal link between increased *Enterobacteriaceae* in RYGB and health outcomes.

A remarkable increase in the genus *Akkermansia* was displayed in the cecum (23.55 ± 4.85% vs. 4.13 ± 1.18%, mean ± SD) and colon (28.57 ± 3.77% vs. 8.35 ± 4.82%) of HFD treated mice compared to that in SC mice. The genus *Akkermansia* has been shown to be reduced by HFD feeding in mice and the administration of *Akkermansia* improved metabolic disorders including IR (45). However, in addition to its beneficial and protective effects on obesity development, the inconsistency in changed abundance of *Akkermansia* responding to HFD treatment has also been demonstrated (46–48). The inconsistent response of the genus could be attributed to the variation in the dietary composition that impact the growth of *Akkermansia* directly by changing the nutrient environment or indirectly through cross-feeding interactions in the gut microbiota (45). In addition, host and environmental factors, such as inflammation and differences in initial microbial composition, may drive the alteration in the abundance of *Akkermensia* (47, 48). Furthermore, in the current study, the presence of *E. coli* exacerbated the severity of metabolic disorders induced by HFD without changing the abundance of *Akkermansia*, suggesting the complex and multifactorial etiology of obesity (49). Therefore, additional research is necessary to characterize the mechanism through which certain dietary components modulate the abundance of the commensal bacterium and functional consequences of the modulation as a basis to understand the role of gut microbes in complex diseases such as obesity and diabetes.

In summary, the commensal *E. coli* strain fills an ecological niche in the gastrointestinal tract with minimal impacts on the overall microbial structure. However, under long-term HFD feeding conditions, commensal *E. coli* aggravated high-fat induced glucose dysregulation with increased adiposity and inflammation. Without a drastic increase in the abundance of *E. coli* after HFD treatment, the enhanced translocation of bacterial-derived products such as LPS may contribute to the impaired glucose homeostasis as indicated by systemic proinflammatory responses. The finding highlights the effect of *E. coli* strain as a member of highly complex commensal communities in the gut on host metabolism in the context of HFD intervention. This proof of concept study suggests the importance to investigate the role of the individual gut commensal bacterium in the pathogenesis of obesity and T2D, and therefore develop strategies to manipulate these commensal bacteria to improve metabolic outcomes.

3.5. References

1. Ley RE, Backhed F, Turnbaugh P, Lozupone CA, Knight RD, Gordon JI. 2005. Obesity alters gut microbial ecology. Proc Natl Acad Sci 102:11070–11075.
2. Turnbaugh PJ, Bäckhed F, Fulton L, Gordon JI. 2008. Diet-induced obesity is linked to marked but reversible alterations in the mouse distal gut microbiome. Cell Host Microbe 3:213–223.
3. Bäckhed F, Manchester JK, Semenkovich CF, Gordon JI. 2007. Mechanisms underlying the resistance to diet-induced obesity in germ-free mice. Proc Natl Acad Sci 104:979–984.
4. Rabot S, Membrez M, Bruneau A, Gérard P, Harach T, Moser M, Raymond F, Mansourian R, Chou CJ. 2010. Germ-free C57BL/6J mice are resistant to high-fat-diet-induced insulin resistance and have altered cholesterol metabolism. FASEB J 4:4948–4959.

5. Ridaura VK, Faith JJ, Rey FE, Cheng J, Duncan AE, Kau AL, et al. 2013. Gut microbiota from twins discordant for obesity modulate metabolism in mice. Science 341:1241–1263.
6. Turnbaugh PJ, Ley RE, Mahowald MA, Magrini V, Mardis ER, Gordon JI. 2006. An obesity-associated gut microbiome with increased capacity for energy harvest. Nature 44:1027–1031.
7. Boutagy NE, McMillan RP, Frisard MI, Hulver MW. 2016. Metabolic endotoxemia with obesity: is it real and is it relevant? Biochimie 124:11–20.
8. Canfora EE, Jocken JW, Blaak EE. 2015. Short-chain fatty acids in control of body weight and insulin sensitivity. Nat Rev Endocrinol 11:577–591.
9. Wahlström A, Sayin SI, Marschall HU, Bäckhed F. 2016. Intestinal crosstalk between bile acids and microbiota and its impact on host metabolism. Cell Metab 24:41–50.
10. Cani PD, Amar J, Iglesias MA, Poggi M, Knauf C, Bastelica D, Neyrinck AM, Fava F, Tuohy KM, Chabo C, Waget A, Delmée E, Cousin B, Sulpice T, Chamontin B, Ferrières J, Tanti J-F, Gibson GR, Casteilla L, Delzenne NM, Alessi MC, Burcelin R. 2007. Metabolic endotoxemia initiates obesity and insulin resistance. Diabetes 56:1761–1772.
11. Caesar R, Reigstad CS, Bäckhed HK, Reinhardt C, Ketonen M, Lundén GÖ, Cani PD, Bäckhed F. 2012. Gut-derived lipopolysaccharide augments adipose macrophage accumulation but is not essential for impaired glucose or insulin tolerance in mice. Gut 12:1701–1707.
12. Sun S, Ji Y, Kersten S, Qi L. 2012. Mechanisms of inflammatory responses in obese adipose tissue. Annu Rev Nutr 32:261–286.
13. Raetz CRH, Whitfield C. 2002. Lipopolysaccharide endotoxins. Annu Rev Biochem 71:635–700.
14. Caesar R, Tremaroli V, Kovatcheva-Datchary P, Cani PD, Bäckhed F. 2015. Crosstalk between gut microbiota and dietary lipids aggravates WAT inflammation through TLR signaling. Cell Metab 22:658–668.
15. Vatanen T, Kostic AD, D'Hennezel E, Siljander H, Franzosa EA, Yassour M, Kolde R, Vlamakis H, Arthur TD, Hämäläinen AM, Peet A, Tillmann V, Uibo R, Mokurov S, Dorshakova N, Ilonen J, Virtanen SM, Szabo SJ, Porter JA, Lähdesmäki H,

Huttenhower C, Gevers D, Cullen TW, Knip M, Xavier RJ. 2016. Variation in microbiome LPS immunogenicity contributes to autoimmunity in humans. Cell 165:1551.

16. Santacruz A, Collado MC, García-Valdés L, Segura MT, Marítn-Lagos JA, Anjos T, Martí-Romero M, Lopez RM, Florido J, Campoy C, Sanz Y. 2010. Gut microbiota composition is associated with body weight, weight gain and biochemical parameters in pregnant women. Br J Nutr 104:83–92.
17. Murugesan S, Ulloa-Martínez M, Martínez-Rojano H, Galván-Rodríguez FM, Miranda-Brito C, Romano MC, et al. 2015. Study of the diversity and short-chain fatty acids production by the bacterial community in overweight and obese Mexican children. Eur J Clin Microbiol Infect Dis 34:1337–1346.
18. Fei N, Zhao L. 2013. An opportunistic pathogen isolated from the gut of an obese human causes obesity in germfree mice. ISME J 7:880–884.
19. Nguyen AT, Mandard S, Dray C, Deckert V, Valet P, Besnard P, et al. 2014. Lipopolysaccharides-mediated increase in glucose-stimulated insulin secretion: involvement of the GLP-1 pathway. Diabetes 63:471–482.
20. Tenaillon O, Skurnik D, Picard B, Denamur E. 2010. The population genetics of commensal *Escherichia coli*. Nat Rev Microbiol 8:207–217.
21. Kim YG, Sakamoto K, Seo SU, Pickard JM, Gillilland MG, Pudlo NA, Hoostal M, Li X, Wang TD, Feehley T, Stefka AT, Schmidt TM, Martens EC, Fukuda S, Inohara N, Nagler CR, Núñez G. 2017. Neonatal acquisition of Clostridia species protects against colonization by bacterial pathogens. Science 356:315–319.
22. Tomas J, Reygner J, Mayeur C, Ducroc R, Bouet S, Bridonneau C, et al. 2015. Early colonizing *Escherichia coli* elicits remodeling of rat colonic epithelium shifting toward a new homeostatic state. ISME J 9:46–58.
23. Ju T, Shoblak Y, Gao Y, Yang K, Fouhse J, Finlay BB, So YW, Stothard P, Willing BP. 2017. Initial gut microbial composition as a key factor driving host response to antibiotic treatment, as exemplified by the presence or absence of commensal *Escherichia coli*. Appl Environ Microbiol 83:e01107–17.
24. Ju, T, Willing BP. 2018. Isolation of commensal *Escherichia coli* strains from feces of healthy laboratory mice or rats. Bio-protocol 8:e2780.

25. Heikkinen S, Argmann CA, Champy MF, Auwerx J. 2007. Evaluation of glucose homeostasis. Curr Protoc Mol Biol 77:29B–33B.
26. Folch J, Lees M, Stanley GHS. 1956. A simple method for the isolation and purification of total lipids from animal tissues. J Biol Chem 226:497–509.
27. McArdle BH, Anderson MJ. 2001. Fitting multivariate models to community data: a comment on distance-based redundancy analysis. Ecology 82:290–297.
28. Karlsson CLJ, Önnerfält J, Xu J, Molin G, Ahrné S, Thorngren-Jerneck K. 2012. The microbiota of the gut in preschool children with normal and excessive body weight. Obesity 20:2257–2261.
29. Lupp C, Robertson ML, Wickham ME, Sekirov I, Champion OL, Gaynor EC, Finlay BB. 2007. Host-mediated inflammation disrupts the intestinal microbiota and promotes the overgrowth of *Enterobacteriaceae*. Cell Host Microbe 2:119–129.
30. Yang Y, Smith DL, Keating KD, Allison DB, Nagy TR. 2014. Variations in body weight, food intake and body composition after long-term high-fat diet feeding in C57BL/6J mice. Obesity 22:2147–2155.
31. Ahrén B, Scheurink AJW. 1998. Marked hyperleptinemia after high-fat diet associated with severe glucose intolerance in mice. Eur J Endocrinol 139:461–467.
32. Pan WW, Myers MG. 2018. Leptin and the maintenance of elevated body weight. Nat Rev Neurosci 19:95–105.
33. Sun K, Kusminski CM, Scherer PE. 2011. Adipose tissue remodeling and obesity. J Clin Invest 121:2094–2101.
34. Shimomura I, Shimano H, Korn BS, Bashmakov Y, Horton JD. 1998. Nuclear sterol regulatory element-binding proteins activate genes responsible for the entire program of unsaturated fatty acid biosynthesis in transgenic mouse liver. J Biol Chem 273:35299–35306.
35. Li Z, Xu G, Qin Y, Zhang C, Tang H, Yin Y, et al. 2014. Ghrelin promotes hepatic lipogenesis by activation of mTOR-PPAR signaling pathway. Proc Natl Acad Sci 111:13163–13168.
36. Shoelson SE, Lee J, Goldfine AB. 2006. Inflammation and insulin resistance. J Clin Invest 116:1793–1801.

37. Xu H, Barnes GT, Yang Q, Tan G, Yang D, Chou CJ, et al. 2003. Chronic inflammation in fat plays a crucial role in the development of obesity-related insulin resistance. J Clin Invest 112:1821–1830.
38. Kittana H, Gomes-Neto JC, Heck K, Geis AL, Segura Muñoz RR, Cody LA, Schmaltz RJ, Bindels LB, Sinha R, Hostetter JM, Benson AK, Ramer-Tait AE. 2018. Commensal *Escherichia coli* strains can promote intestinal inflammation via differential interleukin-6 production. Front Immunol 9:2318.
39. Hildebrandt MA, Hoffmann C, Hamady M, Chen YY, Knight R, Bushman FD, Ahima RS, Wu, GD. 2009. High-fat diet determines the composition of the gut microbiome independent of host genotype and phenotype. Gastroenterology 136:A102.
40. Ziętak M, Kovatcheva-Datchary P, Markiewicz LH, Ståhlman M, Kozak LP, Bäckhed F. 2016. Altered microbiota contributes to reduced diet-induced obesity upon cold exposure. Cell Metab 23:1216–1223.
41. Cox LM, Yamanishi S, Sohn J, Alekseyenko A V, Leung JM, Cho I, et al. 2014. Altering the intestinal microbiota during a critical developmental window has lasting metabolic consequences. Cell 158:705–721.
42. Zhang H, DiBaise JK, Zuccolo A, Kudrna D, Braidotti M, Yu Y, Parameswaran P, Crowell MD, Wing R, Rittmann BE, Krajmalnik-Brown R. 2009. Human gut microbiota in obesity and after gastric bypass. Proc Natl Acad Sci. 106:2365–2370.
43. Aron-Wisnewsky J, Prifti E, Belda E, Ichou F, Kayser BD, Dao MC, Verger EO, Hedjazi L, Bouillot JL, Chevallier JM, Pons N, Le Chatelier E, Levenez F, Ehrlich SD, Dore J, Zucker JD, Clément K. 2019. Major microbiota dysbiosis in severe obesity: fate after bariatric surgery. Gut. 68:70–82.
44. Guo Y, Huang ZP, Liu CQ, Qi L, Sheng Y, Zou DJ. 2018. Modulation of the gut microbiome: a systematic review of the effect of bariatric surgery. Eur J Endocrinol. 178:43–56.
45. Everard A, Belzer C, Geurts L, Ouwerkerk JP, Druart C, Bindels LB, et al. 2013. Cross-talk between *Akkermansia muciniphila* and intestinal epithelium controls diet-induced obesity. Proc Natl Acad Sci 110:9066–9071.

46. Dalby MJ, Ross AW, Walker AW, Morgan PJ. 2017. Dietary uncoupling of gut microbiota and energy harvesting from obesity and glucose tolerance in mice. Cell Rep 21:1521–1533.
47. Tomas J, Mulet C, Saffarian A, Cavin J-B, Ducroc R, Regnault B, et al. 2016. High-fat diet modifies the PPAR-γ pathway leading to disruption of microbial and physiological ecosystem in murine small intestine. Proc Natl Acad Sci 113:E5934–E5943.
48. Carmody RN, Gerber GK, Luevano JM, Gatti DM, Somes L, Svenson KL, et al. 2015. Diet dominates host genotype in shaping the murine gut microbiota. Cell Host Microbe 17:72–84
49. Schwartz MW, Seeley RJ, Zeltser LM, Drewnowski A, Ravussin E, Redman LM, et al. 2017. Obesity pathogenesis: an endocrine society scientific statement. Endocr Rev 38:267–296.

Table 3.1. Primers sequences used for qPCR assays

Targeted gene	Primer	Oligonucleotides sequences (5'-3')
SREBP-1c	Forward	GGCACTAAGTGCCCTCAACCT
	Reverse	GCCACATAGATCTCTGCCAGTGT
LDLr	Forward	GAACTCAGGGCCTCTGTCTG
	Reverse	AGCAGGCTGGATGTCTCTGT
PPAR-α	Forward	GCCTGTCTGTCGGGATGT
	Reverse	GGCTTCGTGGATTCTCTTG
PPARγ2	Forward	ATGCACTGCCTATGAGCACT
	Reverse	CAACTGTGGTAAAGGGCTTG
DGAT1	Forward	GTGCACAAGTGGTGCATCAG
	Reverse	CAGTGGGATCTGAGCCATCA
DGAT2	Forward	TTCCTGGCATAAGGCCCTATT
	Reverse	AGTCTATGGTGTCTCGGTTGAC
FASN	Forward	AGGGGTCGACCTGGTCCTCA
	Reverse	GCCATGCCCAGAGGGTGGTT
ACC1	Forward	TGGAGCTAAACCAGCACTCC
	Reverse	GCCAAACCATCCTGTAAGCC
CPT1α	Forward	ATCGTGGTGGTGGGTGTGATAT
	Reverse	ACGCCACTCACGATGTTCTTC
CD36	Forward	GATCGGAACTGTGGGCTCAT
	Reverse	GGTTCCTTCTTCAAGGACAACTTC
LFABP	Forward	GCAGAGCCAGGAGAACTTTGAG
	Reverse	TTTGATTTTCTTCCCTTCATGCA
ApoB	Forward	TCACCATTTGCCCTCAACCTAA
	Reverse	GAAGGCTCTTTGGAAGTGTAAAC
MTTP	Forward	CTCTTGGCAGTGCTTTTTCTCT
	Reverse	GAGCTTGTATAGCCGCTCATT
HMG-CoA reductase	Forward	CAGGATGCAGCACAGAATGT
	Reverse	CTTTGCATGCTCCTTGAACA
G6Pase	Forward	AGGAAGGATGGAGGAAGGAA
	Reverse	TGGAACCAGATGGGAAAGAG
PEPCK	Forward	CATATGCTGATCCTGGGCATAAC
	Reverse	CAAACTTCATCCAGGCAATGTC
FABP4	Forward	AAGGTGAAGAGCATCATAACCCT
	Reverse	TCACGCCTTTCATAACACATTCC
B2M	Forward	CATGGCTCGCTCGGTGAC
	Reverse	CAGTTCAGTATGTTCGGCTTCC
GAPDH	Forward	ATTGTCAGCAATGCATCCTG
	Reverse	ATGGACTGTGGTCATGAGCC

Table 3.2. Metabolic parameters in plasma of SC, HF, and HF_EC mice

Parameters	SC (pg/mL)	HF (pg/mL)	HF_EC (pg/mL)	SEM	*P* value	Detection limit
Amylin	44.24	58.28	59.57	3.85	0.23	13.72
C-peptide	883.88[b]	925.77[ab]	1403.47[a]	92.39	0.03	22.86
GLP-1	55.18	118.84	25.01	19.78	0.16	13.72
GIP	117.91	165.89	152.98	14.19	0.44	0.91
Ghrelin	27.23	38.27	8.36	7.26	0.28	2.29
Insulin	376.73[b]	792.46[a]	992.90[a]	84.53	< 0.01	22.86
Leptin	1302.24[b]	2453.25[b]	4394.36[a]	374.63	< 0.01	22.86
PYY	97.10	75.93	104.31	7.87	0.32	2.29
Glucagon	97.40	88.93	87.47	8.43	0.88	4.57
PP	20.53	21.98	39.77	11.68	0.83	2.29
Resistin	16041.64	16813.19	17880.27	869.02	0.71	30.29

Table 3.3. Metabolic parameters in plasma of SC and SC_EC mice

Parameters	SC (pg/mL)	SC_EC (pg/mL)	SEM	*P* value	Detection limit
Amylin	59.63	66.87	7.68	0.650	13.72
C-peptide	745.89	719.15	40.61	0.756	22.86
GLP-1	52.75	85.65	18.42	0.341	13.72
GIP	270.23	202.32	32.85	0.318	0.91
Ghrelin	37.77	67.00	9.02	0.113	2.29
Insulin	337.80	503.14	89.66	0.671	22.86
Leptin	1016.17	1248.27	138.26	0.420	22.86
PYY	88.58	86.85	7.09	0.908	2.29
Glucagon	74.57	105.10	8.29	0.083	4.57
PP	37.11	32.01	2.54	0.332	2.29
Resistin	29729.89	36105.73	2675.81	0.246	30.29

Table 3.4. The relative abundance of predominant fecal bacterial phyla and genera

	SC	HF	HF_EC	SEM	*P* value	FDR_*P* value
Phylum						
p__Actinobacteria	0.16	0.27	0.16	0.03	0.131	0.131
p__Bacteroidetes	69.90^{a}	45.15^{b}	42.56^{b}	2.86	<0.001	<0.01
p__Firmicutes	19.27^{b}	23.73^{ab}	28.44^{b}	1.56	0.033	0.057
p__Proteobacteria	1.47	0.85	0.78	0.12	0.104	0.121
p__Verrucomicrobia	8.34^{b}	29.36^{a}	27.79^{a}	2.15	<0.001	<0.01
p__Tenericutes	0.81^{a}	0.02^{b}	0.03^{b}	0.10	<0.01	<0.01
Genus						
Actinobacteria						
g__*Bifidobacterium*	0.12	0.17	0.10	0.02	0.443	0.505
g__*Adlercreutzia*	0.03^{b}	0.10^{a}	0.06^{ab}	0.01	0.031	0.060
Bacteroidetes						
g__*Bacteroides*	18.16	20.09	17.25	1.58	0.961	0.961
f__*Rikenellaceae*;g__	22.55^{a}	7.02^{b}	6.76^{b}	1.76	<0.001	<0.01
f_*S24-7*;g_	29.17^{a}	18.05^{b}	13.08^{b}	1.81	<0.01	<0.01
Firmicutes						
g__*Lactococcus*	0.00^{b}	0.13^{a}	0.10^{a}	0.02	<0.001	<0.01
g__*Turicibacter*	0.26^{a}	0.08^{b}	0.24^{ab}	0.04	0.027	0.055
o__Clostridiales;f__;g__	12.74	11.94	12.89	1.09	0.827	0.869
f__*Clostridiaceae*;g__	0.13^{b}	0.78^{a}	0.53^{a}	0.09	<0.01	<0.01
g__*Clostridium*	0.03	0.02	0.01	0.00	0.760	0.820
g__*Dehalobacterium*	0.18	0.14	0.15	0.01	0.733	0.813
f__*Lachnospiraceae*;g__	1.44^{a}	1.01^{ab}	0.68^{b}	0.11	0.020	0.044
g__*Coprococcus*	0.14	0.10	0.26	0.03	0.394	0.462
g__*Dorea*	0.18^{b}	0.33^{ab}	0.46^{a}	0.04	0.019	0.043

g__*[Ruminococcus]*	0.27[b]	0.70[a]	0.39[ab]	0.06	0.007	0.018
f__*Peptococcaceae*;g__	0.00[b]	0.56[a]	0.38[a]	0.06	<0.001	<0.01
f__*Ruminococcaceae*;Other	0.84[a]	0.27[b]	0.25[b]	0.08	<0.01	<0.01
f__*Ruminococcaceae*;g__	0.71[b]	2.83[a]	4.52[a]	0.39	<0.001	<0.01
g__*Oscillospira*	1.33[b]	2.68[ab]	3.26[a]	0.24	<0.01	<0.01
g__*Ruminococcus*	0.20[b]	1.04[ab]	1.56[a]	0.19	<0.01	0.006
f__Enterococcaceae;Other	0.00[b]	0.01[a]	0.01[a]	0.00	0.002	0.006
f__*Erysipelotrichaceae*;g__	0.01[b]	0.23[a]	0.14[a]	0.03	<0.001	<0.01
g__*Allobaculum*	0.39	0.53	0.18	0.07	0.394	0.462
g__*Anaerostipes*	0.01	0.00	0.02	0.00	0.049	0.083
g__*Lactobacillus*	0.34	0.17	0.05	0.05	0.059	0.098
f__*[Mogibacteriaceae]*;g__	0.03	0.01	0.02	0.01	0.281	0.385
f__*Lachnospiraceae*;Other	0.03[a]	0.00[b]	0.00[b]	0.00	<0.001	<0.01
Proteobacteria						
g__*Sutterella*	1.47[a]	0.84[ab]	0.54[b]	0.13	0.026	0.055
f__*Enterobacteriaceae*;g__	0.00[b]	0.00[b]	0.14[a]	0.03	<0.001	<0.01
Verrucomicrobia						
g__*Akkermansia*	8.35[b]	29.36[a]	27.78[a]	2.15	<0.001	<0.01
Tenericutes						
g__*Anaeroplasma*	0.74[a]	0.00[b]	0.00[b]	0.09	<0.001	<0.01
o__RF39;f__;g__	0.06[a]	0.02[b]	0.03[ab]	0.01	0.043	0.076

The relative abundance data (%) were presented as the mean ± pooled standard error of the mean (SEM). The non-parametric Kruskal Wallis test with the Dwass, Steel, Critchlow-Fligner multiple comparisons post-hoc procedure was used to compare the differences between treatment groups. The *P* value and false discovery rate (FDR)-adjusted *P* value were shown. For all treatment, n = 8. [a,b,c] Means that do not share a common letter are significantly different. $\alpha = 0.05$.

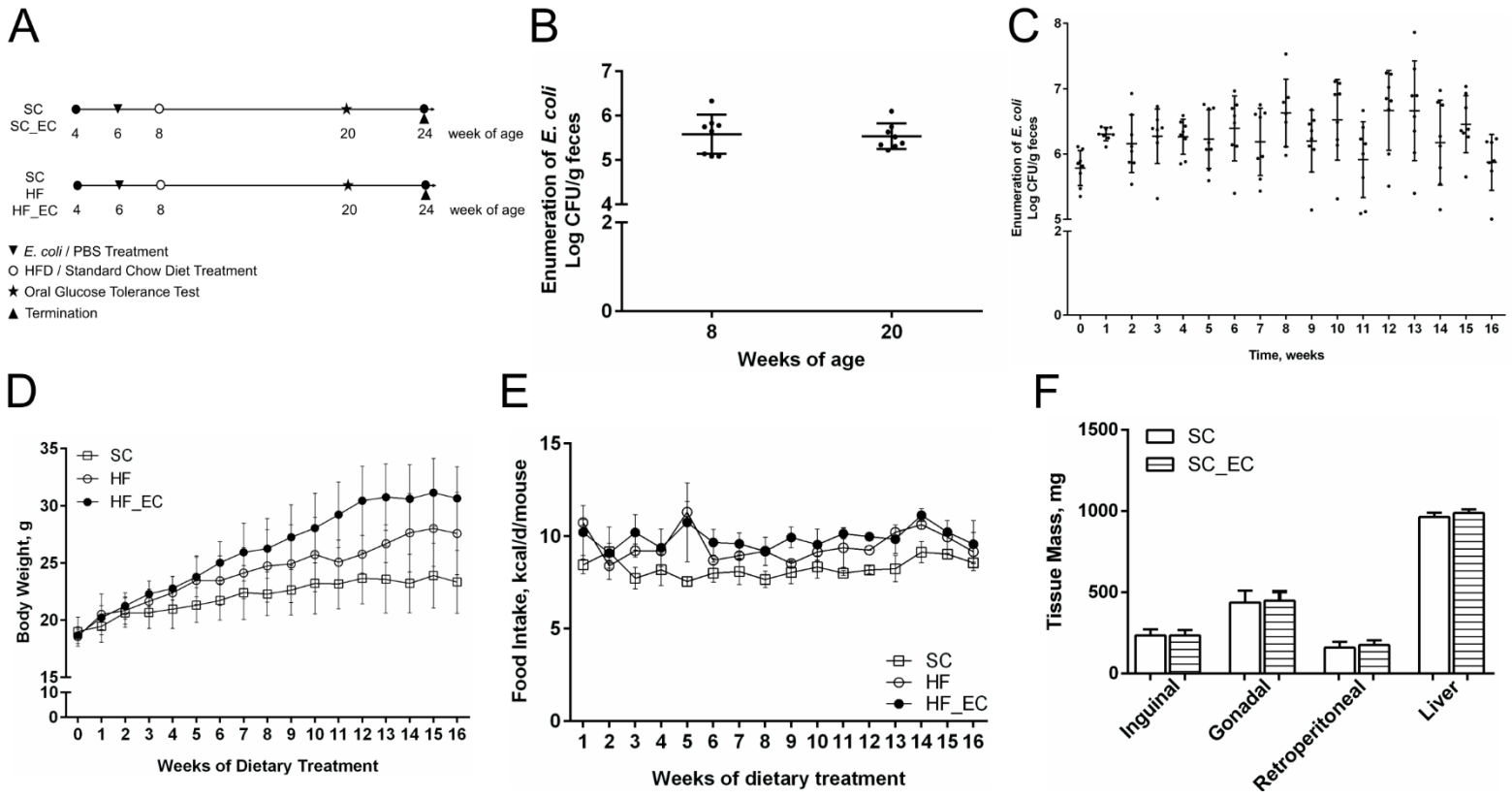

Figure 3.1. A) Experimental protocol. **B**) Enumeration of fecal *E. coli* under standard chow diet treatment. **C**) Enumeration of fecal *E. coli* during 16 weeks of HFD treatment. **D**) Body weight during 16 weeks of HFD treatment. **E**) Food intake during 16 weeks of HFD treatment. **F**) Tissue (fat, liver) mass in SC and SC_EC mice after 16 weeks of standard chow diet treatment. For all treatment, n = 8. Data are shown as mean ± SD. [a,b] Means that do not share a common letter are significantly different. $\alpha = 0.05$.

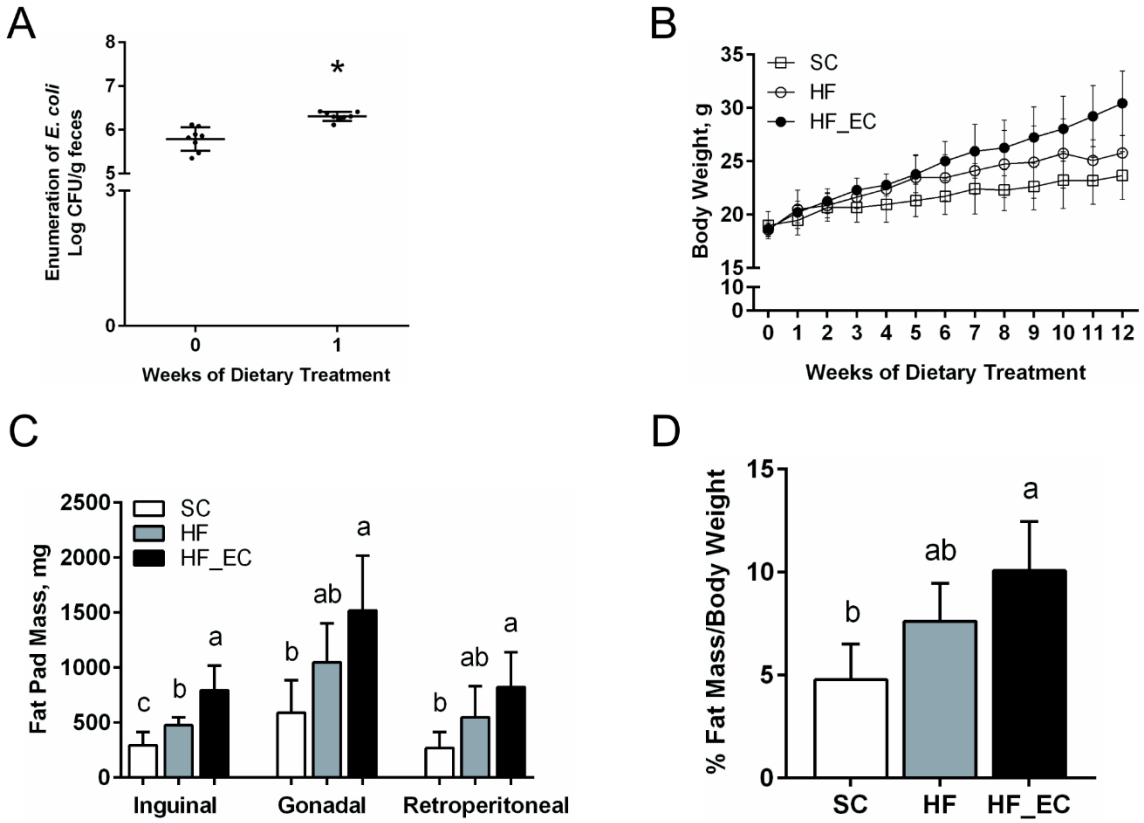

Figure 3.2. A) Enumeration of fecal *E. coli* one week after HFD treatment. **B**) Body weight of SC, HF, HF_EC mice in 12 weeks of dietary treatment. **C**) Fat pad mass of SC, HF, and HF_EC mice after 16 weeks of dietary treatments. **D**) Percentage of fat mass relative to body weight after 16 weeks of dietary treatment. For all treatment, n = 8. Data are shown as mean ± SD. [a,b,c] Means that do not share a common letter are significantly different. $\alpha = 0.05$.

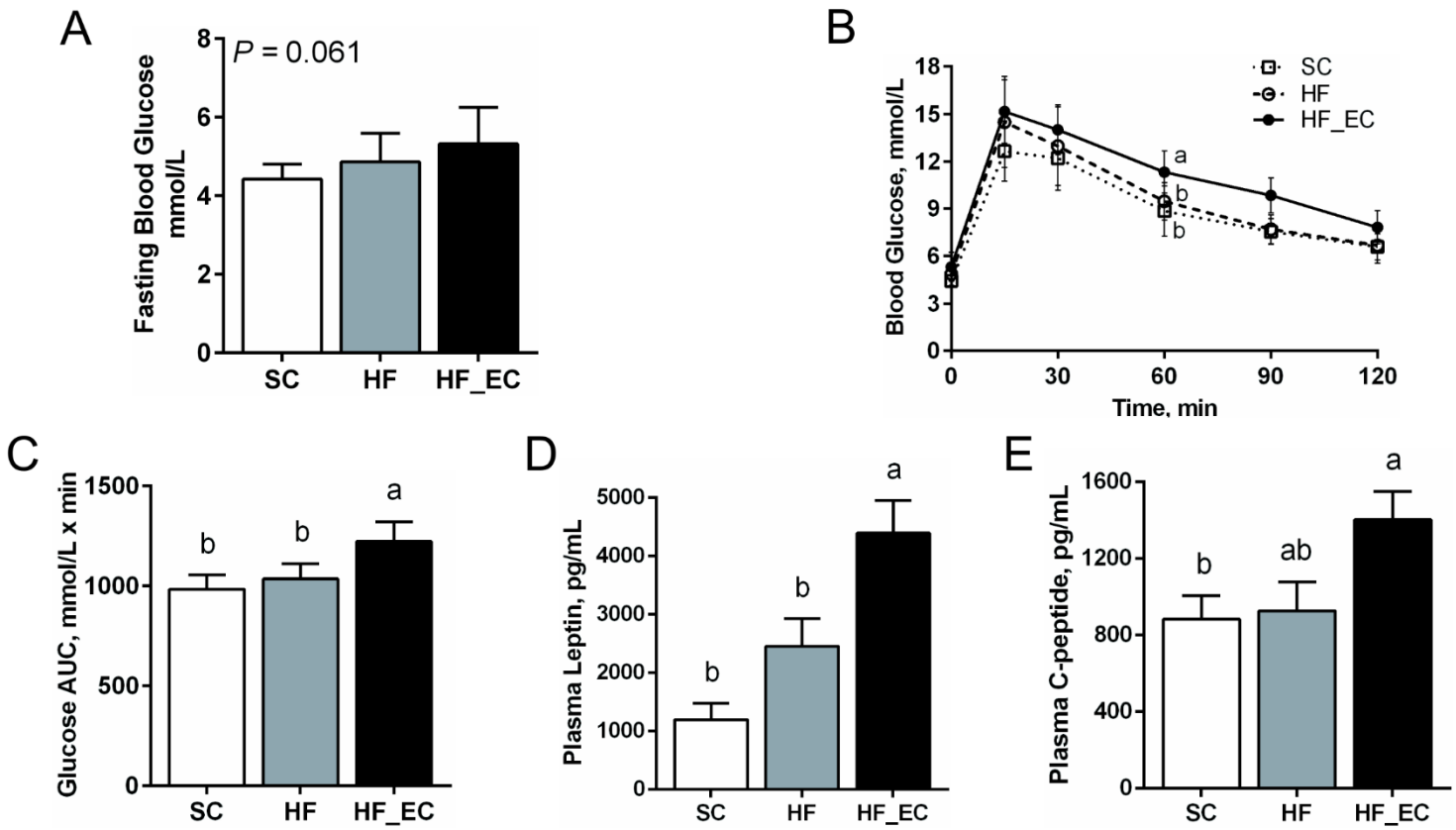

Figure 3.3. A-C) OGTT results of SC, HF, HF_EC mice after 12 weeks of dietary treatment. **A**) Fasting blood glucose levels. **B**) Glucose curve in 120 min of the OGTT test. **C**) The AUC value. **D**) Plasma leptin levels after 16 weeks of dietary treatment. **E**) Plasma C-peptide levels after 16 weeks of dietary treatment. For all treatment, n = 8. Data are shown as mean ± SD. [a,b] Means that do not share a common letter are significantly different. $\alpha = 0.05$.

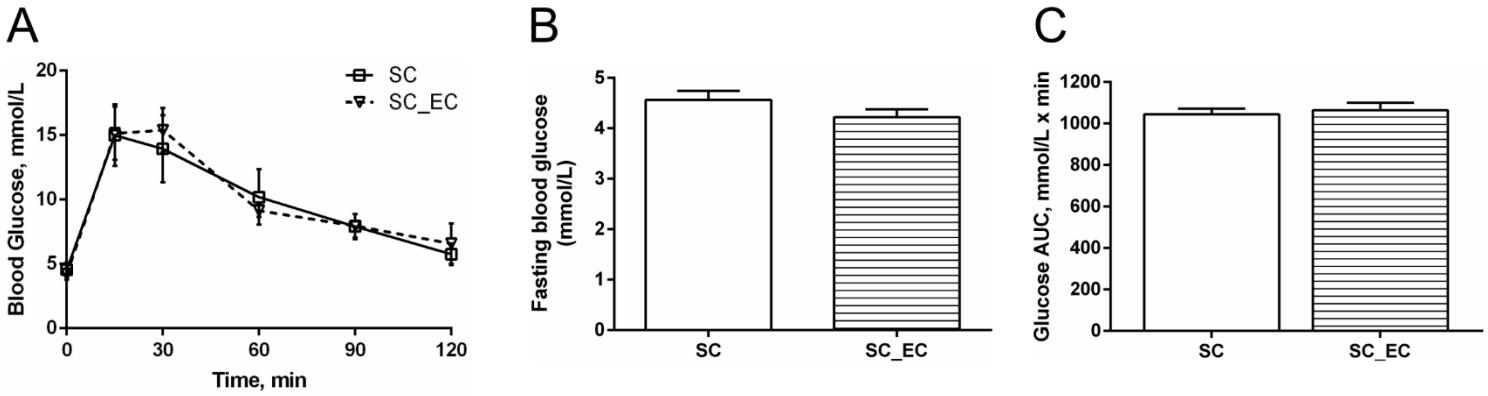

Figure 3.4. A-C) OGTT results of SC and SC_EC mice after 12 weeks of standard chow diet treatment. **A**) Glucose curve in 120 min of the OGTT test. **B**) Fasting blood glucose levels. **C**) The AUC value. For all treatment, n = 8. Data are shown as mean ± SD. [a,b] Means that do not share a common letter are significantly different. $\alpha = 0.05$.

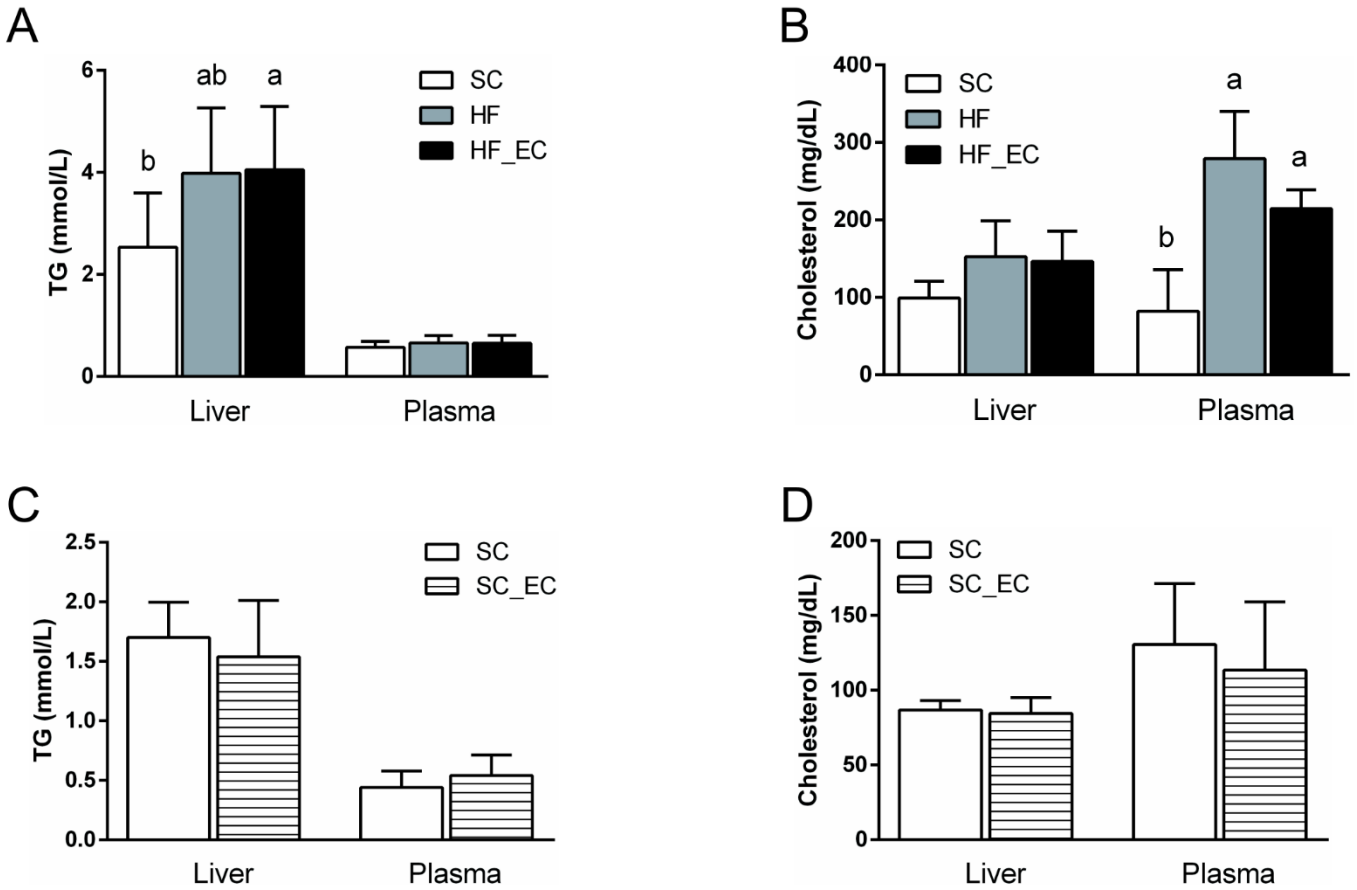

Figure 3.5. Comparisons of plasma and hepatic TG and cholesterol levels. In SC, HF, and HF_EC mice: **A**) Plasma and hepatic TG levels. **B**) Plasma and hepatic cholesterol levels. In SC and SC_EC mice: **C**) Plasma and hepatic TG levels. **D**) Plasma and hepatic cholesterol levels. For all treatment, n = 8. Data are shown as mean ± SD. ^{a,b} Means that do not share a common letter are significantly different. $\alpha = 0.05$.

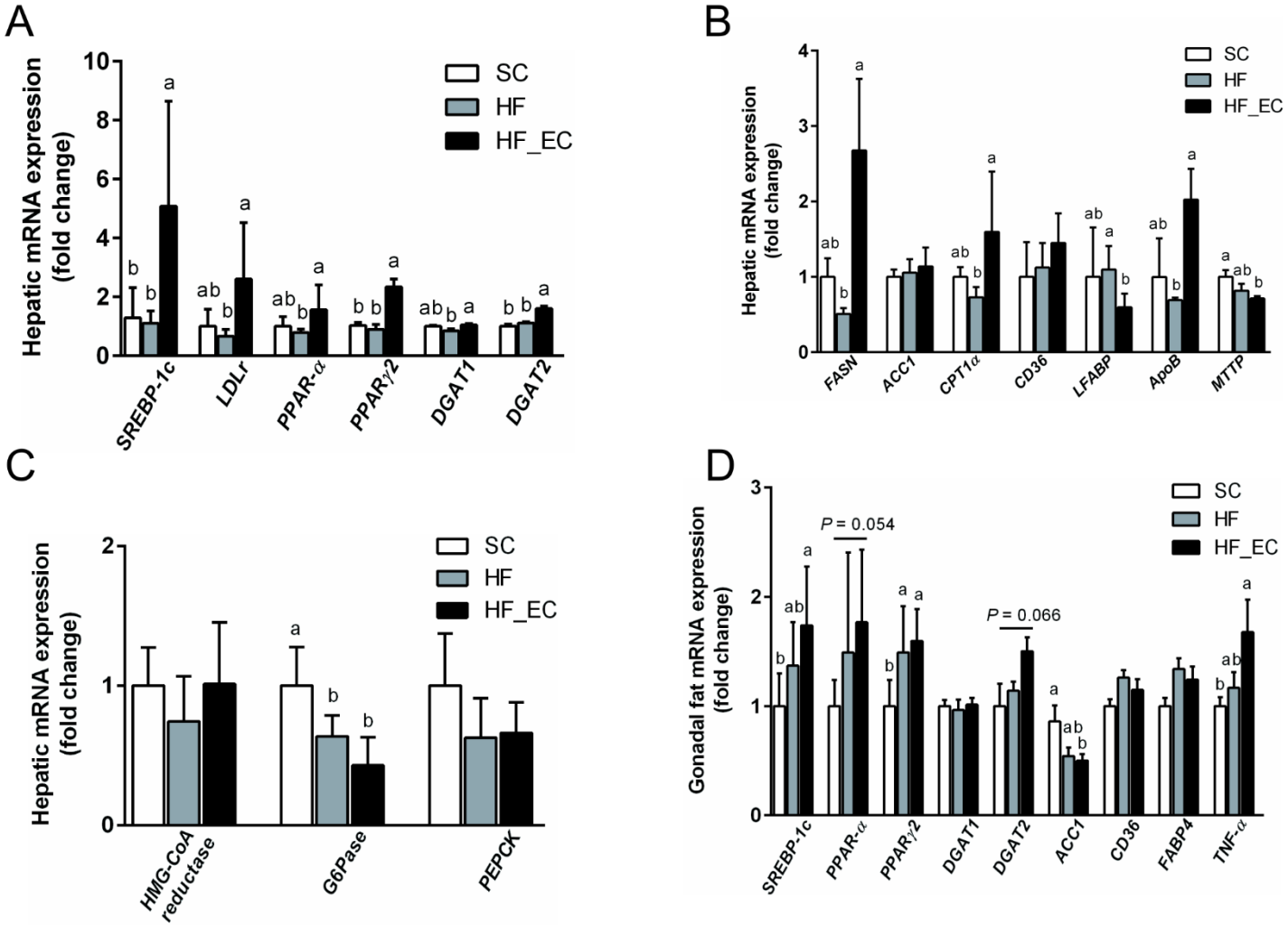
A
Hepatic mRNA expression (fold change)
SC
HF
HF_EC
SREBP-1c
LDLr
PPAR-α
PPARγ2
DGAT1
DGAT2
B
Hepatic mRNA expression (fold change)
FASN
ACC1
CPT1α
CD36
LFABP
ApoB
MTTP
C
Hepatic mRNA expression (fold change)
HMG-CoA reductase
G6Pase
PEPCK
D
Gonadal fat mRNA expression (fold change)
P = 0.054
P = 0.066
FABP4
TNF-α

Figure 3.6. A-C) Hepatic lipogenic gene expression in SC, HF, and HF_EC mice after 16 weeks of dietary treatment. Lipogenesis (*FASN, ACC1*), FA oxidation (*CPT1α*), FA uptake (*CD36, LFABP*), VLDL secretion (*ApoB, MTTP*), gluconeogenesis (*G6Pase, PEPCK*). **D**) Lipogenic gene and inflammatory gene expression in the gonadal fat of SC, HF, and HF_EC mice after 16 weeks of dietary treatment. For all treatment, n = 8. Data are shown as mean ± SD. ^{a,b} Means that do not share a common letter are significantly different. $\alpha = 0.05$.

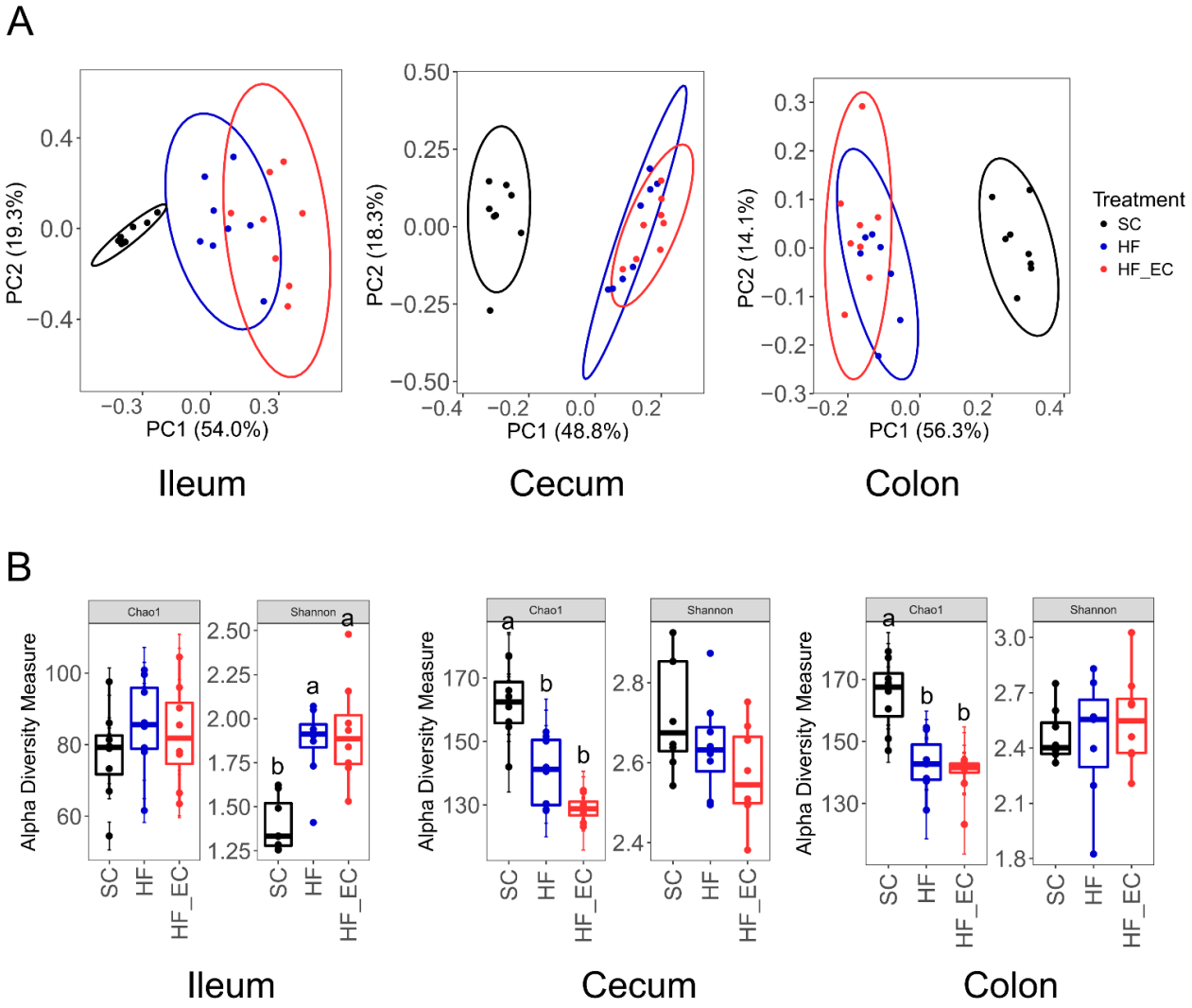
A
PC2 (19.3%)
PC1 (54.0%)
Ileum
PC2 (18.3%)
PC1 (48.8%)
Cecum
PC2 (14.1%)
PC1 (56.3%)
Colon
Treatment
SC
HF
HF_EC
B
Alpha Diversity Measure
Chao1
Shannon
SC
HF
HF_EC
Ileum
Cecum
Colon

Figure 3.7. Microbial structural analysis of contents collected from different intestinal segments. **A**) PCoA plots of bacterial communities based on a Bray-Curtis dissimilarity matrix. Colors represent intestinal sites and within the same intestinal site, each point represents an individual mouse. **B**) Alpha diversity analysis of bacterial communities in ileal, cecal, and colonic contents of mice. Contents were harvested 16 weeks after dietary treatment. For all treatment groups, n = 8. Data are shown as mean ± SEM.

4. CHAPTER 4: DEFINING THE ROLE OF *PARASUTTERELLA*, A PREVIOUSLY UNCHARACTERIZED MEMBER OF THE CORE GUT MICROBIOTA

4.1. Introduction

Parasutterella, a genus of Betaproteobacteria, has been defined as a member of the healthy fecal core microbiome in the human gastrointestinal tract (GIT) (1). Members of the genus *Parasutterella* have also been found in a variety of host species, including mice, rats, dogs, pigs, chickens, turkeys, and calves according to reported sequences available in the Ribosomal Database Project (RDP). The genus *Parasutterella* contains two type strains, *P. excrementihominis* YIT 11859 and *P. secunda* YIT 12071, which were first isolated from human feces (2, 3). 16S ribosomal RNA (rRNA) gene sequence similarities indicate that *Parasutterella* sequences from mice are most closely related to *P. excrementihominis*. In humans, the genus *Parasutterella* has a unique phylogenetic classification (4) as it stands out as one of the most frequently reported taxa within the class Betaproteobacteria in the gut, and is largely represented by a single species, *Parasutterella excrementihominis*. The relative abundance of this species has been associated with different host health outcomes such as inflammatory bowel disease, obesity, diabetes, and fatty liver disease (4–6).

A significant reduction of *Parasutterella* in response to high fat diet (HFD) treatment has been observed in multiple animal models and human studies, indicating a negative correlation between *Parasutterella* abundance and HFD induced metabolic phenotypes including hypothalamic inflammation (7–10). *Parasutterella* has also been identified to respond to antibiotic administration and other dietary interventions such as prebiotic and resistance starch supplementation in human studies and animal trials (11–13). In addition, patients with *Clostridium difficile* infection (CDI) exhibited a dramatic increase in the

abundance of Proteobacteria in the gut, however, within the phylum of Proteobacteria, *Parasutterella* was significantly lower in CDI patients and asymptomatic carriers than in healthy controls (14). An *in vitro* fermentation study, which investigated how the microbial composition of fecal donors impacted fermentation properties of dietary fiber, showed that the abundance of *Parasutterella* decreased during the fermentation and positively correlated with ammonia production (15). These results provide evidence that *Parasutterella* has a role in impacting microbial activities and host responses, however, beyond correlative work, our knowledge of *Parasutterella's* physiological characteristics is extremely limited. With a growing number of studies correlating *Parasutterella* with diverse outcomes, including beneficial and detrimental, it becomes essential that we begin to understand the basic role of this microbe and its uncharacterized metabolites in the microbial ecosystem and host physiology.

The alteration of microbially-derived metabolites is an important mechanism through which changes in gut microbial activity generate functional consequences for host health outcomes (16, 17). Several microbially generated metabolites derived from substrates including carbohydrates, aromatic amino acids, bile acids, and choline have been identified as regulatory molecules. For instance, short-chain fatty acids (SCFAs) play a crucial role in linking diet, gut microbiota, and host immune response (18), and aromatic amino acid metabolites such as indole derivatives enhance epithelial barrier integrity (19). Additionally, the modulatory effects of microbial-derived bile acid metabolites on the farnesoid X receptor (FXR) signaling pathway are recognized to influence bile acid profile and host lipid metabolism (20). The identification of these molecules provides new insights into the microbe-microbe and microbe-host interactions, though there are still a considerable number

of yet-to-be described microbial-derived metabolites. Specifically, when pursuing the functionalities of a gut commensal bacterium that has not been well characterized, the assessment of their contribution to gut metabolite profiling becomes a sufficient and valid approach to deepen our understanding of lifestyle and physiological characteristics.

Different experimental models and detection methodologies have been established to unravel metabolic functionalities of the gut microbiota including *in vitro* fermentation models, human clinical trials, humanized germ-free mouse models, and monocolonization of germ-free mice in combination with targeted or untargeted metabolomic approaches (21, 22). *In vitro* characterization of metabolic capabilities of gut commensal bacteria is a simpler approach, however, it is limited by culturability and required growth conditions. For example, many gut bacteria will only grow to pinpoint colonies and have a limited ability to grow in broth culture (23). The animal model integrates the interaction between the microbe and host to improve the understanding of the holobiont. In the current study, the murine *Parasutterella* strain was successfully isolated and physiological characteristics were identified based on the draft genome and *in vitro* culture results. The isolate was subsequently introduced to *Parasutterella*-free mice harboring a complex microbiota, to investigate the capability of *Parasutterella* to colonize the mouse GIT and its effects on the microbial community, intestinal metabolite profiling, and host physiology. The results provide the first indication of the role of *Parasutterella* in the GIT and improve our understanding of the mechanism through which it may influence host health outcomes.

4.2. Materials and methods

4.2.1. Bacterial strain isolation. The mouse *Parasutterella* strain, *Parasutterella* mc1, was isolated from feces of healthy phosphatidylethanolamine N-methyltransferase

knockout mice using two different types of selective media including the Gifu Anaerobic Medium (GAM) agar at pH value of 6.0 and GAM supplemented with 4 μg/mL oxacillin, as modified from previously published methods (2, 3). Feces were collected immediately after defecation into 1x phosphate-buffered saline (PBS, pH = 7.4) supplemented with 0.05% (w/v) L-cysteine HCl, transferred into an anaerobic chamber (Sheldon, Cornelius, Oregon) containing the anaerobic gas mixture of 85% N_2, 10% CO_2, and 5% H_2, homogenized, diluted, spread on selective agar, and incubated at 37°C for 3 days.

4.2.2. PCR amplification of 16S rRNA gene sequences. The 16S rRNA gene sequence identification of colonies isolated from the selective media was conducted by a colony polymerase chain reaction (PCR) using primers for bacterial 16S rRNA gene, 27f and 1492r (Integrated DNA Technologies, Coralville, IA) as previously described (24, 25). Each 50 μL PCR mixture solution consisted of 2 μL of 10 μM forward primer 27f, 2 μL of 10 μM reverse primer 1492r, 2 μL of 10 mM deoxynucleotide triphosphate mix (Invitrogen, Carlsbad, CA), 5 μL of 10x Taq polymerase buffer (Invitrogen), 2 μL of 50 mM $MgCl_2$ (Invitrogen), 0.5 μL of 1 U/μL Taq polymerase (Invitrogen), and a small amount of colony. The thermal cycling program included an initial 10-min denaturation step at 94°C, 35 cycles of 94°C for 30 s, 58°C for 30 s, and 72°C for 1 min 40s, and a final 7-min extension at 72°C. PCR products were visualized by 1% agarose gel electrophoresis followed by the SYBR Safe DNA gel staining (Invitrogen).

4.2.3. Bacterial strain culture. To test the effect of supplementing asparagine (Asn) and aspartate (Asp) on the growth of *Parasutterella*, the isolate was cultured in 5 mL of GAM at 37°C anaerobically with an initial inoculum density of 10^2 CFUs/mL. At 48 h of growth, filter-sterilized amino acid solutions were added to the bacterial culture at 2 mM (L-

asparagine and L-aspartate, Sigma Aldrich, St. Louis, MO, USA) and the GAM control group received the same volume of sterile water. Bacterial cells were enumerated at 72 h of growth using GAM agar and CFUs per mL culture were then calculated. Experiments were performed in triplicate and repeated twice.

In mouse colonization studies, the bacterial strain was cultivated in 5 mL of GAM medium at 37°C for 72 h. The culture medium containing approximately 1.0×10^7 CFUs/mL of *Parasutterella* was centrifuged to harvest bacterial cells, cell pellets were resuspended in 1 x PBS supplemented with 0.05% (w/v) L-cysteine and mice were subsequently exposed to *Parasutterella* by administering 1mL of the bacterial suspension to the bedding (10^7 CFUs).

4.2.4. Scanning electron microscopy. Colonies growing on GAM agar after 3 days incubation were fixed in electron microscope fixative (2.5% of glutaraldehyde and 2% of paraformaldehyde in 0.1 M phosphate buffer) for a minimum of two hours. The specimen was washed using 50%, 70%, 90%, and 100% ethanol and subsequently washed with a mixture of hexamethyldisilazane (HMDS) reagent and ethanol. After being rinsed with HMDS for two times, the specimen was left to air-dry overnight in the fume hood. The dry specimen was mounted on a 1/2'' aluminum SEM stub. The stub was sputtered with Au/Pd in a Hummer 6.2 sputter coater (Anatech Ltd, Springfield, VA). The cell morphology was then observed using a Philips/FEI (XL30) Scanning Electron Microscope.

4.2.5. Whole genome sequencing of mouse *Parasutterella* isolate. Whole genome sequencing of *Parasutterella* isolate was performed on an Illumina Miseq Platform as described previously (26). Libraries were sequenced using a V3 MiSeq cartridge (Illumina, San Diego, CA) with paired-end reads generated (2 x 300 bp). The draft genome was assembled and annotated with SPAdes assembler (27) and Prokka (v1.12) (28), respectively.

The circular map of the whole genome was generated using the CGView Comparison Tools (29).

4.2.6. Quantitative PCR (qPCR) assay for detecting mouse *Parasutterella* isolate. A set of PCR primers (Paraf/Parar) targeting the 16S rRNA gene of the mouse *Parasutterella* isolate was designed (amplicon size, 276 bp). Primers were checked against 16S rRNA gene sequences of the genus *Parasutterella* (n = 705), which were retrieved from RDP website (release 11.5; http://rdp.cem.msu.edu/). All sequences were obtained as good quality, nearly full-length (> 1,200 bp) using the feature Hierarchy Browser program. Sequences of primers are listed in Table 4.1. The specificity of primers was validated by testing them against DNA isolated from *Parasutterella* free and *Parasutterella* positive mice based on previously obtained 16S rRNA gene amplicon sequencing results. The DNA isolated from the *Parasutterella* isolate was used as a positive control. Sanger sequencing was used to validate the amplicon generated from *Parasutterella* positive mice.

qPCR reaction was performed using the PerfeCTa SYBR Green Supermix (Quantabio, Gaithersburg, MD) on an ABI StepOne™ real-time System (Applied Biosystems, Foster City, CA). The amplification program contained an initial denaturation step at 94°C for 3 min followed by 40 cycles of denaturation at 94°C for 10 s and annealing at 60°C for 30 s. The sensitivity of primers was determined using DNA isolated from the *Parasutterella* free and *Parasutterella* positive mice with a cutoff cycle threshold (Ct) of 34.

To construct standards for quantifying *Parasutterella* 16S rRNA gene copy numbers in feces using the qPCR method, amplicons from the colony PCR of *Parasutterella* isolate generated by Paraf/Parar primers were purified using the GeneJET PCR purification kit (Thermo Scientific, Nepean, ON) according to manufacturer's instructions. Purified PCR

products were ligated into the competent *E. coli* cells using the TOPO TA cloning kit (Invitrogen, Carlsbad, CA). The plasmid DNA was extracted from overnight cultures using the GeneJet Plasmid Miniprep kit (Thermo Scientific, Nepean, ON) and inserts were verified by the Sanger sequencing. The concentration of the plasmid DNA was adjusted, and ten-fold serial dilutions were performed to construct standards. CT values at different dilutions were averaged and plotted relative to corresponding copy numbers.

4.2.7. Quantification of metabolite concentrations in bacterial cultures. Bacterial cultures grown for 0, 24, 48, 72, 96, and 120 h in GAM broth were homogenized in 3.5 % perchloric acid ($HClO_4$) and incubated at 4°C overnight to remove proteins. The supernatant was collected after centrifuging at 10,000 g for 10 min. Compounds were separated using High-Performance Liquid Chromatography (HPLC) equipped with an Aminex 87H cation-exchange column (Bio-Rad, Mississauga, Ontario) at 70°C. A 5 mM H_2SO4 solution was used as the solvent and the flow rate was 0.4 mL/min. Metabolites were monitored with a UV detector at 210 nm or 240 nm, and external standards were used for quantification.

4.2.8. Mice. Six to eight week old female C57BL/6J mice (Jackson Laboratory, Bar Harbor, ME) were housed in the animal facility at the University of Alberta. Mice were kept under specific pathogen-free (SPF) conditions with sterilized filter-topped cages and standard chow diet (LabDiet®, 5053). All the mice were screened with designed primers (Paraf/Parar, Table 4.1) and sixteen mice that did not harbor *Parasutterella* were selected. Mice were randomly grouped into four cages with 4 mice per cage by a blinded lab animal technician and balanced for average body weight. Cages were allocated into 2 treatments: control (CON) and *Parasutterella* colonization (PARA). Preliminary results showed that the exposure to *Parasutterella* by oral gavage or administration to the bedding resulted in successful

colonization of the mouse intestine. Therefore, in the current study, the PARA group was exposed to *Parasutterella* mc1 by administering 1 mL of the bacterial suspension with the concentration of 10^7 CFUs/mL to the bedding while the CON group received PBS (Figure 4.1A). Body weight was recorded weekly and mice were euthanized by CO_2 asphyxiation six weeks after *Parasutterella*/PBS treatment. Contents from ileum, cecum, and colon were collected and liver, intestinal tissue, and blood were harvested. Protocols employed were approved by the University of Alberta's Animal Care Committee and in accordance with the guideline of the Canadian Council on the Use of Laboratory Animals. The colonization experiment was repeated three times with the total sample size of 24 for each treatment and the untargeted metabolomic analysis was repeated twice with the total sample size of 16 for each treatment.

4.2.9. Characterization of gut microbial composition. DNA was extracted from ileal, cecal, and colonic contents after *Parasutterella*/PBS treatment as well as from feces before the treatment. The DNA extraction, amplicon library construction, paired-end sequencing and data analysis were performed using protocols and pipelines published previously (26).

4.2.10. Ultrahigh Performance Liquid Chromatography-Electrospray Ionization/Fourier Transform Mass Spectrometry (UPLC-ESI/FTMS). Frozen cecal contents were lyophilized and homogenized in 80% aqueous methanol (25 μL/mg) and supernatants were subsequently collected after centrifugation at 15,000 rpm for 20 min. Supernatants were profiled by UPLC-ESI/FTMS in positive and negative ionization mode with a pooled quality-control sample injected for every eight samples. Samples were analyzed in a random way using a computerized list of random numbers. The UPLC-FTMS systems

consisted of an acquity UPLC system (Walters, MA, USA) coupled with an LTQ-Orbitrap Fusion mass spectrometer (Thermo Scientific, Nepean, ON), which was operated in a survey scan and Fourier transform MS detection mode.

To maximize chromatographic separations, analytes were separated on a C4 column (dimension, 2.1 x 50 mm; particle size, 1.7 μm), a C18 column (dimension, 2.1 x 100 mm; particle size, 1.7 μm), and a HILIC column (dimension, 2.1 x 100 mm; particle size, 1.7 μm), respectively. For separations performed on the C4 column, the UPLC mobile phase consisted of 0.01% formic acid in water (solution A) and 0.01% formic acid in acetonitrile (solution B) for binary gradient elution to detect and quantify phospholipids and other very hydrophobic lipids. The phospholipid depletion-solid phase extraction (PD-SPE) was conducted before being injected onto the C18 UPLC column according to the previously established method (30). The mobile phase for the C18 column consisted of 0.01% formic acid in water (solution A) and 0.01% formic acid in isopropanol-acetonitrile (1:2) for binary gradient elution to detect and quantify non-phospholipid metabolites. To perform separation on HILIC column, analytes were loaded onto reversed-phase C18 solid phase extraction (SPE) cartridge to collect flow-through fractions which were subsequently dried under a gentle nitrogen gas flow. Residues were reconstituted in 70% acetonitrile and injected on HILIC column using mobile phase comprised 5 mM NH4Ac (solution A) and acetonitrile (solution B) for chromatographic separation, which was good at detecting and relatively quantifying very polar metabolites such as sugars and nucleotides. The flow rate for all three types of columns was 0.35 mL/min and chromatographic temperature conditions were 40°C (C4 and HILIC column) and 50°C (C18 column). Mass spectrometry data were collected in full scan mode at 2 Hz with a detection range of 80 to 1,000 mass/charge (m/z) at 60,000 FWHM (m/z 400).

Chromatography retention times were 1.15-19.05 min for C4, 0.90-33.16 min for C18, and 0.91-8.89 min for HILIC column.

Each of the six UPLC-MS datasets (3 LC methods x two ionization modes) were processed using XCMS (version 3.2.0, https://xcmsonline.scripps.edu/) for peak detection, retention time shift correction, peak grouping, and alignment. Significant features between two treatments were searched against databases including METLIN (31), HMDB (32) and LIPID MAPS (33) to obtain mass-matched metabolite candidates. Allowable mass errors for all the database searches were less than 4 p.p.m. The retention time was taken into consideration when multiple hits were retrieved from the database to identify the potential metabolites. In addition, the retention time was considered for identifying metabolites with available chemical standards including bile acids and phospholipids. The identities of assigned metabolites, especially for those with their authentic compounds commercially available, were confirmed by UPLC-MS/MS using the collision-induced dissociation, in combination with MS/MS library searching against METLIN, HMDB or MSBANK (https://massbank.eu/MassBank/).

4.2.11. RNA isolation and cDNA synthesis. Liver and distal ileum tissue were snap frozen in liquid nitrogen and preserved at -80°C until RNA extraction. A GeneJET RNA purification Kit (Thermo Scientific, Nepean, ON) was used following manufacturer's instructions. The quality of extracted RNA was verified by gel electrophoresis using a 2x RNA GEL Loading Dye (Thermo Scientific, Nepean, ON) and 1 μg of total RNA was used for reverse transcription with the qScript Flex cDNA synthesis kit (Quantabio, Gaithersburg, MD).

4.2.12. Gene expression analysis. Hepatic gene and ileal gene expression were analyzed by qPCR using the PerfeCTa SYBR Green Supermix (Quantabio, Gaithersburg, MD). Primer sequences for ileal bile acid transporter genes as well as liver bile acid synthesis genes are listed in Table 4.1. A thermal cycling program of 94°C for 3 min followed by 40 cycles of 94°C for 10 s and 60°C for 30 s was applied on an ABI StepOne™ real-time System (Applied Biosystems, Foster City, CA) in accordance with manufacturer's recommendations. Beta-actin (*β-actin*) gene was used as the housekeeping gene for normalization. The $2^{-\Delta\Delta Ct}$ method was used to calculate the fold change of gene expression in PARA group compared with the CON group.

4.2.13. Serum cholesterol analysis. At termination, blood was collected via heart puncture and subsequently centrifuged to collect serum. The serum samples were stored at -80°C until further analysis. The serum total cholesterol was determined using a commercial colorimetric kit (Wako Diagnostics, Richmond, VA) following the manufacturer's instruction.

4.2.14. Colonic cytokine detection. Colon tissue was snap frozen and stored at -80°C until protein extraction. The protein extraction and quantification were performed as described previously (26). The MSD Proinflammatory Panel 1 (mouse) kit (Meso Scale Discovery, Gaithersburg, MD) was applied to quantify cytokines according to manufacturer's recommendations.

4.2.15. Data analysis and visualization. For microbial composition analysis, the comparison of individual taxa/OTUs between groups were performed using the Mann-Whitney U test. Nonparametric multivariate analysis of variance (NP-MANOVA) was used to identify the difference between groups using the adonis function in the vegan package (R

v3.4.4). The principal coordinate analysis (PCoA) based on a Bray-Curtis dissimilarity matrix was plotted using the phyloseq package (R v3.4.4) (34). For metabolomic data analysis, the Metaboanalyst (35) was used to conduct the data normalization, univariate and multivariate analysis. The quality of UPLC-FTMS data were controlled by filtering missing values and interquartile range (IQR). Quality-controlled data were normalized by log-transformation and proceeded to statistical analyses. Fold change values between two groups were calculated using datasets before normalization. Corrections of *P* values generated from the Student's t-test or Mann-Whitney U test were conducted for multiple testing by the Benjamini–Hochberg procedure (false discovery rate, FDR; *q*-value). Features with a *q*-value less than 0.05 were considered as statistically significant indicated as follows: ##, *q*-value < 0.01; #, *q*-value < 0.05. For the determination of body weight, gene expression, 16S rRNA gene copy numbers (log-transformed) and cytokine levels, the Shapiro-Wilk test was performed to check the normality of data distribution and the Student's t-test was used to compare the difference between two treatments. *P* values indicate statistical significance as follows: **, $P < 0.01$; *, $P < 0.05$. R (v3.4.4) and GraphPad Prism were used for visualizing results.

4.2.16. Accession number(s). The whole genome sequence of the mouse *Parasutterella* isolate was deposited in the Sequence Read Archive (SRA) under accession number SRP157402. Raw sequence reads of the 16S rRNA gene amplicon data are available through the SRA with accession number SRP157661.

4.3. Results

4.3.1. *Parasutterella* can be successfully isolated from mouse intestine using the selective media. *Parasutterella* mc1 was isolated from the selective media including GAM (pH = 6.0) and GAM supplemented with 4 μg/mL oxacillin inoculated with a 10^{-6} serially

diluted fecal sample. Colonies of *Parasutterella* appeared entire, circular, convex, and translucent with a diameter of 0.5 to 0.7 mm after 72 h of incubation on GAM agar at 37°C (Figure 4.2A). Cells of *Parasutterella* were Gram-negative, obligately anaerobic cocci or coccobacilli (0.5-0.8 × 1.0-1.5 μm in size) (Figure 4.2A). When grown in GAM broth up to 120 h at 37°C anaerobically, *Parasutterella* produced no visible turbidity and no changes in glucose, fructose or lactate were detected in the broth culture. However, the *Parasutterella* strain produced approximately 2.5 mM succinate after 72 h of growth, indicating that *Parasutterella* is a succinate-producing bacterium (Figure 4.2B).

Parasutterella mc1 shared 93% 16S rRNA sequence identity with the type strain *P. excrementihominis* YIT 11859 which was isolated from human feces (Figure 4.1B). The complete genome size of *Parasutterella* is 2.8 Mb with a G+C content of 44.1 mol% (Figure 4.2C). Detailed information including the number of total raw reads, contigs, N50, and the accession number of deposited sequence data is provided in Table 4.2. There are 2,648 unique genes predicted and the absence of genes for transporting and metabolizing exogenous sugars was consistent with the asaccharolytic characteristic of *Parasutterella* shown in broth culture (2, 3). In accordance with the presence of genes encoding L-asparaginase, aspartate ammonia-lyase, and putative aspartate dehydrogenase, asparagine was the most rapid and preferred amino acids metabolized by *Parasutterella* in GAM broth (Figure 4.3; Figure 4.4). Supplementing L-asparagine and L-aspartate at 2 mM in the GAM broth culture of *Parasutterella* at 48 h of growth increased bacterial counts at 72 h compared to that in the GAM broth control ($P < 0.05$) (Figure 4.5A). In addition, there were no identified hits of toxin virulence factors (VFs)-related genes in the genome of *Parasutterella* mc1, which

suggests that *Parasutterella* is either a commensal or symbiotic member of the gut microbiota.

4.3.2. *Parasutterella* isolate readily colonized the mouse GIT without shifting the microbial structure. SPF C57BL/6J mice were screened using a set of designed PCR primers targeting the 16S rRNA gene of the *Parasutterella* isolate to select sixteen *Parasutterella*-free individuals. We were able to confidently detect the presence of *Parasutterella* down to the 10^6 CFUs/g of feces using the qPCR system. With a single environmental exposure, *Parasutterella* rapidly and stably colonized the mouse GIT through the duration of the study, representing an average of 9.31 ± 0.16 log10 16S rRNA gene copies per gram of feces (Figure 4.5B). *Parasutterella* was successfully isolated using the selective media from mouse feces six weeks after environmental inoculation, verifying the stable colonization of *Parasutterella*. The colonization of the *Parasutterella* isolate in the mouse GIT did not significantly affect body weight (Figure 4.1C). The success of *Parasutterella* to colonize the mature mouse gut after a single exposure demonstrated that the microbe fills the ecological niche in the GIT.

The gut microbiota of the CON and PARA groups was characterized by sequencing 16S rRNA gene amplicons from ileal, cecal, and colonic contents. The sequencing obtained 20,086 ± 7,581 (mean ± standard deviation) quality-controlled and chimera-checked reads per sample. The successful colonization of *Parasutterella* did not cause a significant shift in gut microbiota structure as revealed by the PERMANOVA analysis (Figure 4.6A). Specifically, there was no significant difference in the structural pattern between the CON and PARA group at all three intestinal sites, which was evaluated using Bray-Curtis and unweighted UniFrac distance matrices with 999 random permutations (adonis, $P > 0.05$). Instead, the

microbial community was segregated by intestinal sites which explained 39.3% variation in bacterial composition (adonis, $P < 0.001$, 999 permutations). The richness and evenness of the microbial community, indicated by alpha-diversity index (Chao1 and Shannon index), did not vary between the CON and PARA group at each intestinal site (Figure 4.6B).

To assess the abundance of different gut microbes in the CON and PARA group, all sequences were assigned to taxonomy using RDP Classifier. In accordance with the separation of the overall microbial structure by intestinal sites, the regional variation played a key role in shaping the microbial community. However, at each intestinal site, there were no notable changes in microbial abundance profile between two treatments. *Parasutterella* was the only significantly changed genus between the CON and PARA group, contributing the average of 0.64%, 1.88%, and 1.71% of the 16S rRNA gene reads in the ileum, cecum, and colon, respectively (Figure 4.6C).

4.3.3. UPLC-FTMS demonstrated the effect of *Parasutterella* colonization on the cecal metabolome. The UPLC-FTMS methodology was optimized to determine the metabolomic profile of cecal contents from the CON and PARA group collected six weeks after *Parasutterella* exposure. To detect as many metabolites as possible, the UPLC-FTMS-based untargeted approach was used which contained three types of chromatographic conditions (C4, C18, and HILIC column) with two ionization modes (ESI in positive and negative mode, +/-) to generate six possible combinations. The reverse-phase UPLC-FTMS on C18 column with the negative ionization mode generated the largest number of features (2,165 features) and characterized the most significantly different features (105 features) between the CON and PARA group (Table 4.3). Principle component analysis (PCA) of all detected features revealed a distinct clustering between the CON and PARA group based on

the C18-ESI- dataset (Figure 4.7A). The separation was also displayed using features that were differently presented between treatment groups analyzed by Student's t-test (n = 8 per treatment, $P < 0.05$) (Figure 4.8). In total, 132 of 8,990 detected features differentiated the CON and PARA group and the colonization of *Parasutterella* significantly impacted features detected by C18-ESI- approach to the greatest extent, indicating the changed profile of non-phospholipid metabolites in cecal contents (Figure 4.7B; Table 4.4, 4.5). The result showed that the presence of *Parasutterella* changed the cecal metabolomic profile even though the colonization did not result in a significant shift in microbial community structure.

4.3.4. The colonization of *Parasutterella* altered levels of identifiable metabolites. The untargeted metabolomic analysis approach allowed us to detect metabolite features broadly and extensively. However, the identification of metabolites based on detected mass spectra remains challenging due to limited standard reference materials and difficulties in distinguishing the biological source for commonly shared metabolites across the host and gut microbiota (22, 36, 37). In the current study, univariate and multivariate approaches were performed on features detected from the CON and PARA group, and features with a *q*-value less than 0.05 were selected for metabolite identification. Pure standards including certain bile acids were obtained and analyzed under the identical chromatographic condition and ionization mode to validate the spectra from samples.

Approximately 40% of features within 132 significantly differentiated features remained unidentified, which revealed a substantial proportion of yet-to-be described microbial associated metabolites. Though the identification of significant metabolites was incomplete, certain metabolites and pathways consistently associated with gut microbial activity were observed. With the colonization of *Parasutterella*, the level of tryptophan

metabolites, 3-Methyldixyindole (m/z 162.0559, ESI-), indole-2-carboxylic acid (m/z 160.0404, ESI-), and indole-3-carboxylic acid (m/z 160.0403, ESI-) were increased, whereas the abundance of kynurenic acid (m/z 188.0351, ESI-) and nicotinic acid (m/z 122.0248, ESI-) were decreased (q-value < 0.05, Figure 4.9). 3-Methyldixyindole exhibited an 8.3-fold increase and kynurenic acid showed an 11.2-fold decrease in the PARA group compared to the CON group, which were the most notable changes in tryptophan metabolism. The metabolism of another aromatic amino acid, tyrosine, was also altered by *Parasutterella* colonization, as indicated by reduced levels of *p*-Cresol (m/z 107.0503, ESI-) and *p*-Cresol sulfate (m/z 187.0069, ESI-), but elevated ethylphenol (m/z 121.0659, ESI-) and a tyrosine derivative predicted as N-Hydroxy-L-tyrosine or DOPA (m/z 196.0613, ESI-) (q-value < 0.05, Figure 4.9). *p*-Cresol and *p*-Cresol sulfate were decreased 5.6-fold and 43.4-fold in the PARA group compared to that in the CON group, whereas the ethylphenol and the tyrosine derivative in the PARA group were increased 2.1-fold and 84.3-fold than that in the CON group, respectively. Overall, the result indicated that the presence of *Parasutterella* significantly changed aromatic amino acid metabolism in the gut including tryptophan and tyrosine catabolism, and changes in microbial associated metabolites indicated an altered functionality of the gut microbial community to utilize these aromatic amino acids.

Microbial associated metabolites, mesobilirubinogen (m/z 591.3173, ESI-) and purine metabolites including inosine (m/z 267.073, ESI-), hypoxanthine (m/z 135.0311, ESI-), and xanthine (m/z 151.0261, ESI-) were altered in *Parasutterella* colonized mice. The bilirubin derived compound, mesobilirubinogen was significantly increased (q-value < 0.05, 2.4-fold change) in the PARA group, indicating an enhanced metabolism of conjugated bilirubin by the gut microbiota (Figure 4.9). Altered purine metabolites were observed in the PARA group

as indicated by remarkably decreased inosine (74.4-fold difference) and xanthine (9.3-fold difference), and increased hypoxanthine (3.4-fold change) (q-value < 0.05, Figure 4.9). Alterations in these microbial-derived metabolites revealed a distinct metabolomic signature between the CON and PARA group.

Noteworthy changes in bile acids were consistent between repeated experiments and were identified as significant before FDR correction, indicating that *Parasutterella* may actively participate in bile acid metabolism and homeostasis. A reduction in the level of cholic acid (CA, m/z 407.2794, ESI-, 2.9-fold change), taurocholic acid (TCA, m/z 514.2825, ESI-, 2.2-fold change), taurodeoxycholic acid (TDCA, m/z 522.2859, ESI+, 2.0-fold change), 7-ketodeoxycholic acid or its isomers (7-keto DCA, m/z 405.2640, ESI-, 2.8-fold change), and glycolithocholic acid sulfate (glycol-LCA sulfate, m/z 512.2677, ESI-, 2.3-fold change) was observed in the PARA group, indicating alterations in bile acid metabolism (Figure 4.10A). Though changes in bile acids between the CON and PARA group were not significant based on the q-value, the consistent decrease in these bile acid metabolites clearly suggested that the presence of *Parasutterella* influenced bile acid profiling in cecal contents. The concomitant increase in taurine (m/z 124.0073, ESI-, 2.0-fold change) concentration further indicated changes in bile acid metabolism, including the process of deconjugating primary bile acids (Figure 4.10A). Overall, bile acid components detected by the current chromatographic conditions were consistently impacted by *Parasutterella* colonization.

4.3.5. Alterations in bile acid profile were consistent with hepatic and ileal gene expression. Previous studies have indicated correlations between the abundance of *Parasutterella* and alterations of bile acid metabolites in the gut (9, 38–40). To follow up on differences in bile acid profiles observed, we evaluated the host gene expression of bile acid

transporters in the ileum and the FXR signaling pathway. Gene expression of ileal bile acid-binding protein (*Ibabp*) in the PARA group was significantly lower than that in the CON group ($P < 0.05$), and the organic solute transporter β (*Ostβ*) tended to be reduced in the PARA group ($P = 0.05$), which was consistent with the reductions in bile acid metabolites. mRNA levels of ileal genes in the FXR signaling pathway, including the small heterodimer partner (*Shp*, $P < 0.05$) and the fibroblast growth factor 15 (*Fgf15*, $P = 0.08$) were decreased in the PARA group. The regulatory effect of the gut microbiota on bile acid synthesis through modulating the FXR signaling pathway has been demonstrated (20). Therefore, we further measured the associated liver gene encoding the rate-limiting enzyme in bile acid synthesis, cholesterol 7α-hydroxylase (*Cyp7a1*). The expression of *Cyp7a1* was significantly higher in *Parasutterella* colonized mice than that in control mice, which indicated an enhanced bile acid synthesis in the PARA group. Other liver genes related to bile acid synthesis including *Cyp8b1* and *Cyp27a1* were not affected by *Parasutterella* colonization, supporting the role of FXR signaling in the *Cyp7a1* regulation. The *Cyp7a1* expression has been correlated with decreased serum cholesterol in human and mouse studies (41, 42), accordingly, serum cholesterol was measured. Despite a numerical decrease consistent with the hypothesis no significant difference in serum cholesterol concentration was observed (Figure 4.10B).

4.3.6. The presence of *Parasutterella* did not impact the colonic cytokine expression. To investigate if the colonization of *Parasutterella* affects the immune response in the gut, a panel of colonic cytokines were measured by enzyme-linked immunosorbent assay (ELISA). *Parasutterella* colonization did not alter the level of detected colonic cytokines except for a tendency to reduce the IL-1β expression ($P = 0.092$, Figure 4.11), which indicated that the colonization of *Parasutterella* did not induce host innate immune

responses and further supported the role of *Parasutterella* as a commensal or symbiotic gut microbe.

4.4. Discussion

The genus *Parasutterella* has been recognized for approximately ten years and increasing studies have shown its relationship with different health outcomes. However, beyond correlations between the abundance change and host phenotype, our understanding of metabolic features and functionalities of *Parasutterella* remains limited. In the current study, the murine *Parasutterella* was successfully isolated and characterized for its genomic features and metabolic characteristics. A tractable model was subsequently used by adding a single bacterium, *Parasutterella* mc1, to a complex microbial community to investigate the role *Parasutterella* plays in affecting the microbial ecosystem and host physiology. *Parasutterella* successfully thrived in the mouse GIT without shifting microbial structure, but significantly altered the cecal metabolome including multiple biological processes and pathways.

It has been described that the genus *Parasutterella* was largely unreactive in biochemical characterization and only limited end products of metabolism have been identified (4). Type strains of the genus *Parasutterella*, *P. excrementihominis* YIT 11859 and *P. secunda* YIT 12071, were asaccharolytic in the analytical profile index (API) test systems and exhibited weak growth in peptone-yeast extract medium, which could not be enhanced by adding glucose, succinate, or lactate to the broth (2, 3). In the current study, the mouse isolate showed no turbidity when grown in GAM broth for up to 120 h, which was consistent with previously reported biochemical characteristics. The bacterial density reached 10^7 CFUs/mL in the initial 48 h of growth, however, failed to significantly increase in the following 72 h of culture. The rapid growth of bacterial cells in the first 48 h was accompanied by the depletion

of asparagine and a slight decrease of aspartate in the medium, as validated by nuclear magnetic resonance (NMR) analysis (Figure 4.4). The supplementation of asparagine and aspartate in the bacterial culture stimulated the growth in the following 24 h (Figure 4.5A). Therefore, in agreement with the presence of genes encoding amino acid utilizing enzymes in the genome, the asaccharolytic genus, *Parasutterella*, is likely to rely on amino acids such as asparagine, aspartate, and serine to support its metabolic activities and physiological functions. In addition, the preferential catabolism of the non-essential amino acids (NEAAs) for the host may indicate the adaptation of *Parasutterella* to the gut environment which contains readily available NEAAs.

Importantly, it is the first study showing *Parasutterella* produces succinate as a fermentative end-product. Succinate production in feces has been positively correlated with the relative abundance of genera including *Bacteroides*, *Lactobacillus*, and *Parasutterella* in a dextran sulfate sodium (DSS)-induced colitis mouse model (43). The current study provided direct evidence for succinate accumulation in the broth culture of *Parasutterella*. Additionally, despite the fact that succinate is an intermediate compound in the intestinal metabolism, we observed elevated levels of succinate in *Parasutterella* colonized mice when measured on a C8 column (ESI-, m/z 117.01934, Figure 4.5C). When grown in GAM broth for 72 h, *Parasutterella* produced about 2.5 mM succinate whereas *Bacteroides fragilis*, one of the well-identified succinate producers, was able to produce 100 mM succinate under the same condition. However, the amount of succinate generated by *Parasutterella* was substantial when the significant difference in growth rate and bacterial density between *Parasutterella* and *Bacteroides* was taken into consideration. Succinate, as one of the key intermediate metabolites produced by the gut microbiota, plays an important role in cross-

feeding metabolic pathways (44). The capacity of *Parasutterella* to produce succinate indicates one potential way *Parasutterella* supports interspecies metabolic interactions within the gut ecosystem.

Surprisingly, with a single environmental exposure, the *Parasutterella* isolate successfully colonized the mature mouse gut without causing significant shifts in bacterial composition and host innate immune response. Although *Parasutterella* has been described as an obligate anaerobe, it was able to persist sufficiently long to colonize the mouse intestine. It has been reported that some strict anaerobic bacteria such as members of Bacteroides can survive and even grow in the presence of low oxygen concentration (45). We hypothesize that the defined obligate anaerobe, *Parasutterella*, could protect itself from certain level of oxygen through yet-to-be characterized mechanisms. It is possible that the colonization of *Parasutterella* led to strain-level differences in the gut microbiota that was not detected by 16S rRNA sequencing analysis, however, a lack of changes in the overall microbial structure demonstrated that *Parasutterella* fills the ecological niche and persists in the gut microbial community. The transmission of *Parasutterella* has been observed between mother and vaginally born infants, with the relative abundance gradually increasing to 12-months of age, indicating that *Parasutterella* is one of the early colonizers in the newborn gut and increases in response to dietary change and host development (46). A study using a germ-free mouse model reconstituted with neonatal microbiota indicated that bacterially derived succinate promoted the colonization of strict anaerobic bacteria, Clostridiales, to protect mice from infection (47). It was assumed that succinate enhanced the growth of Clostridiales through an indirect mechanism which boosted the consumption of oxygen by aerobic or facultative anaerobic bacteria (47). Being one of the early colonizers as well as succinate

producing commensal bacteria, *Parasutterella* may play a role in microbial interactions and infection resistance especially early in life.

Due to the limited ability to characterize *Parasutterella* using a culture-based approach, we propose that the colonization of *Parasutterella* in a controlled animal model provides greater insight into its functionality. Despite limited effects on microbial composition, notable changes in the cecal metabolic profile including tryptophan, tyrosine, bilirubin, purine, and bile acid metabolism were observed. The presence of *Parasutterella* influenced the microbial metabolism of aromatic amino acids, as indicated by changes in the abundance of metabolites generated from tryptophan and tyrosine. The decreased level of *p*-Cresol and *p*-Cresol sulfate and increased level of ethylphenol as well as a tyrosine derivative demonstrated an altered tyrosine metabolism. Various species of the gut microbiota have been characterized to be capable of converting tyrosine to *p*-Cresol and ethylphenol including *Clostridium*, *Bifidobacterium*, *Bacteroides fragilis*, and *E. coli* (48). The impact on tryptophan metabolism by *Parasutterella* colonization was indicated by the altered abundance of tryptophan metabolites including kynurenic acid, nicotinic acid, 3-Methyldixyindole, indole-2-carboxylic acid and indole-3-carboxylic acid in cecal contents. Tryptophan, as one of the essential amino acids in mammals, can be co-metabolized by the host and gut microbiota through multiple pathways in the GIT. Representative microbial metabolites produced from tryptophan in the intestine include tryptamine, indole, indole acetic acid, indole-propionic acid, and 3-Methylindole (skatole) (49, 50). 3-Methyldioxyindole has been considered as a potential *in vivo* oxidation product of skatole (51, 52), which performs as a marker of altered tryptophan metabolism (53, 54). Indole-3-carboxylic acid is a side-chain shortened product of indole-3-acetic acid that has been reported to be produced in the culture

medium by certain gut bacterial species (50). The increased abundance of 3-Methyldioxyindole and indole-3-carboxylic acid in cecal contents suggests that the colonization of *Parasutterella* enhanced the deamination and chain shortening procedure of tryptophan metabolism in the gut. On the other hand, the concentration of kynurenic acid and nicotinic acid generated from the kynurenine pathway were reduced by the presence of *Parasutterella*, indicating the impact of *Parasutterella* colonization on pathway interactions in tryptophan metabolism (Figure 4.5D).

In addition, purine derivatives were identified to be differentiated between the CON and PARA group, including inosine, hypoxanthine, and xanthine. Purine derived metabolites have been reported to modulate immune responses of immune cells and gut mucosal barrier (55, 56). A study using mouse DSS-induced colitis model identified that hypoxanthine potentially modulates the energy balance of intestinal epithelium and performs a critical role in maintaining intestinal barrier function (56). Therefore, in the current study, the elevated level of hypoxanthine resulting from *Parasutterella* colonization may exert potential beneficial effects on the intestinal mucosal homeostasis. Inosine has been reported to inhibit the Treg cell deficiency-induced autoimmunity in mice and the administration of *Lactobacillus reuteri* restored the reduction of plasma inosine (57). The restored plasma inosine was associated with decreased levels in feces, implying that *L. reuteri* may promote the absorption of inosine in the intestine (57). In the current study, the cecal abundance of inosine was significantly reduced (74.4-fold change) by the presence of *Parasutterella*, which may indicate a potential alteration in plasma inosine level and immunomodulatory effects. Future work integrating blood metabolomics approach will be helpful to underpin the effect of *Parasutterella* colonization on systematic metabolism and function.

Bile acids, in addition to facilitate the absorption of lipid-soluble nutrients in the intestine, have been recognized as important endocrine signaling molecules that impact host physiology, including metabolic processes (58, 59). In the current study, bile acid metabolism was changed in *Parasutterella* colonized mice as indicated by the reduced abundance of detected primary bile acids (CA and TCA) and certain secondary bile acids (TDCA, 7-keto DCA, and glycol-LCA) in cecal contents. The genus *Parasutterella* has been inversely correlated with fecal deoxycholic acid (DCA) and lithocholic acid (LCA) levels in a non-alcoholic steatohepatitis-hepatocellular carcinoma mouse model (9). Another study using a humanized microbiota mouse model showed a positive association between *Parasutterella* and beta-muricholic acid as well as 7-ketoDCA in feces (38). Patients with recurrent *Clostridium difficile* infection who were cured by autologous fecal microbiota transplantation had increased relative abundance of *Clostridium XIVa* members, *Holdemania*, and *Parasutterella*. The authors hypothesized that these taxa may play an active role in bile acid metabolism, especially the secondary bile acid biosynthesis (39). In addition, a remarkable reduction of *Parasutterella excrementihominis* in alcoholic hepatitis (AH) patients suggested that *Parasutterella* species may exert protective effects on liver health (40). Interestingly, the secondary bile acid ursodeoxycholic acid (UDCA) was identified as a hepatoprotective molecule in the healthy control group (40), which may indicate a correlative relationship between the presence of *Parasutterella* and increased secondary bile acid in healthy people. In agreement with these previous reports, our results showed that *Parasutterella* participated in bile acid metabolism, however, due to the limitation of chromatographic conditions in the current study we were unable to demonstrate changes in all bile acid species. In addition, bile acid metabolism is a complex biochemical process including multiple reactions performed by

diverse gut microbes. Even though our study used a well-controlled system by adding one single bacterium to a mature microbial community, we could not eliminate the microbial interaction in bile acid transformation. The changes in detected bile acid metabolites may be attributed to the colonization of *Parasutterella* itself or indirect consequences such as altering the activities of other bacteria by *Parasutterella*. Due to a paucity of information regarding the capability of *Parasutterella* to utilize bile acids, future work will focus on the mechanism driving altered bile acid metabolism by *Parasutterella* colonization.

Consistent with bile acid modifications, the gene expression of ileal bile acid transporters, including *Ibabp* and *Ostβ,* was decreased. I-BABP actively interacts with FXR signaling pathway to modulate FXR expression in the small intestine (60) and the Ost-α/β complex can be induced by FXR as well as bile acids (61). Moreover, FXR has been reported to be antagonized by certain bile acids such as the tauro-conjugated muricholic acid (T-MCA) in mice, and consequently modulate the expression of *Cyp7a1* in the liver (20, 59). In the current study, the reduction in gene expression of bile acid transporters as well as the inhibition of FXR signaling pathway matched the elevated expression of liver *Cyp7a1* gene, which revealed that the colonization of *Parasutterella* modified bile acid metabolites and thereby impacted bile acid transport and synthesis. These effects on bile acid transporters and FXR signaling pathway may be exerted directly by *Parasutterella* or indirectly via microbial interactions. Additionally, there was no significant difference in serum cholesterol levels between the CON and PARA group, which may be explained by the normal physiological state of mice. Future studies incorporating a HFD treatment will be helpful to investigate the effect of *Parasutterella*-induced *Cyp7a1* expression on host physiology.

In summary, the result demonstrated the potential metabolic functionality of *Parasutterella* as a member of the gut microbiota. It is the first study to reveal the chemical 'fingerprint' of *Parasutterella* and highlight the potential to impact the host physiology via modulating the abundance or the function of commensal bacteria in the gut. Additionally, the controlled model system of adding a single commensal microorganism to a complex community can be applied to investigate other commensal species of interest.

4.5. References

1. Willing BP, Dicksved J, Halfvarson J, Andersson AF, Lucio M, Zheng Z, Järnerot G, Tysk C, Jansson JK, Engstrand L. 2010. A pyrosequencing study in twins shows that GI microbial profiles vary with inflammatory bowel disease phenotypes. Gastroenterology 139:1844–1854.
2. Nagai F, Morotomi M, Sakon H, Tanaka R. 2009. *Parasutterella excrementihominis* gen. nov., sp. nov., a member of the family *Alcaligenaceae* isolated from human faeces. Int J Syst Evol Microbiol 59:1793–1797.
3. Morotomi M, Nagai F, Watanabe Y. 2011. *Parasutterella secunda* sp. nov., isolated from human faeces and proposal of *Sutterellaceae* fam. nov. in the order Burkholderiales. Int J Syst Evol Microbiol 61:637–643.
4. Morotomi M. 2014. The family *Sutterellaceae*. p. 1005–1012. In: Rosenberg E, DeLong EF, Lory S, Stackebrandt E, Thompson F (ed), The prokaryotes: Alphaproteobacteria and Betaproteobacteria, 4th ed. Springer, Berlin, Heidelberg.
5. Shin NR, Whon TW, Bae JW. 2015. Proteobacteria: microbial signature of dysbiosis in gut microbiota. Trends Biotechnol 33:496–503.
6. Blasco-Baque V, Coupé B, Fabre A, Handgraaf S, Gourdy P, Arnal JF, Courtney M, Schuster-Klein C, Guardiola B, Tercé F, Burcelin R, Serino M. 2017. Associations between hepatic miRNA expression, liver triacylglycerols and gut microbiota during metabolic adaptation to high-fat diet in mice. Diabetologia 60:690–700.
7. Kreutzer C, Peters S, Schulte DM, Fangmann D, Türk K, Wolff S, van Eimeren T, Ahrens M, Beckmann J, Schafmayer C, Becker T, Kerby T, Rohr A, Riedel C, Heinsen

FA, Degenhardt F, Franke A, Rosenstiel P, Zubek N, Henning C, Freitag-Wolf S, Dempfle A, Psilopanagioti A, Petrou-Papadaki H, Lenk L, Jansen O, Schreiber S, Laudes M. 2017. Hypothalamic inflammation in human obesity is mediated by environmental and genetic factors. Diabetes 66:2407–2415.

8. Zhang C, Zhang M, Pang X, Zhao Y, Wang L, Zhao L. 2012. Structural resilience of the gut microbiota in adult mice under high-fat dietary perturbations. ISME J 6:1848–1857.
9. Xie G, Wang X, Huang F, Zhao A, Chen W, Yan J, Zhang Y, Lei S, Ge K, Zheng X, Liu J, Su M, Liu P, Jia W. 2016. Dysregulated hepatic bile acids collaboratively promote liver carcinogenesis. Int J Cancer 139:1764–1775.
10. Danneskiold-Samsøe NB, Andersen D, Radulescu ID, Normann-Hansen A, Brejnrod A, Kragh M, Madsen T, Nielsen C, Josefsen K, Fretté X, Fjære E, Madsen L, Hellgren LI, Brix S, Kristiansen K. 2017. A safflower oil based high-fat/high-sucrose diet modulates the gut microbiota and liver phospholipid profiles associated with early glucose intolerance in the absence of tissue inflammation. Mol Nutr Food Res 61:1600528.
11. Everard A, Lazarevic V, Derrien M, Girard M, Muccioli GM, Neyrinck AM, Possemiers S, Van Holle A, François P, de Vos WM, Delzenne NM, Schrenzel J, Cani PD. 2011. Responses of gut microbiota and glucose and lipid metabolism to prebiotics in genetic obese and diet-induced leptin-resistant mice. Diabetes 60:2775–2786.
12. Metzler-Zebeli BU, Schmitz-Esser S, Mann E, Grüll D, Molnar T, Zebeli Q. 2015. Adaptation of the cecal bacterial microbiome of growing pigs in response to resistant starch type 4. Appl Environ Microbiol 81:8489–8499.
13. Staley C, Kaiser T, Beura LK, Hamilton MJ, Weingarden AR, Bobr A, Kang J, Masopust D, Sadowsky MJ, Khoruts A. 2017. Stable engraftment of human microbiota into mice with a single oral gavage following antibiotic conditioning. Microbiome 5:87.
14. Zhang L, Dong D, Jiang C, Li Z, Wang X, Peng Y. 2015. Insight into alteration of gut microbiota in *Clostridium difficile* infection and asymptomatic *C. difficile* colonization. Anaerobe 34:1–7.

15. Brahma S, Martínez I, Walter J, Clarke J, Gonzalez T, Menon R, Rose DJ. 2017. Impact of dietary pattern of the fecal donor on *in vitro* fermentation properties of whole grains and brans. J Funct Foods 29:281–289.
16. Postler TS, Ghosh S. 2017. Understanding the holobiont: how microbial metabolites affect human health and shape the immune system. Cell Metab 26:110–130.
17. Krishnan S, Alden N, Lee K. 2015. Pathways and functions of gut microbiota metabolism impacting host physiology. Curr Opin Biotechnol 36:137–145.
18. Maslowski KM, Vieira AT, Ng A, Kranich J, Sierro F, Yu D, Schilter HC, Rolph MS, Mackay F, Artis D, Xavier RJ, Teixeira MM, Mackay CR. 2009. Regulation of inflammatory responses by gut microbiota and chemoattractant receptor GPR43. Nature 461:1282–1286.
19. Bansal T, Alaniz RC, Wood TK, Jayaraman A. 2010. The bacterial signal indole increases epithelial-cell tight-junction resistance and attenuates indicators of inflammation. Proc Natl Acad Sci. USA 107:228–233.
20. Sayin SI, Wahlström A, Felin J, Jäntti S, Marschall HU, Bamberg K, Angelin B, Hyötyläinen T, Orešič M, Bäckhed F. 2013. Gut microbiota regulates bile acid metabolism by reducing the levels of tauro-beta-muricholic acid, a naturally occurring FXR antagonist. Cell Metab 17:225–235.
21. Kostic AD, Howitt MR, Garrett WS. 2013. Exploring host-microbiota interactions in animal models and humans. Genes Dev 27:701–718.
22. Marcobal A, Kashyap PC, Nelson TA, Aronov PA, Donia MS, Spormann A, Fischbach MA, Sonnenburg JL. 2013. A metabolomic view of how the human gut microbiota impacts the host metabolome using humanized and gnotobiotic mice. ISME J 7:1933–1943.
23. Stewart EJ. 2012. Growing unculturable bacteria. J Bacteriol 194:4151–4160.
24. Weisburg WG, Barns SM, Pelletier DA, Lane DJ. 1991. 16S ribosomal DNA amplification for phylogenetic study. J Bacteriol 173:697–703.
25. Ju, T, Willing BP. 2018. Isolation of commensal *Escherichia coli* strains from feces of healthy laboratory mice or rats. Bio-protocol 8:e2780.
26. Ju T, Shoblak Y, Gao Y, Yang K, Fouhse J, Finlay BB, So YW, Stothard P, Willing BP. 2017. Initial gut microbial composition as a key factor driving host response to

antibiotic treatment, as exemplified by the presence or absence of commensal *Escherichia coli*. Appl Environ Microbiol 83:e01107–17.

27. Bankevich A, Nurk S, Antipov D, Gurevich AA., Dvorkin M, Kulikov AS, Lesin VM, Nikolenko SI, Pham S, Prjibelski AD, Pyshkin AV, Sirotkin AV, Vyahhi N, Tesler G, Alekseyev MA, Pevzner PA. 2012. SPAdes: a new genome assembly algorithm and its applications to single-cell sequencing. J Comput Biol 19:455–477.
28. Seemann T. 2014. Prokka: rapid prokaryotic genome annotation. Bioinformatics 30:2068–2069.
29. Grant JR, Arantes AS, Stothard P. 2012. Comparing thousands of circular genomes using the CGView Comparison Tool. BMC Genomics 13:202.
30. Han J, Liu Y, Wang R, Yang J, Ling V, Borchers CH. 2015. Metabolic profiling of bile acids in human and mouse blood by LC-MS/MS in combination with phospholipid-depletion solid-phase extraction. Anal Chem 87:1127–1136.
31. Smith CA, O'Maille G, Want EJ, Qin C, Trauger SA, Brandon TR, Custodio DE, Abagyan R, Siuzdak G. 2005. METLIN: a metabolite mass spectral database. Ther Drug Monit 27:747–751.
32. Wishart DS, Jewison T, Guo AC, Wilson M, Knox C, Liu Y, Djoumbou Y, Mandal R, Aziat F, Dong E, Bouatra S, Sinelnikov I, Arndt D, Xia J, Liu P, Yallou F, Bjorndahl T, Perez-Pineiro R, Eisner R, Allen F, Neveu V, Greiner R, Scalbert A. 2013. HMDB 3.0-the human metabolome database in 2013. Nucleic Acids Res 41:D801–D807.
33. Fahy E, Sud M, Cotter D, Subramaniam S. 2007. LIPID MAPS online tools for lipid research. Nucleic Acids Res 35:W606–W612.
34. McMurdie PJ, Holmes S. 2013. Phyloseq: an R package for reproducible interactive analysis and graphics of microbiome census data. PLoS One 8:e61217.
35. Xia J, Sinelnikov IV, Han B, Wishart DS. 2015. MetaboAnalyst 3.0-making metabolomics more meaningful. Nucleic Acids Res 43:W251–W257.
36. Schrimpe-Rutledge AC, Codreanu SG, Sherrod SD, McLean JA. 2016. Untargeted metabolomics strategies-challenges and emerging directions. J Am Soc Mass Spectrom 27:1897–1905.
37. Alonso A, Marsal S, Julia A. 2015. Analytical methods in untargeted metabolomics: state of the art in 2015. Front Bioeng Biotechnol 3:23–43.

38. Dey N, Wagner VE, Blanton LV, Cheng J, Fontana L, Haque R, Ahmed T, Gordon JI. 2015. Regulators of gut motility revealed by a gnotobiotic model of diet-microbiome interactions related to travel. Cell 163:95–107.
39. Staley C, Kelly CR, Brandt LJ, Khoruts A, Sadowsky MJ. 2016. Complete microbiota engraftment is not essential for recovery from recurrent *Clostridium difficile* infection following fecal microbiota transplantation. MBio 7:e01965–16.
40. Llopis M, Cassard AM, Wrzosek L, Boschat L, Bruneau A, Ferrere G, Puchois V, Martin JC, Lepage P, Le Roy T, Lefèvre L, Langelier B, Cailleux F, González-Castro AM, Rabot S, Gaudin F, Agostini H, Prévot S, Berrebi D, Ciocan D, Jousse C, Naveau S, Gérard P, Perlemuter G. 2016. Intestinal microbiota contributes to individual susceptibility to alcoholic liver disease. Gut 65:830–839.
41. Pullinger CR, Eng C, Salen G, Shefer S, Batta AK, Erickson SK, Verhagen A, Rivera CR, Mulvihill SJ, Malloy MJ, Kane JP. 2002. Human cholesterol 7α-hydroxylase (CYP7A1) deficiency has a hypercholesterolemic phenotype. J Clin Invest 110:109–117.
42. Lin JZ, Martagón AJ, Hsueh WA, Baxter JD, Gustafsson JÅ, Webb P, Phillips KJ. 2012. Thyroid hormone receptor agonists reduce serum cholesterol independent of the LDL receptor. Endocrinology 153:6136–6144.
43. Osaka T, Moriyama E, Arai S, Date Y, Yagi J, Kikuchi J, Tsuneda S. 2017. Meta-analysis of fecal microbiota and metabolites in experimental colitic mice during the inflammatory and healing phases. Nutrients 9:E1329.
44. Fischbach MA, Sonnenburg JL. 2011. Eating for two: how metabolism establishes interspecies interactions in the gut. Cell Host Microbe 10:336–347.
45. Baughn AD, Malamy MH. 2004. The strict anaerobe *Bacteroides fragilis* grows in and benefits from nanomolar concentrations of oxygen. Nature 427:441–444.
46. Bäckhed F, Roswall J, Peng Y, Feng Q, Jia H, Kovatcheva-Datchary P, Li Y, Xia Y, Xie H, Zhong H, Khan MT, Zhang J, Li J, Xiao L, Al-Aama J, Zhang D, Lee YS, Kotowska D, Colding C, Tremaroli V, Yin Y, Bergman S, Xu X, Madsen L, Kristiansen K, Dahlgren J, Wang J. 2015. Dynamics and stabilization of the human gut microbiome during the first year of life. Cell Host Microbe 17:690–703.

47. Kim YG, Sakamoto K, Seo SU, Pickard JM, Gillilland MG, Pudlo NA, Hoostal M, Li X, Wang TD, Feehley T, Stefka AT, Schmidt TM, Martens EC, Fukuda S, Inohara N, Nagler CR, Núñez G. 2017. Neonatal acquisition of Clostridia species protects against colonization by bacterial pathogens. Science 356:315–319.
48. Nicholson JK, Holmes E, Kinross J, Burcelin R, Gibson G, Jia W, Pettersson S. 2012. Host-gut microbiota metabolic interactions. Science 336:1262–1267.
49. Hubbard TD, Murray IA, Perdew GH. 2015. Indole and tryptophan metabolism: endogenous and dietary routes to Ah receptor activation. Drug Metab Dispos 43:1522–1535.
50. Russell WR, Duncan SH, Scobbie L, Duncan G, Cantlay L, Calder AG, Anderson SE, Flint HJ. 2013. Major phenylpropanoid-derived metabolites in the human gut can arise from microbial fermentation of protein. Mol Nutr Food Res 57:523–535.
51. Albrecht CF, Chorn DJ, Wessels PL. 1989. Detection of 3-hydroxy-3-methyloxindole in human urine. Life Sci 45:1119–1126.
52. Skiles GL, Adams JD Jr, Yost GS. 1989. Isolation and identification of 3-Hydroxy-3-methyloxindole, the major murine metabolite of 3-methylindole. Chem Res Toxicol 2:254–259.
53. Zheng X, Xie G, Zhao A, Zhao L, Yao C, Chiu NH, Zhou Z, Bao Y, Jia W, Nicholson JK, Jia W. 2011. The footprints of gut microbial-mammalian co-metabolism. J Proteome Res 10:5512–5522.
54. Zhou Y, Men L, Pi Z, Wei M, Song F, Zhao C, Liu Z. 2018. Fecal metabolomics of type 2 diabetic rats and treatment with Gardenia jasminoides Ellis based on mass spectrometry technique. J Agric Food Chem 66:1591–1599.
55. Haskó G, Sitkovsky MV., Szabó C. 2004. Immunomodulatory and neuroprotective effects of inosine. Trends Pharmacol Sci 25:152–157.
56. Lee JS, Wang RX, Alexeev EE, Lanis JM, Battista KD, Glover LE, Colgan SP. 2018. Hypoxanthine is a checkpoint stress metabolite in colonic epithelial energy modulation and barrier function. J Biol Chem 293:6039–6051.
57. He B, Hoang TK, Wang T, Ferris M, Taylor CM, Tian X, Luo M, Tran DQ, Zhou J, Tatevian N, Luo F, Molina JG, Blackburn MR, Gomez TH, Roos S, Rhoads JM, Liu

Y. 2017. Resetting microbiota by *Lactobacillus reuteri* inhibits T reg deficiency-induced autoimmunity via adenosine A2A receptors. J Exp Med 214:107–123.

58. Swann JR, Want EJ, Geier FM, Spagou K, Wilson ID, Sidaway JE, Nicholson JK, Holmes E. 2011. Systemic gut microbial modulation of bile acid metabolism in host tissue compartments. Proc Natl Acad Sci. USA 108:4523–4530.
59. Wahlström A, Sayin SI, Marschall HU, Bäckhed F. 2016. Intestinal crosstalk between bile acids and microbiota and its impact on host metabolism. Cell Metab 24:41–50.
60. Nakahara M, Furuya N, Takagaki K, Sugaya T, Hirota K, Fukamizu A, Kanda T, Fujii H, Sato R. 2005. Ileal bile acid-binding protein, functionally associated with the farnesoid X receptor or the ileal bile acid transporter, regulates bile acid activity in the small intestine. J Biol Chem 280:42283–42289.
61. Landrier JF, Eloranta JJ, Vavricka SR, Kullak-Ublick GA. 2006. The nuclear receptor for bile acids, FXR, transactivates human organic solute transporter-α and -β genes. Am J Physiol Gastrointest Liver Physiol 290:G476–G485.
62. Spandidos A, Wang X, Wang H, Seed B. 2010. PrimerBank: a resource of human and mouse PCR primer pairs for gene expression detection and quantification. Nucleic Acids Res 38:D792–D799.

Table 4.1. Primers for PCR and qPCR assays

Targeted gene	Primer	Oligonucleotides sequences (5'-3')	Ref
Parasutterella 16S rRNA	Paraf	AACGTRTCCGCTCGTGGGGGAC	NA
	Parar	CGGAATAGCTGGATCAGGCTTG	
Eubacterial 16S rRNA	27f	GGTTACCTTGTTACGACTT	1
	1492r	GGTTACCTTGTTACGACTT	
Mrp2	Forward	GGATGGTGACTGTGGGCTGAT	2
	Reverse	GGCTGTTCTCCCTTCTCATGG	
Mrp3	Forward	TCCCACTTTTCGGAGACAGTAAC	2
	Reverse	ACTGAGGACCTTGAAGTCTTGGA	
Ostα	Forward	TGTTCCAGGTGCTTGTCATCC	2
	Reverse	CCACTGTTAGCCAAGATGGAGAA	
Ostβ	Forward	GATGCGGCTCCTTGGAATTA	2
	Reverse	GGAGGAACATGCTTGTCATGAC	
Ibat	Forward	ACCACTTGCTCCACACTGCTT	2
	Reverse	CGTTCCTGAGTCAACCCACAT	
Ibabp	Forward	CAGGAGACGTGATTGAAAGGG	2
	Reverse	GCCCCCAGAGTAAGACTGGG	
Fxr	Forward	TCCAGGGTTTCAGACACTGG	2
	Reverse	GCCGAACGAAGAAACATGG	
Shp	Forward	CGATCCTCTTCAACCCAGATG	2
	Reverse	AGGGCTCCAAGACTTCACACA	
Fgf15	Forward	ACGTCCTTGATGGCAATCG	2
	Reverse	GAGGACCAAAACGAACGAAATT	
Cyp7a1	Forward	GGGATTGCTGTGGTAGTGAGC	3

Cyp7a1	Reverse	GGTATGGAATCAACCCGTTGTC	3
Cyp8b1	Forward	CCTCTGGACAAGGGTTTTGTG	3
	Reverse	GCACCGTGAAGACATCCCC	
Cyp27a1	Forward	CCAGGCACAGGAGAGTACG	3
	Reverse	GGGCAAGTGCAGCACATAG	
Beta-actin	Forward	CTGTCCCTGTATGCCTCTG	3
	Reverse	ATGTCACGCACGATTTCC	

Table 4.2. Quality metrics of the whole genome sequence of *Parasutterella* mc1

Isolate ID	Accession Number	Total Raw Reads	N50	Number of Contigs
Parasutterella mc1	SRP157402	6,489,082	57,492	130

Table 4.3. Detected features present in cecal contents from the CON and PARA group by UPLC-FTMS equipped with C4, C18, and HILIC column

Treatment	Method	Number of detected features	Min mass (m/z)	Max mass (m/z)	Min retention time (min)	Max retention time (min)
CON	C4, UPLC-FTMS-ESI-	1995	201.113	991.6229	1.15	19.05
PARA	C4, UPLC-FTMS-ESI-	1995	201.113	991.6229	1.15	19.05
CON	C4, UPLC-FTMS-ESI+	1670	105.0699	1050.7123	3.19	17.34
PARA	C4, UPLC-FTMS-ESI+	1670	105.0699	1050.7123	3.19	17.34
CON	C18, UPLC-FTMS-ESI-	2165	105.0016	1101.648	0.91	33.16
PARA	C18, UPLC-FTMS-ESI-	2165	105.0016	1101.648	0.91	33.16
CON	C18, UPLC-FTMS-ESI+	2105	95.0491	918.6891	0.90	33.07
PARA	C18, UPLC-FTMS-ESI+	2105	95.0491	918.6891	0.90	33.07
CON	HILIC, UPLC-FTMS-ESI-	429	87.0452	665.2128	0.91	8.00
PARA	HILIC, UPLC-FTMS-ESI-	429	87.0452	665.2128	0.91	8.00
CON	HILIC, UPLC-FTMS-ESI+	626	90.0549	708.2557	1.00	8.89
PARA	HILIC, UPLC-FTMS-ESI+	626	90.0549	708.2557	1.00	8.89

Table 4.4. Identified features with significantly different abundance between the CON and PARA group by different UPLC-FTMS method (Significances were defined as *q*-value less than 0.05)

Comparison	Method	Sample type	Number of significant features
CON vs. PARA	C4, UPLC-FTMS-ESI-	Cecal content	13
CON vs. PARA	C4, UPLC-FTMS-ESI+	Cecal content	0
CON vs. PARA	C18, UPLC-FTMS-ESI-	Cecal content	105
CON vs. PARA	C18, UPLC-FTMS-ESI+	Cecal content	12
CON vs. PARA	HILIC, UPLC-FTMS-ESI-	Cecal content	0
CON vs. PARA	HILIC, UPLC-FTMS-ESI+	Cecal content	2

Table 4.5. Identified cecal metabolites that were significantly different between the CON and PARA group generated by six chromatographic conditions (Significances were defined as *q*-value less than 0.05)

UPLC-FT/MS C4-ESI-

No.	Mass	RT* (min)	Mean (SD) of CON	Mean (SD) of PARA	*P* value (original)	*q*-value (FDR)	CON/PARA	Assigned metabolite
1	355.1575	10.23	-0.859 (0.512)	0.859 (0.441)	0	0	Down	No match
2	374.1315	10.23	-0.845 (0.621)	0.845 (0.354)	0.00001	0.002	Down	No match
3	381.1732	10.50	-0.873 (0.480)	0.873 (0.414)	0	0	Down	No match
4	383.1888	11.13	-0.883 (0.492)	0.883 (0.344)	0	0	Down	No match
5	402.1627	11.13	-0.868 (0.533)	0.868 (0.368)	0	0	Down	No match
6	442.0892	10.50	-0.856 (0.465)	0.856 (0.502)	0.00001	0.002	Down	No match
7	507.2043	5.44	-0.795 (0.516)	0.795 (0.657)	0.00010	0.0171	Down	No match
8	558.1728	12.67	-0.829 (0.692)	0.829 (0.302)	0.00012	0.0179	Down	No match
9	584.1883	12.75	-0.816 (0.733)	0.816 (0.292)	0.00023	0.0249	Down	No match
10	586.1853	12.75	-0.812 (0.740)	0.812 (0.294)	0.00025	0.0249	Down	No match
11	591.3173	7.63	-0.770 (0.644)	0.770 (0.610)	0.00023	0.0249	Down	Mesobilirubinogen
12	592.3208	7.63	-0.768 (0.658)	0.768 (0.601)	0.00024	0.0249	Down	M+1 isotopic peak of Mesobilirubinogen
13	779.5617	11.65	0.749 (0.492)	-0.749 (0.786)	0.00043	0.0396	Up	Phosphatidic acid (42:4)

UPLC-FT/MS C4-ESI+

No significance

UPLC-FT/MS C18-ESI-

No.	Mass	RT* (min)	Mean (SD) of CON	Mean (SD) of PARA	*P value* (original)	*q*-value (FDR)	CON/PARA	Assigned metabolite
1	105.0016	4.60	-0.827 (0.680)	0.827 (0.344)	0.00003	0.0016	Down	S-Methylthioglycolate
2	107.0503	6.23	0.675 (0.050)	-0.675 (1.049)	0.00268	0.0406	Up	*p*-Cresol
3	108.0204	1.75	-0.827 (0.678)	0.827 (0.349)	0.00003	0.0016	Down	No match
4	111.02	1.05	0.568 (0.111)	-0.568 (1.181)	0.00295	0.0406	Up	Uracil

5	111.0201	1.87	-0.776 (0.802)	0.776 (0.353)	0.0006	0.0134	Down	Uracil
6	111.0202	1.47	0.942 (0.203)	-0.942 (0.272)	0	0	Up	Uracil
7	113.0244	0.92	-0.912 (0.298)	0.912 (0.393)	0	0	Down	No match
8	117.0557	3.68	-0.817 (0.688)	0.817 (0.380)	0.00004	0.0019	Down	3-Hydroxyisovaleric acid
9	119.0503	7.80	0.949 (0.118)	-0.949 (0.264)	0	0	Up	p-Tolualdehyde or 4-Hydroxystyrene
10	121.0659	7.81	-0.746 (0.846)	0.746 (0.392)	0.00047	0.0117	Down	Ethylphenol
11	122.0248	1.48	0.767 (0.178)	-0.767 (0.875)	0.00146	0.0253	Up	Niacin (Nicotinic acid)-vitamin
12	124.0073	0.91	-0.809 (0.704)	0.809 (0.391)	0.00016	0.0053	Down	Taurine
13	125.0356	2.22	0.765 (0.547)	-0.765 (0.710)	0.00027	0.0083	Up	Thymine
14	126.0031	0.91	0.953 (0.142)	-0.953 (0.220)	0	0	Up	No match
15	129.0557	4.69	-0.895 (0.395)	0.895 (0.394)	0	0	Down	No match
16	133.0295	8.27	-0.722 (0.754)	0.722 (0.619)	0.00091	0.0191	Down	No match
17	134.0373	8.27	-0.686 (0.820)	0.686 (0.628)	0.00109	0.0205	Down	No match
18	134.0611	5.42	-0.889 (0.443)	0.889 (0.372)	0	0	Down	No match
19	135.0122	2.20	0.719 (0.180)	-0.719 (0.964)	0.00374	0.0464	Up	No match
20	135.0311	1.61	-0.726 (0.911)	0.726 (0.328)	0.00109	0.0205	Down	Hypoxanthine
21	138.056	5.08	-0.682 (0.863)	0.682 (0.580)	0.00109	0.0205	Down	No match
22	139.1128	11.92	0.747 (0.507)	-0.747 (0.782)	0.00062	0.0134	Up	No match
23	144.0454	9.20	0.927 (0.225)	-0.927 (0.360)	0	0	Up	No match
24	144.0455	6.93	0.765 (0.380)	-0.765 (0.813)	0.00027	0.0083	Up	No match
25	145.0506	4.01	0.866 (0.310)	-0.866 (0.576)	0	0	Up	No match
26	145.0659	6.11	0.726 (0.632)	-0.726 (0.733)	0.00295	0.0406	Up	No match
27	146.0611	6.93	-0.846 (0.458)	0.846 (0.544)	0.00001	0.0007	Down	No match
28	151.0259	1.75	-0.730 (0.306)	0.730 (0.912)	0.00227	0.0359	Down	6,8-Dihydroxypurine
29	151.0261	1.09	0.923 (0.236)	-0.923 (0.377)	0	0	Up	Xanthine
30	152.0292	1.75	0.720 (0.163)	-0.720 (0.965)	0.00375	0.0464	Up	No match
31	158.0822	3.27	-0.710 (0.847)	0.710 (0.524)	0.00124	0.0224	Down	3-isovalerylglycine
32	160.0403	6.70	-0.705 (0.832)	0.705 (0.560)	0.00137	0.0240	Down	Indole-3-carboxylic acid
33	160.0404	5.20	-0.720 (0.642)	0.720 (0.738)	0.00095	0.0196	Down	Indole-2-carboxylic acid
34	162.0559	7.58	-0.748 (0.737)	0.748 (0.568)	0.00046	0.0117	Down	3-Methyldioxyindole

35	163.0592	5.42	-0.774 (0.696)	0.774 (0.539)	0.00021	0.0068	Down	No match
36	164.9863	0.98	0.934 (0.123)	-0.934 (0.365)	0	0	Up	No match
37	165.0749	2.76	0.781 (0.661)	-0.781 (0.558)	0.00016	0.0053	Up	No match
38	171.1502	2.22	0.788 (0.123)	-0.788 (0.841)	0.00104	0.0205	Up	No match
39	173.0818	3.06	0.732 (0.182)	-0.732 (0.941)	0.00295	0.0406	Up	No match
40	173.0818	7.79	-0.746 (0.840)	0.746 (0.407)	0.00048	0.0118	Down	Suberic acid
41	177.0225	4.60	-0.897 (0.148)	0.897 (0.530)	0.00001	0.0007	Down	No match
42	180.0334	1.69	-0.823 (0.404)	0.823 (0.656)	0.00003	0.0016	Down	No match
43	180.0335	0.99	-0.830 (0.496)	0.830 (0.568)	0.00002	0.0012	Down	No match
44	181.0539	2.92	-0.755 (0.580)	0.755 (0.709)	0.00037	0.0102	Down	No match
45	187.0069	3.75	0.889 (0.231)	-0.889 (0.532)	0.00001	0.0007	Up	*p*-Cresol sulfate
46	187.1086	2.73	0.698 (0.578)	-0.698 (0.833)	0.00161	0.0271	Up	Nε-Acetyl-L-lysine
47	188.0351	3.63	0.829 (0.690)	-0.829 (0.308)	0.00295	0.0406	Up	Kynurenic acid
48	190.0542	4.52	-0.896 (0.197)	0.896 (0.521)	0.00016	0.0053	Down	N-Acetyl-DL-methionine
49	192.0426	13.32	0.942 (0.194)	-0.942 (0.279)	0	0	Up	No match
50	195.0521	2.51	0.709 (0.565)	-0.709 (0.821)	0.00126	0.0224	Up	No match
51	196.0072	6.86	-0.801 (0.143)	0.801 (0.809)	0.00062	0.0134	Down	No match
52	196.0613	5.02	-0.873 (0.162)	0.873 (0.611)	0.00016	0.0053	Down	N-Hydroxy-L-tyrosine (DOPA)
53	201.113	11.90	-0.699 (0.643)	0.699 (0.784)	0.0016	0.0271	Down	Sebacic acid
54	202.1083	3.79	0.725 (0.240)	-0.725 (0.940)	0.00297	0.0406	Up	N-lactoyl-Leucine
55	207.0119	8.51	-0.826 (0.103)	0.826 (0.757)	0.00042	0.0109	Down	No match
56	207.0489	5.44	-0.786 (0.729)	0.786 (0.446)	0.00013	0.0053	Down	No match
57	209.0851	7.12	-0.666 (0.861)	0.666 (0.622)	0.00321	0.0430	Down	2-Ethyl-1-hexanol sulfate
58	218.1032	3.46	-0.728 (0.374)	0.728 (0.890)	0.00191	0.0310	Down	Pantothenic acid (vitamin)
59	220.0613	8.12	-0.665 (0.817)	0.665 (0.682)	0.00329	0.0434	Down	Methyl dioxindole-3-acetate
60	221.1544	22.68	-0.820 (0.345)	0.820 (0.698)	0.00004	0.0019	Down	No match
61	222.0405	2.79	0.848 (0.248)	-0.848 (0.661)	0.00295	0.0406	Up	N-acetyl-L-2-aminoadipate (2-) or 2-(Malonylamino) benzoic acid

62	223.0609	8.39	-0.852 (0.288)	0.852 (0.632)	0.00001	0.0007	Down	2-[(4-hydroxyphenyl)methyl]butanedioic acid (may generated from metabolism of flavonoids *in vivo*)
63	225.0073	6.40	-0.780 (0.126)	0.780 (0.859)	0.00126	0.0224	Down	No match
64	227.1286	14.31	-0.881 (0.212)	0.881 (0.568)	0.00002	0.0012	Down	Traumatic acid
65	229.1442	15.65	0.810 (0.293)	-0.810 (0.746)	0.00062	0.0134	Up	Dodecanedioic acid
66	235.1084	3.53	0.660 (0.493)	-0.660 (0.951)	0.00363	0.0462	Up	N-Acetyl-5-methoxykynuramine
67	237.0911	2.40	-0.759 (0.086)	0.759 (0.905)	0.00204	0.0327	Down	No match
68	237.0989	2.80	-0.871 (0.213)	0.871 (0.604)	0.00004	0.0019	Down	No match
69	239.1285	7.48	-0.661 (0.548)	0.661 (0.919)	0.00358	0.0460	Down	No match
70	241.0867	14.58	0.821 (0.639)	-0.821 (0.439)	0.00016	0.0053	Up	Equol
71	242.1758	14.57	0.784 (0.340)	-0.784 (0.788)	0.00049	0.0118	Up	N-Undecanoylglycine
72	243.1962	22.87	0.724 (0.728)	-0.724 (0.643)	0.00086	0.0183	Up	2-Hydroxymyristic acid
73	249.091	1.79	0.729 (0.118)	-0.729 (0.956)	0.00342	0.0444	Up	Methionyl-Threonine
74	255.0659	11.53	0.718 (0.929)	-0.718 (0.317)	0.00295	0.0406	Up	No match
75	255.066	7.31	-0.665 (0.783)	0.665 (0.721)	0.00331	0.0434	Down	No match
76	255.1598	17.81	0.919 (0.283)	-0.919 (0.361)	0	0	Up	di-Hydroxytetradecanedioic acid
77	256.0588	0.95	-0.743 (0.117)	0.743 (0.932)	0.00267	0.0406	Down	No match
78	262.0862	3.79	0.836 (0.661)	-0.836 (0.327)	0.00016	0.0053	Up	Methionyl-Asparagine or its isomers (small peptide)
79	263.0437	2.14	-0.743 (0.725)	0.743 (0.596)	0.00031	0.0089	Down	No match
80	265.1475	30.60	-0.786 (0.109)	0.786 (0.848)	0.00113	0.0210	Down	No match
81	267.073	2.62	0.878 (0.263)	-0.878 (0.558)	0.00016	0.0053	Up	Inosine
82	267.073	3.13	-0.751 (0.450)	0.751 (0.808)	0.00042	0.0109	Down	Inosine
83	267.0903	5.16	0.791 (0.335)	-0.791 (0.776)	0.00041	0.0109	Up	No match
84	269.0451	13.71	0.951 (0.236)	-0.951 (0.146)	0	0	Up	Trihydroxyflavone
85	270.1271	16.54	0.793 (0.387)	-0.793 (0.746)	0.00109	0.0205	Up	Apigenin or Genistein
86	271.2274	25.53	-0.874 (0.167)	0.874 (0.607)	0.00005	0.0022	Down	2-hydroxyhexadecanoic acid

87	273.0763	13.69	0.881 (0.446)	-0.881 (0.414)	0	0	Up	3-(4-hydroxyphenyl)-3,4-dihydro-2H-1-benzopyran-4,6,7-triol (flavonoid metabolite)
88	282.0838	2.29	-0.782 (0.195)	0.782 (0.841)	0.00100	0.0203	Down	8-Hydroxy-deoxyguanosine or guanosine
89	283.0244	14.83	-0.806 (0.268)	0.806 (0.766)	0.00037	0.0102	Down	No match
90	285.1703	6.56	-0.668 (0.948)	0.668 (0.476)	0.00313	0.0423	Down	No match
91	285.1703	8.56	-0.695 (0.572)	0.695 (0.843)	0.00173	0.0288	Down	No match
92	286.6217	16.08	-0.659 (0.777)	0.659 (0.739)	0.00368	0.0464	Down	No match
93	287.6115	11.83	0.874 (0.578)	-0.874 (0.248)	0.00031	0.0089	Up	No match
94	291.0541	6.52	-0.729 (0.202)	0.729 (0.941)	0.00297	0.0406	Down	No match
95	291.121	11.93	-0.744 (0.098)	0.744 (0.931)	0.00265	0.0406	Down	No match
96	294.6012	12.41	-0.388 (1.329)	0.388 (0.179)	0.00186	0.0306	Down	No match
97	299.2585	25.00	0.775 (0.871)	-0.775 (0.105)	0.00031	0.0089	Up	Hydroxystearic acid
98	307.0715	12.45	0.600 (1.148)	-0.600 (0.058)	0.00062	0.0134	Up	No match
99	321.0643	4.67	0.787 (0.602)	-0.787 (0.603)	0.00013	0.0053	Up	No match
100	325.1837	30.61	-0.673 (0.475)	0.673 (0.939)	0.00281	0.0406	Down	No match
101	327.217	16.81	0.802 (0.753)	-0.802 (0.324)	0.00062	0.0134	Up	hydroxy-fatty acid (FA), $C_{18}H_{34}O_6$
102	329.0659	14.20	-0.786 (0.657)	0.786 (0.547)	0.00295	0.0406	Down	Flavonoid related metabolite
103	342.2643	24.69	0.879 (0.569)	-0.879 (0.231)	0.00002	0.0012	Up	Dodecanoylcarnitine
104	482.2573	10.85	0.831 (0.543)	-0.831 (0.521)	0.00002	0.0012	Up	No match
105	503.3367	15.04	0.808 (0.523)	-0.808 (0.615)	0.00006	0.0026	Up	No match

UPLC-FT/MS C18-ESI+

No.	**Mass**	**RT* (min)**	**Mean (SD) of CON**	**Mean (SD) of PARA**	***P* value (original)**	***q*-value (FDR)**	**CON/PARA**	**Assigned metabolite**
1	251.1642	6.55	0.695 (0.750)	-0.695 (0.691)	0.00016	0.0288	Up	No match
2	269.1747	6.55	0.666 (0.804)	-0.666 (0.695)	0.00031	0.0391	Up	No match
3	284.2947	29.16	-0.748 (0.601)	0.748 (0.709)	0.00045	0.0473	Down	Sphingosine (m18:1)
4	327.2682	18.54	-0.840 (0.434)	0.840 (0.585)	0.00001	0.0063	Down	1-Phenyl-1,3-heptadecanedione
5	352.193	28.84	0.796 (0.478)	-0.796 (0.683)	0.00009	0.0284	Up	No match

6	355.2633	18.54	-0.841 (0.452)	0.841 (0.566)	0.00001	0.0063	Down	5beta-Chola-3,8(14),11-trien-24-oic Acid
7	372.2617	16.43	0.743 (0.240)	-0.743 (0.908)	0.00016	0.0288	Up	No match
8	373.2738	18.54	-0.808 (0.474)	0.808 (0.653)	0.00006	0.0252	Down	3-Oxo-5β-chol-1-en-24-oic Acid
9	378.2089	29.19	0.750 (0.604)	-0.750 (0.702)	0.00016	0.0288	Up	(6RS)-22-oxo-23,24,25,26,27-pentanorvitamin D3 6,19-sulfur dioxide adduct
10	393.2094	6.54	0.766 (0.811)	-0.766 (0.377)	0.00026	0.0365	Up	No match
11	498.3247	15.02	0.752 (0.590)	-0.752 (0.708)	0.00040	0.0459	Up	No match
12	592.3211	16.06	-0.776 (0.794)	0.776 (0.370)	0.00019	0.0300	Down	No match

FT/MS HILIC-ESI-

No significance

FT/MS HILIC-ESI+

No.	**Mass**	**RT* (min)**	**Mean (SD) of CON**	**Mean (SD) of PARA**	***P* value (original)**	***q*-value (FDR)**	**CON/PARA**	**Assigned metabolite**
1	195.1228	1.01	-0.786 (0.367)	0.786 (0.773)	0.00014	0.0328	Down	No match
2	239.149	1.00	-0.802 (0.501)	0.802 (0.649)	0.00007	0.0328	Down	No match

***RT: retention time**

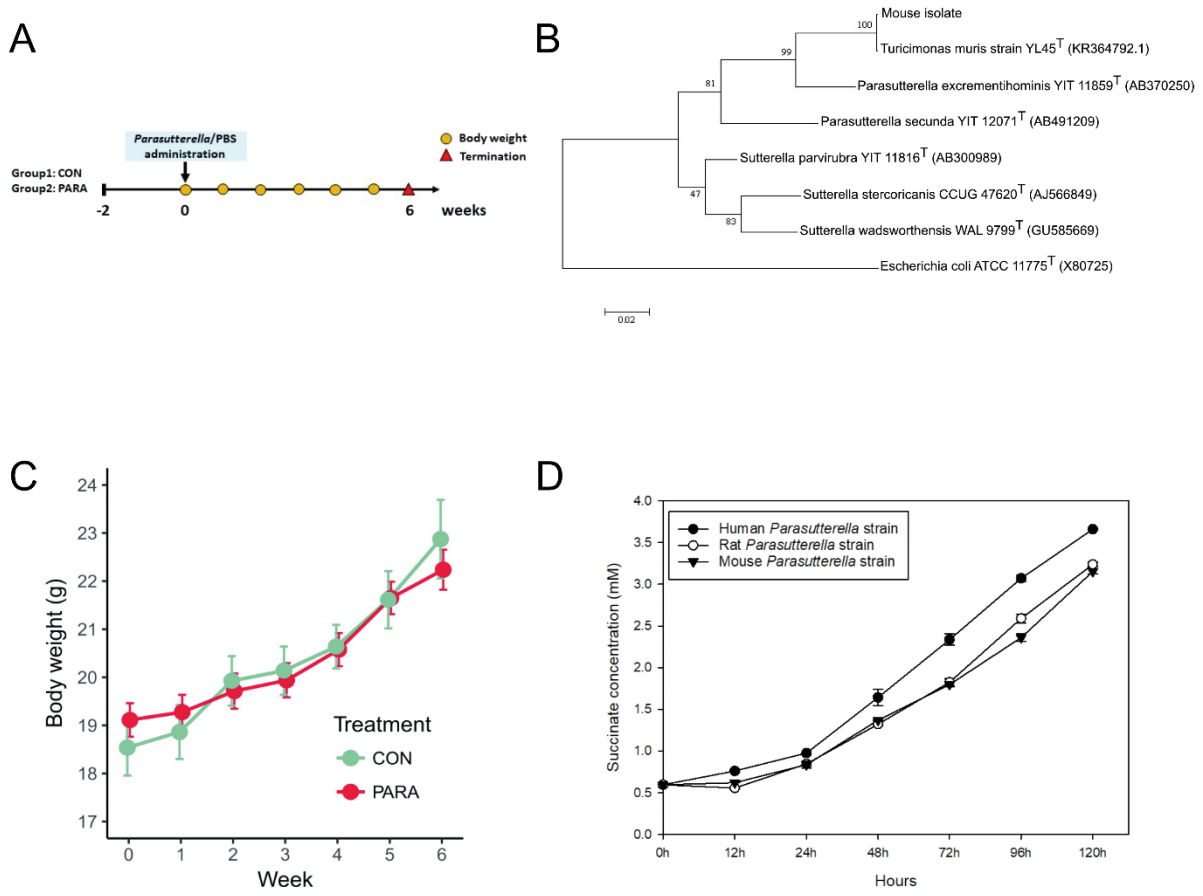

Figure 4.1. A) The timeline for mouse colonization study. C57BL/6J mice, screened and identified as *Parasutterella*-free individuals, were exposed to the murine isolate/PBS and euthanized after six weeks. **B**) Maximum likelihood phylogenetic tree based on 16S rRNA gene sequences of the mouse *Parasutterella* isolate and type strains within the family *Sutterellaceae.* Sequence belonging to the *E. coli* type strain was used as the outgroup. For each node bootstrap values (1,000 replicates) greater than 50% are indicated. **C**) The body weight of the CON and PARA group during the experimental period. For all treatment groups, n = 8. Data are shown as mean ± SEM. **D**) Quantified succinate concentration in the broth culture with human, rat and mouse *Parasutterella* isolate.

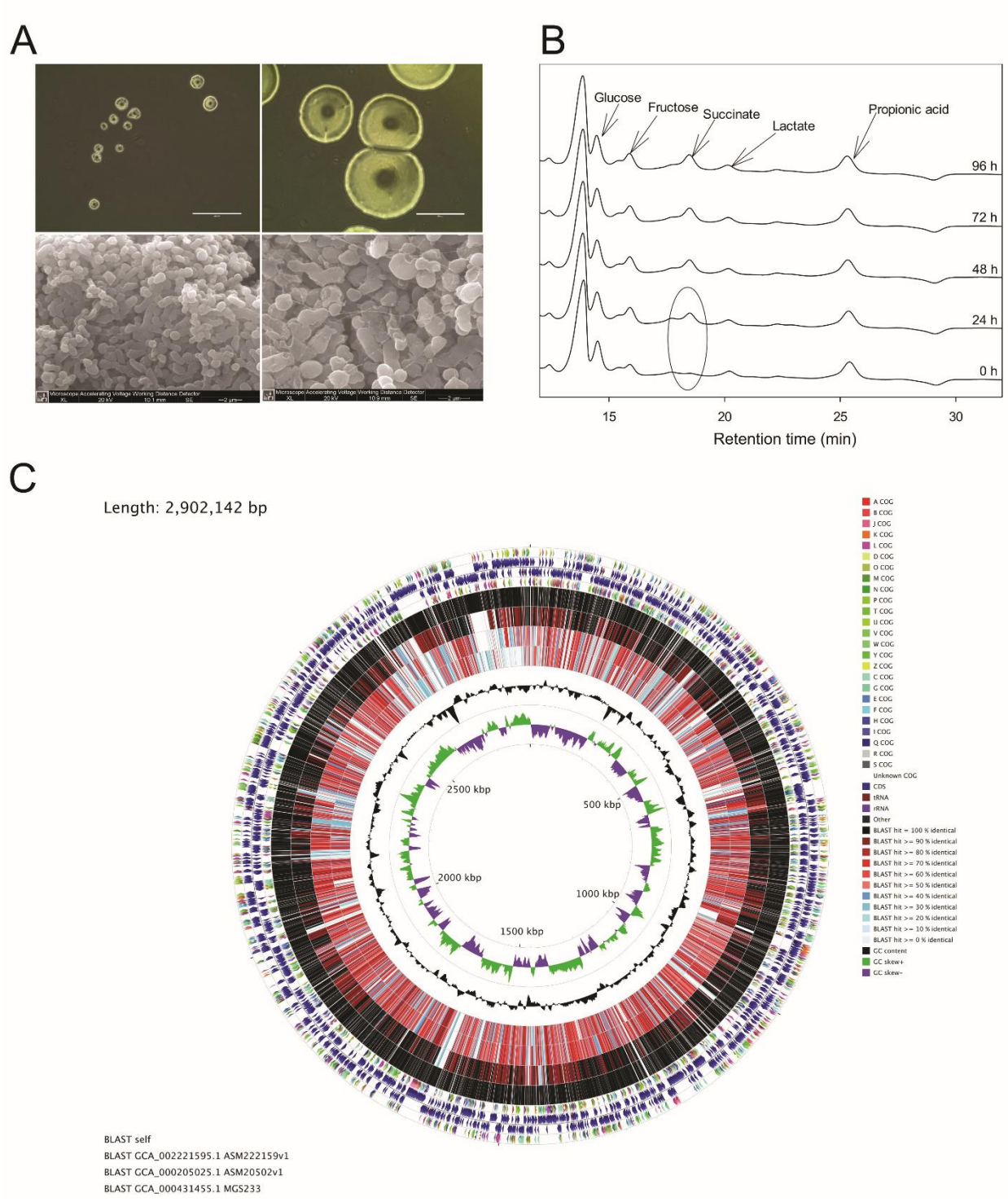

Figure 4.2. Morphology, metabolite production and whole genome visualization of *Parasutterella* mc1. **A**) Top: Colonies of *Parasutterella* mc1 formed on fastidious anaerobic agar (FAA, left) and GAM agar (right), respectively. Bright field, magnification, 100x; Scale

bars, 400 μm. Bottom: Scanning electron microscopy (SEM) micrographs of *Parasutterella* mc1 grown on GAM agar, showing 15,000x (left) and 20,000x (right) magnification, respectively. **B**) HPLC chromatogram showing metabolite profile in GAM broth with *Parasutterella* mc1 collected at 0 h, 24 h, 48 h, 72 h, and 96 h. **C**) Circular genome map of *Parasutterella* mc1 generated with CGView comparison tools. From the outer to inner circles: the first (outermost) and fourth ring depicting Clusters of Orthologous Groups (COG) categories of protein coding genes on the forward and reverse strands, respectively. The second and third rings show the location of protein coding, tRNA, and rRNA genes on the forward and reverse strands, respectively. The fifth, sixth, seventh, and eighth ring depict BLAST comparisons (expected threshold = 0.1) between *Parasutterella* mc1 coding sequences (CDS) translations and the translation from *Parasutterella* mc1, *Turicimonas muris* YL45 (ASM222159v1), *Parasutterella excrementihominis* YIT 11859 (ASM20502v1), and *Parasutterella excrementihominis* CAG:233 (MGS233), respectively. The ninth ring (black plot) depicts GC content and the innermost plot represents GC skew. Both base composition plots were generated using a sliding window of 10,000 nt.

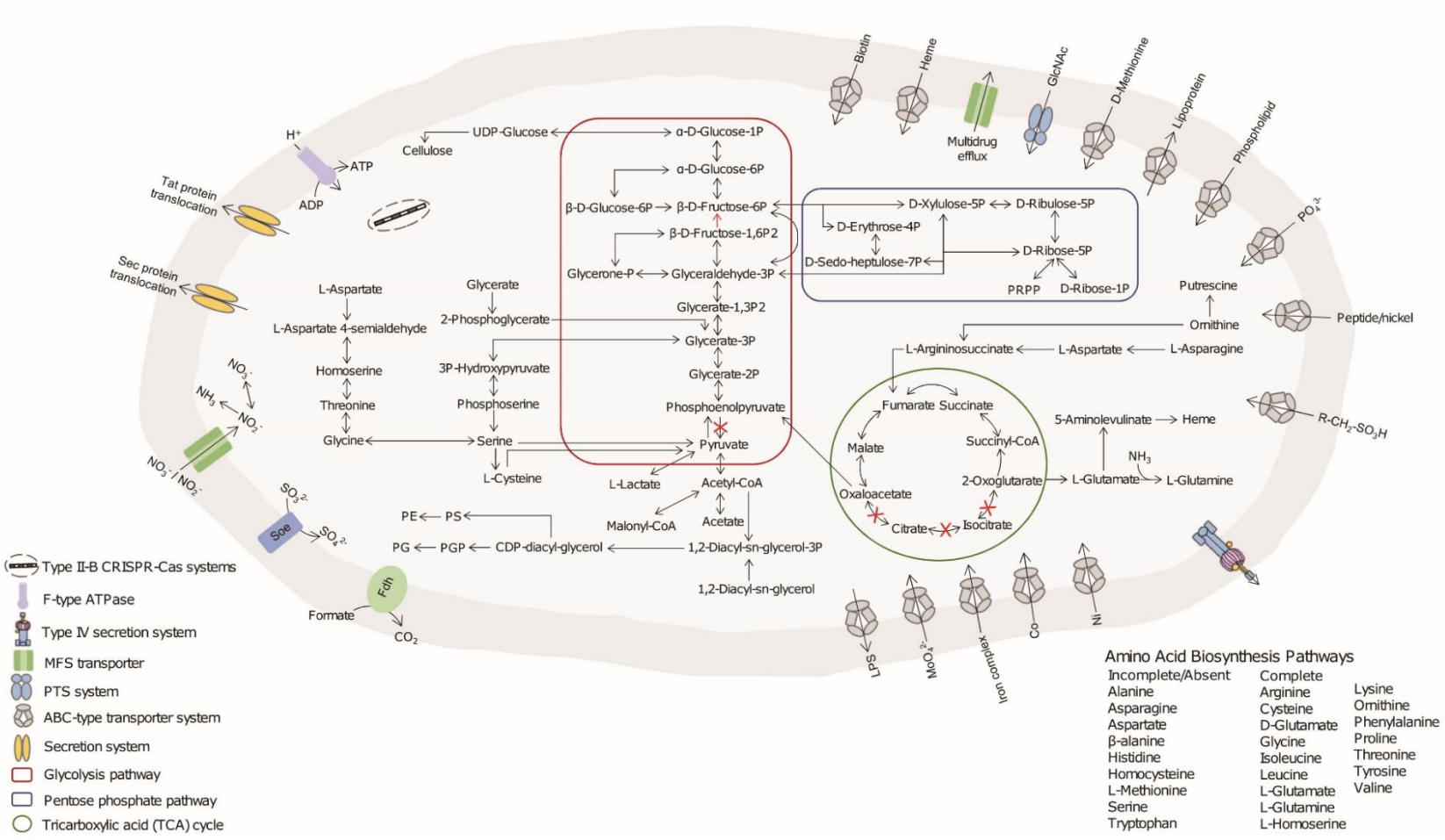
Biotin
Heme
Multidrug efflux
GlcNAc
D-Methionine
Lipoprotein
Phospholipid
PO_4^{-2}
H+
ATP
ADP
Tat protein translocation
Sec protein translocation
UDP-Glucose
Cellulose
α-D-Glucose-1P
α-D-Glucose-6P
β-D-Glucose-6P
β-D-Fructose-6P
β-D-Fructose-1,6P2
Glycerone-P
Glyceraldehyde-3P
D-Xylulose-5P
D-Ribulose-5P
D-Erythrose-4P
D-Sedo-heptulose-7P
D-Ribose-5P
PRPP
D-Ribose-1P
Putrescine
Ornithine
Peptide/nickel
L-Aspartate
L-Aspartate 4-semialdehyde
Homoserine
Threonine
Glycine
Glycerate
2-Phosphoglycerate
3P-Hydroxypyruvate
Phosphoserine
Serine
L-Cysteine
Glycerate-1,3P2
Glycerate-3P
Glycerate-2P
Phosphoenolpyruvate
Pyruvate
L-Lactate
Acetyl-CoA
Malonyl-CoA
Acetate
L-Argininosuccinate
L-Aspartate
L-Asparagine
Fumarate
Succinate
Malate
Succinyl-CoA
Oxaloacetate
Citrate
Isocitrate
2-Oxoglutarate
5-Aminolevulinate
Heme
L-Glutamate
L-Glutamine
NH_3
$R\text{-}CH_2\text{-}SO_3H$
NO_3^-
NO_2^-
NO_3^-/NO_2^-
SO_3^{-2}
SO_4^{-2}
Soe
PE
PS
PG
PGP
CDP-diacyl-glycerol
1,2-Diacyl-sn-glycerol-3P
1,2-Diacyl-sn-glycerol
Fdh
Formate
CO_2
LPS
MoO_4^{-2}
Iron complex
Co
Ni
Type II-B CRISPR-Cas systems
F-type ATPase
Type IV secretion system
MFS transporter
PTS system
ABC-type transporter system
Secretion system
Glycolysis pathway
Pentose phosphate pathway
Tricarboxylic acid (TCA) cycle
Amino Acid Biosynthesis Pathways
Incomplete/Absent
Alanine
Asparagine
Aspartate
β-alanine
Histidine
Homocysteine
L-Methionine
Serine
Tryptophan
Complete
Arginine
Cysteine
D-Glutamate
Glycine
Isoleucine
Leucine
L-Glutamate
L-Glutamine
L-Homoserine
Lysine
Ornithine
Phenylalanine
Proline
Threonine
Tyrosine
Valine

Figure 4.3. Selected genomic features of *Parasutterella* mc1. Predicted metabolic pathways and physiological capabilities are shown based on the annotation of the draft genome. Periplasma (gray) and cytoplasma (light gray) are shown bounded by outer and inner membranes, respectively.
PRPP, Phosphoribosyl pyrophosphate; PGP, Phosphatidylglycerophosphate; PS, Phosphatidylserine; PE, Phosphatidylethanolamine; PG, Phosphatidylglycerol; Fdh, Formate dehydrogenase; Soe, Sulfite dehydrogenase (quinone)

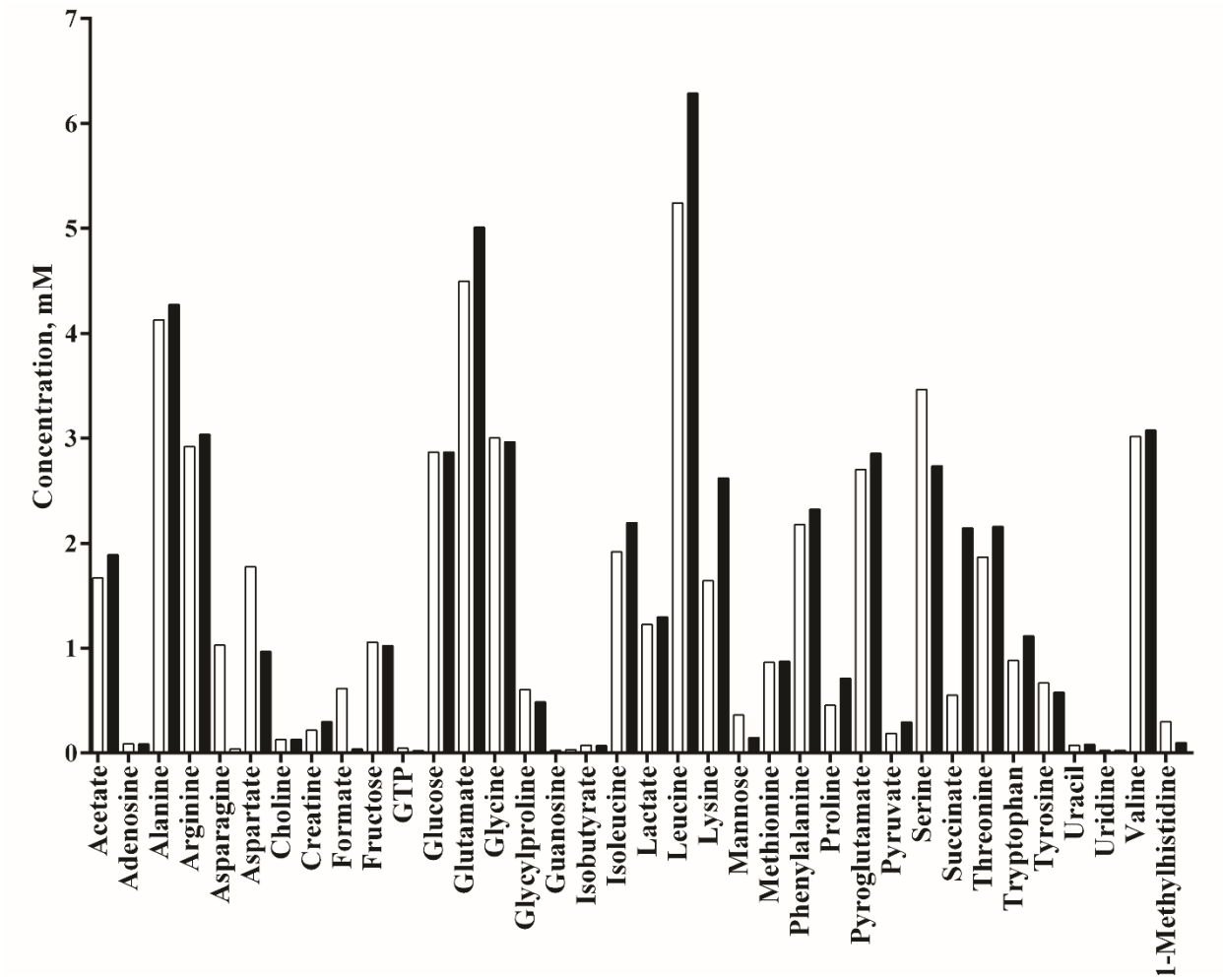

Figure 4.4. The comparison of metabolite concentrations between the GAM broth (white bar) and the *Parasutterella* culture (black bar) collected at 48 h of growth. The identification and quantification of metabolites were conducted by NMR.

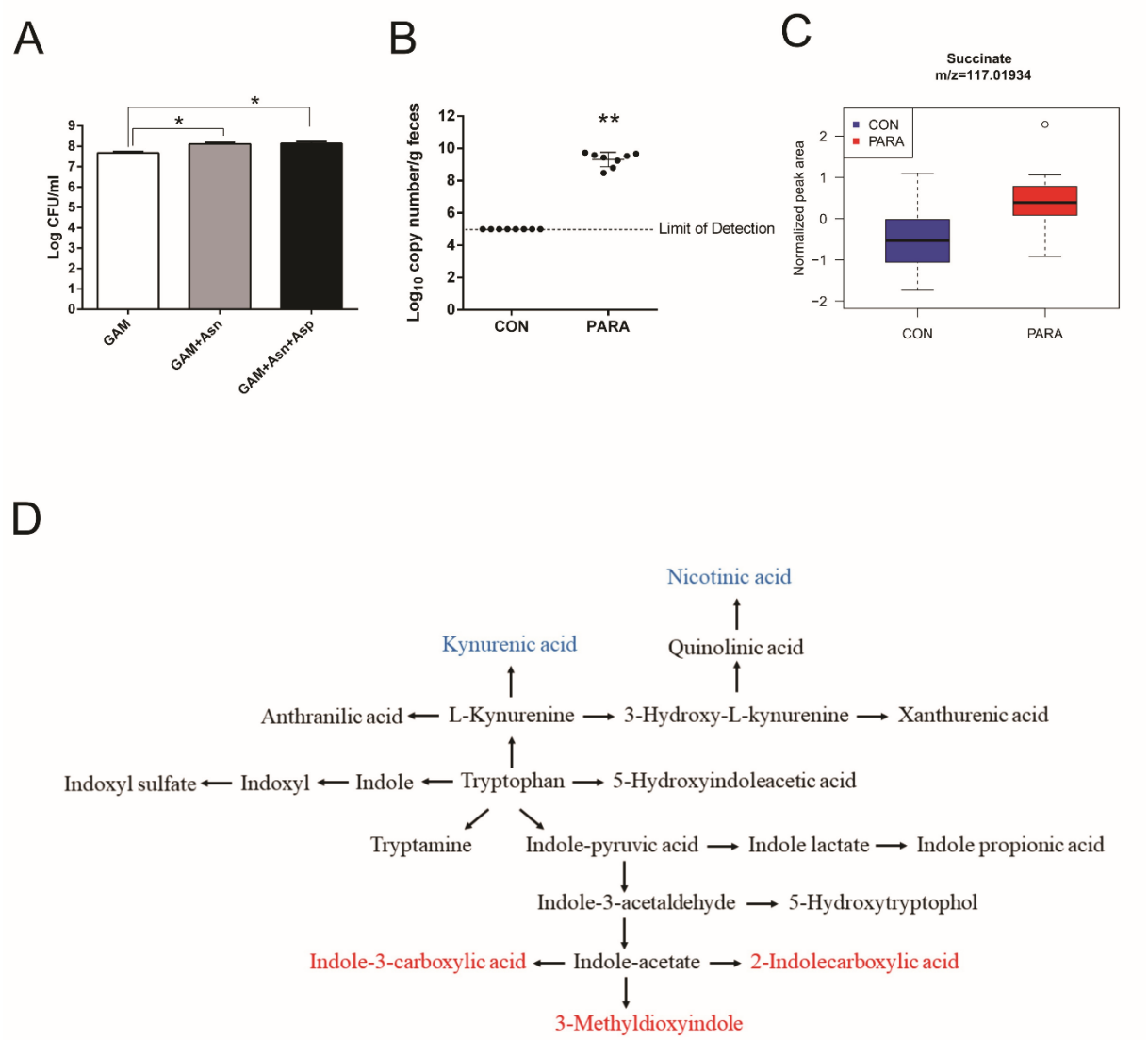

Figure 4.5. A) Enumeration of *Parasutterella* in GAM, GAM supplemented with asparagine (Asn), and GAM supplemented with Asn plus aspartate (Asp) at 72 h of growth. Asn and Asp were added at 48 h of growth. For all treatment group, n = 3. Data are shown as mean ± SEM. *, $P < 0.05$. **B**) qPCR quantification of *Parasutterella* 16S rRNA gene copies in feces of CON and PARA mice. Results are expressed as log10 16S rRNA gene copies per gram of feces and 5 log10 copy numbers was set as the detection of limit (Ct = 34). For each treatment group, n = 8. Data are shown as mean ± SEM. **, $P < 0.01$. **C**) Succinate

concentration in cecal contents from CON and PARA mice. Boxes represent the 25th to 75th percentile and lines within boxes represent the median. Circles represent values beyond 1.5 times the interquartile range. n = 8. $P = 0.049$. **D**) Potential pathways for tryptophan-indole metabolism by the host and gut microbiota (adapted from Reference 46, 49). The red color denoted tryptophan metabolites in cecal contents with increased abundance by *Parasutterella* colonization, while the blue color denoted decreased tryptophan metabolites by *Parasutterella* colonization.

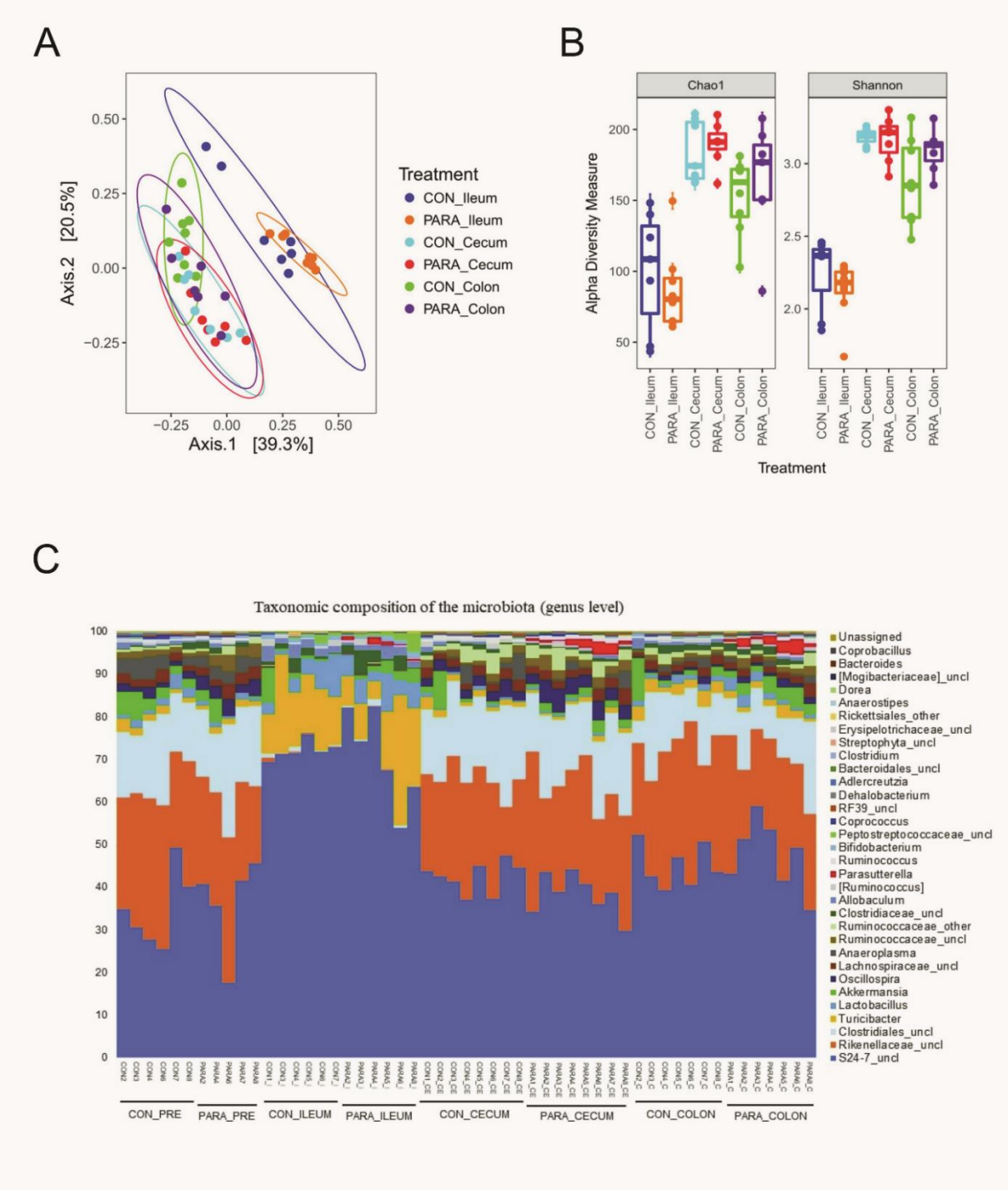

Figure 4.6. Microbial structural analysis of contents collected from different intestinal segments. **A**) PCoA plot of bacterial communities based on a Bray-Curtis dissimilarity matrix. Colors represent intestinal sites and within the same intestinal site, each point

represents an individual mouse. For all treatment groups, n = 8. **B**) Alpha diversity analysis of bacterial communities in ileal, cecal, and colonic contents of mice. All contents were harvested six weeks after *Parasutterella*/PBS administration. Data are shown as mean ± SEM. **C**) Bar chart indicating microbial community profiles between groups, summarized down to the genus level. Microbial compositions of two groups before experimental treatment are labeled as CON_PRE and PARA_PRE.

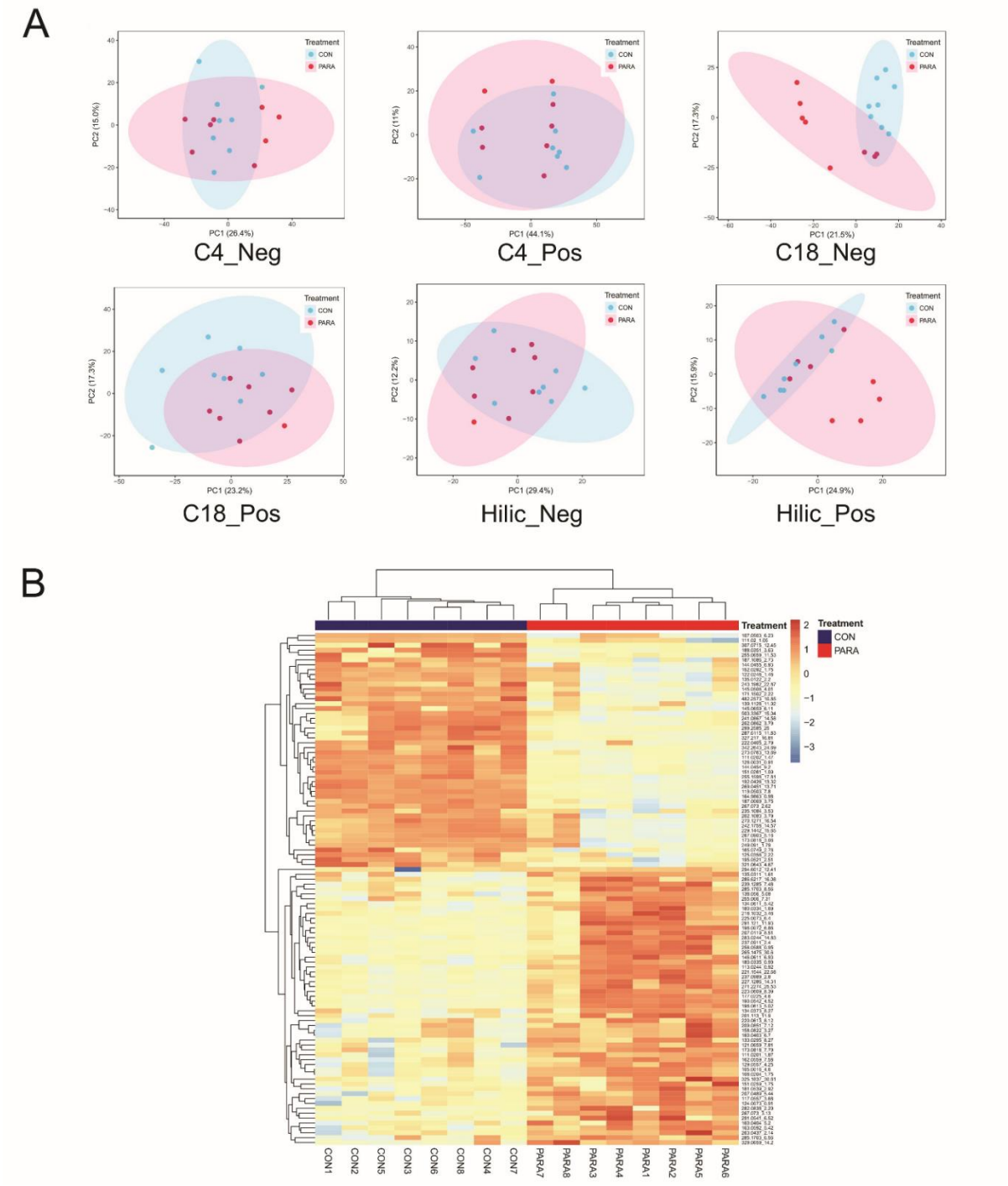

Figure 4.7. *Parasutterella* colonization altered the cecal metabolite profile. **A**) PCA plot of features that were detected from the CON and PARA group. Cecal metabolite features were generated from six chromatographic conditions (n = 8 per treatment). Each dot represents an

individual mouse. **B**) Heatmap of changed features detected from cecal samples based on the C18-ESI- dataset. Features significantly increased or decreased in the PARA group compared to the CON group are shown, *q*-value < 0.05. Each column represents an individual mouse (n = 8 per treatment).

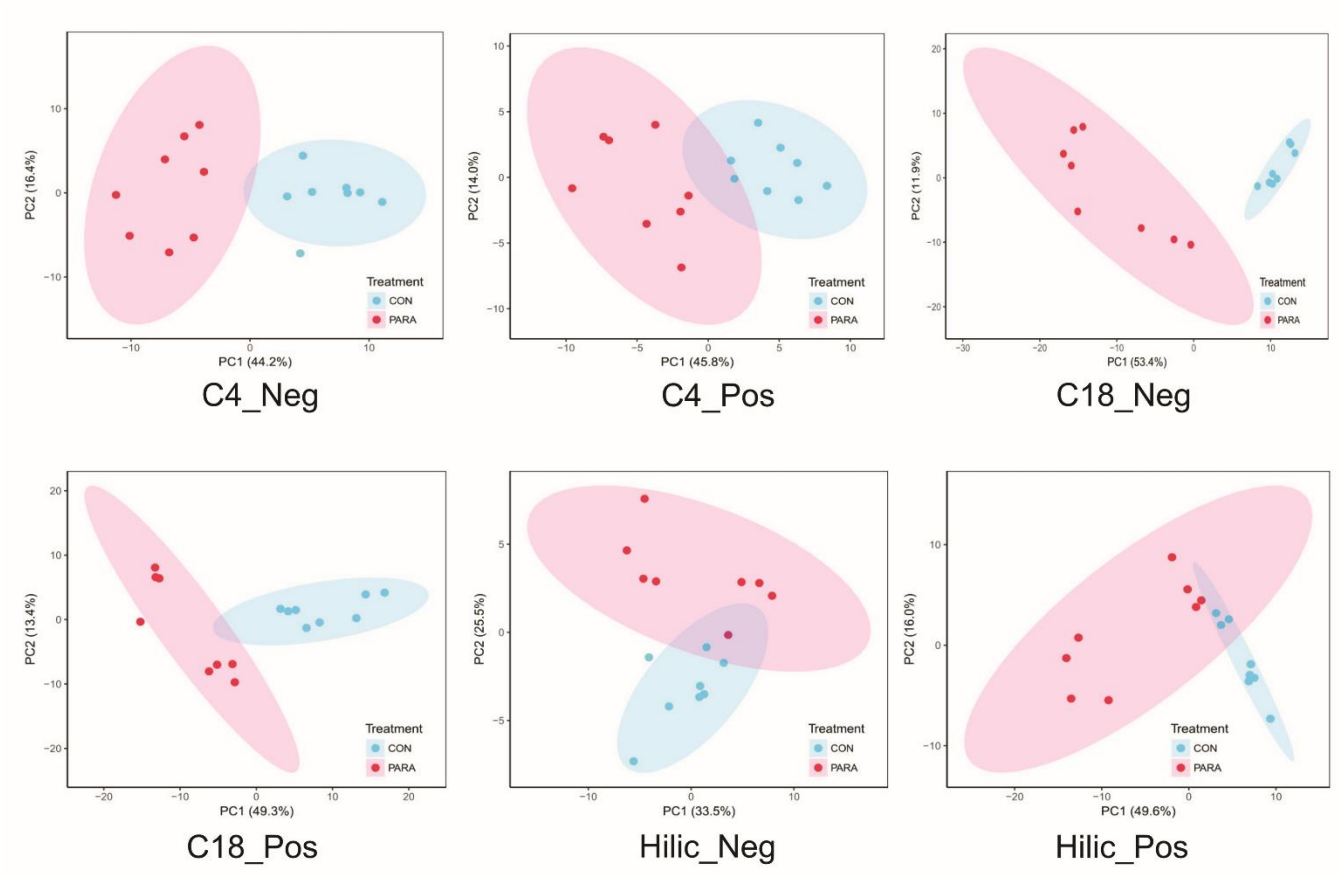

Figure 4.8. PCA plot of features that were differently presented between the CON and PARA group analyzed by Student's t-test. Cecal metabolite features were generated from six chromatographic conditions (n = 8 per treatment). Each dot represents an individual mouse.

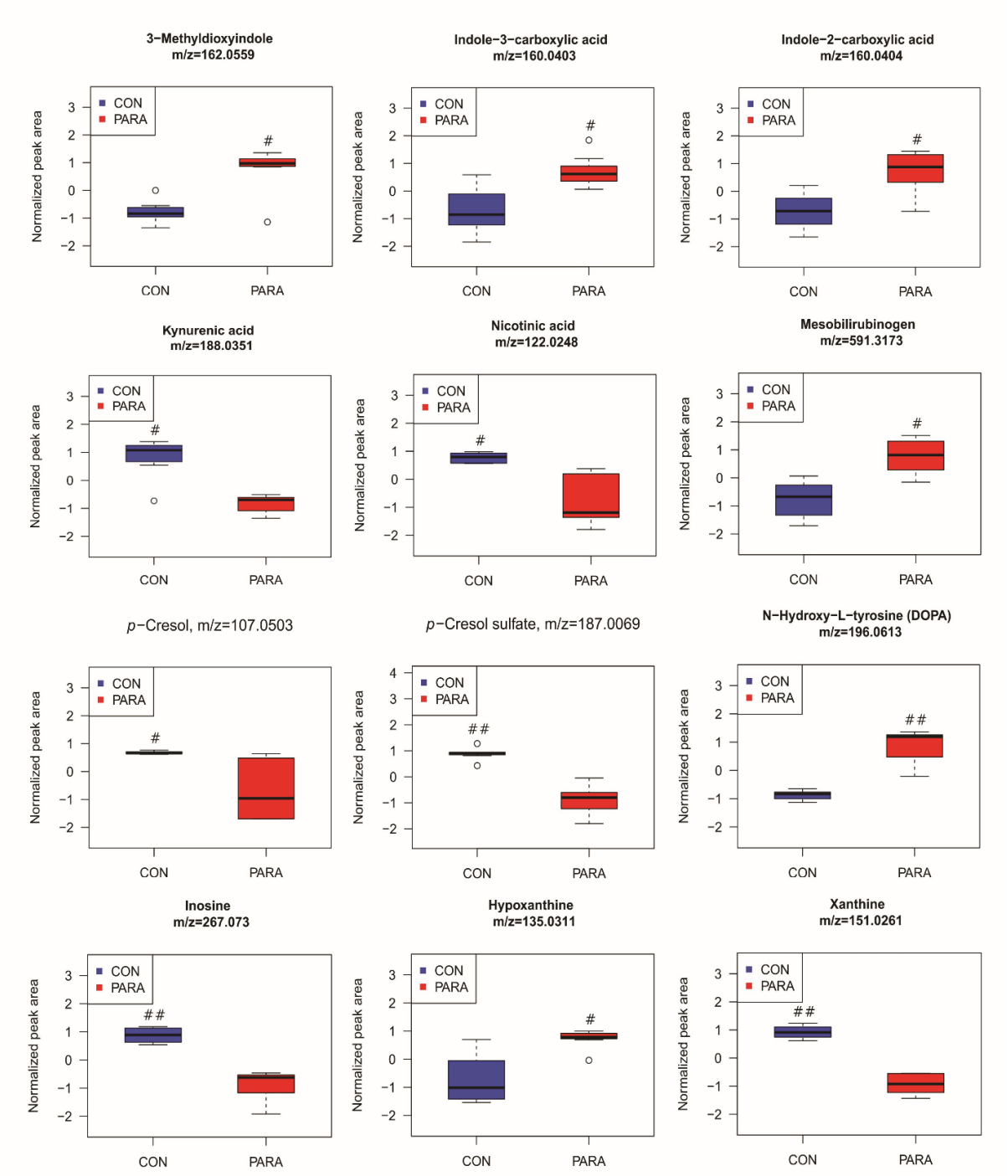

Figure 4.9. *Parasutterella* colonization induced changes in cecal metabolites. Changed metabolites associated with tryptophan metabolism (3-Methyldixyindole, indole-3-carboxylic acid, indole-2-carboxylic acid, kynurenic acid, and nicotinic acid), tyrosine metabolism (*p*-

Cresol, *p*-Cresol sulfate, and N-Hydroxy-L-tyrosine or DOPA), and purine metabolism (inosine, hypoxanthine, and xanthine). Data are presented as box plots, where boxes represent the 25th to 75th percentile and lines within boxes represent the median. Circles represent values beyond 1.5 times the interquartile range. Significance was indicated as follows, ##, *q*-value < 0.01; #, *q*-value < 0.05. Eight biological replicates from CON and PARA mice were plotted.

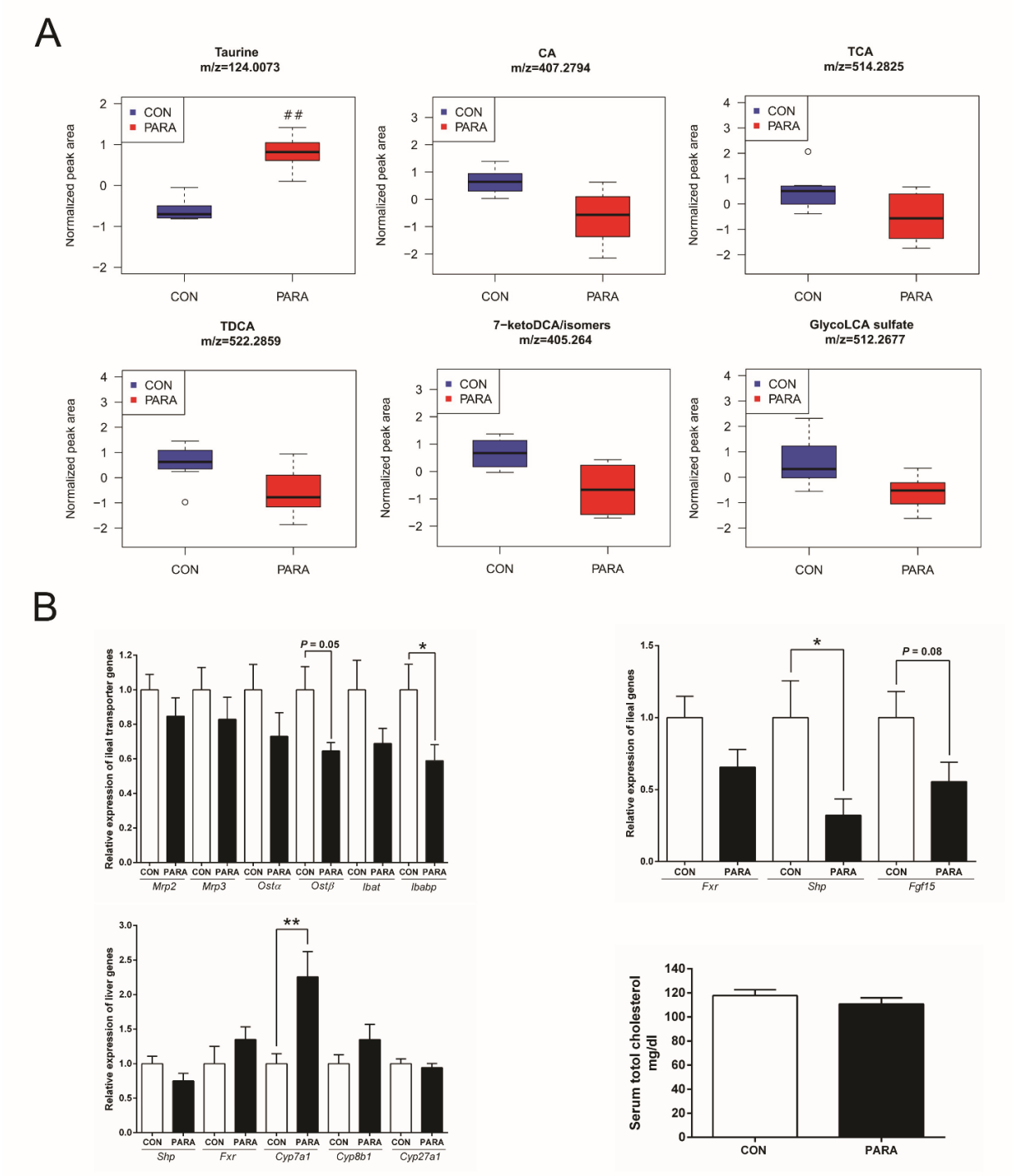

Figure 4.10. Bile acid metabolites and host gene expression**. A**) Changes in bile acid derivatives in cecal contents of the CON and PARA group. Normalized values are presented

as box plots, where boxes represent the 25th to 75th percentile and lines within boxes represent the median. Circles represent values beyond 1.5 times the interquartile range. Eight biological replicates from CON and PARA mice were plotted for taurine, CA, TCA, TDCA, 7-ketoDCA or its isomers, and Glyco-LCA sulfate. ##, q-value < 0.01. **B**) qPCR assay results of gene expression. Top left: Ileal bile acid transporters including *Mrp2, Mrp3, Ostα, Ostβ, Ibat,* and *Ibabp*. Top right: Ileal FXR signaling pathway including *Fxr, Shp*, and *Fgf15*. Bottom left: Liver FXR and bile acid synthesis genes including *Shp, Fxr, Cyp7a1, Cyp8b1*, and *Cyp27a1*. Bottom right: Serum cholesterol concentration of CON and PARA mice. For all treatment group, n = 8. Data are shown as mean ± SEM. **, $P < 0.01$; *, $P < 0.05$.

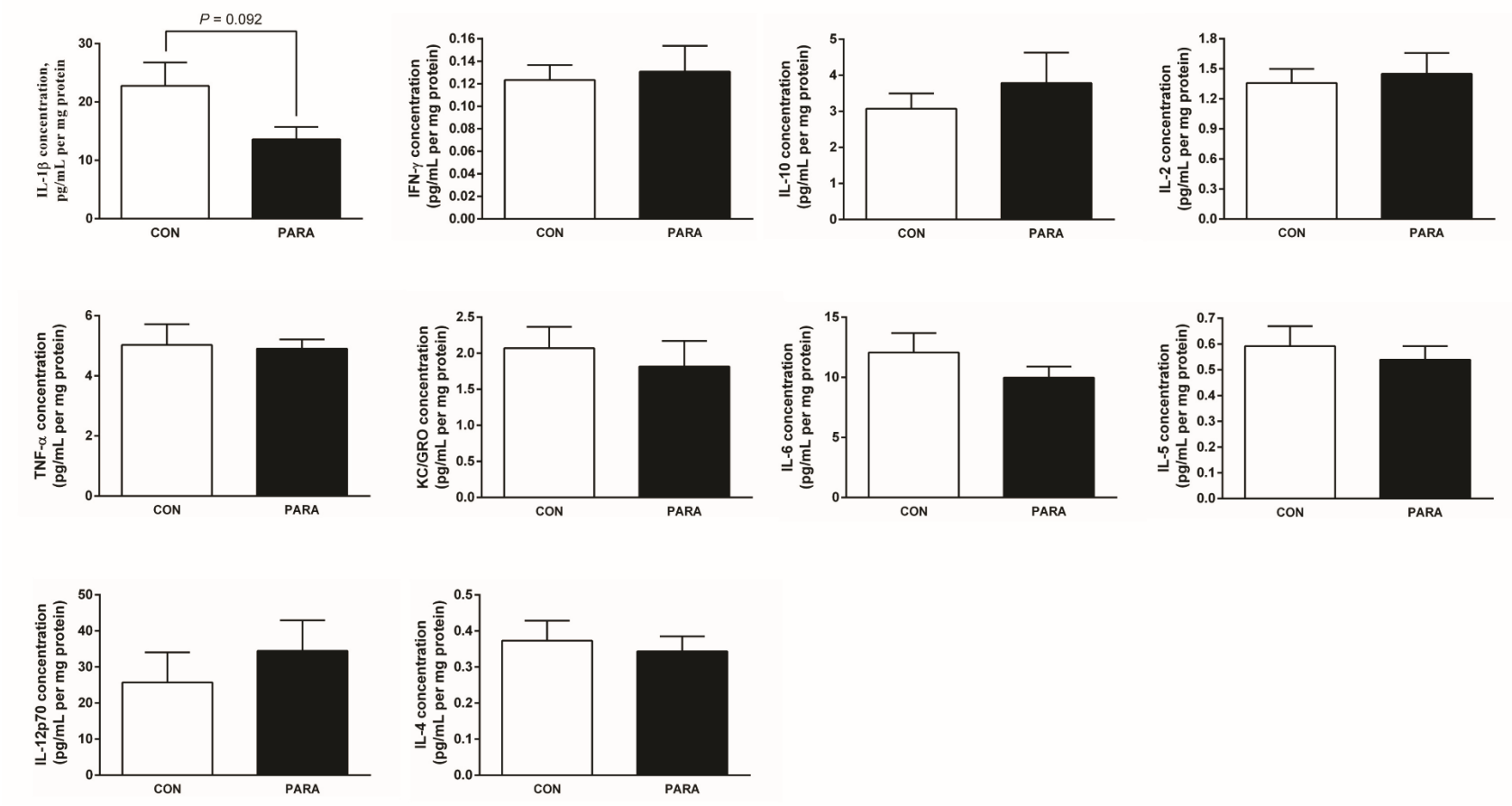

Figure 4.11. Colonic cytokine analysis results of IL-1β, IFN-γ, IL-10, IL-2, TNF-α, KC/GRO, IL-6, IL-5, IL-12p70, and IL-4. Colonic tissue samples were collected six weeks after *Parasutterella*/PBS treatment. For all treatment groups, n = 8. Data are shown as mean ± SEM.

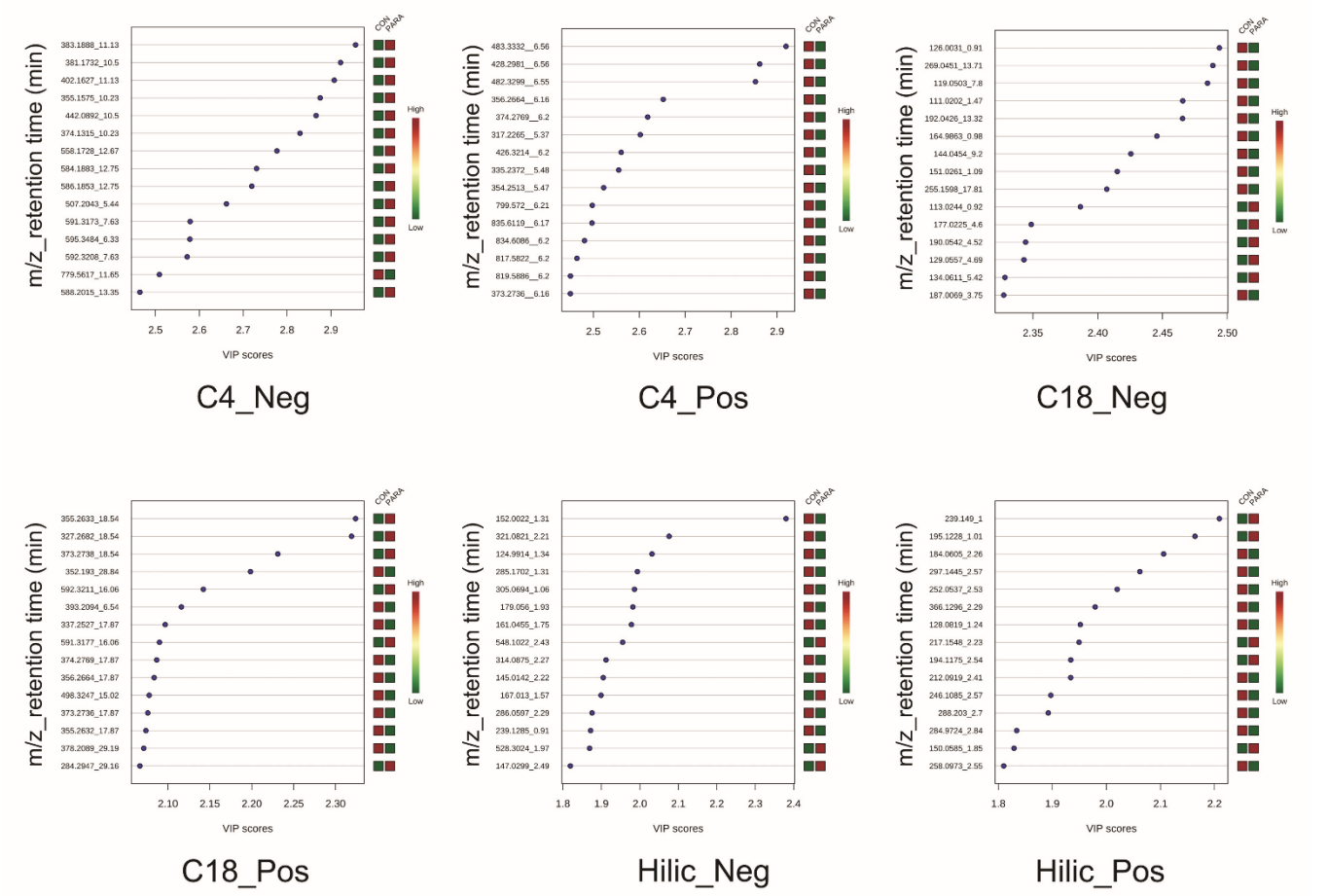

Figure 4.12. Top features ranked by PLS-DA VIP scores. Cecal metabolite features were generated from six chromatographic conditions (n = 8 per treatment). Features were indicated by the m/z value and the retention time (min).

5. CHAPTER 5: HOST SPECIFICITY OF *PARASUTTERELLA* STRAINS IN THE INTESTINAL COLONIZATION

5.1. Introduction

The symbiotic relationship between gut microbes and the host ranges from the mutualism and commensalism to parasitism (1). The mechanism shaping the microbial symbiosis in the gastrointestinal tract (GIT) remains to be fully elucidated. While the gut microbiome has been recognized as a complex and dynamic ecosystem in which microbial species are in continual flux, a question remains of how bacterial lineages are selected and what makes the community particularly suited to the host (2). From the ecological perspective, multiple theories such as the niche theory and the neutral theory have been proposed to explain the assembly process of microbial communities (2). The niche theory is based on deterministic factors in shaping and maintaining the gut microbial community. In contrast, the neutral theory suggests that the assembly of local communities can be explained by stochastic processes, considering the fitness of species within communities are functionally equivalent (2). Evidence suggests that these theories are jointly responsible for shaping the assembly of the gut microbiota (3).

It has been suggested that the co-speciation exerts a significant effect on the evolution of the gut microbial community in mammals, indicating that certain gut microbes may co-evolve with the host (4). During the assembly process of gut microbial communities, the environment presented by the host provides important forces in selecting strains that colonize and persist in the gut as a member of communities (5). The adaptation of microbes to a given gut environment may play an important role in microbial persistence as it can greatly facilitate

the colonization and compete with others (6). Being adapted to the ecological niche featured by a variety of characteristics such as specialized nutrient availability and immune compartment primarily drives the colonization success of certain microbial lineages (3). However, currently our understanding of the host specificity of vertebrate gut symbionts is not well understood, and particularly for those microbes that have not been well characterized.

The host adaptation of gut bacterial species is exemplified by *Lactobacillus reuteri*, which has diversified into distinct phylogenetic lineages inhabiting the gastrointestinal tract (GIT) of humans, pigs, mice, rats, and chickens (7). Mono-colonizing germ-free mice with *L. reuteri* demonstrated that the formation of epithelial biofilm in the forestomach depends on the host origin of strains (8). Specifically, the adherence to the forestomach epithelium was restricted to rodent strains and genes involved in biofilm formation were lineage-specific (8). Administering a mixed bacterial culture composed of *L. reuteri* strains from different host origins to germ-free mice showed that rodent strains became predominant, representing a significantly higher relative abundance in feces than non-rodent lineages (9). On the forestomach epithelium, rodent isolates comprised around 97% of the total *L. reuteri* population, suggesting the host specificity of *L. reuteri* strains in the ecological niche (10). In contrast, the human lineage did not exhibit an elevated ecological fitness in the human study, implying the absence of the niche that *L. reuteri* occupies in the human gut (9). Collectively, these results provided clear evidence for the specific evolution of *L. reuteri* with rodent hosts.

As a common bacterial inhabitant in GIT, the genus *Parasutterella* has been found in the human and animal gut (11). The unique phylogenetic classification and the diversification of *Parasutterella* make the genus an attractive model microorganism to study the host

adaptation of gut commensal bacteria. Previously, we successfully established a mouse model harboring a complex microbial community with an absence of *Sutterellaceae* species to study the effect of *Parasutterella* colonization on host physiology (11). Therefore, in the current study, we tried to isolate *Parasutterella* strains from different hosts and confirmed their ability to colonize the established mouse model. A competitive study was subsequently conducted using the human and mouse strain to investigate if *Parasutterella* strains are host-adapted during colonization. The findings provided more information about the commensal lifestyle of the genus *Parasutterella* and contributed to the understanding of host-microbe interactions from an ecological perspective.

5.2. Materials and methods

5.2.1. Strains, media, and growth conditions. Bacterial strains used in this study were isolated from human, mouse, chicken, and pig feces. The detailed procedure of isolation has been described previously (11). The Gifu Anaerobic Medium (GAM) agar supplemented with 4 μg/mL oxacillin was used as the selective agar.

In mouse colonization studies, bacterial strains were cultivated in 5 mL of GAM medium at 37°C for 72 h. The culture medium containing approximately 1.0×10^7 colony forming units (CFUs)/mL was centrifuged at 5,000 x g for 10 min to harvest bacterial cells. Cell pellets were resuspended in 1 x phosphate-buffered saline (PBS) supplemented with 0.05% (w/v) L-cysteine and mice were subsequently exposed to bacterial strains by oral gavage.

5.2.2. 16S rRNA gene amplification for Sanger sequencing. The 16S rRNA gene sequence identification of colonies on selective media was conducted by a colony polymerase chain reaction (PCR) using primers for bacterial 16S rRNA gene, 27f and 1492r (12). The PCR

reaction and program has been described in Chapter 4. Sequences were searched against the NCBI 16S rRNA sequence and Ribosomal Database Project database.

5.2.3. Mice. Six- to ten-week-old Swiss-Webster mice not harboring *Sutterellaceae* species were housed in the Axenic Mouse Research Unit at the University of Alberta. Mice were kept under specific pathogen-free (SPF) conditions with sterilized filter-topped ISOCages and standard chow diet. Mice were randomly grouped into cages with 3 to 4 mice per cage by a blinded lab animal technician and balanced with respect to sex and body weight. To confirm if bacterial strains were capable of colonizing the mouse gut, strains isolated from human, mouse, pig, and chicken were inoculated to two cages of mice by oral gavage. The colonization was detected from feces by assessing the 16S rRNA gene libraries and culture paired with colony PCR and Sanger sequencing.

In the competitive study, cages were allocated into 3 treatments: colonization with the mouse *Parasutterella* strain (M); colonization with the human *Parasutterella* strain (H), and colonization with a mixture of mouse and human strain (HM). Mice were exposed to *Parasutterella* strains by oral gavage with 0.1 mL of the bacterial suspension (1×10^6 CFUs). Fecal samples were collected on day 0, 14, and 28. At day 14, the human *Parasutterella* strain was added to the M group whereas the mouse *Parasutterella* strain was added to the H group. The HM group received PBS. The protocols employed were approved by the University of Alberta's Animal Care Committee and in accordance with the guideline of the Canadian Council on the Use of Laboratory Animals.

5.2.4. Characterization of gut microbial composition. DNA was extracted from feces after *Parasutterella* strain inoculation as well as from feces collected at day 0. The microbial

composition was assessed using 16S rRNA gene amplicon sequencing of the V3-V4 region on the Miseq platform. The DNA extraction, amplicon library construction, paired-end sequencing, and data analysis were performed using protocols and pipelines published previously (13).

5.2.5. Comparative pathway analysis. The genome of the mouse strain *Parasutterella* mc1 was assembled as previously described and annotated using PATRIC (11, 14). Human strains deposited in PATRIC database including the type strain *P. excrementihominis* YIT 11859, *P. excrementihominis* UBA 11789, and *P. excrementihominis* UBA 9121 were included for comparing key pathways inter-species using PATRIC's Comparative Pathway Tool.

5.2.6. Data analysis and visualization. 16S rRNA gene sequences of mouse and human *Parasutterella* share a high similarity. Therefore, the relative abundance of each strain from microbial taxonomic profiling data was obtained based on the OTU level. The comparison of individual taxa/OTUs between groups was performed using the Kruskal-Wallis test (SAS 9.4). The permutational multivariate analysis of variance (MANOVA) of the weighted UniFrac distance was used to determine the difference in overall microbial composition across the treatments (adonis function, vegan package, R v3.4.4). The principal coordinate analysis (PCoA) based on a Bray-Curtis dissimilarity matrix was plotted using the phyloseq package (R v3.4.4). *P* values indicate statistical significance as follows: **, $P < 0.01$; *, $P < 0.05$. R (v3.4.4) and GraphPad Prism was used for visualizing results.

5.3. Results

5.3.1. Isolating *Parasutterella* species from different hosts. The GAM agar supplemented with oxacillin performed a high selectivity of *Sutterellaceae* species. We had

successfully isolated *Parasutterella* species from human, rat, and mouse gut (11). Based on previous results from taxonomic profiling by 16S rRNA sequencing, the pig and chicken individuals harboring *Sutterellaceae* species in the gut were targeted. The isolated pig strain shares 95.1% 16S rRNA sequence identity with the type strain *Duodenibacillus massiliensis* Marseille-P2968, a new *Sutterellaceae* species isolated from human duodenum, whereas it shares 92.8% identity with the type stain *P. secunda* YIT 12071 (15). The chicken isolate shared high similarity with the type strain *P. secunda* JCM 16078 (98.8% identity). The result demonstrated that strains isolated from pig and chicken are members of the family *Sutterellaceae* and phylogenetically closed to *P. secunda*. However, due to the limitation of identifying new species based on the 16S rRNA gene similarity and a paucity of information about *Parasutterella* species in hosts such as pig, further analysis of genomic features is necessary to define the isolate. Human and mouse isolates have been characterized as *Parasutterella* species that share 99% and 93% 16S rRNA sequence identity with *P. excrementihominis* YIT 11859, respectively (Figure 5.1A).

5.3.2. Colonizing mouse GIT with different *Sutterellaceae* species. To test if isolates with different host origins were capable of colonizing the mouse GIT, Swiss-Webster mice were exposed to each isolate by oral gavage. The colonization was checked after two weeks by 16S rRNA gene PCR amplification from feces and culturing live bacteria. We could not detect pig and chicken isolates after exposure, indicating that *P. secunda* and the pig *Sutterellaceae* strain failed to colonize mouse GIT above our limit of detection (~10^4 CFUs/g). The human and mouse *Parasutterella* strain rapidly and stably colonized the mouse gut, which is consistent

with previous studies conducted in SPF C57BL/6J mice. Therefore, the human and mouse *Parasutterella* strain were selected for the competitive colonization experiment.

5.3.3. Competitive colonization between human and mouse *Parasutterella* isolate. To perform the competitive colonization study, mice were exposed to the mouse *Parasutterella* strain, the human *Parasutterella* strain, and a mixture comprising both strains. The timeline for the competitive colonization study was described in Figure 5.1B. We characterized the microbial composition before and after the colonization with *Parasutterella*. The 16S rRNA gene amplicon sequencing resulted in an average of 22,448 ± 12,420 (mean ± SD) reads per sample after the quality control and chimera removal. At day 0, there was no significant difference in microbial structure (R^2 = 0.147, P = 0.103, adonis) and alpha diversity between treatment groups as reflected by Chao1 and Shannon indexes (Figure 5.2). After being exposed to *Parasutterella* strains, at day 14, the microbial structure was significantly different between treated groups (R^2 = 0.300, P = 0.002). Specifically, there were no difference in microbial structure between the M group and HM group, however, microbial communities in the H group were significantly shifted from that in the M and HM group. Because human *Parasutterella* did not colonize the HM group this data suggests that the human *Parasutterella* strain has a stronger impact on the intestinal environment and microbial population. After receiving the opposing strain in the H and M group at day 14, the difference in microbial structure observed vanished when detected at day 28 (R^2 = 0.147, P = 0.103).

To assess the relative abundance of each *Parasutterella* strain, sequences were assigned to taxonomy using RDP Classifier. At day 0, there was no OTU assigned to the family *Sutterellaceae*, validating the available niche in the mouse gut for *Parasutterella* colonization.

At day 14, both the mouse and human *Parasutterella* were able to colonize the mouse GIT when administered separately. However, the mouse *Parasutterella* showed a better ecological fitness as reflected by a higher relative abundance in the gut microbial population compared to the human strain in the H group (2.67 ± 2.44% vs. 0.55 ± 0.44%, mean ± SD, $P < 0.05$). When inoculating a mixture of both strains, the mouse *Parasutterella* outcompeted the human strain as the OTU representing the human strain could not be detected in HM mice. In contrast, the mouse *Parasutterella* strain represented the *Sutterellaceae* family with an average of 4.27 ± 4.23% (mean ± SD) of the total bacterial population. This phenotype was consistently observed at day 28 in the HM group, confirming that the human strain lacks the ability to colonize and persist in mouse GIT when the mouse lineage is present.

The opposing strain was inoculated to the H and M group to investigate if the added strain survives in the niche that has been occupied. In mice pre-colonized with the mouse *Parasutterella* strain, the human strain failed to fill in the niche as indicated by the absence of human *Parasutterella* in the M group at day 28. In addition, the inoculation of the human strain did not affect the colonization level of the mouse strain. In contrast, in mice pre-colonized with the human *Parasutterella* strain, the human strain became undetected in some individuals after the mouse strain colonized. About 40% of mice still harbored the human strain, however, the colonization abundance of the human strain was significantly reduced from 0.38 ± 0.17% to 0.03 ± 0.02% (mean ± SD, $P < 0.05$) of the microbiota in these mice. The mouse strain became the predominant strain in the gut pre-colonized with the human *Parasutterella*. Taken together, these results demonstrated the host adaptation of *Parasutterella* strains in colonizing mouse GIT as the mouse strain is able to outcompete the human lineage.

In addition, as the colonization of the human strain significantly drove microbial communities, we analyzed the difference in the microbial composition at the genus level. The relative abundance of genera classified as unclassified_*S24-7*, unclassified_Clostridiales, *Ruminoccaceae*_other, and unclassified_*RF39* was significantly different between the M and H group. Specifically, the colonization of the human *Parasutterella* largely decreased the abundance of members from the order Clostridiales. In contrast, the relative abundance of the unclassified_*S24-7* from Bacteroidales was significantly reduced by mouse strain colonization. The relative abundance of these two genera in the M and H group was comparable at day 0, indicating the changed microbial profile was induced by the presence of human and mouse strain.

5.3.4. Comparative pathway analysis. The whole genome sequencing of human *Parasutterella* isolate remains to be performed. Due to the high identity of 16S rRNA gene sequence between our human isolate and the type strain *P. excrementihominis* YIT 11859 isolated from human feces, we used the reported genome of *P. excrementihominis* YIT 11859 as well as the other two human strains retrieved from the PATRIC database to conduct the comparative pathway analysis. Among representative pathways, human strains share some genes that are missing from the mouse lineage, including genes encoding enoyl-CoA hydratase, gamma-glutamyltransferase, and an enzyme interconverts keto- and enol- groups. These genes are involved in pathways associated with lipid and amino acid metabolism as well as xenobiotic biodegradation and metabolism. The type strain *P. excrementihominis* YIT 11859 contains unique genes encoding isomerases and phosphoric diester hydrolases. In contrast, only one unique feature was detected in the genome of the mouse strain compared to human strains,

which is annotated as a gene encoding acetate/propionate kinase. When searching predicted protein sequences against the NCBI database, the enzyme shares 86.5% similarity with the propionate kinase in *E. coli*, however, with low sequence coverage as the predicted enzyme contains much fewer amino acids compared to that in *E. coli* (107 vs. 402 amino acids). These genomic features and associated pathways need further experimental validation.

5.4. Discussion

The host specificity of gut commensal microbes during intestinal colonization varies among microbial species as evidenced by *E. coli* and *L. reuteri*. In particular, The genetic structure of commensal *E. coli* lineages is shaped by both the host and the environment as the prevalence of phylogenetic groups of *E. coli* among different hosts is not clearly associated with particular hosts (16). In contrast, *L. reuteri* species have shown host specialization as reflected by phenotypic characteristics as well as genomic features (1). However, understanding the commensal niche and lifestyle of gut microbes is complex and challenging, which requires the integration of ecological and evolutionary perspectives (17). Investigating factors shaping the genetic structure of gut commensal microbes will help us develop strategies to promote host-microbial mutualism.

Numerous factors such as diet, environment, host genetics and disease states could shape the highly selected microbial community in the GIT (18–20). Reciprocally transplanting the gut microbiota into germ-free zebrafish and mouse recipients suggested the selective pressure from host genetics and physiology on the maintenance of specific gut microbial community (21). In addition, interactions between the dynamics within microbial communities and the host habitat contributes to the assembly of the gut microbiota (17). To date, most studies

investigating the host specificity of commensal microbes are based on germ-free animals such as mice and zebrafish. The model used in the current study incorporated interactions between the colonizing habitat and the complex microbial community to investigate the adaptation of commensals to a given gut environment.

Parasutterella species have been widely found in humans and a variety of animals. However, our understanding of the genus was mainly based on culture-independent techniques and largely relied on 16S rRNA gene sequences. The limited cultivation of *Parasutterella* species from different hosts makes it difficult to characterize the microbial function and its interactions with the host. In the current study, we aimed to isolate *Parasutterella* species from multiple hosts as the previously characterized taxonomic profile revealed the presence of *Parasutterella* in hosts in addition to humans and rodents. Using the selective media, we were able to successfully isolate *Parasutterella* species from human, mouse, chicken, and rat GIT, however, the characterization of the pig isolate needs further confirmation. The pig and chicken isolates failed to colonize the mouse GIT, indicating a highly selected bacterial lineage in the family *Sutterellaceae*. In humans, two species have been identified in the genus *Parasutterella* which are represented by the type strain *P. excrementihominis* YIT 11859 and *P. secunda* YIT 12071 (22, 23). Based on *Parasutterella* sequences deposited in the RDP database, *P. excrementihominis* seems to be the predominant species harbored in the human population whereas no sequences representing *P. secunda* has been reported in rodents. These results suggested the diversification of the genus *Parasutterella* that may provide evidence supporting the co-evolution between the host and gut commensal microbes.

We performed a competitive colonization study subsequently using the human and mouse *Parasutterella* strain. Previous experiments indicated that both strains can rapidly and stably colonize the mouse GIT with a complex microbiota when administering the bacterial cells to the bedding material. To avoid any confounding factors with respect to variations in the exposure to bacterial cells, we colonized mice with the strains by oral gavage in this study. The mouse and human strain exhibited a similar ecological fitness when they colonized the mouse GIT separately. When mice were exposed to a mixture of both strains, the mouse strain completely outcompeted the human strain as reflected by undetected human *Parasutterella* sequences in feces. In mouse gut pre-colonized with the mouse strain, the human strain was unable to colonize and persist in the gut. On the contrary, the mouse strain was able to occupy the niche even though the human strain had colonized. The result is consistent with the niche theory that the mouse strain, as a stronger competitor, shows a better fitness in the ecological niche than the human strain (2). In addition, it has been shown in zebrafish that the model bacterium *Aeromona veronii* became a more prolific colonizer through later adaptations by immigration from the environment and interhost transmission (24). One of the identified traits for the improved adaptation was an increased rate of transit into the gut from the environment as the rapid colonization could be an advantage to outcompete other colonizers (25). From this perspective, the mouse strain may have evolved with multiple traits to become a better colonizer in the mouse gut compared to the human strain.

The human and mouse GIT shares similar compartments, however, with some noticeable differences in the structure and physiology. One of the important traits for a microbe to colonize the gut is the adaptation to the gut immune system. Previous experiments using

mouse model colonized with the human strain demonstrated significant increases in the expression of colonic genes interleukin-22 (*IL-22*) and regenerating islet-derived protein 3β (*Reg3β*) (unpublished data), whereas the phenotype was not observed in mouse strain-colonized mice (11). Therefore, the immune tolerance to host-adapted gut commensals may contribute to the success of colonization and persistence. The interaction between strains with the host intestinal immune system need to be further investigated.

The comparative pathway analysis indicated some differences in genomic features between human and mouse *Parasutterella* strains. Human strains contain unique genes encoding enoyl-CoA hydratase, Gamma-glutamyltransferase, and an enzyme interconverts keto- and enol- groups involving in pathways including lipid and other amino acids metabolism as well as xenobiotics biodegradation and metabolism. The annotated gene encoding acetate/propionate kinase was unique in the mouse strain. The acetate/propionate kinase in *E. coli* is one of the major routes of propionate production in anaerobic growth, which generates propionate from L-threonine (26). However, the protein sequence detected in the mouse *Parasutterella* are much shorter than that in *E. coli*. In the description of the type strain *P. excrementihominis* YIT 11859, a trace amount of propionate was detected as an end product of metabolism (22). In our previous study, we did not observe significant changes in propionate or acetate production using High-Performance Liquid Chromatography (HPLC) (11). More investigations incorporating an improved sensitivity in analyzing metabolites as well as functional validation are necessary to fully understand the metabolism of this gut commensal bacterium. These features indicated differences in the genome potential between human and mouse strains, however, a more comprehensive analysis of genomes needs to be performed.

The colonization of the human and mouse strain induced differences in microbial structure, suggesting the strain-specific interaction with local microbial communities. At day 28, no differences in the microbial structure were observed between groups, which was consistent with the successful colonization of the mouse strain in the H group, leading to the removal of the human *Parasutterella*'s impact. Mice colonized with the mouse strain harbored a significantly higher abundance of Clostridiales, whereas the human strain-colonized mice contained a higher proportion of Bacteroidales. The phenotype could be explained by either the mouse strain stimulated the growth of Clostridiales, the major butyrate producer, or the presence of human strain led to a reduction in Clostridiales. It has been shown that neutralizing IL-22 increased the abundance of Clostridiales and the antimicrobial peptide Reg3β titrated Clostridia abundance in its colonic niche (27). We have observed a stimulatory effect of *Reg3β* by the human strain in mouse colon, which could contribute to changes in Clostridia abundance. On the other hand, as a succinate producer, *Parasutterella* could potentially enhance the colonization of Clostridia by boosting the consumption of oxygen by aerobic and facultative anaerobic bacteria (28). With better ecological fitness, the mouse strain may exert stronger interactions with the microbial community than the human strain. Future research focusing on characterizing interactions between *Parasutterella* strains and the host immune system as well as the microbial community will give a clearer explanation of the strain-specific microbial structure.

In addition, as the host adaptation of *L. reuteri* varied in different hosts, including another host for competitive colonization experimental setup will provide more information about the lifestyle of the symbiont, *Parasutterella*. Taken together, the result showed that the

mouse *Parasutterella* was able to not only outcompete the human strain when they were introduced to the mouse GIT at the same time, but also that the mouse strain was able to overcome a pre-colonized human strain. The elevated ecological fitness of the mouse strain raises a question as to what factors contribute to the competitive advantage. Future work to unravel the mechanism by which the *Parasutterella* strain becomes host adapted will help us understand the assembly and development of the gut microbiota.

5.5. References

1. Walter J, Britton RA, Roos S. 2011. Host-microbial symbiosis in the vertebrate gastrointestinal tract and the *Lactobacill*us reuteri paradigm. Proc Natl Acad Sci 108:4645–4652.
2. Vonaesch P, Anderson M, Sansonetti PJ. 2018. Pathogens, microbiome and the host: Emergence of the ecological Koch's postulates. FEMS Microbiol Rev 42:273–292.
3. Walter J, Ley R. 2011. The human gut microbiome: ecology and recent evolutionary changes. Annu Rev Microbiol 65:411–429.
4. Groussin M, Mazel F, Sanders JG, Smillie CS, Lavergne S, Thuiller W, Alm EJ. 2017. Unraveling the processes shaping mammalian gut microbiomes over evolutionary time. Nat Commun 8:14319.
5. Smillie CS, Sauk J, Gevers D, Friedman J, Sung J, Youngster I, Hohmann EL, Staley C, Khoruts A, Sadowsky MJ, Allegretti JR, Smith MB, Xavier RJ, Alm EJ. 2018. Strain tracking reveals the determinants of bacterial engraftment in the human gut following fecal microbiota transplantation. Cell Host Microbe 23:229–240.
6. Martino ME, Joncour P, Leenay R, Gervais H, Shah M, Hughes S, Gillet B, Beisel C, Leulier F. 2018. Bacterial adaptation to the host's diet is a key evolutionary force shaping Drosophila-*Lactobacillus* symbiosis. Cell Host Microbe 24:109–119.e6.
7. Frese SA, Benson AK, Tannock GW, Loach DM, Kim J, Zhang M, Oh PL, Heng

NCK, Patil PB, Juge N, MacKenzie DA, Pearson BM, Lapidus A, Dalin E, Tice H, Goltsman E, Land M, Hauser L, Ivanova N, Kyrpides NC, Walter J. 2011. The evolution of host specialization in the vertebrate gut symbiont *Lactobacillus reuteri*. PLoS Genet 7:e1001314.

8. Frese SA, Mackenzie DA, Peterson DA, Schmaltz R, Fangman T, Zhou Y, Zhang C, Benson AK, Cody LA, Mulholland F. 2013. Molecular characterization of host-specific biofilm formation in a vertebrate gut symbiont. PLoS Genet 9:e1004057.

9. Duar RM, Frese SA, Lin XB, Fernando SC, Burkey TE, Tasseva G, Peterson DA, Blom J, Wenzel CQ, Szymanski CM, Walter J. 2017. Experimental evaluation of host adaptation of *Lactobacillus reuteri* to different vertebrate species. Appl Environ Microbiol 83:e00132–17.

10. Oh PL, Benson AK, Peterson DA, Patil PB, Moriyama EN, Roos S, Walter J, Lantbruksuniversitet S. 2010. Diversification of the gut symbiont *Lactobacillus reuteri* as a result of host-driven evolution. ISME J 4:377–387.

11. Ju T, Kong JY, Stothard P, Willing BP. 2019. Defining the role of *Parasutterella*, a previously uncharacterized member of the core gut microbiota. ISME J 13:1520–1534.

12. Weisburg WG, Barns SM, Pelletier DA, Lane DJ. 1991. 16S ribosomal DNA amplification for phylogenetic study. J Bacteriol 173:697–703.

13. Ju T, Shoblak Y, Gao Y, Yang K, Fouhse J, Finlay BB, So YW, Stothard P, Willing BP. 2017. Initial gut microbial composition as a key factor driving host response to antibiotic treatment, as exemplified by the presence or absence of commensal *Escherichia coli*. Appl Environ Microbiol 83:e01107–17.

14. Wattam AR, Brettin T, Davis JJ, Gerdes S, Kenyon R, Machi D, Mao C, Olson R, Overbeek R, Pusch GD, Shukla MP, Stevens R, Vonstein V, Warren A, Xia F, Yoo H. 2018. Assembly, annotation, and comparative genomics in PATRIC, the all bacterial bioinformatics resource center. p 79–101. *In* Setubal JC, Stoye J, Stadler P (ed), Comparative genomics. 1st ed, Humana Press, New York, NY.

15. Mailhe M, Ricaboni D, Benezech A, Lagier JC, Fournier PE, Raoult D. 2017. 'Duodenibacillus massiliensis' gen. nov., sp. nov., a new species identified in human duodenum. New Microbes New Infect 17:43–44.

16. Tenaillon O, Skurnik D, Picard B, Denamur E. 2010. The population genetics of commensal *Escherichia coli.* Nat Rev Microbiol 8:207–217.

17. Ley RE, Peterson DA, Gordon JI. 2006. Ecological and evolutionary forces shaping microbial diversity in the human intestine. Cell 124:837–848.

18. Amato KR. 2013. Co-evolution in context: The importance of studying gut microbiomes in wild animals. Microbiome Sci Med 1:10–29.

19. Goodrich JK, Waters JL, Poole AC, Sutter JL, Koren O, Blekhman R, Beaumont M, Van Treuren W, Knight R, Bell JT, Spector TD, Clark AG, Ley RE. 2014. Human genetics shape the gut microbiome. Cell 159:789–799.

20. Turnbaugh PJ, Hamady M, Yatsunenko T, Cantarel BL, Duncan A, Ley RE, Sogin ML, Jones WJ, Roe BA, Affourtit JP, Egholm M, Henrissat B, Heath AC, Knight R, Gordon JI. 2009. A core gut microbiome in obese and lean twins. Nature 457:480–484.

21. Rawls JF, Mahowald MA, Ley RE, Gordon JI. 2006. Reciprocal gut microbiota transplants from zebrafish and mice to germ-free recipients reveal host habitat selection. Cell 127:423–433.

22. Nagai F, Morotomi M, Sakon H, Tanaka R. 2009. *Parasutterella excrementihominis* gen. nov., sp. nov., a member of the family *Alcaligenaceae* isolated from human faeces. Int J Syst Evol Microbiol 59:1793–1797.

23. Morotomi M, Nagai F, Watanabe Y. 2011. *Parasutterella secunda* sp. nov., isolated from human faeces and proposal of *Sutterellaceae* fam. nov. in the order Burkholderiales. Int J Syst Evol Microbiol 61:637–643.

24. Robinson CD, Klein HS, Murphy KD, Parthasarathy R, Guillemin K, Bohannan BJM. 2018. Experimental bacterial adaptation to the zebrafish gut reveals a primary role for immigration. PLoS Biol 16:e2006893.

25. Wiles TJ, Jemielita M, Baker RP, Schlomann BH, Logan SL, Ganz J, Melancon E, Eisen JS, Guillemin K, Parthasarathy R. 2016. Host gut motility promotes competitive exclusion within a model intestinal microbiota. PLoS Biol 14:e1002517.

26. Heßlinger C, Fairhurst SA, Sawers G. 1998. Novel keto acid formate-lyase and propionate kinase enzymes are components of an anaerobic pathway in *Escherichia coli* that degrades L-threonine to propionate. Mol Microbiol 27:477–492.

27. Stefka AT, Feehley T, Tripathi P, Qiu J, McCoy K, Mazmanian SK, Tjota MY, Seo G-Y, Cao S, Theriault BR, Antonopoulos DA, Zhou L, Chang EB, Fu Y-X, Nagler CR. 2014. Commensal bacteria protect against food allergen sensitization. Proc Natl Acad Sci 111:13145–13150.

28. Kim YG, Sakamoto K, Seo SU, Pickard JM, Gillilland MG, Pudlo NA, Hoostal M, Li X, Wang TD, Feehley T, Stefka AT, Schmidt TM, Martens EC, Fukuda S, Inohara N, Nagler CR, Núñez G. 2017. Neonatal acquisition of Clostridia species protects against colonization by bacterial pathogens. Science 356:315–319.

Table 5.1. The relative abundance of predominant bacterial phyla and genera in feces collected at day 14

	H	M	HM	SEM	*P* value
Phylum					
p__Actinobacteria	0.05	0.09	0.08	0.01	0.399
p__Bacteroidetes	25.53[a]	6.98[b]	12.82[ab]	2.21	<0.01
p__Firmicutes	57.83[b]	75.39[a]	70.03[ab]	2.17	<0.01
p__Proteobacteria	0.41	2.38	4.31	0.64	0.107
p__Verrucomicrobia	3.92	1.95	2.96	0.43	0.103
p__Tenericutes	11.09[ab]	13.10[a]	8.02[b]	0.90	0.027
Genus					
Actinobacteria					
g__*Adlercreutzia*	0.05	0.09	0.08	0.01	0.399
Bacteroidetes					
f_*S24-7*;g_	25.53[a]	6.96[b]	12.81[ab]	2.21	<0.01
Firmicutes					
g__*Turicibacter*	1.49	3.07	1.61	0.54	0.920
o__Clostridiales;Other;Other	0.03	0.02	0.11	0.02	0.125
o__Clostridiales;f__;g__	29.70[b]	41.27[a]	39.55[ab]	1.94	0.010
f__*Clostridiaceae*;g__	0.50	0.33	0.35	0.06	0.432
g__*Clostridium*	0.18	0.16	0.21	0.04	0.488
g__*Dehalobacterium*	0.09	0.13	0.15	0.01	0.216
f__*Lachnospiraceae*;g__	5.29	5.17	3.69	0.34	0.063
g__*Coprococcus*	0.34	0.53	0.56	0.05	0.129
g__*Dorea*	0.19	0.20	0.23	0.02	0.902
g__*[Ruminococcus]*	0.20	0.34	0.40	0.05	0.147
g__*rc4-4*	1.14	1.28	0.73	0.14	0.472

f__*Peptococcaceae*;g__	0.47	0.32	0.50	0.07	0.326
f__*Ruminococcaceae*;Other	1.43[b]	3.10[a]	2.92[ab]	0.26	0.018
f__*Ruminococcaceae*;g__	6.18	5.68	6.12	0.28	0.973
g__*Oscillospira*	6.53	8.32	6.55	0.36	0.086
g__*Ruminococcus*	1.14	1.06	1.45	0.08	0.196
f__*Erysipelotrichaceae*;g__	0.13	0.07	0.10	0.02	0.588
g__*Coprobacillus*	0.01	0.02	0.03	0.00	0.895
g__*Anaerostipes*	0.23	0.20	0.17	0.03	0.510
g__*Lactobacillus*	2.11	3.26	4.75	0.55	0.266
f__*[Mogibacteriaceae]*;g__	0.26	0.18	0.13	0.02	0.114
g__*Anaerovorax*	0.11	0.15	0.08	0.01	0.229
Proteobacteria					
g__*Parasutterella*	0.41	1.77	4.61	0.64	0.140
Verrucomicrobia					
g__*Akkermansia*	3.93	1.95	2.96	0.43	0.051
Tenericutes					
g__*Anaeroplasma*	10.89	12.84	9.69	0.94	0.115
o__RF39;f__;g__	0.20[ab]	0.47[a]	0.11[b]	0.05	0.019

The relative abundance data (%) were presented as the mean ± pooled standard error of the mean (SEM). The non-parametric Kruskal Wallis test with the Dwass, Steel, Critchlow-Fligner multiple comparisons post-hoc procedure was used to compare the difference between treatment groups. For all treatment, n = 8 - 9. [a,b,c] Means that do not share a common letter are significantly different. $\alpha = 0.05$.

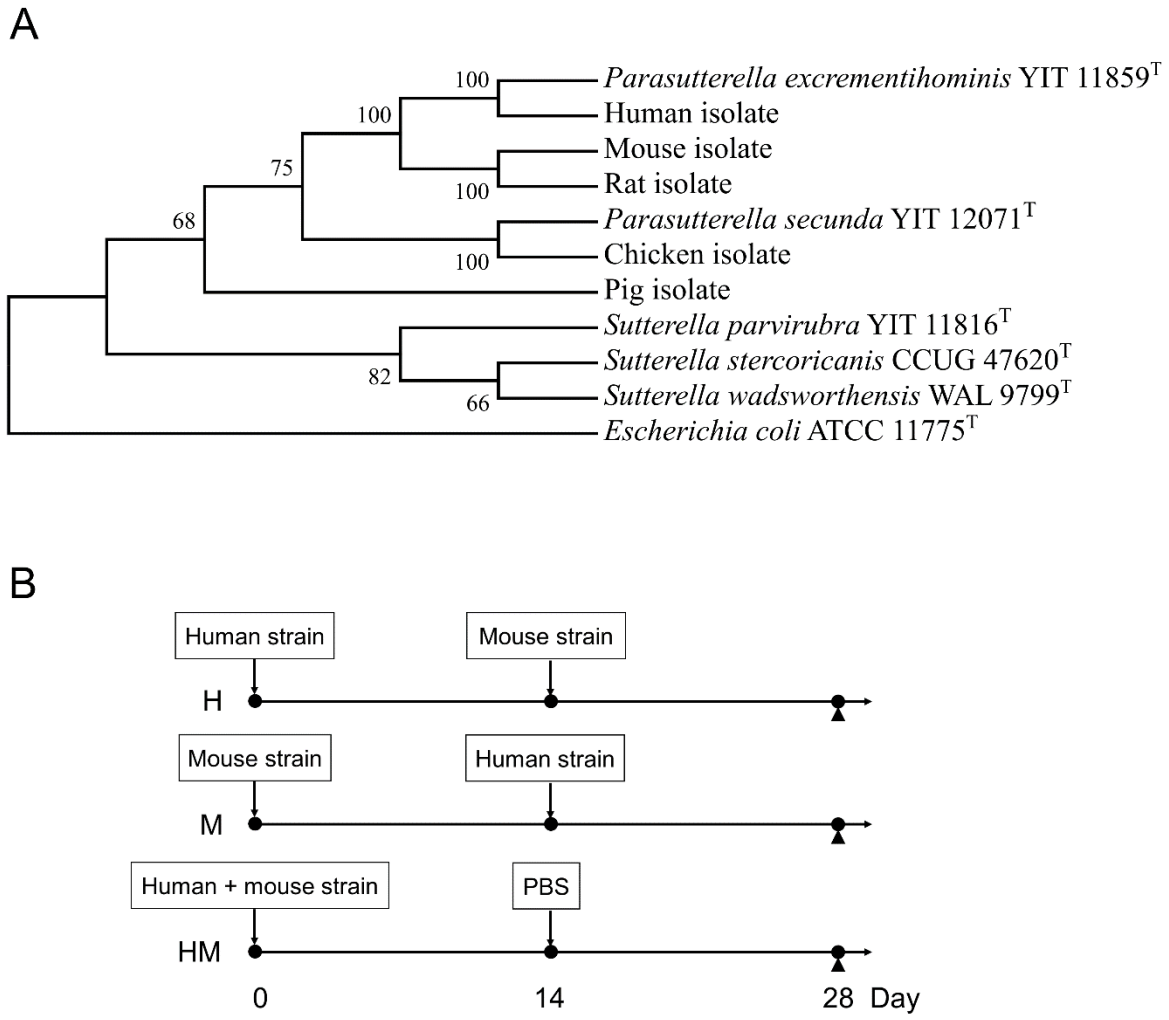

Figure 5.1. A) Maximum likelihood phylogenetic tree based on 16S rRNA gene sequences of *Sutterellaceae* isolates and type strains within the family *Sutterellaceae.* The sequence belonging to *E. coli* type strain was used as the outgroup. For each node bootstrap values (1,000 replicates) greater than 50% are indicated. **B**) The timeline for the competitive colonization study. Swiss-Webster mice, screened and identified as *Parasutterella*-free individuals, were exposed to the human and mouse *Parasutterella* isolate. Fecal samples were collected on day 0, 14, 28. For all treatment, n = 8 - 9.

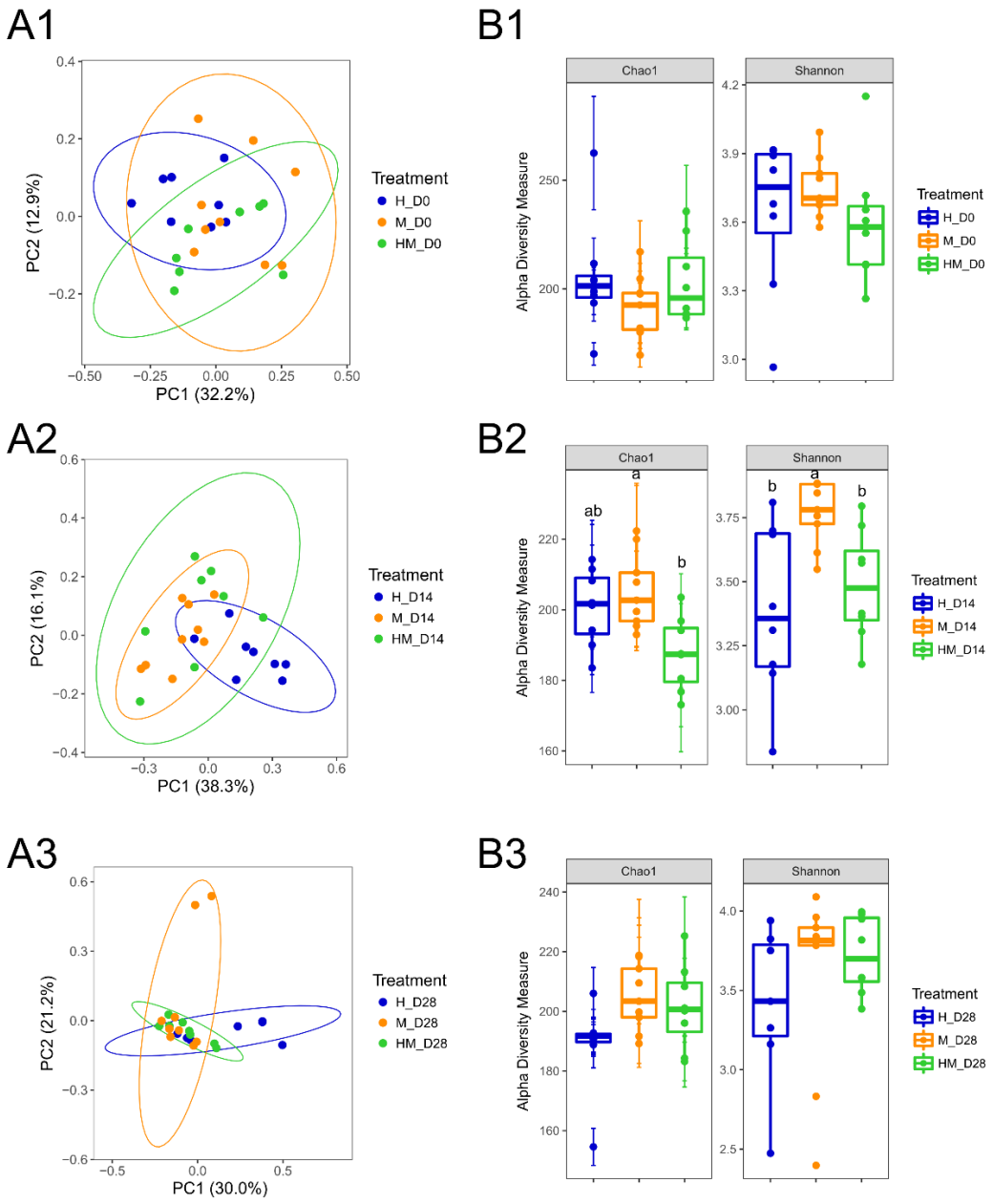

Figure 5.2. Microbial structural analysis of the fecal microbiota collected on day 0, 14, and 28. **A1, A2, A3)** PCoA plots of bacterial communities based on a Bray-Curtis dissimilarity matrix. Colors represent treatments and each point represents an individual mouse. **B1, B2, B3**) Alpha diversity analysis of fecal bacterial communities was reflected by Chao1 and Shannon indexes. For all treatment groups, n = 8 - 9. Data are shown as mean ± SEM. [a,b,c] Means that do not share a common letter are significantly different. $\alpha = 0.05$.

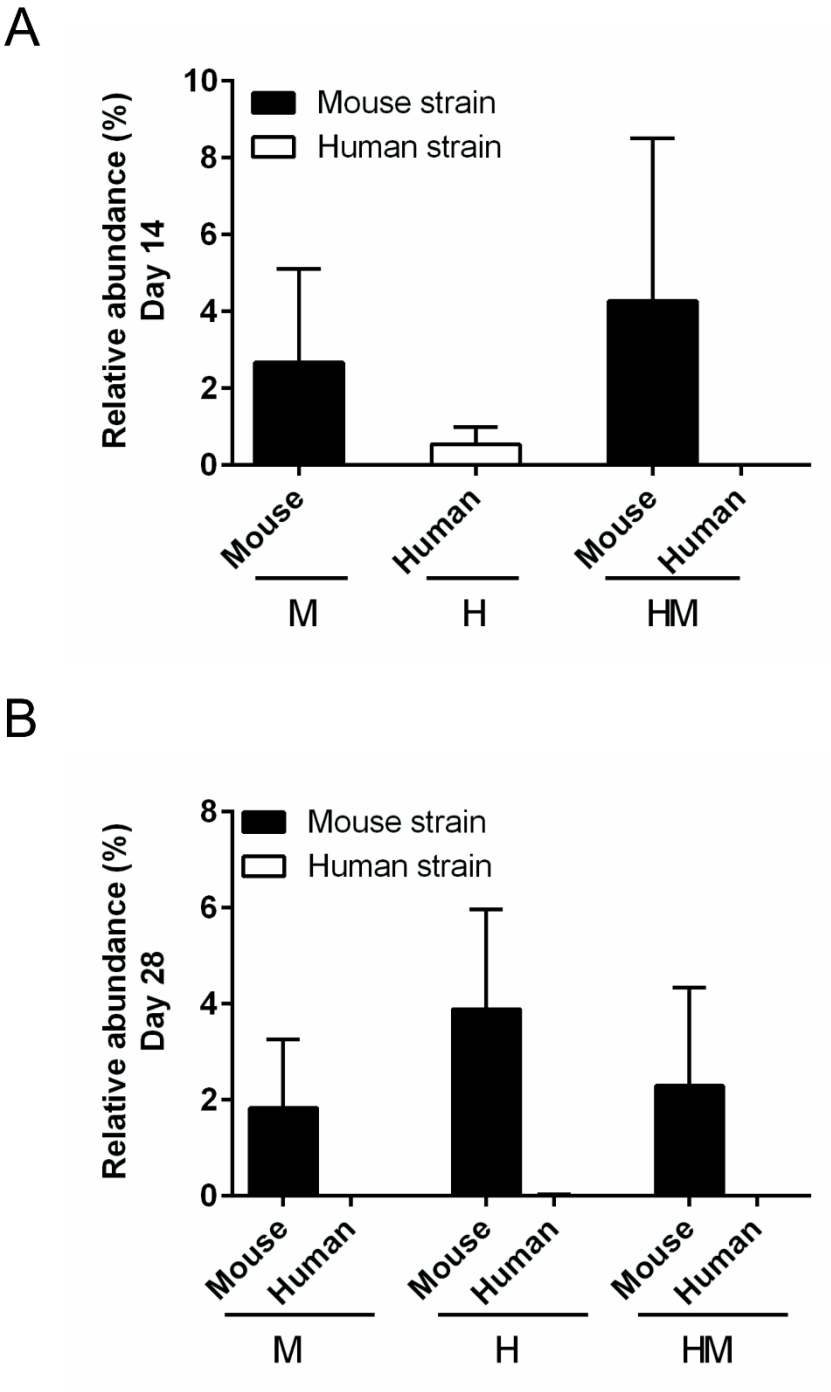

Figure 5.3. The relative abundance of the mouse and human *Parasutterella* isolate in feces collected at **A**) day 14 and **B**) day 28. Data are shown as mean ± SD. For all treatment group, n = 8 - 9.

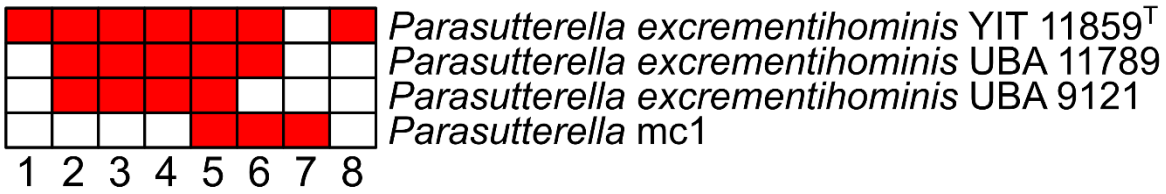

Figure 5.4. Comparative pathway analysis based on the whole genome annotation of *Parasutterella* species. No. 1 to 8 represent genes encoding following enzymes: 1. Isomerases, 2. Enoyl-CoA hydratase, 3. Gamma-glutamyltransferase, 4. Enzyme interconverting keto- and enol- groups, 5. Hexosyltransferases, 6. Enzyme transferring groups other than amino-acyl groups, 7. Acetate kinase, 8. Phosphoric diester hydrolases. The red color indicated the presence of the gene whereas the white color represented the absence of the gene.

6. CHAPTER 6: GENERAL DISCUSSION

6.1. Defining a healthy gut microbiome

The definition of a healthy gut microbiome is beginning to emerge with our increased understanding of the structure and function of the gut microbiota and its role in shaping host physiology (1, 2). From a microbial ecological perspective, the stability of the gut microbial community, which refers to the ability to resist stress or perturbation (resistance) and to return to an equilibrium state afterwards (resilience), can be considered as a functional property to describe the health of the gut microbiome (3, 4). The concept of stability reveals the key feature of healthy states of the gut microbiome, however, the considerable variation in microbial composition between individuals makes it difficult to define the healthy gut microbiome by an idealized set of specific microbes (5, 6). An alternative hypothesis is to define a healthy gut microbiome by a complement of metabolic and other functional capabilities within the gastrointestinal tract (GIT) that promote a stable host-associated ecology rather than specific microbial populations (2). This healthy "functional core" concept is based on the conserved metabolic pathways compared to the varied taxonomic profile of the gut microbiome among individuals (1). Given that the inclusion of *Parasutterella* did not result in any new detectable metabolites in the absence of its colonization supports the concept of functional redundancy across species in the GIT.

Nevertheless, the set of functional capabilities indicating a healthy gut microbiome remains to be fully defined (1, 7). Culture-independent techniques have provided an important tool to explore functional pathways of the gut microbiome, however, there is a substantial proportion of microbial gene families in the gut microbial metagenome needs to

be functionally characterized (2). We need more investigations into microbial cultivation for biological characterization and experimental validation to improve interpretations of microbiome profiling, which will ultimately help define the core function of the healthy gut microbiome. As exemplified by the approach adopted for investigating physiological characterizations of *Parasutterella*, microbial cultivation, in combination with high-throughput culture-independent assays broaden our knowledge of the biology and lifestyle of this previously uncharacterized bacterial genus. In addition, currently, while many studies in gut microbiome field focus on a pathogenic lifestyle of specified gut microbes, such as *E. coli*, investigating the role of these microbes as a member of the gut commensal community will help to demonstrate the ecological and evolutionary forces shape the population (8).

6.2. Pursuing causation and mechanism in gut microbiome research

Changes in gut microbial communities have been widely associated with host health outcomes, including beneficial and deleterious, illustrating the important role the gut microbiome plays in impacting host physiology (9). However, it is difficult to conclude whether the altered gut microbial composition causes physiological changes in the host or the altered microbial population is the consequence reflecting a changed ecological niche (10). Demonstrating the direct causal relationship is necessary to advance the current correlative research.

Indeed, a growing number of studies have pioneered research on unraveling mechanisms by which gut microbes impact host health outcomes using a range of experimental approaches (11). Using gnotobiotic colonization of germ-free mice with each of 53 single microbial strains derived from the human gut demonstrated specialized

immunomodulatory effects exerted by phylogenetically diverse human gut microbes (12). There are, however, substantial limitations to use the monocolonized mouse model. For example, this is evidenced by the weak ability of both the human and mouse *Parasutterella* strain to monocolonize germ-free mice, as well as different immunostimulatory properties of these two strains shown in the cell culture system (unpublished data). Regardless of the limitation, such studies provide a foundation for investigating interactions between individual gut microbe and the host immune system. Another study colonized germ-free mice with subsets of randomly selected combinations of gut microbes isolated from a human donor identified certain bacterial strains modulating host physiology such as adiposity and immunity (13). The study provided a platform to systematically identify the contribution of the gut microbiota to host health outcomes, though the engraftment efficacy of human strains may vary (14).

In our studies, we successfully established a well-controlled mouse model by adding a single mouse bacterial strain to a complex gut microbial community that did not harbor the strain. By comparing outcomes between gut communities that differ only in the presence of the single bacterial strain, the effect of the microorganism can be tested as a member of a complex community. *Parasutterella* mc1 and *E. coli* strain used as model microorganisms in studies can rapidly and stably colonize the mouse GIT with minimal impact on the microbial community structure. The capability of colonizing the mouse gut with a mature microbial ecosystem, especially by *Parasutterella* as a strict anaerobe with largely unreactive characteristics *in vitro*, indicates that these commensal bacteria fill a unique ecological niche in the gut. This approach can be used, for example, to further investigate the role of these two

commensal bacteria with different perturbations or test other gut commensal microbes of interest.

Advantages of minimizing interindividual variations in the baseline gut microbiota using the mouse model could facilitate research unlocking mechanisms of host-microbe interactions. A study where human-derived *Bifidobacterium longum* was administered to human subjects, demonstrated that orally administering *B. longum* AH1206 led to stable long-term persistence in the GIT of 30% of individuals. The different efficacy of engraftment was attributed to the variation in resident *B. longum* and microbial function of utilizing specific carbohydrates, which limited niche opportunities for probiotics to colonize (15). This suggests that using this approach may not work for all bacteria and in all contexts. However, the mouse model allows better control variations in the pre-treatment gut microbiome, providing a strong tool for mechanistic research. The mechanism of the interaction between the host and gut commensal microbes can further provide predictions of the colonization and persistence of these commensal microbes in different hosts, and ultimately advance the application of these symbionts. In addition, mouse-derived microbes were preferred to be used in this mouse model representing natural colonization. However, illustrating the shared microbial function between mice and other hosts including human gut microbiota can overcome the limitation of using mouse strains.

6.3. Focusing on the commensal lifestyle of gut microbes

Evidence has revealed the enrichment of *E. coli* and *Parasutterella* in the gut under certain conditions such as intestinal inflammation and microbiota dysbiosis as discussed in Chapter 1. However, based on correlations, we cannot conclude if these bacterial genera

initiate the physiological process or whether the enrichment is due to their ability to outcompete other commensals to thrive in the inflamed gut by utilizing byproducts of inflammation. As members of gut commensal microbiota, *Parasutterella* and *E. coli* represent a relatively low abundance (below 1% of the total bacterial community) in the specific-pathogen-free (SPF) C57BL/6J mice fed a standard chow diet (16, 17). The fluctuation in populations of *E. coli* and *Parasutterella* indicates that these two bacterial genera have co-evolved with the host to occupy the ecological niche in the gut. Specifically, the genus *Parasutterella* performed as a fastidious microorganism and exhibited an asaccharolytic characteristic, however, it can be easily transmitted to the host by a single environmental exposure, suggesting a unique surviving approach of the bacterial genus. The host adaptation of the mouse *Parasutterella* strain in the intestinal colonization provided further evidence suggesting the co-evolution of the commensal bacterium and the host. *E. coli*, as the predominant *Enterobacteriaceae* in the gut, shows limited impact on host physiology as a commensal bacterium. However, the metronidazole treatment significantly reduced the gut microbial diversity, allowing for blooms of *E. coli* (16, 18). With respect to the development of obesity and type 2 diabetes (T2D), the presence of *E. coli* induced glucose intolerance and increased adiposity only in mice on a high-fat diet (HFD) regime. Collectively, it is likely that *E. coli* as a member of the gut commensal microbiota performs as a reservoir of microbial molecules such as the Lipopolysaccharides (LPS), which can contribute to inflammation upon the disruption of the intestinal barrier. The involvement of the genus *Parasutterella* in the inflammatory state remains to be clearly elucidated.

The microbiome development in early life provides a different context in which *E. coli* and *Parasutterella* may be actively involved in immune education and gut microbiota establishment. It is possible that the host would have responded differently to *Parasutterella* and *E. coli* differently if they had been exposed in early life. This is an avenue of possible future exploration. Collectively, understanding the commensal lifestyle will help guide efforts to develop strategies to maintain the intestinal homeostasis and beneficial interactions between the host and gut commensal microbes.

6.4. Integration of multi-omics technologies for microbiome research

Over the past decade, the technological development in the field of next-generation sequencing, metabolomics, and bioinformatics has greatly advanced our understanding of the role gut microbiota plays in health and disease. The integration of multiple approaches including culturomics, metagenomic sequencing, metatranscriptomics, and metabolomics provides an opportunity to identify and characterize the biology and function of gut commensal microbes that have remained poorly characterized (1, 19). In the study defining the role of *Parasutterella* in the gut, we combined the untargeted and targeted metabolomic analysis to investigate the effect of *Parasutterella* colonization on gut metabolite profile as intestinal metabolites participate in a variety of physiological processes. Intestinal metabolites are the result of both microbial and host-associated factors, providing great potential to link microbial community and host metabolism and immunity (19). Uncovering the knowledge of the function of a vast number of microbial-derived metabolites in physiology and pathophysiology is a work in progress. As the field of metabolomics is still maturing, much

work remains to be done to explore the role of metabolites produced by the gut microbiota and the relevance with host health outcomes (19).

In my study, I aimed to detect as many metabolites as possible by using multiple chromatographic conditions. However, the assignments/identifications of features in the untargeted mass spectrometry-based metabolomic analysis remain challenging due to incomplete metabolite databases and a lack of standard reference materials (20). I was able to identify certain microbial-derived metabolites, although a considerable proportion of detected features are yet to be characterized. Among the confidently identified metabolites including aromatic amino acids, bilirubin, purine, and bile acid derivatives, the relationship between the altered bile acid profile resulted from the presence of *Parasutterella* and host physiology was further demonstrated. The rest of detected metabolites changed by the colonization of *Parasutterella* need to be further validated. Nevertheless, to date many metabolites produced by the gut microbiota remain poorly explored. For example, the bioactivity of bilirubin metabolites, which were impacted by *Parasutterella* colonization, have not been explored. Integrating blood metabolomic analysis in the future will help to investigate the impact of *Parasutterella* presence on systemic metabolism and function. Furthermore, as discussed in Chapter 1, it has been suggested that *Parasutterella* might exert a protective role in liver injury, therefore, it will be worthwhile to investigate the mechanism by which *Parasutterella* reduces inflammation and improves liver function. Regarding the influence of *Parasutterella* on bile acid metabolism, the genus *Parasutterella* may modulate liver health through bile acid metabolisms impacting the gut-liver axis.

6.5. Translating research into practical application

Mechanistic studies in gut microbiome research could lead to the development of practical applications to maintain proper gut function and host health (11). Manipulating the gut microbial population and function helps to maintain beneficial host-microbe interactions. As common inhabitants of the GIT, *Parasutterella* and *E. coli* have been found in humans and a variety of animals. Understanding the biology of these genera as gut commensals will facilitate the development of strategies for manipulating the population by different perturbations such as diet and lifestyle. For instance, blooms of *E. coli* and the resulting inflammatory response after antibiotic treatment created a compelling argument for personalized medication based on individual variations in the gut microbiota. With respect to the impact of *E. coli* colonization on the development of obesity and metabolic syndrome on a HFD regime, the approach can be developed targeting a reduction of *E. coli* abundances such as dietary intervention or phage therapy, to improve glycemic control and prevent obesity as well as metabolic syndrome. Furthermore, the role of *Parasutterella* in influencing gut metabolite profile and related pathways may potentially exert beneficial impact under certain circumstances such as *Clostridium difficile* infection (CDI) and liver injury. However, the question remains if there is a strain-specific phenotype or whether these traits are consistent in human or other animals, which needs further validation.

6.6. Limitations of the thesis

Studies included in the thesis are based on a mouse model system in the context of a complex microbial community. Compared to the germ-free mouse model, the model system provides a relatively natural tool to investigate the impact of two model microorganisms,

Parasutterella and *E. coli*, on the gut microbial community and host physiology. The study characterized the role of commensal *E. coli* in the host response to antibiotic treatment or dietary interventions. The biology, lifestyle, and interactions with the host of a previously uncharacterized bacterial genus *Parasutterella* have been investigated. Although findings supported the hypothesis that the presence of commensal bacterial species drives changes in host physiology, there are still some limitations that should be acknowledged.

In these studies, functional characteristics of the gut microbiota remain to be investigated. The taxonomic profiling by 16S rRNA gene amplicon sequencing method gave limited information about the microbial function. Although the metabolomic analysis demonstrated the impact of the presence of a single bacterium on intestinal metabolite pool and host physiology, changes in metabolomic profile may be a direct effect of the added bacterium or an indirect effect from microbe-microbe interactions. Incorporating results from metagenomic sequencing approach allows functional analyses of the gut microbiota, which will help identify the core microbial trait. Profiling metabolites in intestinal contents showed the impact of *Parasutterella* on the ecosystem directly, however, further investigation integrating circulating metabolites should be included to reflect the regulation of the bacterium on host systemic metabolism.

The presence of the commensal *E. coli* strain contributed to the glucose metabolism in the context of HFD intervention, however, the mechanisms have not been fully elucidated in the current study. Previous research has indicated that impaired glucose metabolism resulted from the combination of altered gut epithelial cell physiology by HFD treatment and increased translocations of microbial ligands (21). In the current study, changes in intestinal

barrier function need to be further analyzed. To link the commensal *E. coli*, LPS, and obese phenotypes, LPS deficient mutants of *E. coli* species or TLR4$^{-/-}$ mouse model will help unravel causal relationships.

Chapter 5 presented a set of preliminary data regarding the host specificity of *Parasutterella* in intestinal colonization. The study has raised some interesting questions about microbial traits in colonizing ecological niches. *P. secunda* has not been detected in rodents whereas most of the bacterial prevalence has been reported in human studies, indicating a unique environmental requirement for the species, which remains to be characterized. The mouse strain was able to outcompete and overcome human *P. excrementihominis* strain in colonizing the mouse gut, suggesting the host adaptation of the mouse strain. However, the mechanism of the host specificity need to be studied with respect to differences in functional traits between bacterial species. Also, impacts of different species on the gut microbial community and host immune response need to be validated. Approaches including the whole genome sequencing, metagenomic sequencing, and the analysis of host immune responses will provide a fundamental basis for understanding the lifestyle and function of the genus *Parasutterella*.

6.7. Future directions

In the current study, we successfully established a well-controlled and tractable mouse model to investigate the biology and function of gut commensal bacteria, *Parasutterella* and *E. coli*, providing insights into how these bacterial genera may contribute to host health. The model will facilitate further studies of exploring the causal mechanism of alterations in microbial population and host responses. It has been suggested that species that can provide

key roles in metabolism, signaling, immunomodulation, and other aspects in the gut microbial community may be more temporally stable than other species (2). The genus *Parasutterella* is able to persist in the gut environment, contributing to the assembly of the gut microbiome. The fluctuation of *Parasutterella* abundance in inflammation as discussed in Chapter 1 highlighted the potential immunomodulatory role of *Parasutterella* that has not been well demonstrated. It is interesting to study whether the LPS produced by *Parasutterella* has a unique function potential in interacting with the host immune system. In addition, in the current study, the taxonomic profiling performed by16S rRNA amplicon sequencing has limitations to reveal functional and strain-levels changes in the microbial community. Coupling the functional analysis using metagenomic sequencing approach and metabolomic analysis will provide a more comprehensive approach demonstrating dynamic changes in microbial activity and function resulted from *Parasutterella* colonization. Furthermore, the role of *Parasutterella* in the metabolism of aromatic amino acids, bilirubin, and purine can be a direction for future research.

It is intriguing that *E. coli* colonization led to glucose intolerance and increased adiposity with a moderate increase in *E. coli* abundance after HFD treatment even though it represented less than 0.1% of the bacterial community. It will be worthwhile to investigate the mechanism driving the impaired glucose metabolism by *E. coli*, without a drastic enrichment, in combination with HFD particularly regarding the gut barrier function. We cannot rule out strain-level variations as the genomic potential may vary among commensal *E. coli* species. In mice treated with metronidazole, we colonized the mouse gut by different commensal *E. coli* strains, indicating that both *E. coli* strains isolated from mouse feces

induced a similar host response. Future studies considering a more diverse commensal *E. coli* strains can be conducted to exploit these phenotypes. More importantly, studying the difference in the function of commensal *E. coli* strains provides a tool for developing therapeutics targeting specified strains due to a high diversity within the genus *E. coli*. It is possible that certain *E. coli* strains do not exert the same stimulatory effects on host metabolism such as glucose intolerance, or some strains can even provide protective effects. Therefore, research focusing on genomic and biological features at low taxonomic levels may help identify specified traits of microbial species, define the feature of the ecosystem within which the microbial species are included, and ultimately support beneficial host-microbe interactions.

6.8. References

1. Bäckhed F, Fraser CM, Ringel Y, Sanders ME, Sartor RB, Sherman PM, Versalovic J, Young V, Finlay BB. 2012. Defining a healthy human gut microbiome: Current concepts, future directions, and clinical applications. Cell Host Microbe 12:611–622.
2. Lloyd-Price J, Abu-Ali G, Huttenhower C. 2016. The healthy human microbiome. Genome Med 8:51.
3. Shade A, Peter H, Allison SD, Baho DL, Berga M, Bürgmann H, Huber DH, Langenheder S, Lennon JT, Martiny JBH, Matulich KL, Schmidt TM, Handelsman J. 2012. Fundamentals of microbial community resistance and resilience. Front Microbiol 3:417–436.
4. Lozupone CA, Stombaugh JI, Gordon JI, Jansson JK, Knight R. 2012. Diversity, stability and resilience of the human gut microbiota. Nature 489:220–230.
5. Xu Z, Malmer D, Langille MGI, Way SF, Knight R. 2014. Which is more important for classifying microbial communities: Who's there or what they can do? ISME J 8:2357–2359.

6. Shafquat A, Joice R, Simmons SL, Huttenhower C. 2014. Functional and phylogenetic assembly of microbial communities in the human microbiome. Trends Microbiol 22:261–266.
7. Nicholson JK, Holmes E, Kinross J, Burcelin R, Gibson G, Jia W, Pettersson S. 2012. Host-gut microbiota metabolic interactions. Science 336:1262–1267.
8. Tenaillon O, Skurnik D, Picard B, Denamur E. 2010. The population genetics of commensal *Escherichia coli*. Nat Rev Microbiol 8:207–217.
9. Cani PD. 2018. Human gut microbiome: hopes, threats and promises. Gut 67:1716–1725.
10. Meijnikman AS, Gerdes VE, Nieuwdorp M, Herrema H. 2018. Evaluating causality of gut microbiota in obesity and diabetes in humans. Endocr Rev 39:133–153.
11. Fischbach MA. 2018. Microbiome: focus on causation and mechanism. Cell 174:785–790.
12. Geva-Zatorsky N, Sefik E, Kua L, Pasman L, Tan TG, Ortiz-Lopez A, Yanortsang TB, Yang L, Jupp R, Mathis D, Benoist C, Kasper DL. 2017. Mining the human gut microbiota for immunomodulatory organisms. Cell 168:928–943.
13. Faith JJ, Ahern PP, Ridaura VK, Cheng J, Gordon JI. 2014. Identifying gut microbe-host phenotype relationships using combinatorial communities in gnotobiotic mice. Sci Transl Med 6:220ra11.
14. Staley C, Kaiser T, Beura LK, Hamilton MJ, Weingarden AR, Bobr A, Kang J, Masopust D, Sadowsky MJ, Khoruts A. 2017. Stable engraftment of human microbiota into mice with a single oral gavage following antibiotic conditioning. Microbiome 5:87.
15. Maldonado-Gómez MX, Martínez I, Bottacini F, O'Callaghan A, Ventura M, van Sinderen D, Hillmann B, Vangay P, Knights D, Hutkins RW, Walter J. 2016. Stable engraftment of *Bifidobacterium longum* AH1206 in the human gut depends on individualized features of the resident microbiome. Cell Host Microbe. 20:515–526.
16. Ju T, Shoblak Y, Gao Y, Yang K, Fouhse J, Finlay BB, So YW, Stothard P, Willing BP. 2017. Initial gut microbial composition as a key factor driving host response to

antibiotic treatment, as exemplified by the presence or absence of commensal *Escherichia coli*. Appl Environ Microbiol 83:e01107–17.

17. Ju T, Kong JY, Stothard P, Willing BP. 2019. Defining the role of *Parasutterella*, a previously uncharacterized member of the core gut microbiota. ISME J 13:1520–1534.
18. Zeng MY, Inohara N, Nuñez G. 2017. Mechanisms of inflammation-driven bacterial dysbiosis in the gut. Mucosal Immunol 10:18–26.
19. Sonnenburg JL, Bäckhed F. 2016. Diet-microbiota interactions as moderators of human metabolism. Nature 535:56–64.
20. Schrimpe-Rutledge AC, Codreanu SG, Sherrod SD, McLean JA. 2016. Untargeted metabolomics strategies-challenges and emerging directions. J Am Soc Mass Spectrom 27:1897–1905.
21. Thaiss CA, Levy M, Grosheva I, Zheng D, Soffer E, Blacher E, Braverman S, Tengeler AC, Barak O, Elazar M, Ben-Zeev R, Lehavi-Regev D, Katz MN, Pevsner-Fischer M, Gertler A, Halpern Z, Harmelin A, Aamar S, Serradas P, Grosfeld A, Shapiro H, Geiger B, Elinav E. 2018. Hyperglycemia drives intestinal barrier dysfunction and risk for enteric infection. Science 359:1376–1383.

BIBLIOGRAPHY

Abraham C, Medzhitov R. 2011. Interactions between the host innate immune system and microbes in inflammatory bowel disease. Gastroenterology 140:1729–1737.

Adeolu M, Alnajar S, Naushad S, Gupta RS. 2016. Genome-based phylogeny and taxonomy of the 'Enterobacteriales': Proposal for enterobacterales ord. nov. divided into the families *Enterobacteriaceae*, *Erwiniaceae* fam. nov., *Pectobacteriaceae* fam. nov., *Yersiniaceae* fam. nov., *Hafniaceae* fam. nov., Morgane. Int J Syst Evol Microbiol 66:5575.

Aevarsson A, Seger K, Turley S, Sokatch JR, Hol WG. 1999. Crystal structure of 2-oxoisovalerate and dehydrogenase and the architecture of 2-oxo acid dehydrogenase multienzyme complexes. Nat Struct Biol 6:785–792.

Aguirre M, Jonkers DMAE, Troost FJ, Roeselers G, Venema K. 2014. *In vitro* characterization of the impact of different substrates on metabolite production, energy extraction and composition of gut microbiota from lean and obese subjects. PLoS One 9:e113864.

Ahrén B, Scheurink AJW. 1998. Marked hyperleptinemia after high-fat diet associated with severe glucose intolerance in mice. Eur J Endocrinol 139:461–467.

Albrecht CF, Chorn DJ, Wessels PL. 1989. Detection of 3-hydroxy-3-methyloxindole in human urine. Life Sci 45:1119–1126.

Alonso A, Marsal S, Julia A. 2015. Analytical methods in untargeted metabolomics: state of the art in 2015. Front Bioeng Biotechnol 3:23–43.

Amar J, Burcelin R, Ruidavets JB, Cani PD, Fauvel J, Alessi MC, Chamontin B, Ferriéres J. 2008. Energy intake is associated with endotoxemia in apparently healthy men. Am J Clin Nutr 87:1219–1223.

Amarasingham CR, Davis BD. 1965. Regulation of alpha-ketoglutarate dehydrogenase formation in *Escherichia coli*. J Biol Chem 240:3664–3668.

Amato KR. 2013. Co-evolution in context: The importance of studying gut microbiomes in wild animals. Microbiome Sci Med 1:10–29.

An C, Kuda T, Yazaki T, Takahashi H, Kimura B. 2013. Flx pyrosequencing analysis of the effects of the brown-algal fermentable polysaccharides alginate and laminaran on rat cecal microbiotas. Appl Environ Microbiol 79:860–866.

An C, Kuda T, Yazaki T, Takahashi H, Kimura B. 2014. Caecal fermentation, putrefaction and microbiotas in rats fed milk casein, soy protein or fish meal. Appl Microbiol Biotechnol 98:2779–2787.

Antranikian G, Giffhorn F. 1987. Citrate metabolism in anaerobic bacteria. FEMS Microbiol Lett 46:175–198.

Arnold GL, Beaves MR, Pryjdun VO, Mook WJ. 2002. Preliminary study of ciprofloxacin in active Crohn's disease. Inflamm Bowel Dis 8:10–15.

Aron-Wisnewsky J, Prifti E, Belda E, Ichou F, Kayser BD, Dao MC, Verger EO, Hedjazi L, Bouillot JL, Chevallier JM, Pons N, Le Chatelier E, Levenez F, Ehrlich SD,

Dore J, Zucker JD, Clément K. 2019. Major microbiota dysbiosis in severe obesity: fate after bariatric surgery. Gut. 68:70–82.

Avershina E, Lundgård K, Sekelja M, Dotterud C, Storrø O, Øien T, Johnsen R, Rudi K. 2016. Transition from infant- to adult-like gut microbiota. Environ Microbiol 18:2226–2236.

Aziz RK, Bartels D, Best AA, DeJongh M, Disz T, Edwards RA, Formsma K, Gerdes S, Glass EM, Kubal M, Meyer F, Olsen GJ, Olson R, Osterman AL, Overbeek RA, McNeil LK, Paarmann D, Paczian T, Parrello B, Pusch GD, Reich C, Stevens R, Vassieva O, Vonstein V, Wilke A, Zagnitko O. 2008. The RAST Server: rapid annotations using subsystems technology. BMC Genomics 9:75.

Bäckhed F, Fraser CM, Ringel Y, Sanders ME, Sartor RB, Sherman PM, Versalovic J, Young V, Finlay BB. 2012. Defining a healthy human gut microbiome: Current concepts, future directions, and clinical applications. Cell Host Microbe 12:611–622.

Bäckhed F, Manchester JK, Semenkovich CF, Gordon JI. 2007. Mechanisms underlying the resistance to diet-induced obesity in germ-free mice. Proc Natl Acad Sci 104:979–984.

Bäckhed F, Roswall J, Peng Y, Feng Q, Jia H, Kovatcheva-Datchary P, Li Y, Xia Y, Xie H, Zhong H, Khan MT, Zhang J, Li J, Xiao L, Al-Aama J, Zhang D, Lee YS, Kotowska D, Colding C, Tremaroli V, Yin Y, Bergman S, Xu X, Madsen L, Kristiansen K, Dahlgren J, Wang J. 2015. Dynamics and stabilization of the human gut microbiome during the first year of life. Cell Host Microbe 17:690–703.

Bahrami B, Macfarlane S, Macfarlane GT. 2011. Induction of cytokine formation by human intestinal bacteria in gut epithelial cell lines. J Appl Microbiol 110:353–363.

Bankevich A, Nurk S, Antipov D, Gurevich AA., Dvorkin M, Kulikov AS, Lesin VM, Nikolenko SI, Pham S, Prjibelski AD, Pyshkin AV, Sirotkin AV, Vyahhi N, Tesler G, Alekseyev MA, Pevzner PA. 2012. SPAdes: a new genome assembly algorithm and its applications to single-cell sequencing. J Comput Biol 19:455–477.

Bansal T, Alaniz RC, Wood TK, Jayaraman A. 2010. The bacterial signal indole increases epithelial-cell tight-junction resistance and attenuates indicators of inflammation. Proc Natl Acad Sci. USA 107:228–233.

Bartley JM, Zhou X, Kuchel GA, Weinstock GM, Haynes L. 2017. Impact of age, caloric restriction, and influenza infection on mouse gut microbiome: an exploratory study of the role of age-related microbiome changes on influenza responses. Front Immunol 8:1164.

Baughn AD, Malamy MH. 2004. The strict anaerobe *Bacteroides fragilis* grows in and benefits from nanomolar concentrations of oxygen. Nature 427:441–444.

Bermudez-Brito M, Plaza-Díaz J, Fontana L, Muñoz-Quezada S, Gil A. 2013. *In vitro* cell and tissue models for studying host–microbe interactions: a review. Br J Nutr 109:S27–S34.

Biggs MB, Medlock GL, Moutinho TJ, Lees HJ, Swann JR, Kolling GL, Papin JA. 2017. Systems-level metabolism of the altered Schaedler flora, a complete gut microbiota. ISME J 11:426–438.

Bindels LB, Neyrinck AM, Claus SP, Le Roy CI, Grangette C, Pot B, Martinez I, Walter J, Cani PD, Delzenne NM. 2015. Synbiotic approach restores intestinal homeostasis and prolongs survival in leukaemic mice with cachexia. ISME J 10:1456–1470.

Bjerrum L, Engberg RM, Leser TD, Jensen BB, Finster K, Pedersen K. 2006. Microbial community composition of the ileum and cecum of broiler chickens as revealed by molecular and culture-based techniques. Poult Sci 85:1151–1164.

Blasco-Baque V, Coupé B, Fabre A, Handgraaf S, Gourdy P, Arnal JF, Courtney M, Schuster-Klein C, Guardiola B, Tercé F, Burcelin R, Serino M. 2017. Associations between hepatic miRNA expression, liver triacylglycerols and gut microbiota during metabolic adaptation to high-fat diet in mice. Diabetologia 60:690–700.

Bologna FP, Andreo CS, Drincovich MF. 2007. *Escherichia coli* malic enzymes: two isoforms with substantial differences in kinetic properties, metabolic regulation, and structure. J Bacteriol 189:5937–5946.

Boutagy NE, McMillan RP, Frisard MI, Hulver MW. 2016. Metabolic endotoxemia with obesity: is it real and is it relevant? Biochimie 124:11–20.

Brahma S, Martínez I, Walter J, Clarke J, Gonzalez T, Menon R, Rose DJ. 2017. Impact of dietary pattern of the fecal donor on *in vitro* fermentation properties of whole grains and brans. J Funct Foods 29:281–289.

Brandl K, Plitas G, Schnabl B, DeMatteo RP, Pamer EG. 2007. MyD88-mediated signals induce the bactericidal lectin RegIIIγ and protect mice against intestinal *Listeria monocytogenes* infection. J Exp Med 204:1891–1900.

Brugiroux S, Beutler M, Pfann C, Garzetti D, Ruscheweyh HJ, Ring D, Diehl M, Herp S, Lötscher Y, Hussain S, Bunk B, Pukall R, Huson DH, Münch PC, McHardy AC, McCoy KD, MacPherson AJ, Loy A, Clavel T, Berry D, Stecher B. 2016. Genome-guided design of a defined mouse microbiota that confers colonization resistance against *Salmonella enterica* serovar Typhimurium. Nat Microbiol 2:16215.

Buck D, Spencer ME, Guest JR. 1985. Primary structure of the succinyl-CoA synthetase of *Escherichia coli*. Biochemistry 24:6245–6252.

Buffie CG, Jarchum I, Equinda M, Lipuma L, Gobourne A, Viale A, Ubeda C, Xavier J, Pamer EG. 2012. Profound alterations of intestinal microbiota following a single dose of clindamycin results in sustained susceptibility to *Clostridium difficile*-induced colitis. Infect Immun 80:62–73.

Caesar R, Reigstad CS, Bäckhed HK, Reinhardt C, Ketonen M, Lundén GÖ, Cani PD, Bäckhed F. 2012. Gut-derived lipopolysaccharide augments adipose macrophage accumulation but is not essential for impaired glucose or insulin tolerance in mice. Gut 12:1701–1707.

Caesar R, Tremaroli V, Kovatcheva-Datchary P, Cani PD, Bäckhed F. 2015. Crosstalk between gut microbiota and dietary lipids aggravates WAT inflammation through TLR signaling. Cell Metab 22:658–668.

Campbell HA, Mashburn LT, Boyse EA, Old LJ. 1967. Two L-asparaginases from *Escherichia coli* B. Their separation, purification, and antitumor activity. Biochemistry 6:721–730.

Canesso MCC, Lacerda, NL, Ferreira CM, Gonçalves, JL, Almeida D, Gamba C, Pedroso SH, Moreira C, Martins FS, Nicoli JR, Teixeira MM, Godard ALB, Vieira AT. 2014. Comparing the effects of acute alcohol consumption in germ-free and conventional mice: the role of the gut microbiota. BMC Microbiol 14:240.

Canfora EE, Jocken JW, Blaak EE. 2015. Short-chain fatty acids in control of body weight and insulin sensitivity. Nat Rev Endocrinol 11:577–591.

Cani PD, Amar J, Iglesias MA, Poggi M, Knauf C, Bastelica D, Neyrinck AM, Fava F, Tuohy KM, Chabo C, Waget A, Delmée E, Cousin B, Sulpice T, Chamontin B, Ferrières J, Tanti J-F, Gibson GR, Casteilla L, Delzenne NM, Alessi MC, Burcelin R. 2007. Metabolic endotoxemia initiates obesity and insulin resistance. Diabetes 56:1761–1772.

Cani PD, Bibiloni R, Knauf C, Waget A, Neyrinck AM, Delzenne NM, Burcelin R. 2008. Changes in gut microbiota control metabolic endotoxemia-induced inflammation in high-fat diet-induced obesity and diabetes in mice. Diabetes 57:1470–1481.

Cani PD. 2018. Human gut microbiome: hopes, threats and promises. Gut 67:1716–1725.

Caporaso JG, Kuczynski J, Stombaugh J, Bittinger K, Bushman FD, Costello EK, Fierer N, Peña AG, Goodrich JK, Gordon JI, Huttley GA, Kelley ST, Knights D, Koenig JE, Ley RE, Lozupone CA, McDonald D, Muegge BD, Pirrung M, Reeder J, Sevinsky JR, Turnbaugh PJ, Walters WA, Widmann J, Yatsunenko T, Zaneveld J, Knight R. 2010. QIIME allows analysis of high-throughput community sequencing data. Nat Methods 7:335–336.

Carmody RN, Gerber GK, Luevano JM, Gatti DM, Somes L, Svenson KL, et al. 2015. Diet dominates host genotype in shaping the murine gut microbiota. Cell Host Microbe 17:72–84

Caroff M, Karibian D. 2003. Structure of bacterial lipopolysaccharides. Carbohydr Res 338:2431–2447.

Cash HL, Whitham C V, Behrendt CL, Hooper L V. 2006. Symbiotic bacteria direct expression of an intestinal bactericidal lectin. Science 313:1126–1130.

Cecchini G, Schröder I, Gunsalus RP, Maklashina E. 2002. Succinate dehydrogenase and fumarate reductase from *Escherichia coli*. Biochim Biophys Acta 1553:140–157.

Cedar H, Schwartz JH. 1968. Production of L-asparaginase II by *Escherichia coli.* J Bacteriol 96:2043–2048.

Charon MH, Volbeda A, Chabriere E, Pieulle L, Fontecilla-Camps JC. 1999. Structure and electron transfer mechanism of pyruvate:ferredoxin oxidoreductase. Curr Opin Struct Biol 9:663–669.

Chen Y-J, Wu H, Wu S-D, Lu N, Wang Y-T, Liu H-N, Dong L, Liu T-T, Shen X-Z. 2018. *Parasutterella*, in association with irritable bowel syndrome and intestinal chronic inflammation. J Gastroenterol Hepatol 33:1844–1852.

Cheng W, Lu J, Lin W, Wei X, Li H, Zhao X, Jiang A, Yuan J. 2018. Effects of a galacto-oligosaccharide-rich diet on fecal microbiota and metabolite profiles in mice. Food Funct 9:1612–1620.

Chiang JYL. 2009. Bile acids: regulation of synthesis. J Lipid Res 50:1955–1966.

Chiodini RJ, Dowd SE, Chamberlin WM, Galandiuk S, Davis B, Glassing A. 2015. Microbial population differentials between mucosal and submucosal intestinal tissues in advanced Crohn's disease of the ileum. PLoS One 10:e0134382.

Chylinski K, Makarova KS, Charpentier E, Koonin E V. 2014. Classification and evolution of type II CRISPR-Cas systems. Nucleic Acids Res 42:6091–6105.

Cinquin C, Le Blay G, Fliss I, Lacroix C. 2006. New three-stage *in vitro* model for infant colonic fermentation with immobilized fecal microbiota. FEMS Microbiol Ecol 57:324–336.

Clermont O, Christenson JK, Denamur E, Gordon DM. 2013. The Clermont *Escherichia coli* phylo-typing method revisited: improvement of specificity and detection of new phylo-groups. Environ Microbiol Rep 5:58–65.

Collins J, Auchtung JM, Schaefer L, Eaton KA, Britton RA. 2015. Humanized microbiota mice as a model of recurrent *Clostridium difficile* disease. Microbiome 3:35.

Colombel JF, Lemann M, Cassagnou M, Bouhnik Y, Duclos B, Dupas JL, Notteghem B, Mary JY. 1999. A controlled trial comparing ciprofloxacin with mesalazine for the treatment of active Crohn's disease. Groupe d'Etudes Therapeutiques des Affections Inflammatoires Digestives (GETAID). Am J Gastroenterol 94:674–678.

Cordwell SJ. 1999. Microbial genomes and "missing" enzymes: redefining biochemical pathways. Arch Microbiol 172:269–279.

Corfield AP. 2018. The interaction of the gut microbiota with the mucus barrier in health and disease in human. Microorganisms 6:78–135.

Cox LM, Yamanishi S, Sohn J, Alekseyenko A V, Leung JM, Cho I, et al. 2014. Altering the intestinal microbiota during a critical developmental window has lasting metabolic consequences. Cell 158:705–721.

Creely SJ, McTernan PG, Kusminski CM, Fisher FM, Da Silva NF, Khanolkar M, Evans M, Harte AL, Kumar S. 2006. Lipopolysaccharide activates an innate immune system response in human adipose tissue in obesity and type 2 diabetes. Am J Physiol Metab 292:E740–E747.

Curtis MM, Hu Z, Klimko C, Narayanan S, Deberardinis R, Sperandio V. 2014. The gut commensal *Bacteroides thetaiotaomicron* exacerbates enteric infection through modification of the metabolic landscape. Cell Host Microbe 16:759–769.

D'Auria G, Peris-Bondia F, Džunková M, Mira A, Collado MC, Latorre A, Moya A. 2013. Active and secreted IgA-coated bacterial fractions from the human gut reveal an under-represented microbiota core. Sci Rep 3:3515.

Dalby MJ, Ross AW, Walker AW, Morgan PJ. 2017. Dietary uncoupling of gut microbiota and energy harvesting from obesity and glucose tolerance in mice. Cell Rep 21:1521–1533.

Danneskiold-Samsøe NB, Andersen D, Radulescu ID, Normann-Hansen A, Brejnrod A, Kragh M, Madsen T, Nielsen C, Josefsen K, Fretté X, Fjære E, Madsen L, Hellgren LI, Brix S, Kristiansen K. 2017. A safflower oil based high-fat/high-sucrose diet modulates the gut microbiota and liver phospholipid profiles associated with early glucose intolerance in the absence of tissue inflammation. Mol Nutr Food Res 61:1600528.

Dawson PA. 2011. Role of the intestinal bile acid transporters in bile acid and drug disposition. Handb Exp Pharmacol 201:169–203.

De Angelis, Maria and Piccolo, Maria and Vannini, Lucia and Siragusa, Sonya and De Giacomo, Andrea and Serrazzanetti, Diana Isabella and Cristofori, Fernanda and Guerzoni, Maria Elisabetta and Gobbetti, Marco and Francavilla R. 2013. Fecal microbiota and metabolome of children with autism and pervasive developmental disorder not otherwise specified. PLoS One 8:e76993.

De Filippo C, Cavalieri D, Di Paola M, Ramazzotti M, Poullet JB, Massart S, Collini S, Pieraccini G, Lionetti P. 2010. Impact of diet in shaping gut microbiota revealed by a comparative study in children from Europe and rural Africa. Proc Natl Acad Sci 107:14691–14696.

De Gunzburg J, Ghozlane A, Ducher A, Le Chatelier E, Duval X, Ruppé E, Armand-Lefevre L, Sablier-Gallis F, Burdet C, Alavoine L, Chachaty E, Augustin V, Varastet M, Levenez F, Kennedy S, Pons N, Mentré F, Andremont A. 2018. Protection of the human gut microbiome from antibiotics. J Infect Dis 217:628–636.

De Plaen IG, Tan XD, Chang H, Wang L, Remick DG, Hsueh W. 2000. Lipopolysaccharide activates nuclear factor kappaB in rat intestine: role of endogenous platelet-activating factor and tumour necrosis factor. Br J Pharmacol 129:307–314.

Degirolamo C, Rainaldi S, Bovenga F, Murzilli S, Moschetta A. 2014. Microbiota modification with probiotics induces hepatic bile acid synthesis via downregulation of the Fxr-Fgf15 axis in mice. Cell Rep 7:12–18.

Dethlefsen L, Huse S, Sogin ML, Relman DA. 2008. The pervasive effects of an antibiotic on the human gut microbiota, as revealed by deep 16s rRNA sequencing. PLoS Biol 6:e280.

Dethlefsen L, Relman DA. 2011. Incomplete recovery and individualized responses of the human distal gut microbiota to repeated antibiotic perturbation. Proc Natl Acad Sci U S A 1:4554–4561.

Dewhirst FE, Chien CC, Paster BJ, Ericson RL, Orcutt RP, Schauer DB, Fox JG. 1999. Phylogeny of the defined murine microbiota: altered Schaedler flora. Appl Env Microbiol 65:3287–3292.

Dey N, Wagner VE, Blanton LV, Cheng J, Fontana L, Haque R, Ahmed T, Gordon JI. 2015. Regulators of gut motility revealed by a gnotobiotic model of diet-microbiome interactions related to travel. Cell 163:95–107.

Dhillon BK, Laird MR, Shay JA, Winsor GL, Lo R, Nizam F, Pereira SK, Waglechner N, McArthur AG, Langille MGI, Brinkman FSL. 2015. IslandViewer 3: more flexible, interactive genomic island discovery, visualization and analysis. Nucleic Acids Res 43:W104–W108.

Dong LN, Wang JP, Liu P, Yang YF, Feng J, Han Y. 2017. Faecal and mucosal microbiota in patients with functional gastrointestinal disorders: correlation with toll-like receptor 2/toll-like receptor 4 expression. World J Gastroenterol 23:6665–6673.

Drago L, Toscano M, De Grandi R, Grossi E, Padovani EM, Peroni DG. 2016. Microbiota network and mathematic microbe mutualism in colostrum and mature milk collected in two different geographic areas: Italy versus Burundi. ISME J 11:875–884.

Duar RM, Frese SA, Lin XB, Fernando SC, Burkey TE, Tasseva G, Peterson DA, Blom J, Wenzel CQ, Szymanski CM, Walter J. 2017. Experimental evaluation of host adaptation of *Lactobacillus reuteri* to different vertebrate species. Appl Environ Microbiol 83:e00132–17.

Ebbensgaard A, Mordhorst H, Aarestrup FM, Hansen EB. 2018. The role of outer membrane proteins and lipopolysaccharides for the sensitivity of *Escherichia coli* to antimicrobial peptides. Front Microbiol 9:2153.

Edgar RC. 2010. Search and clustering orders of magnitude faster than BLAST. Bioinformatics 26:2460–2461.

Eeckhaut V, Wang J, Van Parys A, Haesebrouck F, Joossens M, Falony G, Raes J, Ducatelle R, Van Immerseel F. 2016. The probiotic butyricicoccus pullicaecorum reduces feed conversion and protects from potentially harmful intestinal microorganisms and necrotic enteritis in broilers. Front Microbiol 7:1416.

Ehmann D, Wendler J, Koeninger L, Larsen IS, Klag T, Berger J, Marette A, Schaller M, Stange EF, Malek NP, Jensen BAH, Wehkamp J. 2019. Paneth cell α-defensins HD-5 and HD-6 display differential degradation into active antimicrobial fragments. Proc Natl Acad Sci 116:3746–3751.

Ericsson AC, Davis JW, Spollen W, Bivens N, Givan S, Hagan CE, McIntosh M, Franklin CL. 2015. Effects of vendor and genetic background on the composition of the fecal microbiota of inbred mice. PLoS One 10:e0116704.

Erny D, De Angelis ALH, Jaitin D, Wieghofer P, Staszewski O, David E, Keren-Shaul H, Mahlakoiv T, Jakobshagen K, Buch T, Schwierzeck V, Utermöhlen O, Chun E, Garrett WS, Mccoy KD, Diefenbach A, Staeheli P, Stecher B, Amit I, Prinz M. 2015. Host microbiota constantly control maturation and function of microglia in the CNS. Nat Neurosci 18:965–977.

Evans SJ, Bassis CM, Hein R, Assari S, Flowers SA, Kelly MB, Young VB, Ellingrod VE, McInnis MG. 2017. The gut microbiome composition associates with bipolar disorder and illness severity. J Psychiatr Res 87:23–29.

Everard A, Belzer C, Geurts L, Ouwerkerk JP, Druart C, Bindels LB, et al. 2013. Cross-talk between *Akkermansia muciniphila* and intestinal epithelium controls diet-induced obesity. Proc Natl Acad Sci 110:9066–9071.

Everard A, Lazarevic V, Derrien M, Girard M, Muccioli GM, Neyrinck AM, Possemiers S, Van Holle A, François P, de Vos WM, Delzenne NM, Schrenzel J, Cani PD. 2011. Responses of gut microbiota and glucose and lipid metabolism to prebiotics in genetic obese and diet-induced leptin-resistant mice. Diabetes 60:2775–2786.

Eykyn SJ, Phillips I. 1976. Metronidazole and anaerobic sepsis. BrMedJ 2:1418–1421.

Fahy E, Sud M, Cotter D, Subramaniam S. 2007. LIPID MAPS online tools for lipid research. Nucleic Acids Res 35:W606–W612.

Faith JJ, Ahern PP, Ridaura VK, Cheng J, Gordon JI. 2014. Identifying gut microbe-host phenotype relationships using combinatorial communities in gnotobiotic mice. Sci Transl Med 6:220ra11.

Fei N, Zhao L. 2013. An opportunistic pathogen isolated from the gut of an obese human causes obesity in germfree mice. ISME J 7:880–884.

Feng Y, Huang Y, Wang Y, Wang P, Song H, Wang F. 2019. Antibiotics induced intestinal tight junction barrier dysfunction is associated with microbiota dysbiosis, activated NLRP3 inflammasome and autophagy. PLoS One 14:e0218384.

Fernández-Calleja JMS, Konstanti P, Swarts HJM, Bouwman LMS, Garcia-Campayo V, Billecke N, Oosting A, Smidt H, Keijer J, van Schothorst EM. 2018. Non-invasive continuous real-time *in vivo* analysis of microbial hydrogen production shows adaptation to fermentable carbohydrates in mice. Sci Rep 8:15351.

Fischbach MA, Sonnenburg JL. 2011. Eating for two: how metabolism establishes interspecies interactions in the gut. Cell Host Microbe 10:336–347.

Fischbach MA. 2018. Microbiome: focus on causation and mechanism. Cell 174:785–790.

Floch MH. 2002. Bile salts, intestinal microflora and enterohepatic circulation. Dig Liver Dis 34:S54–57.

Folch J, Lees M, Stanley GHS. 1956. A simple method for the isolation and purification of total lipids from animal tissues. J Biol Chem 226:497–509.

Francino MP. 2016. Antibiotics and the human gut microbiome: dysbioses and accumulation of resistances. Front Microbiol 6:1543.

Frank RAW, Price AJ, Northrop FD, Perham RN, Luisi BF. 2007. Crystal structure of the e1 component of the *Escherichia coli* 2-oxoglutarate dehydrogenase multienzyme complex. J Mol Biol 368:639–651.

Fratamico PM, DebRoy C, Liu Y, Needleman DS, Baranzoni GM, Feng P. 2016. Advances in molecular serotyping and subtyping of *Escherichia coli*. Front Microbiol 7:644.

Frese SA, Benson AK, Tannock GW, Loach DM, Kim J, Zhang M, Oh PL, Heng NCK, Patil PB, Juge N, MacKenzie DA, Pearson BM, Lapidus A, Dalin E, Tice H, Goltsman E, Land M, Hauser L, Ivanova N, Kyrpides NC, Walter J. 2011. The evolution of host specialization in the vertebrate gut symbiont *Lactobacillus reuteri*. PLoS Genet 7:e1001314.

Frese SA, Mackenzie DA, Peterson DA, Schmaltz R, Fangman T, Zhou Y, Zhang C, Benson AK, Cody LA, Mulholland F. 2013. Molecular characterization of host-specific biofilm formation in a vertebrate gut symbiont. PLoS Genet 9:e1004057.

Frirdich E, Whitfield C. 2005. Lipopolysaccharide inner core oligosaccharide structure and outer membrane stability in human pathogens belonging to the *Enterobacteriaceae*. J Endotoxin Res 11:133–144.

Fritz J V., Desai MS, Shah P, Schneider JG, Wilmes P. 2013. From meta-omics to causality: experimental models for human microbiome research. Microbiome 1:14.

Fuchs TM, Eisenreich W, Heesemann J, Goebel W. 2012. Metabolic adaptation of human pathogenic and related nonpathogenic bacteria to extra- and intracellular habitats. FEMS Microbiol Rev 36:435–462

Furdui C, Ragsdale SW. 2000. The role of pyruvate ferredoxin oxidoreductase in pyruvate synthesis during autotrophic growth by the Wood-Ljungdahl pathway. J Biol Chem 275:28494–28499.

Ge Y, Ezzell RM, Warren HS. 2002. Localization of endotoxin in the rat intestinal epithelium. J Infect Dis 182:873–881.

Ge Z, Feng Y, Dangler CA, Xu S, Taylor NS, Fox JG. 2000. Fumarate reductase is essential for *Helicobacter pylori* colonization of the mouse stomach. Microb Pathog 29:279–287.

Ge Z. 2005. Potential of fumarate reductase as a novel therapeutic target in *Helicobacter pylori* infection. Expert Opin Ther Targets 6:135–146.

Gerritsen J, Smidt H, Rijkers GT, De Vos WM. 2011. Intestinal microbiota in human health and disease: the impact of probiotics. Genes Nutr 6:209–240.

Geva-Zatorsky N, Sefik E, Kua L, Pasman L, Tan TG, Ortiz-Lopez A, Yanortsang TB, Yang L, Jupp R, Mathis D, Benoist C, Kasper DL. 2017. Mining the human gut microbiota for immunomodulatory organisms. Cell 168:928–943.

Goedert JJ, Hua X, Bielecka A, Okayasu I, Milne GL, Jones GS, Fujiwara M, Sinha R, Wan Y, Xu X, Ravel J, Shi J, Palm NW, Feigelson HS. 2018. Postmenopausal breast cancer and oestrogen associations with the IgA-coated and IgA-noncoated faecal microbiota. Br J Cancer 118:471–479.

Goodrich JK, Waters JL, Poole AC, Sutter JL, Koren O, Blekhman R, Beaumont M, Van Treuren W, Knight R, Bell JT, Spector TD, Clark AG, Ley RE. 2014. Human genetics shape the gut microbiome. Cell 159:789–799.

Goodrich ME, McGee DW. 1999. Effect of intestinal epithelial cell cytokines on mucosal B-cell IgA secretion: enhancing effect of epithelial-derived IL-6 but not TGF-β on IgA^+ B cells. Immunol Lett 67:11–14.

Grant JR, Arantes AS, Stothard P. 2012. Comparing thousands of circular genomes using the CGView Comparison Tool. BMC Genomics 13:202.

Green JDF, Laue ED, Perham RN, Ali ST, Guest JR. 1995. Three-dimensional structure of a lipoyl domain fromthe dihydrolipoyl acetyltransferase component of the pyruvate dehydrogenase multienzyme complex of *Escherichia coli*. J Mol Biol 248:328–343.

Groussin M, Mazel F, Sanders JG, Smillie CS, Lavergne S, Thuiller W, Alm EJ. 2017. Unraveling the processes shaping mammalian gut microbiomes over evolutionary time. Nat Commun 8:14319.

Guccione E, Del Rocio Leon-Kempis M, Pearson BM, Hitchin E, Mulholland F, Van Diemen PM, Stevens MP, Kelly DJ. 2008. Amino acid-dependent growth of *Campylobacter jejuni*: key roles for aspartase (AspA) under microaerobic and oxygen-limited conditions and identification of AspB (Cj0762), essential for growth on glutamate. Mol Microbiol 69:77–93.

Guo C, Li Y, Wang P, Li Y, Qiu C, Li M, Wang D, Zhao R, Li D, Wang Y, Li S, Dai W, Zhang L. 2018. Alterations of gut microbiota in cholestatic infants and their correlation with hepatic function. Front Microbiol 9:2682.

Guo S, Al-Sadi R, Said HM, Ma TY. 2013. Lipopolysaccharide causes an increase in intestinal tight junction permeability *in vitro* and *in vivo* by inducing enterocyte membrane expression and localization of TLR-4 and CD14. Am J Pathol 182:375–387.

Guo S, Nighot M, Al-Sadi R, Alhmoud T, Nighot P, Ma TY. 2015. Lipopolysaccharide regulation of intestinal tight junction permeability is mediated by TLR4 signal transduction pathway activation of FAK and MyD88. J Immunol 195:4999–5010.

Guo Y, Huang ZP, Liu CQ, Qi L, Sheng Y, Zou DJ. 2018. Modulation of the gut microbiome: a systematic review of the effect of bariatric surgery. Eur J Endocrinol. 178:43–56.

Guslandi M. 2005. Antibiotics for inflammatory bowel disease: do they work? Eur J Gastroenterol Hepatol 17:145–147.

Haller D, Bode C, Hammes WP, Pfeifer AM, Schiffrin EJ, Blum S. 2000. Non-pathogenic bacteria elicit a differential cytokine response by intestinal epithelial cell/leucocyte co-cultures. Gut 47:79–87.

Han J, Liu Y, Wang R, Yang J, Ling V, Borchers CH. 2015. Metabolic profiling of bile acids in human and mouse blood by LC-MS/MS in combination with phospholipid-depletion solid-phase extraction. Anal Chem 87:1127–1136.

Haskó G, Sitkovsky MV., Szabó C. 2004. Immunomodulatory and neuroprotective effects of inosine. Trends Pharmacol Sci 25:152–157.

He B, Hoang TK, Wang T, Ferris M, Taylor CM, Tian X, Luo M, Tran DQ, Zhou J, Tatevian N, Luo F, Molina JG, Blackburn MR, Gomez TH, Roos S, Rhoads JM, Liu Y. 2017. Resetting microbiota by *Lactobacillus reuteri* inhibits T reg deficiency-induced autoimmunity via adenosine A2A receptors. J Exp Med 214:107–123.

Heikkinen S, Argmann CA, Champy MF, Auwerx J. 2007. Evaluation of glucose homeostasis. Curr Protoc Mol Biol 77:29B–33B.

Heßlinger C, Fairhurst SA, Sawers G. 1998. Novel keto acid formate-lyase and propionate kinase enzymes are components of an anaerobic pathway in *Escherichia coli* that degrades L-threonine to propionate. Mol Microbiol 27:477–492.

Hiemstra PS. 2001. Epithelial antimicrobial peptides and proteins: their role in host defence and inflammation. Paediatr Respir Rev 2:306–310.

Hildebrandt MA, Hoffmann C, Hamady M, Chen YY, Knight R, Bushman FD, Ahima RS, Wu, GD. 2009. High-fat diet determines the composition of the gut microbiome independent of host genotype and phenotype. Gastroenterology 136:A102.

Hoare A, Bittner M, Carter J, Alvarez S, Zaldívar M, Bravo D, Valvano MA, Contreras I. 2006. The outer core lipopolysaccharide of *Salmonella enterica* serovar Typhi is required for bacterial entry into epithelial cells. Infect Immun 74:1555–1564.

Hoebler C, Gaudier E, De Coppet P, Rival M, Cherbut C. 2006. MUC genes are differently expressed during onset and maintenance of inflammation in dextran sodium sulfate-treated mice. Dig Dis Sci 51:381–389.

Hofmann AF, Mysels KJ. 1992. Bile acid solubility and precipitation *in vitro* and *in vivo*: the role of conjugation, pH, and Ca_2^+ ions. J Lipid Res 33:617–626.

Honda K, Littman DR. 2016. The microbiota in adaptive immune homeostasis and disease. Nature 535:75–84

Horvath P, Barrangou R. 2010. CRISPR/Cas, the immune system of bacteria and archaea. Science 327:167–170.

Hoshino K, Takeuchi O, Kawai T, Sanjo H, Ogawa T, Takeda Y, Takeda K, Akira S. 1999. Cutting edge: Toll-like receptor 4 (TLR4)-deficient mice are hyporesponsive to lipopolysaccharide: evidence for TLR4 as the Lps gene product. J Immunol 162:3749–3752.

Hu S, Li A, Huang T, Lai J, Li J, Sublette ME, Lu H, Lu Q, Du Y, Hu Z, Ng CH, Zhang H, Lu J, Mou T, Lu S, Wang D, Duan J, Hu J, Huang M, Wei N, Zhou W, Ruan L, Li MD, Xu Y. 2019. Gut microbiota changes in patients with bipolar depression. Adv Sci 0:1900752.

Hu X, Wang T, Liang S, Li W, Wu X, Jin F. 2015. Antibiotic-induced imbalances in gut microbiota aggravates cholesterol accumulation and liver injuries in rats fed a high-cholesterol diet. Appl Microbiol Biotechnol 99:9111–9122.

Hu Y, Yang X, Qin J, Lu N, Cheng G, Wu N, Pan Y, Li J, Zhu L, Wang X, Meng Z, Zhao F, Liu D, Ma J, Qin N, Xiang C, Xiao Y, Li L, Yang H, Wang J, Yang R, Gao GF, Wang J, Zhu B. 2013. Metagenome-wide analysis of antibiotic resistance genes in a large cohort of human gut microbiota. Nat Commun 4:2151.

Huang C, Chen J, Wang J, Zhou H, Lu Y, Lou L, Zheng J, Tian L, Wang X, Cao Z, Zeng Y. 2017. Dysbiosis of intestinal microbiota and decreased antimicrobial peptide level in paneth cells during hypertriglyceridemia-related acute necrotizing pancreatitis in rats. Front Microbiol 8:776.

Hubbard TD, Murray IA, Perdew GH. 2015. Indole and tryptophan metabolism: endogenous and dietary routes to Ah receptor activation. Drug Metab Dispos 43:1522–1535.

Hugenholtz F, de Vos WM. 2018. Mouse models for human intestinal microbiota research: a critical evaluation. Cell Mol Life Sci 75:149–160.

Ikeyama N, Ohkuma M, Sakamoto M. 2019. Draft genome sequence of *Mesosutterella multiformis* jcm 32464T, a member of the family *Sutterellaceae*, isolated from human feces. Microbiol Resour Announc 8:e00478–19.

Isaac S, Scher JU, Djukovic A, Jiménez N, Littman DR, Abramson SB, Pamer EG, Ubeda C. 2017. Short- and long-term effects of oral vancomycin on the human intestinal microbiota. J Antimicrob Chemother 72:128–136.

Jacobson AN, Choudhury BP, Fischbach MA. 2018. The biosynthesis of lipooligosaccharide from *Bacteroides thetaiotaomicron*. MBio 9:e02289–17.

Jang L-G, Choi G, Kim S-W, Kim B-Y, Lee S, Park H. 2019. The combination of sport and sport-specific diet is associated with characteristics of gut microbiota: an observational study. J Int Soc Sports Nutr 16:21.

Jang SE, Lim SM, Jeong JJ, Jang HM, Lee HJ, Han MJ, Kim DH. 2018. Gastrointestinal inflammation by gut microbiota disturbance induces memory impairment in mice. Mucosal Immunol 11:369–379.

Jernberg C, Löfmark S, Edlund C, Jansson JK. 2007. Long-term ecological impacts of antibiotic administration on the human intestinal microbiota. ISME J 1:56–66.

Jernberg C, Löfmark S, Edlund C, Jansson JK. 2010. Long-term impacts of antibiotic exposure on the human intestinal microbiota. Microbiology 156:3216–3223.

Jiang H, Ling Z, Zhang Y, Mao H, Ma Z, Yin Y, Wang W, Tang W, Tan Z, Shi J, Li L, Ruan B. 2015. Altered fecal microbiota composition in patients with major depressive disorder. Brain Behav Immun 48:186–194.

Joice R, Yasuda K, Shafquat A, Morgan XC, Huttenhower C. 2014. Determining microbial products and identifying molecular targets in the human microbiome. Cell Metab 20:731–741.

Jones B V, Begley M, Hill C, Gahan CGM, Marchesi JR. 2008. Functional and comparative metagenomic analysis of bile salt hydrolase activity in the human gut microbiome. Proc Natl Acad Sci 105:13580–13585.

Jones SA, Chowdhury FZ, Fabich AJ, Anderson A, Schreiner DM, House AL, Autieri SM, Leatham MP, Lins JJ, Jorgensen M, Cohen PS, Conway T. 2007. Respiration of *Escherichia coli* in the mouse intestine. Infect Immun 75:4891–4899.

Joyce MA, Fraser ME, James MNG, Bridger WA, Wolodko WT. 2000. ADP-binding site of *Escherichia coli* succinyl-CoA synthetase revealed by X-ray crystallography. Biochemistry 39:17–25.

Ju T, Kong JY, Stothard P, Willing BP. 2019. Defining the role of *Parasutterella*, a previously uncharacterized member of the core gut microbiota. ISME J 13:1520–1534.

Ju T, Shoblak Y, Gao Y, Yang K, Fouhse J, Finlay BB, So YW, Stothard P, Willing BP. 2017. Initial gut microbial composition as a key factor driving host response to antibiotic treatment, as exemplified by the presence or absence of commensal *Escherichia coli*. Appl Environ Microbiol 83:e01107–17.

Ju, T, Willing BP. 2018. Isolation of commensal *Escherichia coli* strains from feces of healthy laboratory mice or rats. Bio-protocol 8:e2780.

Kararli TT. 1995. Comparison of the gastrointestinal anatomy, physiology, and biochemistry of humans and commonly used laboratory animals. Biopharm Drug Dispos 16:351–380.

Karlsson CLJ, Önnerfält J, Xu J, Molin G, Ahrné S, Thorngren-Jerneck K. 2012. The microbiota of the gut in preschool children with normal and excessive body weight. Obesity 20:2257–2261.

Kashyap PC, Marcobal A, Ursell LK, Smits SA, Sonnenburg ED, Costello EK, Higginbottom SK, Domino SE, Holmes SP, Relman DA, Knight R, Gordon JI,

Sonnenburg JL. 2013. Genetically dictated change in host mucus carbohydrate landscape exerts a diet-dependent effect on the gut microbiota. Proc Natl Acad Sci 110:17059–17064.

Kasper DL. 1976. Chemical and biological characterization of the lipopolysaccharide of *Bacteroides fragilis* subspecies fragilis. J INFECT DIS 134:59–66.

Katsuma S, Hirasawa A, Tsujimoto G. 2005. Bile acids promote glucagon-like peptide-1 secretion through TGR5 in a murine enteroendocrine cell line STC-1. Biochem Biophys Res Commun 329:386–390.

Kau AL, Planer JD, Liu J, Rao S, Yatsunenko T, Trehan I, Manary MJ, Liu TC, Stappenbeck TS, Maleta KM, Ashorn P, Dewey KG, Houpt ER, Hsieh CS, Gordon JI. 2015. Functional characterization of IgA-targeted bacterial taxa from undernourished Malawian children that produce diet-dependent enteropathy. Sci Transl Med 7:276ra24.

Kayagaki N, Wong MT, Stowe IB, Ramani SR, Gonzalez LC, Akashi-Takamura S, Miyake K, Zhang J, Lee WP, Muszyński A, Forsberg LS, Carlson RW, Dixit VM. 2013. Noncanonical inflammasome activation by intracellular LPS independent of TLR4. Science 341:1246–1249.

Keilbaugh S a, Shin ME, Banchereau RF, McVay LD, Boyko N, Artis D, Cebra JJ, Wu GD. 2005. Activation of RegIIIbeta/gamma and interferon gamma expression in the intestinal tract of SCID mice: an innate response to bacterial colonisation of the gut. Gut 54:623–629.

Kennedy EA, King KY, Baldridge MT. 2018. Mouse microbiota models: comparing germ-free mice and antibiotics treatment as tools for modifying gut bacteria. Front Physiol 9:1534.

Kern M, Simon J. 2008. Characterization of the NapGH quinol dehydrogenase complex involved in *Wolinella succinogenes* nitrate respiration. Mol Microbiol 69:1137–1152.

Kerr TA, Saeki S, Schneider M, Schaefer K, Berdy S, Redder T, Shan B, Russell DW, Schwarz M. 2002. Loss of nuclear receptor SHP impairs but does not eliminate negative feedback regulation of bile acid synthesis. Dev Cell 2:713–720.

Kim HJ, Huh D, Hamilton G, Ingber DE. 2012. Human gut-on-a-chip inhabited by microbial flora that experiences intestinal peristalsis-like motions and flow. Lab Chip 12:2165–2174.

Kim YG, Sakamoto K, Seo SU, Pickard JM, Gillilland MG, Pudlo NA, Hoostal M, Li X, Wang TD, Feehley T, Stefka AT, Schmidt TM, Martens EC, Fukuda S, Inohara N, Nagler CR, Núñez G. 2017. Neonatal acquisition of Clostridia species protects against colonization by bacterial pathogens. Science 356:315–319.

Kittana H, Gomes-Neto JC, Heck K, Geis AL, Segura Muñoz RR, Cody LA, Schmaltz RJ, Bindels LB, Sinha R, Hostetter JM, Benson AK, Ramer-Tait AE. 2018. Commensal *Escherichia coli* strains can promote intestinal inflammation via differential interleukin-6 production. Front Immunol 9:2318.

Klein G, Müller-Loennies S, Lindner B, Kobylak N, Brade H, Raina S. 2013. Molecular and structural basis of inner core lipopolysaccharide alterations in *Escherichia coli*: incorporation of glucuronic acid and phosphoethanolamine in the heptose region. J Biol Chem 288:8111–8127.

Knappe J, Sawers G. 1990. A radical-chemical route to acetyl-CoA: the anaerobically induced pyruvate formate-lyase system of *Escherichia coli*. FEMS Microbiol Lett 6:383–398.

Kok DEG, Rusli F, van der Lugt B, Lute C, Laghi L, Salvioli S, Picone G, Franceschi C, Smidt H, Vervoort J, Kampman E, Müller M, Steegenga WT. 2018. Lifelong calorie restriction affects indicators of colonic health in aging C57Bl/6J mice. J Nutr Biochem 56:152–164.

Kong F, Singh RP. 2010. A human gastric simulator (HGS) to study food digestion in human stomach. J Food Sci 75:E627–E635.

Kostic AD, Howitt MR, Garrett WS. 2013. Exploring host-microbiota interactions in animal models and humans. Genes Dev 27:701–718.

Kreutzer C, Peters S, Schulte DM, Fangmann D, Türk K, Wolff S, van Eimeren T, Ahrens M, Beckmann J, Schafmayer C, Becker T, Kerby T, Rohr A, Riedel C, Heinsen FA, Degenhardt F, Franke A, Rosenstiel P, Zubek N, Henning C, Freitag-Wolf S, Dempfle A, Psilopanagioti A, Petrou-Papadaki H, Lenk L, Jansen O, Schreiber S, Laudes M. 2017. Hypothalamic inflammation in human obesity is mediated by environmental and genetic factors. Diabetes 66:2407–2415.

Krishnan S, Alden N, Lee K. 2015. Pathways and functions of gut microbiota metabolism impacting host physiology. Curr Opin Biotechnol 36:137–145.

Kubo A, Stephens RS. 2001. Substrate-specific diffusion of select dicarboxylates through *Chlamydia trachomatis* PorB. Microbiology 147:3135–3140.

Kuhn KA, Manieri NA, Liu TC, Stappenbeck TS. 2014. IL-6 stimulates intestinal epithelial proliferation and repair after injury. PLoS One 9:e114195.

Kurilshikov A, Wijmenga C, Fu J, Zhernakova A. 2017. Host genetics and gut microbiome: challenges and perspectives. Trends Immunol 38:633–647.

Lacroix C, de Wouters T, Chassard C. 2015. Integrated multi-scale strategies to investigate nutritional compounds and their effect on the gut microbiota. Curr Opin Biotechnol 32:149–155.

Lambeth DO. 2006. Reconsideration of the significance of substrate-level phosphorylation in the citric acid cycle. Biochem Mol Biol Educ 34:21–29.

Landrier JF, Eloranta JJ, Vavricka SR, Kullak-Ublick GA. 2006. The nuclear receptor for bile acids, FXR, transactivates human organic solute transporter-α and -β genes. Am J Physiol Gastrointest Liver Physiol 290:G476–G485.

Langdon A, Crook N, Dantas G. 2016. The effects of antibiotics on the microbiome throughout development and alternative approaches for therapeutic modulation. Genome Med 8:39.

Larmonier CB, Laubitz D, Hill FM, Shehab KW, Lipinski L, Midura-Kiela MT, McFadden R-MT, Ramalingam R, Hassan KA, Golebiewski M, Besselsen DG,

Ghishan FK, Kiela PR. 2013. Reduced colonic microbial diversity is associated with colitis in NHE3-deficient mice. Am J Physiol Liver Physiol 305:G667–G677.

Lawley TD, Walker AW. 2013. Intestinal colonization resistance. Immunology 138:1–11.

Lee JS, Wang RX, Alexeev EE, Lanis JM, Battista KD, Glover LE, Colgan SP. 2018. Hypoxanthine is a checkpoint stress metabolite in colonic epithelial energy modulation and barrier function. J Biol Chem 293:6039–6051.

Lefebvre P, Cariou B, Lien F, Kuipers F, Staels B. 2009. Role of bile acids and bile acid receptors in metabolic regulation. Physiol Rev 89:147–191.

Leushacke M, Barker N. 2014. *Ex vivo* culture of the intestinal epithelium: Strategies and applications. Gut 63:1345–1354.

Lewis BB, Buffie CG, Carter RA, Leiner I, Toussaint NC, Miller LC, Gobourne A, Ling L, Pamer EG. 2015. Loss of microbiota-mediated colonization resistance to *Clostridium difficile* infection with oral vancomycin compared with metronidazole. J Infect Dis 212:1656–1665.

Ley RE, Backhed F, Turnbaugh P, Lozupone CA, Knight RD, Gordon JI. 2005. Obesity alters gut microbial ecology. Proc Natl Acad Sci 102:11070–11075.

Ley RE, Peterson DA, Gordon JI. 2006. Ecological and evolutionary forces shaping microbial diversity in the human intestine. Cell 124:837–848.

Li H, Limenitakis JP, Fuhrer T, Geuking MB, Lawson MA, Wyss M, Brugiroux S, Keller I, Macpherson JA, Rupp S, Stolp B, Stein J V., Stecher B, Sauer U, McCoy KD, Macpherson AJ. 2015. The outer mucus layer hosts a distinct intestinal microbial niche. Nat Commun 6:8292.

Li J, Hao H, Cheng G, Liu C, Ahmed S, Shabbir MAB, Hussain HI, Dai M, Yuan Z. 2017. Microbial shifts in the intestinal microbiota of *Salmonella* infected chickens in response to enrofloxacin. Front Microbiol 8:1711.

Li N, Wang Q, Wang Y, Sun A, Lin Y, Jin Y, Li X. 2019. Fecal microbiota transplantation from chronic unpredictable mild stress mice donors affects anxiety-like and depression-like behavior in recipient mice via the gut microbiota-inflammation-brain axis. Stress 24:1–11.

Li R, Wang H, Shi Q, Wang N, Zhang Z, Xiong C, Liu J, Chen Y, Jiang L, Jiang Q. 2017. Effects of oral florfenicol and azithromycin on gut microbiota and adipogenesis in mice. PLoS One 12:e0181690.

Li X, Rezaei R, Li P, Wu G. 2011. Composition of amino acids in feed ingredients for animal diets. Amino Acids 40:1159–1168.

Li Z, Xu G, Qin Y, Zhang C, Tang H, Yin Y, et al. 2014. Ghrelin promotes hepatic lipogenesis by activation of mTOR-PPAR signaling pathway. Proc Natl Acad Sci 111:13163–13168.

Lin JZ, Martagón AJ, Hsueh WA, Baxter JD, Gustafsson JÅ, Webb P, Phillips KJ. 2012. Thyroid hormone receptor agonists reduce serum cholesterol independent of the LDL receptor. Endocrinology 153:6136–6144.

Litvak Y, Bäumler AJ. 2019. The founder hypothesis: a basis for microbiota resistance, diversity in taxa carriage, and colonization resistance against pathogens. PLOS Pathog 15:e1007563.

Litvak Y, Byndloss MX, Bäumler AJ. 2018. Colonocyte metabolism shapes the gut microbiota. Science 362:eaat9076.

Litvak Y, Mon KKZ, Nguyen H, Chanthavixay G, Liou M, Velazquez EM, Kutter L, Alcantara MA, Byndloss MX, Tiffany CR, Walker GT, Faber F, Zhu Y, Bronner DN, Byndloss AJ, Tsolis RM, Zhou H, Bäumler AJ. 2019. Commensal *Enterobacteriaceae* protect against *Salmonella* colonization through oxygen competition. Cell Host Microbe 25:128–139.

Liu Q, Li F, Zhuang Y, Xu J, Wang J, Mao X, Zhang Y, Liu X. 2019. Alteration in gut microbiota associated with hepatitis B and non-hepatitis virus related hepatocellular carcinoma. Gut Pathog 11:1.

Llopis M, Cassard AM, Wrzosek L, Boschat L, Bruneau A, Ferrere G, Puchois V, Martin JC, Lepage P, Le Roy T, Lefèvre L, Langelier B, Cailleux F, González-Castro AM, Rabot S, Gaudin F, Agostini H, Prévot S, Berrebi D, Ciocan D, Jousse C, Naveau S, Gérard P, Perlemuter G. 2016. Intestinal microbiota contributes to individual susceptibility to alcoholic liver disease. Gut 65:830–839.

Lloyd-Price J, Abu-Ali G, Huttenhower C. 2016. The healthy human microbiome. Genome Med 8:51.

Löfmark S, Edlund C, Nord CE. 2010. Metronidazole is still the drug of choice for treatment of anaerobic infections. Clin Infect Dis 50:16–23.

Loonen LMP, Stolte EH, Jaklofsky MTJ, Meijerink M, Dekker J, van Baarlen P, Wells JM. 2014. REG3γ-deficient mice have altered mucus distribution and increased mucosal inflammatory responses to the microbiota and enteric pathogens in the ileum. Mucosal Immunol 7:939–947.

Lotz M, Gütle D, Walther S, Ménard S, Bogdan C, Hornef MW. 2006. Postnatal acquisition of endotoxin tolerance in intestinal epithelial cells. J Exp Med 203:973–984.

Low DE, Shahinas D, Silverman M, Sittler T, Chiu C, Kim P, Allen-Vercoe E, Weese S, Wong A, Pillaij DR. 2012. Toward an understanding of changes in diversity associated with fecal microbiome transplantation based on 16s rRNA gene deep sequencing. MBio 3:e00338–12.

Lozupone CA, Stombaugh JI, Gordon JI, Jansson JK, Knight R. 2012. Diversity, stability and resilience of the human gut microbiota. Nature 489:220–230.

Lu C, Sun T, Li Y, Zhang D, Zhou J, Su X. 2018. Microbial diversity and composition in different gut locations of hyperlipidemic mice receiving krill oil. Appl Microbiol Biotechnol 102:355–366.

Luna RA, Oezguen N, Balderas M, Venkatachalam A, Runge JK, Versalovic J, Veenstra-VanderWeele J, Anderson GM, Savidge T, Williams KC. 2017. Distinct microbiome-neuroimmune signatures correlate with functional abdominal pain in children with autism spectrum disorder. Cell Mol Gastroenterol Hepatol 3:218–230.

Lupp C, Robertson ML, Wickham ME, Sekirov I, Champion OL, Gaynor EC, Finlay BB. 2007. Host-mediated inflammation disrupts the intestinal microbiota and promotes the overgrowth of *Enterobacteriaceae*. Cell Host Microbe 2:119–129.

Ma K, Saha PK, Chan L, Moore DD. 2006. Farnesoid X receptor is essential for normal glucose homeostasis. J Clin Invest 116:1102–1109.

Macdonald IA, Bokkenheuser VD, Winter J, McLernon AM, Mosbach EH. 1983. Degradation of steroids in the human gut. J Lipid Res 24:675–700.

Macfarlane GT, Gibson GR, Cummings JH. 1992. Comparison of fermentation reactions in different regions of the human colon. J Appl Bacteriol 72:57–64.

Mailhe M, Ricaboni D, Benezech A, Lagier JC, Fournier PE, Raoult D. 2017. 'Duodenibacillus massiliensis' gen. nov., sp. nov., a new species identified in human duodenum. New Microbes New Infect 17:43–44.

Maldonado-Gómez MX, Martínez I, Bottacini F, O'Callaghan A, Ventura M, van Sinderen D, Hillmann B, Vangay P, Knights D, Hutkins RW, Walter J. 2016. Stable engraftment of *Bifidobacterium longum* AH1206 in the human gut depends on individualized features of the resident microbiome. Cell Host Microbe. 20:515–526.

Marcobal A, Kashyap PC, Nelson TA, Aronov PA, Donia MS, Spormann A, Fischbach MA, Sonnenburg JL. 2013. A metabolomic view of how the human gut microbiota impacts the host metabolome using humanized and gnotobiotic mice. ISME J 7:1933–1943.

Mark AR, Clore GM, James GO, Angela MG, Richard NP, Ettore A, Kazuyasu S. 1992. Three-dimensional solution structure of the e3-binding domain of the dihydrolipoamide succinyltransferase core from the 2-oxoglutarate dehydrogenase multienzyme complex of *Escherichia coli*. Biochemistry 31:3463–3471.

Martin CR, Osadchiy V, Kalani A, Mayer EA. 2018. The brain-gut-microbiome axis. Cell Mol Gastroenterol Hepatol 6:133–148.

Martin G, Kolida S, Marchesi JR, Want E, Sidaway JE, Swann JR. 2018. *In vitro* modeling of bile acid processing by the human fecal microbiota. Front Microbiol 9:1153.

Martino ME, Joncour P, Leenay R, Gervais H, Shah M, Hughes S, Gillet B, Beisel C, Leulier F. 2018. Bacterial adaptation to the host's diet is a key evolutionary force shaping Drosophila-*Lactobacillus* symbiosis. Cell Host Microbe 24:109–119.e6.

Martinson JNV, Pinkham N V., Peters GW, Cho H, Heng J, Rauch M, Broadaway SC, Walk ST. 2019. Rethinking gut microbiome residency and the *Enterobacteriaceae* in healthy human adults. ISME J.

Marzorati M, Vanhoecke B, De Ryck T, Sadaghian Sadabad M, Pinheiro I, Possemiers S, Van Den Abbeele P, Derycke L, Bracke M, Pieters J, Hennebel T, Harmsen HJ, Verstraete W, Van De Wiele T. 2014. The HMITM module: a new tool to study the host-microbiota interaction in the human gastrointestinal tract *in vitro*. BMC Microbiol 14:133.

Maseda D, Zackular JP, Trindade B, Kirk L, Roxas JL, Rogers LM, Washington MK, Du L, Koyama T, Viswanathan VK, Vedantam G, Schloss PD, Crofford LJ, Skaar EP, Aronoff DM. 2019. Nonsteroidal anti-inflammatory drugs alter the microbiota and

exacerbate *Clostridium difficile* colitis while dysregulating the inflammatory response. MBio 10:e02282–18.

Maslowski KM, Vieira AT, Ng A, Kranich J, Sierro F, Yu D, Schilter HC, Rolph MS, Mackay F, Artis D, Xavier RJ, Teixeira MM, Mackay CR. 2009. Regulation of inflammatory responses by gut microbiota and chemoattractant receptor GPR43. Nature 461:1282–1286.

McArdle BH, Anderson MJ. 2001. Fitting multivariate models to community data: a comment on distance-based redundancy analysis. Ecology 82:290–297.

McMurdie PJ, Holmes S. 2013. Phyloseq: an R package for reproducible interactive analysis and graphics of microbiome census data. PLoS One 8:e61217.

Meijnikman AS, Gerdes VE, Nieuwdorp M, Herrema H. 2018. Evaluating causality of gut microbiota in obesity and diabetes in humans. Endocr Rev 39:133–153.

Metzler-Zebeli BU, Schmitz-Esser S, Mann E, Grüll D, Molnar T, Zebeli Q. 2015. Adaptation of the cecal bacterial microbiome of growing pigs in response to resistant starch type 4. Appl Environ Microbiol 81:8489–8499.

Midtvedt T. 1974. Microbial bile acid transformation. Am J Clin Nutr 27:1341–1347.

Milani C, Duranti S, Bottacini F, Casey E, Turroni F, Mahony J, Belzer C, Delgado Palacio S, Arboleya Montes S, Mancabelli L, Lugli GA, Rodriguez JM, Bode L, de Vos W, Gueimonde M, Margolles A, van Sinderen D, Ventura M. 2017. The first microbial colonizers of the human gut: composition, activities, and health implications of the infant gut microbiota. Microbiol Mol Biol Rev 81:e00036–17.

Minekus M, Marteau P, Havenaar R, Huis in 't Veld JHJ. 1995. A multicompartmental dynamic computer-controlled model simulating the stomach and small intestine. Altern to Lab Anim 23:197.

Minekus M, Smeets-Peeters M, Havenaar R, Bernalier A, Fonty G, Marol-Bonnin S, Alric M, Marteau P, Huis In't Veld JHJ. 1999. A computer-controlled system to simulate conditions of the large intestine with peristaltic mixing, water absorption and absorption of fermentation products. Appl Microbiol Biotechnol 1:108–114.

Molly K, Vande Woestyne M, Verstraete W. 1993. Development of a 5-step multi-chamber reactor as a simulation of the human intestinal microbial ecosystem. Appl Microbiol Biotechnol 39:254–258.

Monteiro MA. 2001. Helicobacter pylori: A wolf in sheep's clothing: The glycotype families of *Helicobacter pylori* lipopolysaccharides expressing histo-blood groups: structure, biosynthesis, and role in pathogenesis. Adv Carbohydr Chem Biochem 57:99–158.

Moon C, Baldridge MT, Wallace MA, Burnham CAD, Virgin HW, Stappenbeck TS. 2015. Vertically transmitted faecal IgA levels determine extra-chromosomal phenotypic variation. Nature 521:90–93.

Morgun A, Dzutsev A, Dong X, Greer RL, Sexton DJ, Ravel J, Schuster M, Hsiao W, Matzinger P, Shulzhenko N. 2015. Uncovering effects of antibiotics on the host and microbiota using transkingdom gene networks. Gut 64:1732–1743.

Morishita T, Yajima M. 1995. Incomplete operation of biosynthetic and bioenergetic functions of the citric acid cycle in multiple auxotrophic Lactobacilli. Biosci Biotechnol Biochem 59:251–255.

Morotomi M, Nagai F, Watanabe Y. 2011. *Parasutterella secunda* sp. nov., isolated from human faeces and proposal of *Sutterellaceae* fam. nov. in the order Burkholderiales. Int J Syst Evol Microbiol 61:637–643.

Morotomi M. 2014. The family *Sutterellaceae*. p. 1005–1012. In: Rosenberg E, DeLong EF, Lory S, Stackebrandt E, Thompson F (ed), The prokaryotes: Alphaproteobacteria and Betaproteobacteria, 4th ed. Springer, Berlin, Heidelberg.

Murugesan S, Ulloa-Martínez M, Martínez-Rojano H, Galván-Rodríguez FM, Miranda-Brito C, Romano MC, et al. 2015. Study of the diversity and short-chain fatty acids production by the bacterial community in overweight and obese Mexican children. Eur J Clin Microbiol Infect Dis 34:1337–1346.

Nagai F, Morotomi M, Sakon H, Tanaka R. 2009. *Parasutterella excrementihominis* gen. nov., sp. nov., a member of the family *Alcaligenaceae* isolated from human faeces. Int J Syst Evol Microbiol 59:1793–1797.

Nakahara M, Furuya N, Takagaki K, Sugaya T, Hirota K, Fukamizu A, Kanda T, Fujii H, Sato R. 2005. Ileal bile acid-binding protein, functionally associated with the farnesoid X receptor or the ileal bile acid transporter, regulates bile acid activity in the small intestine. J Biol Chem 280:42283–42289.

Nataro JP, Kaper BJ. 1998. Diarrheagenic *Escherichia coli*. Clin Microbiol Rev 11:142–201.

Natividad JM, Hayes CL, Motta JP, Jury J, Galipeau HJ, Philip V, Garcia-Rodenas CL, Kiyama H, Bercik P, Verdu EF. 2013. Differential induction of antimicrobial REGIII by the intestinal microbiota and *Bifidobacterium breve* NCC2950. Appl Environ Microbiol 79:7745–7754.

Netzer R, Krause M, Rittmann D, Peters-Wendisch PG, Eggeling L, Wendisch VF, Sahm H. 2004. Roles of pyruvate kinase and malic enzyme in *Corynebacterium glutamicum* for growth on carbon sources requiring gluconeogenesis. Arch Microbiol 182:354–363.

Nguyen AT, Mandard S, Dray C, Deckert V, Valet P, Besnard P, et al. 2014. Lipopolysaccharides-mediated increase in glucose-stimulated insulin secretion: involvement of the GLP-1 pathway. Diabetes 63:471–482.

Nguyen TLA, Vieira-Silva S, Liston A, Raes J. 2015. How informative is the mouse for human gut microbiota research? Dis Model Mech 8:1–16.

Nicholson JK, Holmes E, Kinross J, Burcelin R, Gibson G, Jia W, Pettersson S. 2012. Host-gut microbiota metabolic interactions. Science 336:1262–1267.

Nieuwdorp M, Gilijamse PW, Pai N, Kaplan LM. 2014. Role of the microbiome in energy regulation and metabolism. Gastroenterology 146:1525–1533.

Noble EE, Hsu TM, Jones RB, Fodor AA, Goran MI, Kanoski SE. 2017. Early-life sugar consumption affects the rat microbiome independently of obesity. J Nutr 147:20–28.

Nolte JC, Schürmann M, Schepers CL, Vogel E, Wübbeler JH, Steinbüchel A. 2014. Novel characteristics of succinate coenzyme a (succinate-coa) ligases: Conversion of malate to malyl-coa and coa-thioester formation of succinate analogues *in vitro*. Appl Environ Microbiol 80:166–176.

O'Flaherty S, Briner Crawley A, Theriot CM, Barrangou R. 2018. The *Lactobacillus* bile salt hydrolase repertoire reveals niche-specific adaptation. mSphere 3:e00140–18.

O'Neil DS, Stewart CJ, Chu DM, Goodspeed DM, Gonzalez-Rodriguez PJ, Shope CD, Aagaard KM. 2017. Conditional postnatal deletion of the neonatal murine hepatic circadian gene, Npas2, alters the gut microbiome following restricted feeding. Am J Obstet Gynecol 217:218.e1–218.e15.

Oh PL, Benson AK, Peterson DA, Patil PB, Moriyama EN, Roos S, Walter J, Lantbruksuniversitet S. 2010. Diversification of the gut symbiont *Lactobacillus reuteri* as a result of host-driven evolution. ISME J 4:377–387.

Osaka T, Moriyama E, Arai S, Date Y, Yagi J, Kikuchi J, Tsuneda S. 2017. Meta-analysis of fecal microbiota and metabolites in experimental colitic mice during the inflammatory and healing phases. Nutrients 9:E1329.

Palm NW, De Zoete MR, Cullen TW, Barry NA, Stefanowski J, Hao L, Degnan PH, Hu J, Peter I, Zhang W, Ruggiero E, Cho JH, Goodman AL, Flavell RA. 2014. Immunoglobulin A coating identifies colitogenic bacteria in inflammatory bowel disease. Cell 158:1000–1010.

Palmer C, Bik EM, DiGiulio DB, Relman DA, Brown PO. 2007. Development of the human infant intestinal microbiota. PLoS Biol 5:e177.

Pan WW, Myers MG. 2018. Leptin and the maintenance of elevated body weight. Nat Rev Neurosci 19:95–105.

Park SJ, Cotter PA, Gunsalus RP. 1995. Regulation of malate dehydrogenase (mdh) gene expression in *Escherichia coli* in response to oxygen, carbon, and heme availability. J Bacteriol 177:6652–6656.

Part VI. 2015. In vitro fermentation models: General introduction. p 175. In: Verhoeckx K, Cotter P, López-Expósito I, Kleiveland C, Lea T, Mackie A, Requena, T., Swiatecka, D., Wichers, H. (ed), The impact of food bioactives on health: *in vitro* and *ex vivo* models. Springer.

Parte AC. 2014. LPSN-List of prokaryotic names with standing in nomenclature. Nucleic Acids Res 42:D613–D616.

Patel MS, Roche TE. 1990. Molecular biology and biochemistry of pyruvate dehydrogenase complexes. FASEB J 4:3224–3233.

Pearce SC, Coia HG, Karl JP, Pantoja-Feliciano IG, Zachos NC, Racicot K. 2018. Intestinal *in vitro* and *ex vivo* models to study host-microbiome interactions and acute stressors. Front Physiol 9:1584.

Pélissier MA, Vasquez N, Balamurugan R, Pereira E, Dossou-Yovo F, Suau A, Pochart P, Magne F. 2010. Metronidazole effects on microbiota and mucus layer thickness in the rat gut. FEMS Microbiol Ecol 73:601–610.

Perez-Cobas AE, Gosalbes MJ, Friedrichs A, Knecht H, Artacho A, Eismann K, Otto W, Rojo D, Bargiela R, von Bergen M, Neulinger SC, Daumer C, Heinsen FA, Latorre A, Barbas C, Seifert J, Santos VM Dos, Ott SJ, Ferrer M, Moya A, Pérez-Cobas AE, Bergen M Von, Däumer C, Martins V, Dos Santos VM. 2012. Gut microbiota disturbance during antibiotic therapy: a multi-omic approach. Gut 62:1591–1601.

Pitson SM, Mendz GL, Srinivasan S, Hazell SL. 1999. The tricarboxylic acid cycle of *Helicobacter pylori*. Eur J Biochem 260:258–267.

Pols TWH, Auwerx J, Schoonjans K. 2010. Targeting the TGR5-GLP-1 pathway to combat type 2 diabetes and non-alcoholic fatty liver disease. Gastroentérologie Clin Biol 34:270–273.

Postler TS, Ghosh S. 2017. Understanding the holobiont: how microbial metabolites affect human health and shape the immune system. Cell Metab 26:110–130.

Prawitt J, Abdelkarim M, Stroeve JHM, Popescu I, Duez H, Velagapudi VR, Dumont J, Bouchaert E, Van Dijk TH, Lucas A, Dorchies E, Daoudi M, Lestavel S, Gonzalez FJ, Oresic M, Cariou B, Kuipers F, Caron S, Staels B. 2011. Farnesoid X receptor deficiency improves glucose homeostasis in mouse models of obesity. Diabetes 60:1861–1871.

Pullinger CR, Eng C, Salen G, Shefer S, Batta AK, Erickson SK, Verhagen A, Rivera CR, Mulvihill SJ, Malloy MJ, Kane JP. 2002. Human cholesterol 7α-hydroxylase (CYP7A1) deficiency has a hypercholesterolemic phenotype. J Clin Invest 110:109–117.

Qian Y, Yang X, Xu S, Wu C, Qin N, Chen S Di, Xiao Q. 2018. Detection of microbial 16S rRNA gene in the blood of patients with Parkinson's disease. Front Aging Neurosci 10:156.

Qin J, Li Y, Cai Z, Li S, Zhu J, Zhang F, Liang S, Zhang W, Guan Y, Shen D, Peng Y, Zhang D, Jie Z, Wu W, Qin Y, Xue W, Li J, Han L, Lu D, Wu P, Dai Y, Sun X, Li Z, Tang A, Zhong S, Li X, Chen W, Xu R, Wang M, Feng Q, Gong M, Yu J, Zhang Y, Zhang M, Hansen T, Sanchez G, Raes J, Falony G, Okuda S, Almeida M, LeChatelier E, Renault P, Pons N, Batto J-M, Zhang Z, Chen H, Yang R, Zheng W, Li S, Yang H, Wang J, Ehrlich SD, Nielsen R, Pedersen O, Kristiansen K, Wang J. 2012. A metagenome-wide association study of gut microbiota in type 2 diabetes. Nature 490:55–60.

Rabot S, Membrez M, Bruneau A, Gérard P, Harach T, Moser M, Raymond F, Mansourian R, Chou CJ. 2010. Germ-free C57BL/6J mice are resistant to high-fat-diet-induced insulin resistance and have altered cholesterol metabolism. FASEB J 4:4948–4959.

Raetz CRH, Whitfield C. 2002. Lipopolysaccharide endotoxins. Annu Rev Biochem 71:635–700.

Rausch P, Künzel S, Suwandi A, Grassl GA, Rosenstiel P, Baines JF. 2017. Multigenerational influences of the Fut2 gene on the dynamics of the gut microbiota in mice. Front Microbiol 8:991.

Rawls JF, Mahowald MA, Ley RE, Gordon JI. 2006. Reciprocal gut microbiota transplants from zebrafish and mice to germ-free recipients reveal host habitat selection. Cell 127:423–433.

Raymond F, Ouameur A a, Déraspe M, Iqbal N, Gingras H, Dridi B, Leprohon P, Plante P-L, Giroux R, Bérubé È, Frenette J, Boudreau DK, Simard J-L, Chabot I, Domingo M-C, Trottier S, Boissinot M, Huletsky A, Roy PH, Ouellette M, Bergeron MG, Corbeil J. 2015. The initial state of the human gut microbiome determines its reshaping by antibiotics. ISME J 10:707–720.

Ridaura VK, Faith JJ, Rey FE, Cheng J, Duncan AE, Kau AL, et al. 2013. Gut microbiota from twins discordant for obesity modulate metabolism in mice. Science 341:1241–1263.

Ridlon JM, Kang D-J, Hylemon PB. 2006. Bile salt biotransformations by human intestinal bacteria. J Lipid Res 47:241–259.

Rieder R, Wisniewski PJ, Alderman BL, Campbell SC. 2017. Microbes and mental health: a review. Brain Behav Immun 66:9–17.

Ritchie LE, Sturino JM, Carroll RJ, Rooney LW, Andrea Azcarate-Peril M, Turner ND. 2015. Polyphenol-rich sorghum brans alter colon microbiota and impact species diversity and species richness after multiple bouts of dextran sodium sulfate-induced colitis. FEMS Microbiol Ecol 91:fiv008.

Rivera-Chávez F, Zhang LF, Faber F, Lopez CA, Byndloss MX, Olsan EE, Xu G, Velazquez EM, Lebrilla CB, Winter SE, Bäumler AJ. 2016. Depletion of butyrate-producing Clostridia from the gut microbiota drives an aerobic luminal expansion of *Salmonella*. Cell Host Microbe 19:443–454.

Robinson CD, Klein HS, Murphy KD, Parthasarathy R, Guillemin K, Bohannan BJM. 2018. Experimental bacterial adaptation to the zebrafish gut reveals a primary role for immigration. PLoS Biol 16:e2006893.

Rojo ÓP, San Román AL, Arbizu EA, Martínez ADLH, Sevillano ER, Martínez AA. 2007. Serum lipopolysaccharide-binding protein in endotoxemic patients with inflammatory bowel disease. Inflamm Bowel Dis 13:269–277.

Rosadini C V., Kagan JC. 2017. Early innate immune responses to bacterial LPS. Curr Opin Immunol 44:14–19.

Rosshart SP, Vassallo BG, Angeletti D, Hutchinson DS, Morgan AP, Takeda K, Hickman HD, McCulloch JA, Badger JH, Ajami NJ, Trinchieri G, Pardo-Manuel de Villena F, Yewdell JW, Rehermann B. 2017. Wild mouse gut microbiota promotes host fitness and improves disease resistance. Cell 171:1015–1028.

Round JL, Palm NW. 2018. Causal effects of the microbiota on immune-mediated diseases. Sci Immunol 3:eaao1603.

Roy CDL. 2001. Succinate:quinone oxidoreductases-what can we learn from *Wolinella succinogenes* quinol:fumarate reductase? FEBS Letters 504:133–141.

Rumney CJ, Rowland IR. 1992. *In vivo* and *in vitro* models of the human colonic flora. Crit Rev Food Sci Nutr 31:299–331.

Russell DW. 2003. The enzymes, regulation, and genetics of bile acid synthesis. Annu Rev Biochem 72:137–174.

Russell WR, Duncan SH, Scobbie L, Duncan G, Cantlay L, Calder AG, Anderson SE, Flint HJ. 2013. Major phenylpropanoid-derived metabolites in the human gut can arise from microbial fermentation of protein. Mol Nutr Food Res 57:523–535.

Sakamoto M, Ikeyama N, Kunihiro T, Iino T, Yuki M, Ohkuma M. 2018. *Mesosutterella multiformis* gen. nov., sp. nov., a member of the family *Sutterellaceae* and *Sutterella megalosphaeroides* sp. nov., isolated from human faeces. Int J Syst Evol Microbiol 68:3942–3950.

Sanos SL, Vonarbourg C, Mortha A, Diefenbach A. 2011. Control of epithelial cell function by interleukin-22-producing RORγt^{+} innate lymphoid cells. Immunology 132:453–465.

Santacruz A, Collado MC, García-Valdés L, Segura MT, Marítn-Lagos JA, Anjos T, Martí-Romero M, Lopez RM, Florido J, Campoy C, Sanz Y. 2010. Gut microbiota composition is associated with body weight, weight gain and biochemical parameters in pregnant women. Br J Nutr 104:83–92.

Sartor RB. 2004. Therapeutic manipulation of the enteric microflora in inflammatory bowel diseases: antibiotics, probiotics, and prebiotics. Gastroenterology 126:1620–1633.

Satoh-Takayama N, Serafini N, Verrier T, Rekiki A, Renauld JC, Frankel G, DiSanto J. 2014. The chemokine receptor CXCR6 controls the functional topography of interleukin-22 producing intestinal innate lymphoid cells. Immunity 41:776–788.

Sayin SI, Wahlström A, Felin J, Jäntti S, Marschall HU, Bamberg K, Angelin B, Hyötyläinen T, Orešič M, Bäckhed F. 2013. Gut microbiota regulates bile acid metabolism by reducing the levels of tauro-beta-muricholic acid, a naturally occurring FXR antagonist. Cell Metab 17:225–235.

Schrimpe-Rutledge AC, Codreanu SG, Sherrod SD, McLean JA. 2016. Untargeted metabolomics strategies-challenges and emerging directions. J Am Soc Mass Spectrom 27:1897–1905.

Schwartz MW, Seeley RJ, Zeltser LM, Drewnowski A, Ravussin E, Redman LM, et al. 2017. Obesity pathogenesis: an endocrine society scientific statement. Endocr Rev 38:267–296.

Seemann T. 2014. Prokka: rapid prokaryotic genome annotation. Bioinformatics 30:2068–2069.

Serino M, Luche E, Gres S, Baylac A, Bergé M, Cenac C, Waget A, Klopp P, Iacovoni J, Klopp C, Mariette J, Bouchez O, Lluch J, Ouarné F, Monsan P, Valet P, Roques C, Amar J, Bouloumié A, Théodorou V, Burcelin R. 2012. Metabolic adaptation to a high-fat diet is associated with a change in the gut microbiota. Gut 61:543–553.

Shade A, Peter H, Allison SD, Baho DL, Berga M, Bürgmann H, Huber DH, Langenheder S, Lennon JT, Martiny JBH, Matulich KL, Schmidt TM, Handelsman J. 2012. Fundamentals of microbial community resistance and resilience. Front Microbiol 3:417–436.

Shafquat A, Joice R, Simmons SL, Huttenhower C. 2014. Functional and phylogenetic assembly of microbial communities in the human microbiome. Trends Microbiol 22:261–266.

Shah P, Fritz J V., Glaab E, Desai MS, Greenhalgh K, Frachet A, Niegowska M, Estes M, Jäger C, Seguin-Devaux C, Zenhausern F, Wilmes P. 2016. A microfluidics-based *in vitro* model of the gastrointestinal human-microbe interface. Nat Commun 7:11535.

Shen B, Hu J, Song H, Wang Z, Fan J, Sun Y, Wang Q. 2019. Antibiotics exacerbated colitis by affecting the microbiota, Treg cells and SCFAs in IL10-deficient mice. Biomed Pharmacother 114:108849.

Shi J, Zhao Y, Wang Y, Gao W, Ding J, Li P, Hu L, Shao F. 2014. Inflammatory caspases are innate immune receptors for intracellular LPS. Nature 514:187–192.

Shimomura I, Shimano H, Korn BS, Bashmakov Y, Horton JD. 1998. Nuclear sterol regulatory element-binding proteins activate genes responsible for the entire program of unsaturated fatty acid biosynthesis in transgenic mouse liver. J Biol Chem 273:35299–35306.

Shin NR, Whon TW, Bae JW. 2015. Proteobacteria: microbial signature of dysbiosis in gut microbiota. Trends Biotechnol 33:496–503.

Shoelson SE, Lee J, Goldfine AB. 2006. Inflammation and insulin resistance. J Clin Invest 116:1793–1801.

Silipo A, Molinaro A. 2010. The diversity of the core oligosaccharide in lipopolysaccharides. Subcell Biochem 53:69–99.

Singh V, Yeoh BS, Xiao X, Kumar M, Bachman M, Borregaard N, Joe B, Vijay-Kumar M. 2015. Interplay between enterobactin, myeloperoxidase and lipocalin 2 regulates *E. coli* survival in the inflamed gut. Nat Commun 6:7113.

Skiles GL, Adams JD Jr, Yost GS. 1989. Isolation and identification of 3-Hydroxy-3-methyloxindole, the major murine metabolite of 3-methylindole. Chem Res Toxicol 2:254–259.

Smillie CS, Sauk J, Gevers D, Friedman J, Sung J, Youngster I, Hohmann EL, Staley C, Khoruts A, Sadowsky MJ, Allegretti JR, Smith MB, Xavier RJ, Alm EJ. 2018. Strain tracking reveals the determinants of bacterial engraftment in the human gut following fecal microbiota transplantation. Cell Host Microbe 23:229–240.

Smith CA, O'Maille G, Want EJ, Qin C, Trauger SA, Brandon TR, Custodio DE, Abagyan R, Siuzdak G. 2005. METLIN: a metabolite mass spectral database. Ther Drug Monit 27:747–751.

Smith K, McCoy KD, Macpherson AJ. 2007. Use of axenic animals in studying the adaptation of mammals to their commensal intestinal microbiota. Semin Immunol 19:59–69.

Somm E, Henry H, Bruce SJ, Bonnet N, Montandon S A, Niederländer NJ, Messina A, Aeby S, Rosikiewicz M, Fajas L, Sempoux C, Ferrari S, Greub G, Pitteloud N. 2018. β-Klotho deficiency shifts the gut-liver bile acid axis and induces hepatic alterations in mice. Am J Physiol Endocrinol Metab 315:E833–E847.

Sonnenburg JL, Bäckhed F. 2016. Diet-microbiota interactions as moderators of human metabolism. Nature 535:56–64.

Spandidos A, Wang X, Wang H, Seed B. 2010. PrimerBank: a resource of human and mouse PCR primer pairs for gene expression detection and quantification. Nucleic Acids Res 38:D792–D799.

Staels B, Handelsman Y, Fonseca V. 2010. Bile acid sequestrants for lipid and glucose control. Curr Diab Rep 10:70–77.

Ståhl AL, Svensson M, Mörgelin M, Svanborg C, Tarr PI, Mooney JC, Watkins SL, Johnson R, Karpman D. 2006. Lipopolysaccharide from enterohemorrhagic *Escherichia coli* binds to platelets through TLR4 and CD62 and is detected on circulating platelets in patients with hemolytic uremic syndrome. Blood 108:167–176.

Staley C, Kelly CR, Brandt LJ, Khoruts A, Sadowsky MJ. 2016. Complete microbiota engraftment is not essential for recovery from recurrent *Clostridium difficile* infection following fecal microbiota transplantation. MBio 7:e01965–16.

Stefka AT, Feehley T, Tripathi P, Qiu J, McCoy K, Mazmanian SK, Tjota MY, Seo G-Y, Cao S, Theriault BR, Antonopoulos DA, Zhou L, Chang EB, Fu Y-X, Nagler CR. 2014. Commensal bacteria protect against food allergen sensitization. Proc Natl Acad Sci 111:13145–13150.

Steimle A, Autenrieth IB, Frick JS. 2016. Structure and function: lipid A modifications in commensals and pathogens. Int J Med Microbiol 306:290–301.

Stewart EJ. 2012. Growing unculturable bacteria. J Bacteriol 194:4151–4160.

Sun EW, De Fontgalland D, Rabbitt P, Hollington P, Sposato L, Due SL, Wattchow DA, Rayner CK, Deane AM, Young RL, Keating DJ. 2017. Mechanisms controlling glucose-induced GLP-1 secretion in human small intestine. Diabetes 66:2144–2149.

Sun K, Kusminski CM, Scherer PE. 2011. Adipose tissue remodeling and obesity. J Clin Invest 121:2094–2101.

Sun S, Ji Y, Kersten S, Qi L. 2012. Mechanisms of inflammatory responses in obese adipose tissue. Annu Rev Nutr 32:261–286.

Surana NK, Kasper DL. 2017. Moving beyond microbiome-wide associations to causal microbe identification. Nature 552:244–247.

Swann JR, Want EJ, Geier FM, Spagou K, Wilson ID, Sidaway JE, Nicholson JK, Holmes E. 2011. Systemic gut microbial modulation of bile acid metabolism in host tissue compartments. Proc Natl Acad Sci. USA 108:4523–4530.

Tenaillon O, Skurnik D, Picard B, Denamur E. 2010. The population genetics of commensal *Escherichia coli*. Nat Rev Microbiol 8:207–217.

Thaiss CA, Levy M, Grosheva I, Zheng D, Soffer E, Blacher E, Braverman S, Tengeler AC, Barak O, Elazar M, Ben-Zeev R, Lehavi-Regev D, Katz MN, Pevsner-Fischer M, Gertler A, Halpern Z, Harmelin A, Aamar S, Serradas P, Grosfeld A, Shapiro H, Geiger B, Elinav E. 2018. Hyperglycemia drives intestinal barrier dysfunction and risk for enteric infection. Science 359:1376–1383.

Thomas C, Gioiello A, Noriega L, Strehle A, Oury J, Rizzo G, Macchiarulo A, Yamamoto H, Mataki C, Pruzanski M, Pellicciari R, Auwerx J, Schoonjans K. 2009.

TGR5-mediated bile acid sensing controls glucose homeostasis. Cell Metab 10:167–177.

Thompson JA, Oliveira RA, Djukovic A, Ubeda C, Xavier KB. 2015. Manipulation of the quorum sensing signal AI-2 affects the antibiotic-treated gut microbiota. Cell Rep 10:1861–1871.

Thuenemann EC, Giuseppina GM, Rich GT, Faulks RM. 2015. Dynamic gastric model (DGM), p 47–59. In: Verhoeckx K, Cotter P, López-Expósito I, Kleiveland C, Lea T, Mackie A, Requena, T., Swiatecka, D., Wichers, H. (ed), The impact of food bioactives on health: *in vitro* and *ex vivo* models. Springer.

Tomas J, Mulet C, Saffarian A, Cavin J-B, Ducroc R, Regnault B, et al. 2016. High-fat diet modifies the PPAR-γ pathway leading to disruption of microbial and physiological ecosystem in murine small intestine. Proc Natl Acad Sci 113:E5934–E5943.

Tomas J, Reygner J, Mayeur C, Ducroc R, Bouet S, Bridonneau C, et al. 2015. Early colonizing *Escherichia coli* elicits remodeling of rat colonic epithelium shifting toward a new homeostatic state. ISME J 9:46–58.

Treuting PM, Dintzis SM. 2012. 12-Lower gastrointestinal tract. p 212–228. In: Treuting PM, Dintzis SM, Liggitt D, Frevert CW, (ed), Comparative anatomy and histology, 1st ed. Academic Press.

Trøseid M, Nestvold TK, Rudi K, Thoresen H, Nielsen EW, Lappegård KT. 2013. Plasma lipopolysaccharide is closely associated with glycemic control and abdominal obesity: evidence from bariatric surgery. Diabetes Care 36:3627–3632.

Tulstrup MV-L, Roager HM, Thaarup IC, Frandsen HL, Frøkiær H, Licht TR, Bahl MI. 2018. Antibiotic treatment of rat dams affects bacterial colonization and causes decreased weight gain in pups. Commun Biol 1:145.

Turnbaugh PJ, Bäckhed F, Fulton L, Gordon JI. 2008. Diet-induced obesity is linked to marked but reversible alterations in the mouse distal gut microbiome. Cell Host Microbe 3:213–223.

Turnbaugh PJ, Hamady M, Yatsunenko T, Cantarel BL, Duncan A, Ley RE, Sogin ML, Jones WJ, Roe BA, Affourtit JP, Egholm M, Henrissat B, Heath AC, Knight R, Gordon JI. 2009. A core gut microbiome in obese and lean twins. Nature 457:480–484.

Turnbaugh PJ, Ley RE, Mahowald MA, Magrini V, Mardis ER, Gordon JI. 2006. An obesity-associated gut microbiome with increased capacity for energy harvest. Nature 44:1027–1031.

Turnbaugh PJ, Ridaura VK, Faith JJ, Rey FE, Knight R, Gordon JI. 2009. The effect of diet on the human gut microbiome: a metagenomic analysis in humanized gnotobiotic mice. Sci Transl Med 1:6ra14.

Turner JR. 2009. Intestinal mucosal barrier function in health and disease. Nat Rev Immunol 9:799–809

Utzschneider KM, Kratz M, Damman CJ, Hullarg M. 2016. Mechanisms linking the gut microbiome and glucose metabolism. J Clin Endocrinol Metab 101:1445–1454.

Vaishnava S, Yamamoto M, Severson KM, Ruhn KA, Yu X, Koren O, Ley R, Wakeland EK, Hooper L V. 2011. The antibacterial lectin RegIIIgamma promotes the spatial segregation of microbiota and host in the intestine. Science 334:255–258.

Van den Abbeele P, Roos S, Eeckhaut V, Mackenzie DA, Derde M, Verstraete W, Marzorati M, Possemiers S, Vanhoecke B, Van Immerseel F, Van de Wiele T. 2012. Incorporating a mucosal environment in a dynamic gut model results in a more representative colonization by Lactobacilli. Microb Biotechnol 5:106–115.

van der Lugt B, Rusli F, Lute C, Lamprakis A, Salazar E, Boekschoten M V., Hooiveld GJ, Müller M, Vervoort J, Kersten S, Belzer C, Kok DEG, Steegenga WT. 2018. Integrative analysis of gut microbiota composition, host colonic gene expression and intraluminal metabolites in aging C57BL/6J mice. Aging (Albany NY) 10:930–950.

Van der Sluis M, De Koning BAE, De Bruijn ACJM, Velcich A, Meijerink JPP, Van Goudoever JB, Büller HA, Dekker J, Van Seuningen I, Renes IB, Einerhand AWC. 2006. Muc2-deficient mice spontaneously develop colitis, indicating that MUC2 is critical for colonic protection. Gastroenterology 131:117–129.

Vatanen T, Kostic AD, D'Hennezel E, Siljander H, Franzosa EA, Yassour M, Kolde R, Vlamakis H, Arthur TD, Hämäläinen AM, Peet A, Tillmann V, Uibo R, Mokurov S, Dorshakova N, Ilonen J, Virtanen SM, Szabo SJ, Porter JA, Lähdesmäki H, Huttenhower C, Gevers D, Cullen TW, Knip M, Xavier RJ. 2016. Variation in microbiome LPS immunogenicity contributes to autoimmunity in humans. Cell 165:1551.

Velazquez EM, Nguyen H, Heasley KT, Saechao CH, Gil LM, Rogers AWL, Miller BM, Rolston MR, Lopez CA, Litvak Y, Liou MJ, Faber F, Bronner DN, Tiffany CR, Byndloss MX, Byndloss AJ, Bäumler AJ. 2019. Endogenous *Enterobacteriaceae* underlie variation in susceptibility to *Salmonella* infection. Nat Microbiol 4:1057–1064.

Venema K, Van Den Abbeele P. 2013. Experimental models of the gut microbiome. Best Pract Res Clin Gastroenterol 27:115–126.

Vinderola G, Matar C, Perdigon G. 2005. Role of intestinal epithelial cells in immune effects mediated by gram-positive probiotic bacteria: involvement of toll-like receptors. Clin Diagn Lab Immunol 12:1075–1084.

Vonaesch P, Anderson M, Sansonetti PJ. 2018. Pathogens, microbiome and the host: Emergence of the ecological Koch's postulates. FEMS Microbiol Rev 42:273–292.

Vrieze A, Out C, Fuentes S, Jonker L, Reuling I, Kootte RS, Van Nood E, Holleman F, Knaapen M, Romijn JA, Soeters MR, Blaak EE, Dallinga-Thie GM, Reijnders D, Ackermans MT, Serlie MJ, Knop FK, Holst JJ, Van Der Ley C, Kema IP, Zoetendal EG, De Vos WM, Hoekstra JBL, Stroes ES, Groen AK, Nieuwdorp M. 2014. Impact of oral vancomycin on gut microbiota, bile acid metabolism, and insulin sensitivity. J Hepatol 60:824–831.

Wahlström A, Sayin SI, Marschall HU, Bäckhed F. 2016. Intestinal crosstalk between bile acids and microbiota and its impact on host metabolism. Cell Metab 24:41–50.

Waidmann M, Bechtold O, Frick J-S, Lehr H-A, Schubert S, Dobrindt U, Loeffler J, Bohn E, Autenrieth IB. 2003. *Bacteroides vulgatus* protects against *Escherichia coli*-induced colitis in gnotobiotic interleukin-2-deficient mice. Gastroenterology 125:162–177.

Walter J, Britton RA, Roos S. 2011. Host-microbial symbiosis in the vertebrate gastrointestinal tract and the *Lactobacill*us reuteri paradigm. Proc Natl Acad Sci 108:4645–4652.

Walter J, Ley R. 2011. The human gut microbiome: ecology and recent evolutionary changes. Annu Rev Microbiol 65:411–429.

Wang J, Lang T, Shen J, Dai J, Tian L, Wang X. 2019. Core gut bacteria analysis of healthy mice. Front Microbiol 10:887.

Wang L, Lee YK, Bundman D, Han Y, Thevananther S, Kim CS, Chua SS, Wei P, Heyman RA, Karin M, Moore DD. 2002. Redundant pathways for negative feedback regulation of bile acid production. Dev Cell 2:721–731.

Watanabe M, Houten SM, Mataki C, Christoffolete MA, Kim BW, Sato H, Messaddeq N, Harney JW, Ezaki O, Kodama T, Schoonjans K, Bianco AC, Auwerx J. 2006. Bile acids induce energy expenditure by promoting intracellular thyroid hormone activation. Nature 439:484–489.

Wattam AR, Brettin T, Davis JJ, Gerdes S, Kenyon R, Machi D, Mao C, Olson R, Overbeek R, Pusch GD, Shukla MP, Stevens R, Vonstein V, Warren A, Xia F, Yoo H. 2018. Assembly, annotation, and comparative genomics in PATRIC, the all bacterial bioinformatics resource center. p 79–101. *In* Setubal JC, Stoye J, Stadler P (ed), Comparative genomics. 1st ed, Humana Press, New York, NY.

Weisburg WG, Barns SM, Pelletier DA, Lane DJ. 1991. 16S ribosomal DNA amplification for phylogenetic study. J Bacteriol 173:697–703.

Wexler HM, Reeves D, Summanen PH, Molitoris E, McTeague M, Duncan J, Wilson KH, Finegold SM. 1996. *Sutterella wadsworthensis* gen. nov., sp. nov., bile-resistant microaerophilic *Campylobacter gracilis*-like clinical isolates. Int J Syst Bacteriol 46:252–258.

Wiles TJ, Jemielita M, Baker RP, Schlomann BH, Logan SL, Ganz J, Melancon E, Eisen JS, Guillemin K, Parthasarathy R. 2016. Host gut motility promotes competitive exclusion within a model intestinal microbiota. PLoS Biol 14:e1002517.

Willing B, Dicksved J, Halfvarson J, Andersson A, Lucio M, Zeng Z, Jarnerot G, Tysk C, Jansson JK, Engstrand L. 2010. A pyrosequencing study in twins shows that GI microbial profiles vary with inflammatory bowel disease phenotypes. Gastroenterology 139:1844–1854.

Willing BP, Russell SL, Finlay BB. 2011. Shifting the balance: antibiotic effects on host-microbiota mutualism. Nat Rev Microbiol 9:233–243.

Willing BP, Vacharaksa A, Croxen M, Thanachayanont T, Finlay BB. 2011. Altering host resistance to infections through microbial transplantation. PLoS One 6:e26988.

Willing BP, Van Kessel AG. 2007. Enterocyte proliferation and apoptosis in the caudal small intestine is influenced by the composition of colonizing commensal bacteria in the neonatal gnotobiotic pig. J Anim Sci 85:3256–3266.

Windmueller HG, Spaeth AE. 1976. Metabolism of absorbed aspartate, asparagine, and arginine by rat small intestine *in vivo*. Arch Biochem Biophys 175:670–676.

Windmueller HG, Spaeth AE. 1980. Respiratory fuels and nitrogen metabolism *in vivo* in small intestine of fed rats. Quantitative importance of glutamine, glutamate, and aspartate. J Biol Chem 255:107–112.

Winter SE, Winter MG, Xavier MN, Thiennimitr P, Poon V, Keestra AM, Laughlin RC, Gomez G, Wu J, Lawhon SD, Popova IE, Parikh SJ, Adams LG, Tsolis RM, Stewart VJ, Bäumler AJ. 2013. Host-derived nitrate boosts growth of *E. coli* in the inflamed gut. Science 339:708–711.

Wishart DS, Jewison T, Guo AC, Wilson M, Knox C, Liu Y, Djoumbou Y, Mandal R, Aziat F, Dong E, Bouatra S, Sinelnikov I, Arndt D, Xia J, Liu P, Yallou F, Bjorndahl T, Perez-Pineiro R, Eisner R, Allen F, Neveu V, Greiner R, Scalbert A. 2013. HMDB 3.0-the human metabolome database in 2013. Nucleic Acids Res 41:D801–D807.

Wlodarska M, Willing B, Keeney KM, Menendez A, Bergstrom KS, Gill N, Russell SL, Vallance BA, Finlay BB. 2011. Antibiotic treatment alters the colonic mucus layer and predisposes the host to exacerbated *Citrobacter rodentium*-induced colitis. Infect Immun 79:1536–1545.

Wolodko WT, Fraser ME, James MN, Bridger WA. 1994. The crystal structure of succinyl-CoA synthetase from *Escherichia coli* at 2.5-A resolution. J Biol Chem 269:10883–10890.

Woods SA, Schwartzbach SD, Guest JR. 1988. Two biochemically distinct classes of fumarase in *Escherichia coli*. Biochim Biophys Acta (BBA)-Protein Struct Mol 954:14–26.

Wu G. 2010. Functional amino acids in growth, reproduction, and health. Adv Nutr 1:31–37.

Wu J, Ren W, Li L, Luo M, Xu K, Shen J, Wang J, Chang G, Lu Y, Qi Y, Xu B, He Y, Hu Y. 2018. Effect of aging and glucagon-like peptide 2 on intestinal microbiota in SD rats. Aging Dis 9:566–577.

Xia J, Sinelnikov IV, Han B, Wishart DS. 2015. MetaboAnalyst 3.0-making metabolomics more meaningful. Nucleic Acids Res 43:W251–W257.

Xiao L, Chen B, Feng D, Yang T, Li T, Chen J. 2019. TLR4 may be involved in the regulation of colonic mucosal microbiota by Vitamin A. Front Microbiol 10:268.

Xie G, Wang X, Huang F, Zhao A, Chen W, Yan J, Zhang Y, Lei S, Ge K, Zheng X, Liu J, Su M, Liu P, Jia W. 2016. Dysregulated hepatic bile acids collaboratively promote liver carcinogenesis. Int J Cancer 139:1764–1775.

Xu H, Barnes GT, Yang Q, Tan G, Yang D, Chou CJ, et al. 2003. Chronic inflammation in fat plays a crucial role in the development of obesity-related insulin resistance. J Clin Invest 112:1821–1830.

Xu J, Chen N, Wu Z, Song Y, Zhang Y, Wu N, Zhang F, Ren X, Liu Y. 2018. 5-aminosalicylic acid alters the gut bacterial microbiota in patients with ulcerative colitis. Front Microbiol 9:1274.

Xu Z, Malmer D, Langille MGI, Way SF, Knight R. 2014. Which is more important for classifying microbial communities: Who's there or what they can do? ISME J 8:2357–2359.

Yang J, Summanen PH, Henning SM, Hsu M, Lam H, Huang J, Tseng CH, Dowd SE, Finegold SM, Heber D, Li Z. 2015. Xylooligosaccharide supplementation alters gut bacteria in both healthy and prediabetic adults: a pilot study. Front Physiol 6:216.

Yang Y, Smith DL, Keating KD, Allison DB, Nagy TR. 2014. Variations in body weight, food intake and body composition after long-term high-fat diet feeding in C57BL/6J mice. Obesity 22:2147–2155.

Ye J, Lv L, Wu W, Li Y, Shi D, Fang D, Guo F, Jiang H, Yan R, Ye W, Li L. 2018. Butyrate protects mice against methionine–choline-deficient diet-induced non-alcoholic steatohepatitis by improving gut barrier function, attenuating inflammation and reducing endotoxin levels. Front Microbiol 9:1967.

Yissachar N, Zhou Y, Ung L, Lai NY, Mohan JF, Ehrlicher A, Weitz DA, Kasper DL, Chiu IM, Mathis D, Benoist C. 2017. An intestinal organ culture system uncovers a role for the nervous system in microbe-immune crosstalk. Cell 168:1135–1148.

Yoneno K, Hisamatsu T, Shimamura K, Kamada N, Ichikawa R, Kitazume MT, Mori M, Uo M, Namikawa Y, Matsuoka K, Sato T, Koganei K, Sugita A, Kanai T, Hibi T. 2013. TGR5 signalling inhibits the production of pro-inflammatory cytokines by in vitro differentiated inflammatory and intestinal macrophages in Crohn's disease. Immunology 139:19–29.

Yoshida N, Emoto T, Yamashita T, Watanabe H, Hayashi T, Tabata T, Hoshi N, Hatano N, Ozawa G, Sasaki N, Mizoguchi T, Amin HZ, Hirota Y, Ogawa W, Yamada T, Hirata KI. 2018. *Bacteroides vulgatus* and *Bacteroides dorei* reduce gut microbial lipopolysaccharide production and inhibit atherosclerosis. Circulation 138:2486–2498.

Zarepour M, Bhullar K, Montero M, Ma C, Huang T, Velcich A, Xia L, Vallance BA. 2013. The mucin Muc2 limits pathogen burdens and epithelial barrier dysfunction during *Salmonella enterica* serovar typhimurium colitis. Infect Immun 81:3672–3683.

Zeng MY, Inohara N, Nuñez G. 2017. Mechanisms of inflammation-driven bacterial dysbiosis in the gut. Mucosal Immunol 10:18–26.

Zhang C, Zhang M, Pang X, Zhao Y, Wang L, Zhao L. 2012. Structural resilience of the gut microbiota in adult mice under high-fat dietary perturbations. ISME J 6:1848–1857.

Zhang F, Zheng W, Guo R, Yao W. 2017. Effect of dietary copper level on the gut microbiota and its correlation with serum inflammatory cytokines in Sprague-Dawley rats. J Microbiol 55:694–702.

Zhang H, DiBaise JK, Zuccolo A, Kudrna D, Braidotti M, Yu Y, Parameswaran P, Crowell MD, Wing R, Rittmann BE, Krajmalnik-Brown R. 2009. Human gut microbiota in obesity and after gastric bypass. Proc Natl Acad Sci. 106:2365–2370.

Zhang L, Dong D, Jiang C, Li Z, Wang X, Peng Y. 2015. Insight into alteration of gut microbiota in *Clostridium difficile* infection and asymptomatic *C. difficile* colonization. Anaerobe 34:1–7.

Zhang X, Wang H, Yin P, Fan H, Sun L, Liu Y. 2017. Flaxseed oil ameliorates alcoholic liver disease via anti-inflammation and modulating gut microbiota in mice. Lipids Health Dis 16:44.

Zhang X, Zhao Y, Xu J, Xue Z, Zhang M, Pang X, Zhang X, Zhao L. 2015. Modulation of gut microbiota by berberine and metformin during the treatment of high-fat diet-induced obesity in rats. Sci Rep 5:14405.

Zheng X, Xie G, Zhao A, Zhao L, Yao C, Chiu NH, Zhou Z, Bao Y, Jia W, Nicholson JK, Jia W. 2011. The footprints of gut microbial-mammalian co-metabolism. J Proteome Res 10:5512–5522.

Zheng Y, Valdez PA, Danilenko DM, Hu Y, Sa SM, Gong Q, Abbas AR, Modrusan Z, Ghilardi N, de Sauvage FJ, Ouyang W. 2008. Interleukin-22 mediates early host defense against attaching and effacing bacterial pathogens. Nat Med 14:282–289.

Zhou D, Pan Q, Xin FZ, Zhang RN, He CX, Chen GY, Liu C, Chen YW, Fan JG. 2017. Sodium butyrate attenuates high-fat diet-induced steatohepatitis in mice by improving gut microbiota and gastrointestinal barrier. World J Gastroenterol 23:60–75.

Zhou Y, Men L, Pi Z, Wei M, Song F, Zhao C, Liu Z. 2018. Fecal metabolomics of type 2 diabetic rats and treatment with Gardenia jasminoides Ellis based on mass spectrometry technique. J Agric Food Chem 66:1591–1599.

Zietak M, Kovatcheva-Datchary P, Markiewicz LH, Ståhlman M, Kozak LP, Bäckhed F. 2016. Altered microbiota contributes to reduced diet-induced obesity upon cold exposure. Cell Metab 23:1216–1223.